

OPERA

LILW degradation processes and products

OPERA-PU-IBR512

Ionising radiation and radioactive substances are used in various fields: e.g., medicine, industry, agriculture, research. However, radioactive waste is produced by using radiation. In the Netherlands, this waste is collected, treated and stored by COVRA (Centrale Organisatie Voor Radioactief Afval). After the waste is stored for at least 100 years it is intended for disposal in a geological repository. There is world-wide scientific and technical consensus that this approach represents the safest long-term option for radioactive waste disposal.

The geological waste disposal is understood as the emplacement of radioactive waste in deep underground geological formations. The objective is to isolate the radioactive waste from the biosphere in order to avoid the exposure of future generations to ionising radiation from the waste. The Dutch research programme focussing on the geological disposal of radioactive waste is called OPERA (OnderzoeksProgramme Eindberging Radioactief Afval).

In the framework of OPERA, researchers of different institutions and scientific areas cooperate on the initial, conditional Safety Cases for the host rock formations Boom Clay and Zechstein rock salt. OPERA is a preliminary or initial safety case and will be developed to set up the research necessary for the eventual development of a repository in the Netherlands.

OPERA is financed by the Dutch Ministry of Economic Affairs and the public limited liability company Electriciteits-Produktie maatschappij Zuid-Nederland (EPZ) and coordinated by COVRA. Further details on OPERA and its outcomes can be accessed at www.covra.nl.

This report concerns a study conducted in the framework of OPERA. The conclusions and viewpoints presented in the report are those of the author(s). COVRA may draw modified conclusions, based on additional literature sources and expert opinions. A .pdf version of this document can be downloaded from www.covra.nl

OPERA-PU-IBR512

Title LILW degradation processes and products

Authors: A. Filby, G. Deissmann, R. Wieggers

Date of publication 26 October 2016

Keywords: LILW, degradation, Cellulose, Plastics, Metals, Source-Term

COVRA N.V.



Summary	1
Samenvatting	1
1. Introduction	2
1.1. Background	2
1.2. Objectives	2
1.3. Realization	2
1.4. Explanation contents	2
2. OPERA waste disposal concept in Boom Clay	3
3. LILW in OPERA	5
3.1. LILW inventory and matrix composition	5
3.1.1. Compacted waste	6
3.1.2. Processed liquid Molybdenum waste and spent ion exchangers	8
3.1.2.1. Processed liquid molybdenum waste	9
3.1.2.2. Processed liquid waste with spent ion exchangers	11
3.1.3. Depleted Uranium	12
3.2. Radionuclide inventory	13
4. Evolution of the Repository Near-Field	13
4.1. Evolution of pH and pore water composition	13
4.2. Evolution of redox conditions	15
4.2.1. Aerobic phase	15
4.2.2. Anaerobic phase	16
5. LILW degradation processes and products	16
5.1. Introduction to cellulose chemistry	16
5.2. Cellulose degradation processes	18
5.2.1. Chemical degradation of cellulose	18
5.2.1.1. Cellulose degradation products	21
5.3. Cellulose degradation kinetics	25
5.3.1. Microbial degradation of cellulose	28
5.3.2. Radiolytic degradation of cellulose	30
5.3.3. Cellulose degradation kinetics: determining factors	31
5.4. Degradation processes of ISA	32
5.4.1. Chemical Degradation	32
5.4.2. Microbial degradation	33
5.4.3. Radiolytic degradation	34
5.5. Plastics	35
5.5.1. Non-aqueous phase liquids	35
5.5.2. Non-halogenated plastics	36
5.5.2.1. Chemical degradation of polyethylene	37
5.5.2.2. Radiolytic degradation of polyethylene	37
5.5.2.3. Microbial degradation of polyethylene	43
5.5.3. Halogenated plastics	44
5.5.3.1. General information on PVC	44
5.5.3.2. Specific additives: Plasticisers	46
5.5.3.3. Specific additives: Stabilisers	47
5.5.3.4. Chemical Degradation of PVC	48
5.5.3.5. Microbial Degradation of PVC	51
5.5.3.6. Radiolytic degradation of PVC	52
5.5.4. Degradation processes of PVC plasticisers	57
5.5.4.1. Chemical and radiolytic degradation	58
5.5.4.2. Microbial degradation	62
5.6. Rubbers	63
5.6.1. General information	63
5.6.2. Chemical degradation	65
5.6.3. Radiolytic degradation	65

5.6.4.	Microbial degradation.....	68
5.7.	Ion exchangers	69
5.7.1.	General information.....	69
5.7.2.	Chemical degradation of ion exchangers.....	70
5.7.3.	Radiolytic degradation of ion exchangers.....	70
5.7.4.	Microbial degradation of polystyrene.....	76
5.8.	Varnish.....	77
5.9.	Cement admixtures.....	77
5.9.1.	Chemical degradation.....	80
5.9.2.	Microbial degradation.....	81
5.9.3.	Radiolytic degradation.....	81
5.10.	Metal corrosion processes and products	82
5.10.1.	Carbon Steel	82
5.10.2.	Zinc	87
5.10.3.	Aluminium	88
5.11.	Behaviour of U ₃ O ₈	90
5.12.	Degradation of processed liquid molybdenum waste	92
5.13.	Gas generation.....	93
5.13.1.	Gas generation processes.....	93
5.13.1.1.	Gas generation due to metal corrosion	93
5.13.1.2.	Gas generation due to microbial activity	95
5.13.1.1.	Volatile radioisotopes	96
5.13.1.1.	Radiolysis of water	97
6.	Radionuclide Source-Terms and Migration in the Near-Field	97
6.1.	Source terms.....	97
6.1.1.	Compacted waste.....	97
6.1.2.	Processed liquid molybdenum waste	98
6.1.3.	Processed liquid waste with ion exchangers.....	98
6.1.4.	(TE)NORM: depleted Uranium	98
6.2.	Radionuclide migration in the near-field	99
6.2.1.	Solubility of radionuclides in a cementitious near-field	99
6.2.2.	Effects of (organic) LILW degradation products on radionuclide solubility ..	104
7.	Conclusions.....	117
8.	References	123
	Appendix 1: Exemplary cement pore water compositions.....	136
	Appendix 2: Additives in polymers	137
	Appendix 3: Complexation constants	139
	Appendix 4: Radionuclide Inventory	142

Summary

This report deals with the degradation processes and products of low-intermediate level waste (LILW) in a potential Dutch nuclear waste repository situated several hundred meters below the sea level in the geological host rock formation Boom Clay. In addition to LILW, large amounts of other materials will be present in the rock formation, e.g. cement, containers, shielding, air. In the first step, the geochemical conditions of the cementitious near-field of the repository were defined. On the basis of the defined conditions, the waste degradation processes and products and their behavior in the repository near-field were investigated and discussed. The particular wastes present in the LILW inventory (i.e. cellulose, plastics, rubbers, metals, depleted uranium) were investigated regarding their chemical, microbial and radiolytic degradation. Furthermore, radionuclide source-terms and the radionuclide migration in the repository near-field are addressed. Finally, the findings of this study are discussed with focus on the many knowledge gaps which were found to exist and further research is proposed.

Samenvatting

Dit rapport behandelt de degradatie processen die optreden bij de eindberging van laag en middel actief afval (LILW) in een mogelijke ondergrondse eindberging welke zich in een kleilaag (Boomsche klei) van enkele honderden meters beneden de zeespiegel bevindt. Naast het betreffende radioactieve afval zullen ook grote hoeveelheden andere materialen in deze eindberging aanwezig zijn, zoals beton, containers, afscherming en lucht. Als eerste stap zijn de geochemische omstandigheden gedefinieerd waar de cementgebonden materialen zich in de near field situatie bevinden. Op basis van deze vastgelegde omstandigheden is vervolgens gekeken naar de degradatie processen die optreden en de producten die hierbij gevormd worden. De specifieke afvalstoffen die in het LILW type afval aanwezig zijn (ondermeer cellulose, plastics, rubbers, metalen en verarmd uranium), zijn nader beschouwd wat betreft de chemische, microbiologische en radiologische degradatie. Verder zijn ook de bronterm en de radionuclide migratie in de near field behandeld. Tot slot zijn de resultaten van deze studie beschouwd met daarbij aandacht voor de ontbrekende informatie en tevens zijn mogelijke vervolgstappen voorgesteld.

1. Introduction

1.1. Background

The five-year research programme OPERA for the geological disposal of radioactive waste began on 7 July 2011 with an open invitation for research proposals. In the OPERA Research plan the different research tasks were described. In this report, the execution and results of the research proposed for Task 5.1.2 LILW degradation processes and products are presented.

1.2. Objectives

In this study the degradation processes and products of low and intermediate level waste (LILW) in a potential Dutch nuclear waste repository located in the geological host rock formation Boom Clay are investigated. The LILW to be disposed will be made up of, e.g., cellulosic materials, plastics, metals and depleted uranium (DU).

To estimate the influence of LILW degradation products on the host rock structure and engineered barrier system (EBS), the chemical and physical processes of LILW degradation need to be known. Thus, the focus of this study is to identify these processes and to quantify possible safety-relevant parameters.

An extensive insight on the LILW degradation behavior and its evolution under the chemical and physical conditions expected in a generic cementitious repository in Boom Clay is given. Besides the investigation of waste form degradation rates also processes that may retain the leached radionuclides in the immediate near-field by interaction with degradation products (e.g. metal corrosion/cement degradation products) are addressed and radionuclide source terms are derived.

1.3. Realization

The approach of this study was to undertake a literature research to investigate the chemical and physical processes relevant for the degradation of LILW and the formation of the degradation products, respectively.

1.4. Explanation contents

Chapter 2 briefly presents the waste disposal concept in Boom Clay in the Netherlands. Furthermore, the LILW inventory and matrix composition are briefly summarized since this data forms the basis for the subsequent chapters.

Chapter 3 gives general information regarding LILW in OPERA.

Chapter 4 discusses the evolution of the repository near-field.

Chapter 5 describes the degradation processes and products of the various low to intermediate level wastes to be disposed.

Chapter 6 deals with the derivation of a radionuclide source-term and the radionuclide migration in the near-field.

Chapter 7 discusses the findings of this study and focusses on knowledge gaps.

Chapter 8 lists the references used in this report.

2. OPERA waste disposal concept in Boom Clay

In this chapter general information regarding the Dutch disposal concept in the Boom Clay is briefly summarized. Furthermore, the LILW inventory and its matrix composition are presented.

For the OPERA study a generic disposal concept was derived [Verhoef 2014]. In this disposal concept the waste is disposed in a Boom Clay formation with a thickness of about 100 metres. All LILW, (TE)NORM and HLW are disposed in the clay formation [Verhoef 2014].

The OPERA disposal facility consists of both surface and underground facilities, as can be seen in Figure 1 [Verhoef 2014].

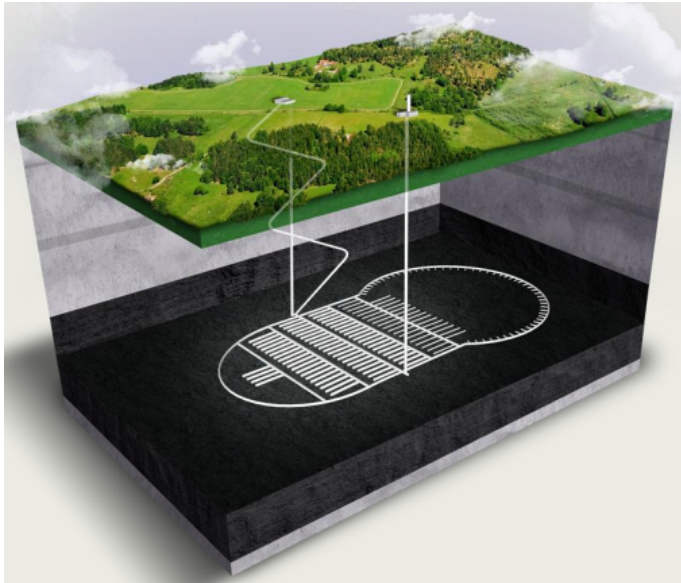


Figure 1: Artist impression of a nuclear waste repository in Boom Clay [Verhoef 2014]

Four disposal sections are distinguished in the disposal concept [Verhoef 2014]:

- Vitrified high-level waste (HLW)
- Spent fuel from research reactors
- Non-heat generating HLW (compacted hulls and ends from nuclear power plants and other non-heat generating waste)
- Low and intermediate level waste (LILW) and (TE)NORM (DU)

The underground facilities contain furthermore a pilot facility and a workshop for maintenance work [Verhoef 2014]. Figure 2 shows the disposal sections of the different wastes in the underground facility.

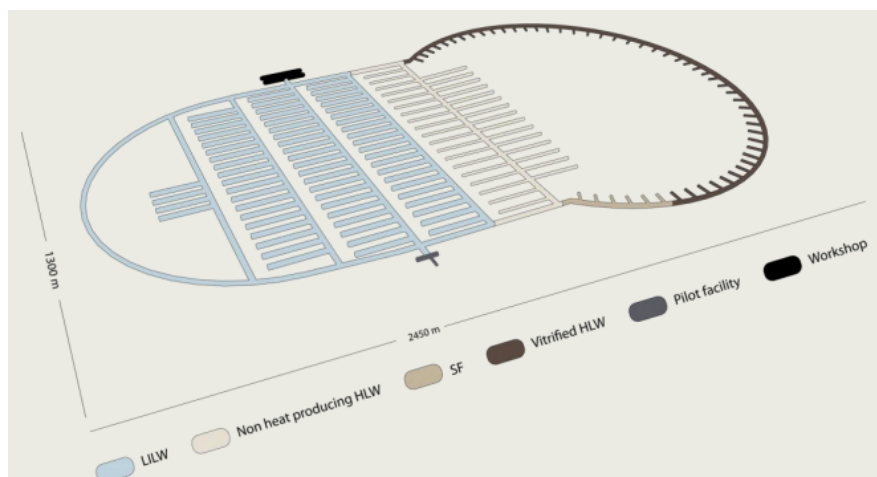


Figure 2: Disposal sections of the underground facility [Verhoef 2014]

The disposal drifts in the particular waste disposal sections are horizontal boreholes that are directly connected to the main gallery or can be accessed through secondary galleries. After the waste is emplaced, the drifts are backfilled with grout and hydraulically sealed off by a plug [Verhoef 2014]. Figure 3 shows a scheme of the waste disposal in the LILW section of the repository.



Figure 3: Scheme of the LILW section with 1,000 L containers [Verhoef 2014]

In the LILW section, the waste containers are stacked on top of each other in the disposal gallery. Regarding the depleted uranium waste, two KONRAD type II containers will be emplaced per gallery section [Verhoef 2014].

The waste disposal concept in the Boom Clay employs various cementitious materials. In [Verhoef 2014b], the following three functions for cementitious materials were defined:

- mechanical support,
- enclosure of emplaced waste and
- containment of waste.

Requirements for the mentioned cementitious materials were given in [Verhoef 2014b]. Low pH cement is not considered in the disposal concept and thus amorphous or reactive silica are not regarded as aggregates. Another requirement is that the cementitious materials should be low in chloride content to limit the concentration of corrosive species. The SO_3 content should also be low in order to limit delayed ettringite formation [Verhoef 2014b].

Since this study deals with LILW degradation processes, only the cementitious materials used in the LILW section of the repository and proposed in [Verhoef 2014b] are briefly

summarized here because they are used as basis for the investigations carried out in this study.

Table 1 gives the composition regarding the cementitious materials proposed for mechanical support according to [Verhoef 2014b].

Table 1: Composition of the cement used as mechanical support (as reinforced concrete segments) [Verhoef 2014b]

Component/parameter	Type	Concentration [kg/m ³]
Cement	CEM II/A to B-(V)	386
Water		125
Plasticiser	Woermann BV 514	1.33
Superplasticiser	Woermann FM 30	3.65
Fine aggregate	Quartz sand: 0-2 m	615
Coarse aggregate	Quartz gravel: 2-8 mm	612
Coarse aggregate	Quartz gravel: 8-16 mm	700

According to [Verhoef 2014b], the reinforced concrete segments are made with CEM I 42.5 R to which fly ash is added 19-23 wt% of CEM I [Westerscheldetunnel 2014].

In [Verhoef 2014b], the proposed composition of the enclosure (backfill) cement is also given. Foamed concrete, consisting of cement, water, foam and (fine) aggregates is suggested and the composition of this material is shown in Table 2.

Table 2: Composition of the enclosure material (backfill - foam concrete) [Verhoef 2014b]

Component	Receipt for 1 m ³ of Aercrete FC 1,200 to 1,600 kg/m ³	Type for OPERA	1200 kg/m ³ [kg/m ³]	1600 kg/m ³ [kg/m ³]
Cement	360 - 400 kg	CEM I	360	400
Water	140 - 160 kg	-	140	160
Fine aggregate	750 - 1,100 kg	Quartz sand: 0-4 mm	750	1,100
Foaming agent Synthetic surfactant	0.57 - 0.36 L	Foaming agent TM 80/23	1	1
Water	21.3 - 13.6 L	water	21.3	13.6
Air	434 - 277 L	Air	0	0

3. LILW in OPERA

3.1. LILW inventory and matrix composition

LILW is generated from activities with radioisotopes in, e.g., research institutes and hospitals. It includes lightly contaminated materials, such as tissues, cloth and plastic, metal or glass objects. Additionally, waste originated from nuclear power plants (i.e. spent ion exchangers) contributes to the amount of LILW [Hart 2014]. Besides that, processed liquid molybdenum waste generated in the framework of isotope production is included in the LILW section. Furthermore, (TE)NORM is also in the LILW section. This waste includes radioactive waste originating from the Uranium enrichment facility URENCO. Besides those wastes, also organic liquid wastes are burned and the organic sludges are present in the waste [Verhoef 2016].

According to [Verhoef 2014b], five types of containers for LILW with volumes of 200, 400, 600, 1,000 or 1,500 L are stored at the COVRA site. The 200 and 600 L drums are made of painted, galvanised steel with a cement infill. The 1,000 and 1,500 L containers are full concrete containers containing a cemented waste form [Verhoef 2014]. Table 3 summarizes the containers for the different LILW waste types according to [Verhoef 2016].

Table 3: Waste containers employed in OPERA [Meeusen 2014]

OPERA waste type	Interim storage container	Waste container at disposal
Depleted Uranium	DV-70 and 200 L containers	Konrad galvanized steel type II container
Compacted waste	200, 400, 600, 1,000, 1,500 L galvanized steel/concrete container	200, 400, 600, 1,000, 1,500 L galvanized steel/concrete container
Processed liquid molybdenum waste	1,000 L concrete containers with magnetite or quartz aggregates	1,000 L concrete containers with magnetite or quartz aggregates
Processed liquid waste with spent ion exchangers	1,000 L concrete containers with magnetite	1,000 L concrete containers with magnetite

According to [Meeusen 2014], the most significant fraction of LILW is stored in 200 L and 1,000 L containers and they make up 98.7 % of the total volume and 98.3 % of the total weight of the LILW stored at COVRA.

The inventory of the LILW waste fractions is made up of all radionuclides stored in five different container types. Table 4 shows an overview of the number of containers with LILW stored at COVRA at February 2013 derived [Meeusen 2014]. Since the 400, 600 and 1,500 L containers represent only a marginal volume/weight, they are not regarded in this study.

Table 4: Number and weight of current LILW inventory [Meeusen 2014]

Container type	Number	Total volume [m ³]	Total weight [t]
200 L	35,431	7,086	16,139
400 L	2	0.8	3
600 L	43	26	87
1,000 L	3,200	3,200	7,791
1,500 L	69	104	322
Total	38,745	10,420	24,342

In the following subsections, the characteristics of the 200, 1,000 and DU waste containers will be discussed.

3.1.1. Compacted waste

Using the data in Table 4, [Hart 2014] calculated an average total weight of a currently stored 200 L container of 456 kg [Meeusen 2014b]. The containers consist of a galvanized steel 200 L barrel in which on average 4 to 7 compressed and perforated pucks (including waste) with a volume of about 90 L are placed. The outer voids between the pressed canisters and the outer barrel are filled with cement [Meeusen 2014]. Figure 4 shows a waste container containing the compacted waste. The wall thickness of the barrel is 1 mm. The container top is not covered with steel. The technical specification of the material of the steel is DX51D- EN10143 for the bottom and DC01 - EN10130 for the sheet steel from the wall (both are low carbon steels). The drum walls are galvanized with a thickness of zinc of 40 µm. Furthermore, the containers are varnished with vinylcopolymer resin [Verhoef 2016].

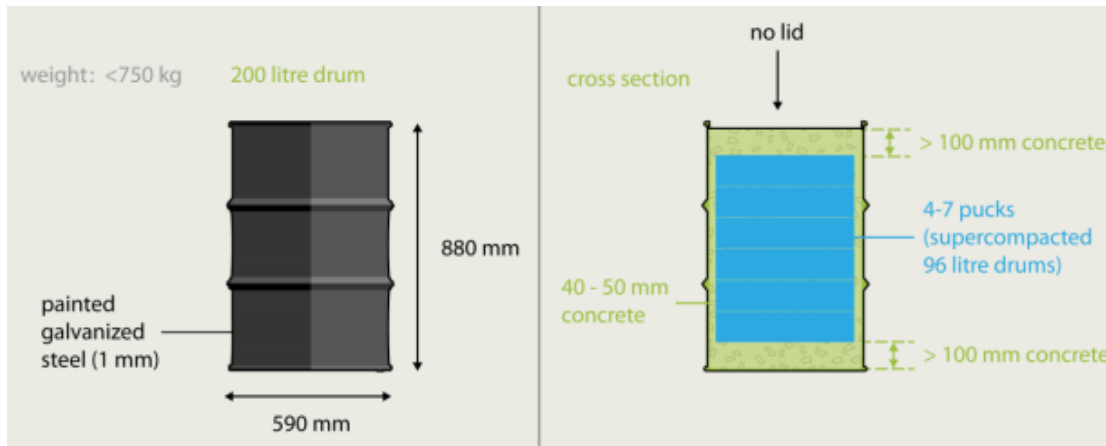


Figure 4: Waste container with super-compacted pucks. Dimensions in mm [Verhoef 2016]

Table 5 shows further technical information of the 200 L containers [Meeusen 2014].

Table 5: Characteristics of 200 L containers in [Meeusen 2014]

200 L container content	Comment	min [kg]	max [kg]
Steel: total per container	(Barrel, compressed canisters, centering iron)	58	118
Cement: total per container		210	240
Plasticiser: total per container	1.4 % of cement weight	2.94	3.36
Zinc: total per (galvanised) container	50-100 μm , 4.4 m^2	1.57	6.71
Paint: total per container	50-100 μm , 2.2 m^2	0.11	0.72
Total tare mass (all packaging materials)	Combined tare weights	272.6	368.8
Total average mass (waste plus packaging)	Based on current COVRA inventory	456	
Remaining net waste (without packaging materials)	Based on current COVRA inventory]	87.2	183.3

In [Meeusen 2014], the net weight fraction of the LILW waste within a 200 L container was estimated by subtracting the masses of steel and concrete from the total average mass of the containers. Using the present average LILW composition and the expected inventory of LILW intended for disposal [Verhoef 2014], the amount of cement/concrete, plasticiser and waste corresponding to 200 L LILW containers was determined (see Table 6).

Table 6: Matrix composition of the 200 L containers intended for disposal [Meeusen 2014]

Material	Total per 200 L container		Total for disposal (x 140,000)	
	min [kg]	max [kg]	min [kg]	max [kg]
concrete	2.10E+02	2.40E+02	2.94E+07	3.36E+07
steel	5.80E+01	1.18E+02	8.12E+06	1.65E+07
stainless steel	0	0	0	0
plasticiser	2.94E+00	3.36E+00	4.12E+05	4.70E+05
zinc	1.57E+00	6.71E+00	2.20E+05	9.40E+05
paint	1.10E-01	7.20E-01	1.54E+04	1.01E+05
net waste	8.72E+01	1.83E+02	1.22E+07	2.57E+07

According to [Verhoef 2016], the compacted solid waste contains contaminated materials and therefore all radionuclides are expected to be present on surfaces. Table 7 shows a quantitative guess (made by COVRA) of the waste matrices of the 90 L cans before their

compaction. As can be seen, the waste is mainly composed of cellulosic materials and metals. However, the error margins of the guess are quite large (up to 20 %).

Table 7: Quantitative guess of waste matrices in 90 L cans prior to their compaction [Verhoef 2016]

Matrix	Specification	Fraction of Matrix	Volume [%]	Margin [%]
Organic material	Cellulosics (paper, clothing, tissue, cardboard, organic sludge etc.)	1	35	20
Metals	Steel	0.75	30	20
	Aluminium	0.25		
Plastics	Halogenated	0.10	25	20
	Non-halogenated	0.90		
Other	Glass, rubber, concrete, inorganic adsorption, materials, salts etc.	1	10	10

By applying the data given in Table 7 on the total amounts of net waste (1.22E+07 - 2.57E+07 kg, see Table 6), the masses of the particular wastes in the 200 L containers can be estimated as shown in Table 8.

Table 8: Estimated mass of different wastes in the 200 L containers

Material	Volume [%]	Total Mass [t]
Organic material	15 - 55	1,830 - 14,135
Metals	10 - 50	1,220 - 12,850
Plastics	5 - 45	610 - 11,565
Other	0 - 20	max. 5,140

Table 9 shows the composition of the cement used for filling the voids between the compacted canisters and the outer barrel of the compacted waste. According to [Verhoef 2016], the moisture content of the concrete supersedes the maximum moisture content of 1 vol% in the waste and the moisture content in the waste can therefore be considered negligible. The concrete is made of blast furnace slag cement, water, aggregates and plasticiser. According to [Verhoef 2016] the moisture content in the waste pucks can be considered negligible as compared to that in the concrete.

Table 9: Composition containment of waste [Verhoef 2016]

Component/Parameter	Type	
Cement	CEM III/B 42.5 LH HS	407-430 kg m ⁻³
Water	-	175-185 kg m ⁻³
Plasticiser	TM OFT-II B84/39 CON. 35% (BT-SPL)	3-5 kg m ⁻³
Fine aggregate	Quartz sand: 0-4 mm	819-972 kg m ⁻³
Coarse aggregate	Quartz gravel: 2-8 mm	891-763 kg m ⁻³

3.1.2. Processed liquid Molybdenum waste and spent ion exchangers

According to [Meeusen 2014], the second largest fraction of LILW is made up of 1,000 L containers (Table 4). In total, there are 12,000 containers intended for disposal [Meeusen 2014, Verhoef 2016].

The containers store processed molybdenum waste, processed ion exchange waste or radiation sources. For OPERA, only processed molybdenum and ion exchange waste are taken into account because the radiation sources amount to less than 1.1 vol% of the processed waste in the past 5 years. In [Verhoef 2016], it was deduced that the amount of processed molybdenum waste is about 2/3 of the amount of the 1,000 L containers. Therefore, in the OPERA disposal concept it is assumed that there are 8,000 of the 1,000 L containers with processed liquid molybdenum waste, whereas 6,000 containers employ magnetite as coarse aggregate and 2,000 utilize quartz. The remaining 4,000 containers thus contain ion exchange waste [Verhoef 2016]. Table 10 shows the matrix composition of the 1,000 L containers.

Table 10: Matrix composition of the 1,000 L containers [Meeusen 2014]

Material	Total per 1000 L container		Total for disposal (x 12,000)	
	min [kg]	max [kg]	min [kg]	max [kg]
Cement	1,000	2,000	1,20E+07	2.40E+07
Concrete	1,600	2,100	1.92E+07	2.52E+07
Steel	50	200	6.00E+07	2.40E+06
Plasticiser	28	57.4	4.37E+05	6.89E+05

In the following subsections, characteristics of the processed molybdenum and ion exchange wastes are discussed.

3.1.2.1. Processed liquid molybdenum waste

Details regarding the processed liquid molybdenum waste can be found in [Verhoef 2016]. However, the important aspects which are also used as basis for the investigations of this report are presented here also. In general, the ⁹⁹Mo production generates two highly alkaline waste streams. Table 11 shows the main characteristics of those highly alkaline waste streams.

Table 11: Main characteristics of the alkaline waste streams [Verhoef 2016]

Component	Unit	Waste Stream I	Reference	Waste stream II	Reference
Liquid produced after production 111 TBq ⁹⁹ Mo	L	13.3	[IAEA 1998a]	8.7	[IAEA 1998a]
NaOH	g/L	244	[IAEA 1998a]	102	[IAEA 1998a]
Aluminium	g/L	Max 38	Covra 2010	-	
NaNO ₃	g/L	-	[IAEA 1998]	29.6	[IAEA 1998]
Uranium	g/L	0.05	[IAEA 1998a]	4 x waste stream I	Common practice
¹³⁷ Cs	GBq per 44 L	Max 600	Covra 2010, A ₂ value	1 / 500 of waste stream I	Common practice
¹⁰⁶ Ru	GBq per 44 L			Max 200	[COVRA, 2010] A ₂ value
Main type of radionuclides		Fission products soluble in alkaline media		Fission products insoluble in alkaline media, lanthanides, Uranium, Americium and Plutonium	

A₂ values are understood as radionuclide specific maximum activities that a vessel of radioactive waste may contain upon collection by COVRA.

Both waste streams are processed with a mobile cementation plant and the radionuclides can be assumed to be homogeneously distributed in the matrix. The cementation plant mixes the waste with mortar in 200 L drums whereas each drum with processed waste contains a sacrificial stirrer made of steel. The radionuclides can thus be assumed to be uniformly distributed [Verhoef 2016]. Zeolite is added in the mixture to limit the leaching of cesium. The composition of the liquid waste mixed with mortar in a 200 L drum is shown Table 12.

Table 12: 180 L processed molybdenum waste per 1,000 L waste container [Verhoef 2016]

Component	Type	Weight [kg]
Cement	CEM III/B 42.6 LH HS	155
Fine aggregate in suspension	EMSAC 500 S 50 wt% water, 50 % silica	74
Retarder	Cugla MMV con. 25% BT	1.6
Admixture	Zeolite / Klino type 1 (Na,K) ₂₋₃ Al ₃ (Al,Si) ₂ Si ₁₃ O ₃₆ ·12 H ₂ O	11
Waste stream	See I and II in Table 11	53 for I
		92 for II
Water	Only for waste stream I	39

According to [Verhoef 2016], one 200 L drum with processed waste is placed in a 1,000 L concrete container. The aggregates in that container are either magnetite (Fe₃O₄) for processed waste stream I or quartz for processed waste stream II. The 200 L drums are closed with a reinforcement lid and the 1,000 L containers are filled up with mortar to remove empty void volume. Furthermore, a reinforcement grid is employed in the concrete containers whereas the reinforcement steel used is FeB 500 HKN [Verhoef 2016]. Table 13 gives the composition of the reinforced concrete containers.

Table 13: Composition of the reinforced concrete containers per m³ without waste [Verhoef 2016]

Component	Type	1,000 L container for waste stream II [kg]	1,000 L container for waste stream I [kg]
Cement	CEM III/A 52.5 N	360	350
	CEM I/52.5 R	-	40
Fine aggregate	Quartz sand: 0-4 mm	820	760
Coarse aggregate	Quartz gravel: 4-16 mm	871	1775
	Magnetite gravel: 2-16 mm		
Superplasticiser	Glenium 51 35%	2.95	1.7
Filler	Foamcarb	200	0
Water		162	154

Figure 5 shows a 200 L drum in the 1,000 L container before concrete is poured into the latter.

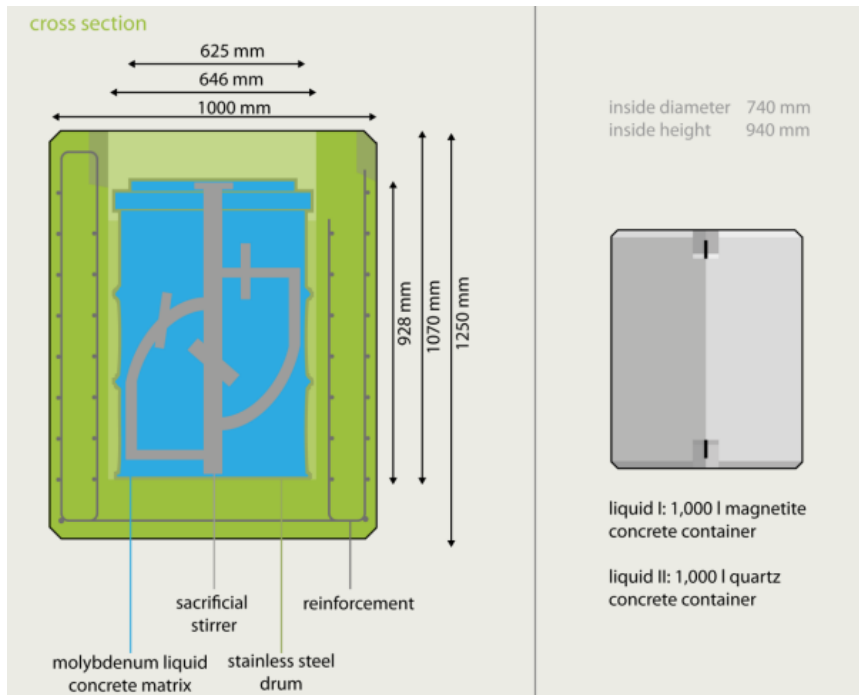


Figure 5: 200 L drum with processed waste in a concrete container. Dimensions in mm [Verhoef 2016]

3.1.2.2. Processed liquid waste with spent ion exchangers

According to [Verhoef 2016], all nuclear and research reactors in the Netherlands and nuclear facilities for molybdenum production generate waste streams with spent ion exchangers. However, only spent ion exchangers from nuclear power plants are conditioned in cement. Spent ion exchangers from research reactors are processed in another way. For example, the exchange resins from the Delft University were thermally decomposed at COVRA and the resulting sludge with the radionuclides was put in 90 L cans and became compacted waste as presented in section 3.1.1 [Verhoef 2016].

The spent ion exchangers from the molybdenum production facility and research reactors in Petten are not processed yet and the waste characteristics are unknown [Verhoef 2016]. Therefore, only ion exchangers from nuclear power plants are considered here.

According to [Verhoef 2016], bead and powdered resins are used in the still running pressurized water reactor (PWR) in the Netherlands. The spent resins are conditioned with sludge in a cementitious matrix. The activities of only a few radionuclides were reported to COVRA (^{137}Cs , ^{134}Cs and ^{60}Co). The characteristics of these waste streams are shown in Table 14.

Table 14: Main characteristics of processed waste streams [Verhoef 2016]

Component	Waste stream I	Waste stream II
Ion exchange resin	Powder max 4.3 kg (wet 6.8 kg) per waste container	Powder max 2.7 kg (wet 5.4 kg) per waste container Beads max 16.8 kg (wet 40 kg) per waste container
Max activity per waste container	^{60}Co : 10 GBq	A_2 values: ^{60}Co : max 400 GBq ^{137}Cs : max 600 GBq

Table 15 shows the cementitious composition of processed liquid waste which is poured into a 200 L drum.

Table 15: Processed waste per 200 L drum [Verhoef 2016]

Component	Type	Weight of waste stream with powder and sludge [kg]	Weight of waste stream with beads, powder and sludge [kg]
Spent ion exchanger	Resin beads	-	16.8 dry resin 23.2 absorbed water
	Resin powder mixed with sludge	94	45
Cement	CEM III/B 42.5 LH HS	242	181
Plasticiser	Sikament	-	3.6
Retarder	Sika Retarder	2.4	1.8
Admixture	Zeolite/Klino type 1 (Na ₂ K) ₆ (Al ₆ Si ₃ O ₇₂) ₂₀ ·6 H ₂ O	12.1	9.1
Admixture	Ca(OH) ₂	15	12
Water	-	97	63.5

According to [Verhoef 2016], the amount of containers with sludge and ion exchange resin is 1/3 of the total amount (12,000) of the 1,000 L containers. 4,000 waste containers are thus presumed to contain sludge and ion exchange resin conditioned at the nuclear power plant. As is described in [Verhoef 2016], in the past 5 years only waste containers containing processed waste with an activity higher than 10 GBq have been delivered to COVRA. In the framework of this study it is therefore assumed that 4,000 waste containers contain bead-based spent ion exchangers. Furthermore, based on the information in [Verhoef 2016], it is assumed that the waste containers have the maximum ⁶⁰Co and ¹³⁷Cs activity upon collection by COVRA. The 1,000 L concrete containers with magnetite as aggregates are presumed to be used considering this high activity.

3.1.3. Depleted Uranium

The largest waste family in volume is depleted uranium (DU) [Verhoef 2016].

DU originating from the URENCO uranium enrichment plant is stored at COVRA in DV-80 containers in the form of uranium oxide (U₃O₈) and is, after its conditioning with cement and re-packing in 7,700 KONRAD type II containers (made of low carbon steel with at least 3 mm thickness), foreseen for geological disposal [Verhoef 2014]. Figure 6 shows a schematic drawing of the KONRAD containers with additional data.

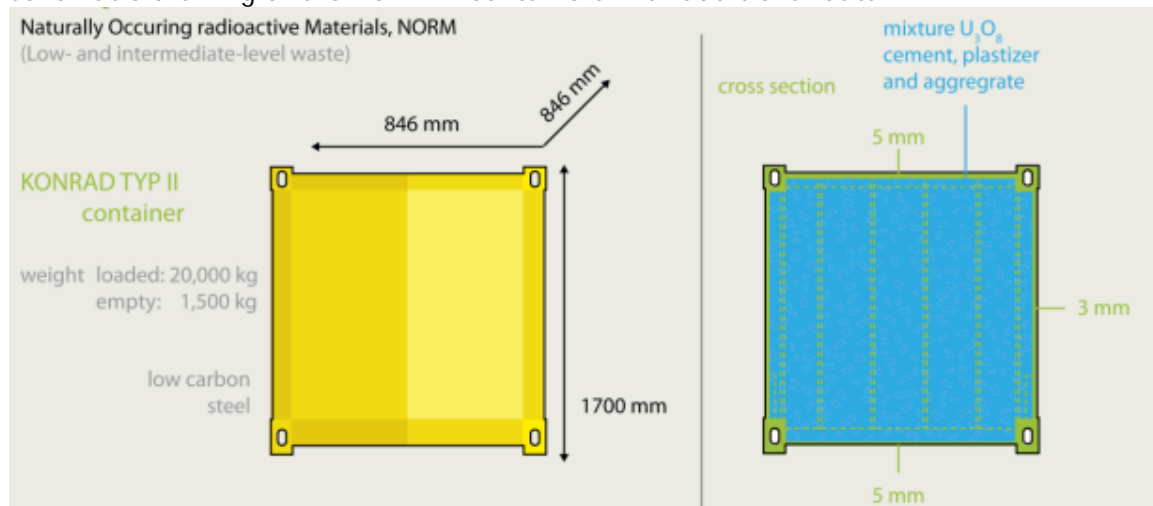


Figure 6: Schematic drawing of KONRAD type II container, dimensions in mm [Verhoef 2016]

In [Verhoef 2014b], it is proposed to employ Portland cement with limestone aggregates because sufficient calcium would then be available to react with traces of UF₆ and precipitate as stable minerals [Kienzler 2013].

Table 16 shows the concrete composition for the conditioning of U_3O_8 . The actual conditioning process of U_3O_8 is explained in [Verhoef 2014b].

Table 16: Concrete composition for the disposal of U_3O_8 [Verhoef 2016, Verhoef 2014b]

Component	Type	
Cement	CEM I / 42.5 N SR O LA (LH)	365 kg/m ³
Water		175 kg/m ³
Superplasticiser	TM OFT-II B84/39 CON. 35 % (BT-SPL)	3.3 kg/m ³
Fine aggregate	U_3O_8 : 0-4 mm	2664 kg/m ³
Coarse aggregate	Limestone: 2-8 mm	911 kg/m ³

N: Usual initial strength, HS High Sulphate resistance, LA Low Alkali content, (LH Low Hydration Heat)

3.2. Radionuclide inventory

In [Verhoef 2016], the radionuclide inventory at the start time of disposal in the year 2130 is calculated and a standardised inventory of radionuclides per waste container has been derived for each waste family. Please refer to [Verhoef 2016] for further information. In Appendix 4 of this report, the radionuclide inventories for the particular waste families are listed.

4. Evolution of the Repository Near-Field

The repository near-field evolution depends on a number of complex, inter-related processes including the nature of the host rock and the infiltrating groundwater. In general, the near-field will be (after closure of the repository) influenced by processes such as heat generation of the emplaced (high-level) waste, radiation of engineered barrier materials (particularly of waste containers), resaturation and degradation of engineered barriers [Randall 2013].

The OPERA waste disposal concept regards the use of cementitious materials to establish a high pH pore water system. Furthermore, cementitious materials also provide a substrate for sorption and thus retardation of the radionuclide transport once the latter are released from the waste containers. Section 4.1 discusses the concept of the evolution of the cement degradation and pore water composition. Section 4.2 deals with the evolution of the redox conditions in the repository near-field.

4.1. Evolution of pH and pore water composition

Cementitious materials are the main constituents of the near-field in the planned repository. These large amounts of hydrated cement will determine the chemical and physical properties of the repository in the near-field for long periods of time [Berner 1992]. Cement degradation will take place due to the disequilibrium arising between the cementitious materials and groundwater infiltrating into the near-field [Wieland 2001]. The cementitious materials cement will leach in order to adjust the chemical composition of the groundwater to a level in equilibrium with the cement matrix.

[Kursten 2015] calculated the pH evolution at the HLW overpack/cement interface. This system consists of the following elements (from the outside to the inside): Gallery lining (CEM II), Backfill/foam concrete (CEM I), Supercontainer buffer (CEM I). The results for the long-term evolution are shown in Figure 7.

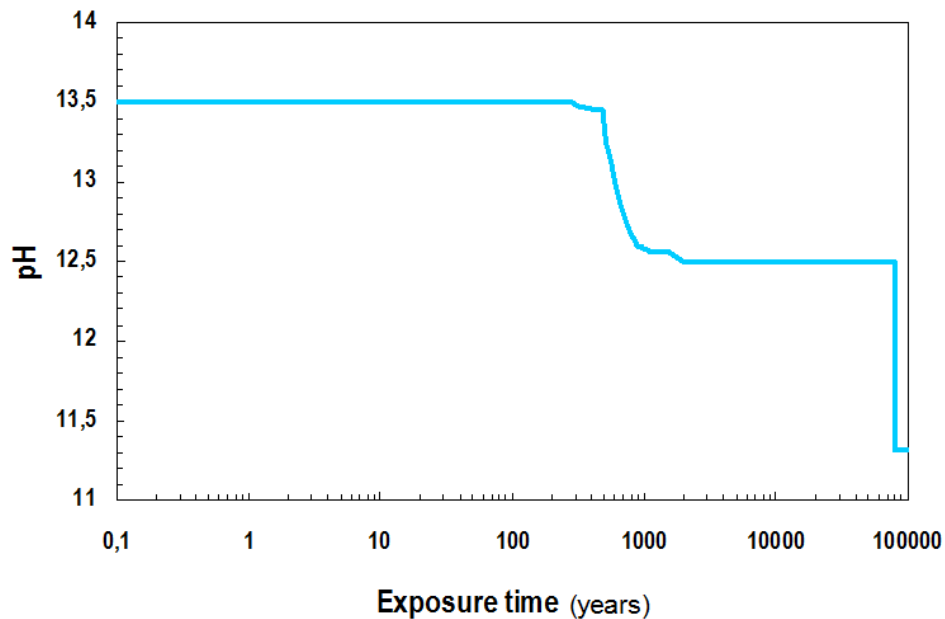


Figure 7: Long-term pH evolution at the cement/HLW overpack interface [Kursten 2015]

In about five years after closure, the system evolution will be characterised by resaturation with inflowing groundwater, consumption of trapped oxygen by aerobic metal corrosion and conditioning of cement pore water to high pH [Kursten 2015]. It can be expected that the super containers maintain their mechanical integrity for many hundreds of years. Gas generation due to the corrosion/degradation of wastes and their containers will take place [Randall 2013]. The cement pore water composition is dominated by dissolution of alkali hydroxides (NaOH and KOH) [Wieland 2002]. According to [Kursten 2015], conditions with pH ~ 13.5 are prevalent for about 1,000 years (Figure 7).

From then on, when the cementitious materials deplete in Na- and K-hydroxides, portlandite ($\text{Ca}(\text{OH})_2$) dissolution will determine the pH at a value of 12.5 [Kursten 2015] (Figure 7). The pH of 12.5 is predicted to persist for at least 80,000 years after which it will drop to a value of 11.3 [Kursten 2015].

The subsequent phase is comparatively more complex and is controlled by the incongruent dissolution of CSH phases, where calcium is preferentially leached from the solid phase until the Ca:Si relation in the CSH is the same as that in solution, after which congruent dissolution of CSH takes places. When CSH is depleted, the pore water composition is controlled by secondary minerals such as calcite [Randall 2013]. When the CSH phases are completely dissolved, the pH of the cement pore fluid will continue to decrease to a value buffered by the host ground water [Krupa 1998].

According to [Kursten 2015], their pH evolution calculations are very conservative because an infinite dilution boundary condition was directly applied at the concrete/clay interface and transport limitations in the Boom Clay are neglected. Furthermore, an unrealistically low rate constant was applied to set calcite as an inert mineral phase. For further details refer to [Kursten 2015].

In the framework of this study, a somewhat similar pH evolution based on these calculations is also expected for the LILW section near-field, whereas furthermore a temperature of 25 °C is assumed.

Regarding the LILW, CEM III cement is employed for the conditioning of the compacted waste, the processed liquid molybdenum waste and the ion exchange resins. As stated above, CEM I is employed as backfill. Thus, in the near field as well as at the backfill/container interface, a likewise pH evolution as shown in Figure 7 can be expected. Regarding the pH values to be expected within the mentioned conditioned wastes, the CEM

III composition is however relevant. [Deissmann 2005] compiled experimental results regarding investigations of cement pore water compositions, i.e. ordinary portland cement (OPC) as well as blast furnace slag (CEM III; whereas CEM III/B contains up to 34 % OPC and CEM III/A contains up to 65 % OPC). According to this compilation, pH values of pore waters extracted from hardened blast furnace cement (CEM III) aged up to 5 a were in the range of 12.8 - 13.7. Thus, the initial pH values within the compacted waste can assumed to be also in the range of the backfill material or slightly lower, respectively.

DU is conditioned with CEM I cement. Thus, pH conditions with initial pH values about 13.5 (comparable to those shown in Figure 7 can be expected in this waste. Exemplary cement pore water compositions in different planned waste repositories can be found in Appendix 1.

To conclude, the evolution of the repository system will be characterised (on the timescale of thousands of years) by the equilibration of the cementitious pore water to high pH and reducing conditions, the continuing anaerobic corrosion of the waste containers (leading to gas release and penetration of their structure), physical and mineralogical changes of the cementitious backfill and the continuing radioactive decay (including ingrowth) of the initial inventory.

4.2. Evolution of redox conditions

The presence or absence of oxygen plays a paramount role for the redox evolution in the repository. [Kursten 2015] carried out preliminary geochemical simulations to understand the long-term evolution of the environmental conditions surrounding the carbon steel overpack used for the HLW. These investigations have shown that the concrete materials will resaturate almost completely (95-98 %) after one to five years.

It can be expected that oxygen will be consumed relatively quickly and that anaerobic corrosion of metal (used, e.g. for waste drums) will begin relatively soon.

The environmental conditions in the LILW section will thus gradually evolve over time from oxic and relatively dry to anoxic and fully saturated. The oxygen initially trapped in the free spaces of the disposal galleries during its construction is assumed to be consumed due to chemical reactions and corrosion processes.

4.2.1. Aerobic phase

It can be assumed that the repository initially contains large volumes of air trapped in the pores of the cementitious materials, the excavation damaged zone and the LILW itself and thus oxidising redox conditions will prevail. The repository near-field is expected to be initially unsaturated and the waste is exposed to the high pH cementitious materials. The degradation of waste and corrosion of metals commences from the moment the waste is placed in contact with the cementitious near-field.

After closure of the repository, due to Boom Clay groundwater seeping into the backfill materials and into the vicinity of the waste materials, the air eventually present will be displaced and oxygen will be dissolved. A complete saturation will take place. The duration of this aerobic phase depends on the amount of oxygen present and the oxidation reaction rates [Neill 1994].

In the aerobic phase, the oxygen eventually present may also react with steel (canisters), other metals and reduced mineral phases (e.g. pyrite) in the excavation damaged zone (EDZ) [Wersin 2003]. The rates of oxygen consumption and metal corrosion are strongly dependent on the water saturation which itself depends on the temperature and the hydraulic conductivity of the Boom Clay and the cementitious materials [Wersin 2003]. Furthermore, it can be assumed that in the case that significant microbial activity occurs, degradation of organic compounds will also enhance the consumption of oxygen [Wersin 2003].

4.2.2. Anaerobic phase

Subsequent to the aerobic phase, the repository conditions will evolve to anaerobic conditions when oxygen is consumed due to corrosion or eventually microbiological processes. Note that microbial activity is highly unlikely, since the geochemical conditions are unfavourable due to high pH and small poresizes [Kursten 2015]. The redox conditions will be influenced by various reactions that occur between the dissolved and solid redox-active materials in the alkaline environment [Wersin 2003]. Due to the large amounts of iron (steel, corrosion products, waste) and the ease of electron transfer between Fe(II) and Fe(III) compared to other redox couples, it can be assumed that iron phases control redox conditions in the repository near-field [Jobe 1997, King 2000]. The corrosion of steel and other reduced metals will furthermore generate high hydrogen pressures and steel corrosion will generate magnetite [Wersin 2003] (see section 5.10.1). The duration of anaerobic conditions is expected to persist indefinitely [Kursten 2015].

[Berner 2003] estimated the redox conditions in reference cement pore water in Opalinus Clay environments (Switzerland). Assuming that redox conditions are principally defined through the $\text{Fe}^{3+}/\text{Fe}^{2+}$ couple and Magnetite is the major corrosion product which is in equilibrium with the cement pore water, [Berner 2003] estimated the possible redox potentials. A sensitivity analyses showed that different combinations of iron bearing solids (including sulphides) might produce an E_H range from -750 to -230 mV at pH ~12.55. Regarding the redox potential of the initial stage pore water (pH ~13.4), [Berner 2003] calculated that this water was much more reducing. It was found that the stability of Fe(III)(OH)_4^- produces an Eh of -430 mV pH 13.44.

5. LILW degradation processes and products

The cementitious backfill employed in the LILW section of the potential repository will result in the generation and persistence of high pH values (see section 4). These alkaline conditions are favourable for reducing the mobility of some radionuclides. On the other hand, these conditions could also promote the chemical degradation of cellulosic materials which are present in significant amounts in the LILW section of the potential repository. Due to the alkaline chemical degradation of cellulosic materials, a range of soluble products may be generated which are able to complex radionuclides and potentially enhance their mobility.

In the following sections, different aspects of cellulose degradation are discussed. Section 5.1 gives an introduction into cellulose chemistry. In sections 5.2, degradation processes and products will be discussed. Section 5.3 deals with the cellulose degradation kinetics. Section 5.4 deals degradation processes of isosaccharinic acid, a major cellulose degradation product.

5.1. Introduction to cellulose chemistry

The cellulosic waste to be deposited in the planned repository is assumed to consist of paper, cloth and tissue [Verhoef 2016], all of which contain mostly cellulose and minor amounts of hemicellulose [Cohen 2006].

Cellulose ($\text{C}_6\text{H}_{10}\text{O}_5$)_n is a linear condensation polymer (polysaccharide) consisting of glucose units (i.e. D-anhydroglucopyranose) linked by β -1,4-glycosidic bonds (see Figure 8) [Askarieh 2000]. Each glucose unit is rotated through approximately 180° relative to its neighbors [Astbury 1944]. Figure 8 shows the structure of cellulose.

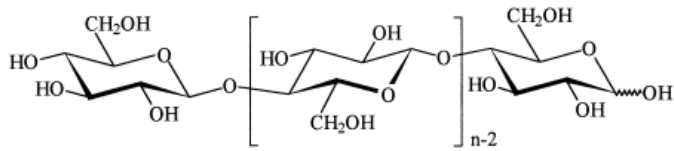


Figure 8: The structure of cellulose [Humphreys 2010]

A popular view is that cellulose can exist in different solid state forms although it is an unbranched polysaccharide. According to the widely accepted “fringed fibril model” of cellulose fibre morphology, proposed by Hearle in 1958, the chains of native cellulose have regions of low order (amorphous) and regions of high order (crystalline), i.e. it is a semi-crystalline material. Linear chains of cellulose run through several crystalline regions as well as amorphous regions (Figure 9) [Shaw 2013]. Material in amorphous regions may not be able to participate in chemical reactions if blocked by a preceding crystalline region.

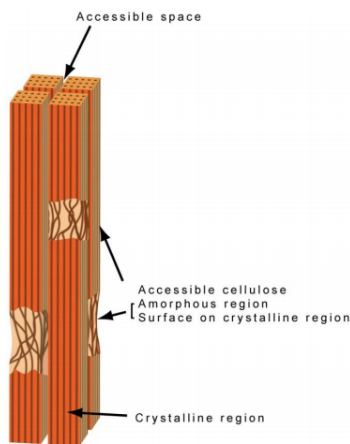


Figure 9: Cellulose microfibril [Shaw 2013]

The term hemicellulose describes the polysaccharide components of plant cell walls other than cellulose. Hemicelluloses are in contrast to cellulose branched polymers which contain a range of different monosaccharides. It consists of shorter polysaccharide chains (500 - 3,000 sugar units) than cellulose (7,000 - 150,000 glucose molecules) [Randall 2013]. According to [Loon 1998], hemicelluloses are primarily modified xylans, galactoglucomannans, glucomannans and arabinogalactans. All of these polysaccharides are made up from a number of sugar residues, whereas the principal ones are: D-xylose, D-mannose, D-glucose, D-galactose, L-arabinose and 4-O-methyl-D-glucuronic acid.

Hardwood hemicelluloses contain 4-O-methylglucuronoxylan (xylan) as the most important hemicellulose (25 - 30 %). Xylan is made up of up to 150 - 200 (1,4)- β -Dxylopyranose units whereas on the average every tenth xylose residue is substituted at C2 by a 4-O-methylglucuronic acid residue. The xylose content in xylan is about 80 % and the 4-O-methylglucuronic acid content is 20 % [Loon 1998]. Figure 10 shows the chemical structure of xylan. In hardwoods, only minor amounts of glucomannan (β -/1,4)-linked D-mannopyranose and D-glucopyranose sub-units) are present [Randall 2013].

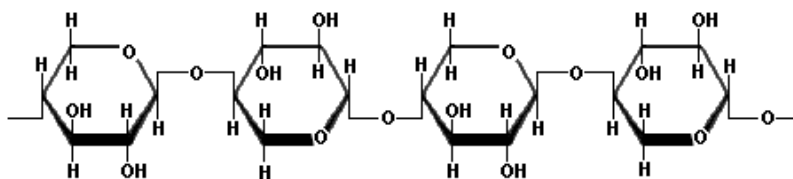


Figure 10: Chemical structure of xylan [Randall 2013]

Softwood hemicelluloses (e.g. pines) contain glucomannan as the main hemicellulose. These are essentially linear polysaccharides composed of β -(1,4)-linked D-mannose and β -(1,4)-linked D-glucose residues, to which are attached various amounts of α -linked D-galactose end groups. Furthermore, significant amounts of arabino-(4-O-methylglucurono)-xylan are present (7-15 %) [Loon 1998].

In contrast to cellulose which is semi-crystalline, strong and resistant to hydrolysis, hemicelluloses with their random amorphous structure with little strength are soluble in alkaline water. Aqueous KOH selectively extracts xylan from the wood. Glucomannan is not released but, however, is soluble in aqueous NaOH. Furthermore, xylan and glucomannan are expected to be soluble in cement pore water which contains both NaOH and KOH [Randall 2013], [Loon 1998].

Since hemicellulose is present in wood, it can be expected that it also will be present in paper. However, its amount in paper is variable and depends strongly on the type of raw material used for production (hardwoods or softwoods) and from the pulping process employed [Loon 1998].

Paper will be present in the LILW inventory probably from contaminated documentation, disposable tissues (e.g. "Kimwipes") and packaging materials. The pulping process removes most of the hemicellulose structures from solution, resulting in a high quantity of pure cellulose (hemicellulose content of $< 10\%$) in the final tissue paper product. According to [Loon 1998], it is difficult to quantify the hemicellulose content, but a value of several percent up to 10 % seems to be a reasonable estimation. The tissues present in the LILW are assumed to be comprised mainly of cellulose itself [Randall 2013]. Organic cotton is assumed to be present in the LILW inventory from clothing and other packaging materials. Cotton wool is made up almost entirely of pure cellulose [Cohen 2006].

5.2. Cellulose degradation processes

A considerable volume of work was already undertaken by various researchers to determine both the processes and rates of degradation of celluloses under cementitious repository conditions. Research was focused on the alkaline decomposition of cellulose, its microbial and also its radiolytic decomposition. In the following sections, these processes will be described.

5.2.1. Chemical degradation of cellulose

Three reaction pathways have been identified which lead to the alkaline degradation of cellulose. These are described as the peeling, stopping and mid-chain scission reactions [Humphreys 2010].

Under alkaline, anaerobic conditions and temperatures $< 170\text{ }^{\circ}\text{C}$ (a temperature of $25\text{ }^{\circ}\text{C}$ is assumed in the LILW part of the repository (see section 4.1)), the predominant mechanism of cellulose degradation was found to be the peeling reaction (Figure 11). This reaction takes place at the reducing end group of the chain and ruptures the 1,4-glycosidic linkage. Thus, the glucose units are progressively eliminated from the reducing end of the chain. As a result, and when no other reactions occur, an isolated chain of cellulose would be expected to degrade completely under alkaline, anaerobic conditions and $< 170\text{ }^{\circ}\text{C}$ [Nevell 1985]. However, this does not happen due to competing reactions taking place at the reducing end-groups, forming end-groups that resist alkaline attack [Machell 1957, Johansson 1978]. The formation of one final degradation product named isosaccharinic acid (ISA) is due to the migration of the carbonyl group of the reducing end anhydroglucose through successive enediols to C3 followed by elimination of the C4-alkoxy group to yield 4-deoxy-2,3-hexodilose. The latter compound is a key intermediate and by a benzilic acid type rearrangement gives ISA isomers [Humphreys 2010].

Reactions that form alkali-stable end-groups (e.g. meta-saccharinic (3-deoxyhexonic acid)) are known as 'stopping' reactions [Askarieh 2000] (Figure 11). Here, a hydroxyl group is eliminated with the formation of metasaccharinic acid which blocks the peeling of the chain. The degradation is slowed down or terminated by the inaccessibility of the crystalline regions of the cellulose ([Knill 2003], [Glaus 2008b]). According to [Askarieh 2000], it is not clear whether cellulose chains that have undergone the stopping reaction will be resistant to further alkaline degradation over the timescales of more than a million years.

The mid-chain scission (Figure 12) describes the scission of the chemically stopped cellulose and does not become a major reaction pathway until a temperature of 170 °C has been reached [Nevell 1985]. However, according to [Askarieh 2000], it is possible that the reaction may take place at lower temperatures at a slow rate or may be initiated by radiolytic processes. The mid-chain scission is understood as the hydroxide-catalysed cleavage of glycosidic links at random sites along the cellulose chain which generates new reducing end groups that may participate in peeling. The mid-chain scission is slow but of long-term relevance (>1,000 a) [Askarieh 2000].

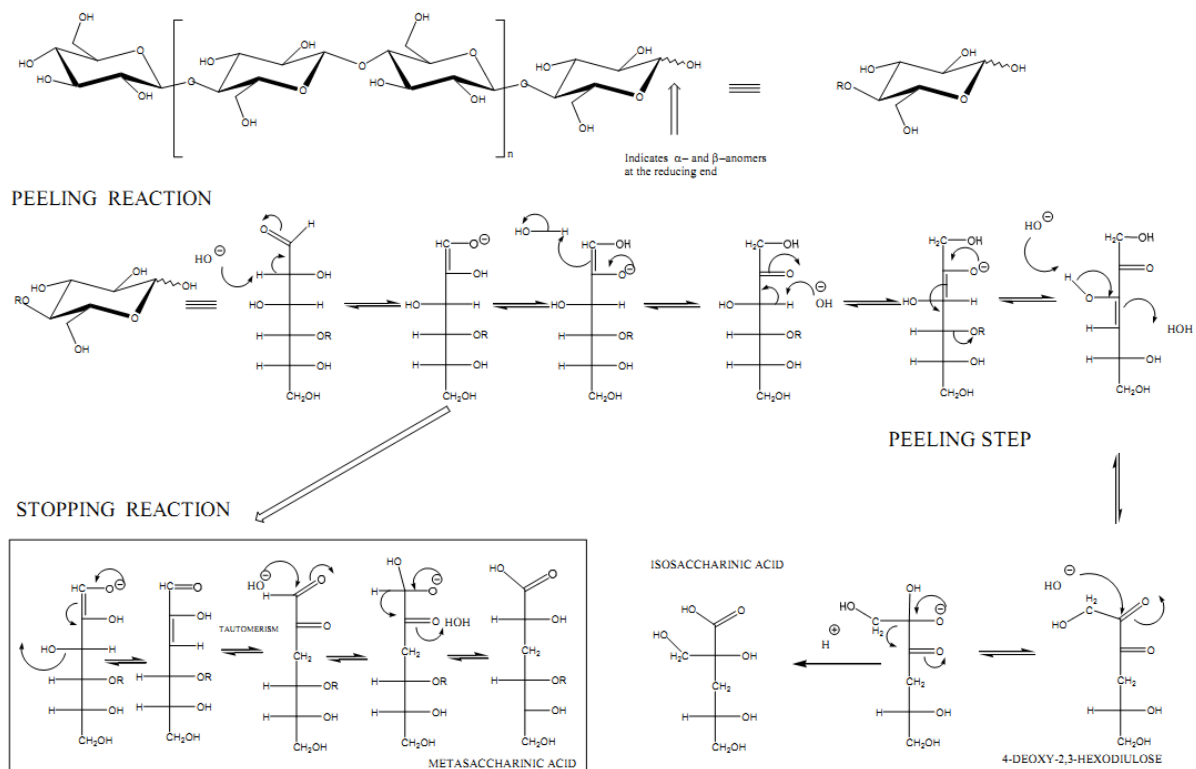


Figure 11: Alkaline cellulose degradation pathways which lead to the formation of ISA and meta-ISA [Humphreys 2010] (see text)

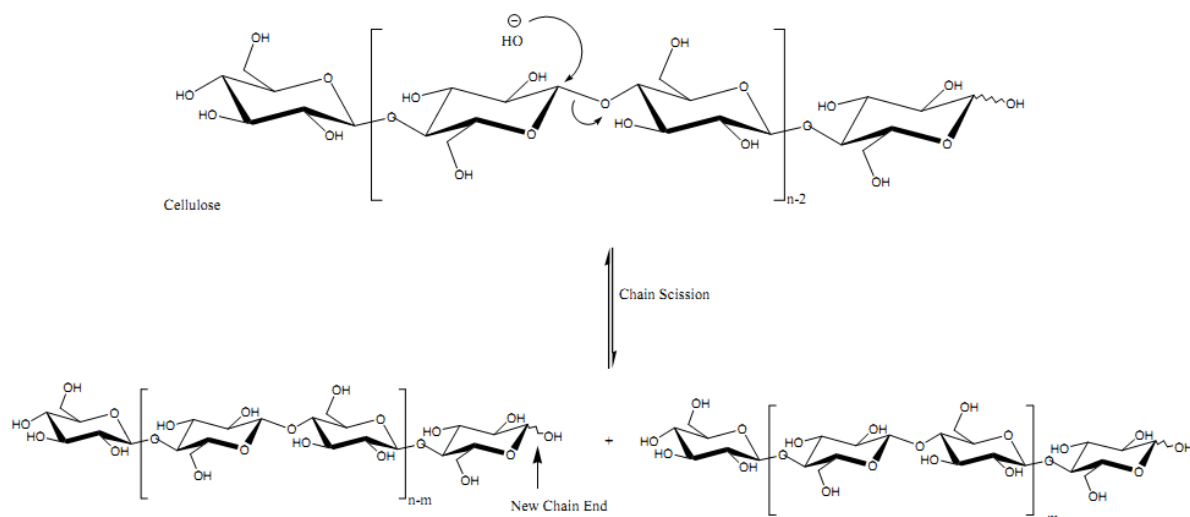


Figure 12: Mid-chain scission of cellulose catalysed under alkaline conditions [Humphreys 2010] (see text)

ISA forms two isomers: α -isosaccharinic acid (3-deoxy-2-C-(hydroxymethyl)-erythro-pentanoic acid) and β -isosaccharinic acid (3-deoxy-2-C (hydroxymethyl)-threopentonic acid) [Randall 2013] (see Figure 13).

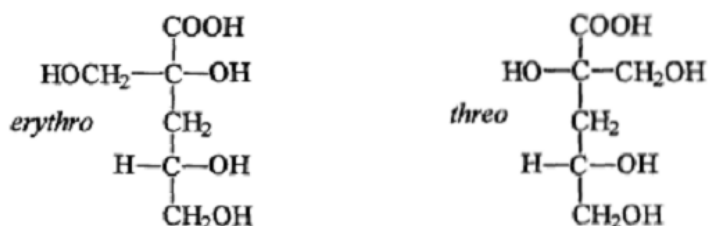


Figure 13: The two ISA isomers [Hurdus 2000]

Under acidic conditions, both isomers of ISA form lactones. The structures are shown in Figure 14.

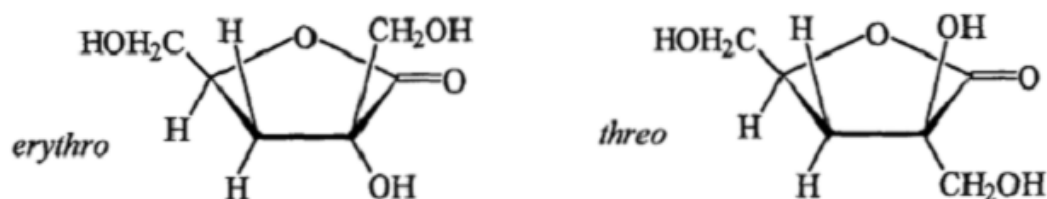


Figure 14: The two isomers of the ISA lactone form [Hurdus 2000]

Under alkaline conditions, ISA is present mainly in the open-chain form as deprotonated anion (Figure 15).

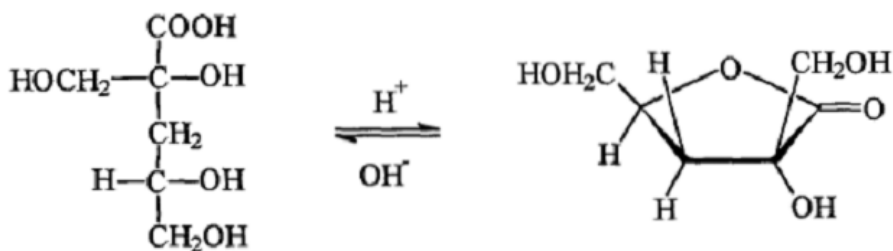


Figure 15: The equilibrium between the ISA acid and lactone forms [Hurdus 2000]

All the mentioned degradation reactions generally result in a decrease in the cellulose molecular chain length and thus appreciable amounts of aliphatic acids including C1-C4 monocarboxylic acids, C4-C6 dicarboxylic acids and various polyhydroxy carboxylic acids and alcohols [Randall 2013]. Since research on cellulose degradation products generated due to alkaline degradation is relatively extensive, the following section is dedicated to this subject.

5.2.1.1. Cellulose degradation products

Cellulosic materials chemically degrade under alkaline conditions and form a range of cellulose degradation products (CDPs) [Humphreys 2010]. Most research focused on chemical degradation of cellulose, and thus the degradation products arising due to chemical degradation are discussed here. The literature concerning radiolytic or microbial degradation products is limited and was already discussed in the sections 5.3.1 and 5.3.2.

[Glaus 1999] investigated the potential role of cellulose degradation products as metal-binding chelates in a nuclear waste repository. Different cellulosic materials (pure cellulose (20 μm spheres)), cotton, Tela tissues and recycling paper) were degraded under the chemical conditions of cement pore water (pH 13.3). [Glaus 1999] used an artificial cement pore water which was a NaOH/KOH solution saturated with respect to $\text{Ca}(\text{OH})_2$ containing 114 mM of Na, 180 mM of K and 2.3 mM of Ca with and a pH of 13.3. The solution was prepared in a glove box in N_2 atmosphere (O_2 , $\text{CO}_2 < 5$ ppm). For the degradation experiments, solid $\text{Ca}(\text{OH})_2$ was kept in the solution to maintain portlandite saturation during the degradation process at a temperature of 25°C. The duration of the experiments was up to 239 days.

The main degradation products of (pure) cellulose were identified to be the diastomeric α -isosaccharinic acid (α -ISA) and β -isosaccharinic acid (β -ISA), which accounted for ~ 80% of the total dissolved organic carbon (DOC) formed (Table 17). Minor components identified by [Glaus 1999] were short chain aliphatic acids such as formic acid, acetic acid, lactic acid and threonic acid comprising less than 10% of the total dissolved organic carbon. The degradation of the other cellulosic materials (cotton, tissues and recycling paper) resulted in lower amounts of α -ISA and β -ISA and in higher yields of small organic acids (acetic acid) and of unidentified acidic compounds.

Table 17: Degradation products of pure Cellulose [Glaus 1999]. The reaction times (days) are given in parentheses

Analytes (acids)	A1 (7)	A3 (40)	A4 (62)	A5 (119)	A6 (181)	A7 (239)
Formic	0.74	3.87	5.13	8.13	10.23	11.87
Acetic	1.11	4.21	4.99	8.19	7.58	9.40
Glycolic	0.23	1.13	1.56	2.41	3.26	3.87
Pyruvic	0.08	0.24	0.27	0.24	0.33	0.31
Glyceric	0.19	1.77	1.99	2.05	2.75	2.84
Lactic	0.50	1.89	2.37	3.65	4.27	4.81
Propionic	n.d. ^b	n.d.	n.d.	n.d.	0.33	0.37
Succinic	<0.05	0.07	0.08	0.12	0.11	0.13
Butyric	n.d.	0.51	n.d.	0.87	1.00	1.21
Threonic	0.49	1.40	1.56	1.61	1.95	2.65
Adipic	n.d.	0.15	0.19	0.30	0.38	0.60
Isosaccharinic ^c	11.6	44.9	59.7	84.5	102	117
DOC	123	317	471	685	784	910

^bn.d.: not detected

^csum of α -ISA and β -ISA (including lactones)

Another study carried out by [Randall 2013] also investigated the degradation of cellulosic material (e.g. paper (Kimwipe tissues), wood shavings and cotton) under alkaline anaerobic conditions. A series of batch experiments were carried out to create a range of cellulosic degradation products likely to form under disposal conditions. The following conditions were applied [Randall 2013]:

- Two aqueous solutions: saturated $\text{Ca}(\text{OH})_2$ and low pH CaCl_2 solutions
- Three temperatures: 25 °C, 50 °C and 80 °C
- Two atmospheric conditions: anaerobic and aerobic

The particular samples were analysed after 1, 3, 6 and 12-month time intervals. The leachates of 36 of these degradation experiments were analysed by a variety of chromatographic and spectroscopic methods and the following key degradation products were identified in the leachate [Randall 2013]:

- ISA was identified in almost all the $\text{Ca}(\text{OH})_2$ samples and was, in terms of concentration, the dominant degradation product. The concentration of ISA was found to be linearly related to the total organic carbon (TOC) and the concentrations as high as 16,900 ppm, although more typically less than 3,000 ppm (~20 mM). Furthermore, the ISA concentrations were generally highest in the Kimwipe and wood samples. Some evidence was found that ISA degrades over the 12-month incubation period. However, this was more marked in the aerobic samples, whereas some of the anaerobic samples indicate an increase in ISA over 12 months [Randall 2013].
- A significant finding of [Randall 2013] was the presence of potentially large concentrations of X-ISA (presumably derived from hemicellulose degradation). X-ISA is structurally similar to ISA and therefore can be expected to exhibit comparable complexing behavior.
- Other organic acids that have been positively identified were lactic, acetic and glycolic acid and additional small concentrations of other low molecular weight organic acids and alcohols.

The cellulose degradation products identified after 1 month of degradation included pyruvate, lactic acid, glycolic acid, 2-hydroxybutyric acid, γ -hydroxybutyric acid, glycerol, glycine, succinic acid, 2,3-dihydroxy-2-methylpropanoate, glyceric acid, 2,3-dihydroxy-

butanoic acid, 3,4-dihydroxy-butanoate, butane-1,2,4-triol, α -hydroxyglutaric acid, 2,4-dihydroxy-2-hydroxymethyl butanoic acid, 2,4,5-trihydroxypentanoic acid, lyxose, 3-hydroxy-3,5-bis(hydroxymethyl)dihydrofuran-2(3H)-one, isosaccharinic acid, dehydroabiatic acid and disaccharide (maltotritol or raffinose) [Randall 2013].

After 12 months of degradation, the following cellulose degradation products were identified: lactic acid, glycolic acid, malic acid, 2-hydroxybutyric acid, 3-hydroxypropionic acid, xylo-isosaccharinic acid, isosaccharinic acid, erthyo-pentonic acid, propanoic acid, octadecanoic acid, hexadecanoic acid, dehydroabiatic acid, 3-deoxypentonic acid and di-n-actyl phthalate [Randall 2013].

According to [Randall 2013], when the measured TOC in the samples is assumed to be present as ISA, this would equate to ISA concentrations presented in Table 18.

Table 18: Equivalent ISA concentrations [Randall 2013]

	1 month	12 months
Cotton wool	2.2E-3 M	8.3E-3 M
Tissue paper	7.4E-3 M	1.8E-2 M
Wood	9.4E-3 M	5E-3 M

A complete summary of the measured degradation products (and solubility data) can be found in [Randall 2013b].

A detailed list of commonly identified alkaline degradation products of cellulose found in different studies is presented in Table 19.

Table 19: Commonly identified alkaline cellulose degradation products (Aldrich cellulose powder) [Knill 2003, Glaus 1999]. Alkali: C = Ca(OH)₂; K = KOH; N = NaOH; L = Lime water. M = major (> 10 %), S = significant (1 - 10 %), T = trace (< 1 %)

Alkaline degradation product (Analytes)	Alkali	Temperature (°C)	Concentration
Methanoic acid (CH ₂ O ₂)	N/K/C	23	S
Acetic acid (C ₂ H ₄ O ₂)	N/K/C	23	S
Hydroxyethanoic acid (C ₂ H ₄ O ₃)	N/K/C	23	S
2-Hydroxy-propanoic acid (2-hydroxy-proionic acid (DL-lactic acid) (3-deoxy-DL-glyceric acid) C ₃ H ₆ O ₃)	N/K/C	23	S
2,3-Dihydroxypropanoic acid (DL-glyceric acid) (3-hydroxy-DL-lactic acid) C ₃ H ₆ O ₄	N/K/C	19-25	S
Butanoic acid (butyric acid) (2,3,4-trideoxytetronic acid) C ₄ H ₈ O ₂	N/K/C	25	S
2S,3R,4-Trihydroxybutanoic acid (D-threo-tetronic acid) (D-threonic acid) C ₄ H ₈ O ₅	N/K/C	25	S
Hexanedioic acid (adipic acid) C ₆ H ₁₀ O ₄	N/K/C	25	T
2-Hydroxymethyl-2,4,5-trihydroxypentanoic acid-1,4-lactone (3-deoxy-2-C-(hydroxymethyl)-D-erythro- and D-threo-pentono-1,4-lactone) (D-glucoisosaccharino-1,4-lactone) C ₆ H ₁₀ H ₅	N/K/C	25	M
2S,4R,5-Trihydroxy-2S-hydroxymethylpentanoic acid (3-deoxy-2-C-(hydroxymethyl)-D-erythro-pentonic acid) (α -D-glucoisosaccharinic acid) C ₆ H ₁₂ O ₆	N/K/C	25	M
2R,4R,5-Trihydroxy-2S-hydroxymethylpentanoic acid (3-deoxy-2-C-(hydroxymethyl)-D-threo-pentonic acid (β -D-glucoisosaccharinic acid) C ₆ H ₁₂ O ₆	N/K/C	25	M

According to Pavasars 1999 and [Glaus 1999], the glucoisosaccharinic acids (α - and β -forms) and their lactones are undoubtedly the major observed alkaline cellulose degradation products. In the experiments of [Pavasars 1999], glucoisosaccharinic acid comprised ~ 70 and 85 % of cellulose degradation products at cellulose to water ratios of 5 and 100 g/l. The experiments of [Glaus 1999] showed that isosaccharinic acid (α - and β -form) also make up between 70 and 85 % of the degradation products. Note that the nature and concentrations of the different products are influenced by temperature and the cellulose type [Glaus 1999]. In general, the concentration of cellulose degradation products in the (cementitious) pore water depends on the cellulose loading in the waste, the extent of degradation of cellulose, the cement porosity, the sorption behavior of ISA on cement, the chemical stability of ISA under the existing alkaline repository conditions and the water flow through the repository [Loon 1998].

It is unlikely that ISA will be generated during the brief time period when oxidising conditions might exist in the LILW waste forms. Initially, air will be present in the voids between the particular containers, so there could be potential for ISA oxidation in cement leachate seeping from containers [Small 2013].

[Glaus 2008b] carried out lab experiments regarding the chemical degradation of cellulose. Four different cellulosic materials (Aldrich purified cellulose, cellulose tissues, cotton and recycling paper) were contacted in closed containers with $\text{Ca}(\text{OH})_2$ and an artificial cement pore water simulating the chemical conditions of the first stage of cement degradation. The composition of this water was: 114 mmol/dm³ Na, 180 mmol/dm³ K, ~ 2 mmol/dm³ Ca and a pH of 13.3. The temperature was kept constant at 25 °C under an inert-gas atmosphere and exclusion of light. After different reaction times the samples were analysed for pH, alkalinity, DOC, α -ISA, β -ISA and other carbohydrates. Figure 16 shows the development of the sum concentration of α -ISA and β -ISA (denoted as ISA) and DOC for the different cellulosic materials. According to [Glaus 2008b], the close position of the ISA and DOC data confirms that the two stereoisomers of ISA are the main products of the alkaline degradation of cellulose.

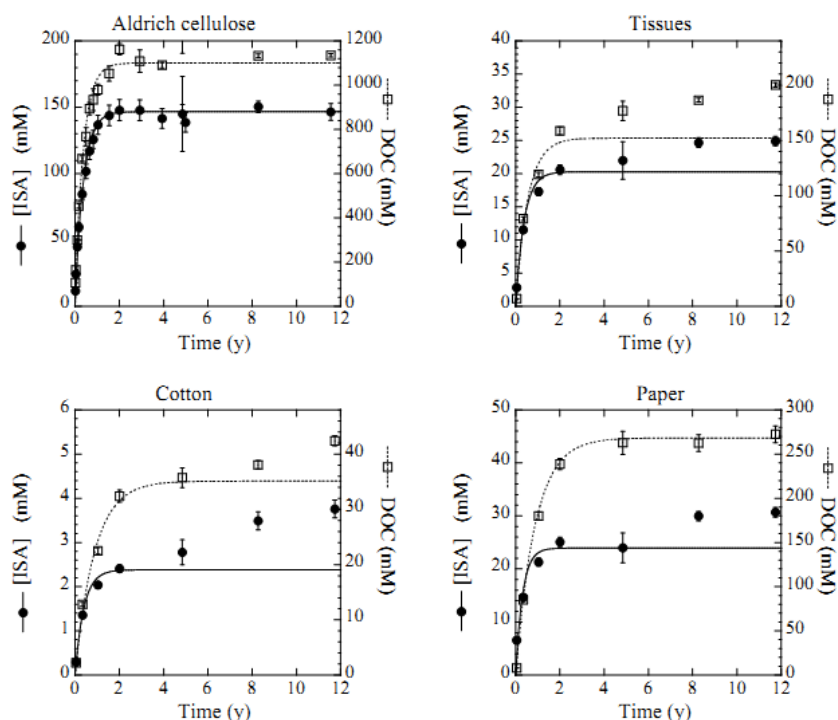


Figure 16: Evolution of ISA and DOC sum concentrations vs. time during the degradation of various cellulose types in cementitious pore water at room temperature. The model (lines) applied to the data represents only the peeling-off process and is based on the reaction rate constants given in [van Loon 1999]

Hemicelluloses will be soluble under the alkaline conditions expected in the repository. The alkaline hydrolysis of hemicellulose components such as glucomannans and galactoglucomannans, which are made up from isomeric aldohexoses, will produce the same degradation products as cellulose, i.e. ISAs with a certain amount of short chain fatty acids [Humphreys 2010].

However, the alkaline hydrolysis of xylans (one of the main components in hemicellulose) has been shown to generate 3-deoxy-2-C-(hydroxymethyl)-tetronic acids (xylosaccharinic acid) as the major degradation product [Alen 1985]. Since hemicelluloses are soluble polysaccharides, their degradation kinetics will not include the physical stopping reactions. Consequently, the peeling process can be expected to lead to complete degradation of hemicelluloses [Humphreys 2010].

Previous studies regarding the rate of alkaline degradation of these substances under repository conditions indicated that celluloses degrade much more slowly than hemicelluloses [Loon 1998].

5.3. Cellulose degradation kinetics

Up to date, there exist conflicting views regarding the question of how much time is needed for cellulose to be degraded in a cementitious nuclear waste repository ([Loon 1998], [Pavasars 1999], [Askarieh 2000], [Knill 2003], [Glaus 2004]). Significant uncertainties exist regarding the cellulose degradation rates. Selected research regarding the cellulose degradation rates is discussed in the subsequent text.

The rates of the peeling, stopping and mid-chain scission reactions determine the extent of the degradation of a specific cellulose [Humphreys 2010]. Consequently, the degradation rates will contribute to the ISA concentrations present in the repository.

The cellulose degradation rate depends, besides the physico-chemical conditions, on the type of cellulose [Askarieh 2000]. According to [Knill 2003], the cellulose supramolecular structure (crystallinity or fibrillary morphology) plays a main role in determining the degradation rate and furthermore the course of the cellulose degradation process. Amorphous cellulose is known to react more readily than crystalline cellulose [Greenfield 1994], because a high supramolecular order of polymer chains generally impedes degradation [Klemm 1998].

At 25 °C, for a fixed degree of polymerization (DP = 1,500, which was found to be a good average value for tissues and paper), degradation proceeds quickly at first, with soluble components and exposed reducing ends being consumed by the peeling reaction [Humphreys 2010]. Then, the degradation rate slows significantly as the number of ends is reduced by stopping reactions [Humphreys 2010]. [Loon 1998] found a (two-phase) kinetic expression to describe the alkaline cellulose degradation at 25 °C:

$$cel\ deg = 1 - \left(\frac{1 - \frac{k_1}{k_t} \cdot (G_r)_0 \cdot (1 - e^{-k_1 t})}{e^{k_{obs} \cdot x_n \cdot t}} \right)$$

where

cel deg is the mole fraction of cellulose degraded,

k_1 is the first order rate constant for the peeling reaction

k_t is the overall first order rate constant for the stopping reaction [h^{-1}]

$k_{obs} \cdot x_n$ is the kinetic constant of alkaline hydrolysis [h^{-1}]

$(G_r)_0$ is the mole fraction of reducing end groups (= 1/DP)

t is the time.

[Loon 1998] used the parameters shown in Table 20. The kinetic parameters k_1/k_t and k_t at 25 °C and $\text{OH}^- = 0.3 \text{ M}$ were taken from measurements the mentioned authors performed in their study. Values for $k_{\text{obs}} \cdot x_n$ were extrapolated from experimentally determined data [Loon 1998]. It was assumed that the pH stays at 13.3. [Loon 1998] stated that this constant high pH reflects a worst case scenario since under this condition the degradation rate will be overestimated and that the calculated amount of ISA produced will therefore reflect an upper limit.

Table 20: Parameters used to calculate the cellulose degradation under the alkaline conditions [Loon 1998]

Parameter	Value
k_1/k_t	25 ± 13
k_t	$(2.6 \pm 0.9) \cdot 10^{-4} / \text{h}$
$k_{\text{obs}} \cdot x_n$	$8.6 \cdot 10^{-10} - 8.6 \cdot 10^{-12} / \text{h}$
Degree of polymerisation (DP)	1500 ± 500
$(G_r)_0$	$(7.5 \pm 2.5) \cdot 10^{-4}$

The described kinetic expression however ignored the rates of the mid-chain scission reactions (alkaline hydrolysis) k_{hydr} ($= 8.6 \times 10^{-10} / \text{h} - 8.6 \times 10^{-12} / \text{h}$ [Loon 1998]). However, k_{hydr} becomes more important when experimental degradation data is extrapolated to cover longer time periods, e.g. 1,000s of years [Humphreys 2010]. In the model from [Loon 1998], 10^5 years would have elapsed before about 60 % cellulose degradation has taken place.

[Pavasars 2003] subjected cellulose powder and softwood sawdust to alkaline degradation under conditions representative of a cementitious environment for periods of 3 and 7 years. It was found that a previously published theoretical model of the degradation kinetics by the same authors gave a good approximation of the experimental data. The major difference to the findings of [Loon 1998] was that they employed values for k_{hydr} ($2 - 3 \times 10^{-6} / \text{h}$ dependent on cellulose loadings). [Pavasars 2003] used the following model to interpret the results of their experimental data:

$$\text{cel deg} = 1 - \left(1 - \left(\frac{k_1}{k_t} (G_r)_0 (1 - e^{-k_t t}) \right) \right) e^{-k_{\text{hydr}} t}$$

When these values for k_{hydr} are used to predict the degree of cellulose degradation for a time period of < 1,000 years, there is now almost complete conversion of the cellulose to ISA.

Differences between the both studies described above were described in a later publication from [Glaus 2004]. [Glaus 2004] carried out further experiments to study the degradation of pure Aldrich cellulose and cotton cellulose at the conditions of an artificial cement pore water (pH 13.3) at elevated temperatures (60 °C and 90 °C) for reaction times between 1 and 2 years. The initial cellulose degradation rates were high but soon reduced. The degradation appeared to stop after approximately one year whereas the degradation rates at elevated temperatures were almost identical for both pure cellulose and cotton cellulose.

[Glaus 2004] concluded that the high initial rates correspond with a high rate for k_{hydr} (equivalent to the number estimated by [Pavasars 2003]) but it could not be explained why degradation slows and then appears to halt. The reaction behaviour of the tested materials could not be explained by the peeling-off process and the slow alkaline hydrolysis at the employed temperatures. It was hypothesised that the alkaline hydrolysis has not been

observed in the experiments, and that cellulose degradation would proceed eventually by another unknown type of reaction.

[Glaus 2004] proposed a three-phase reaction sequence to describe the cellulose degradation:

- 1) The peeling-off of monomeric cellulose units. According to [Glaus 2004], this reaction phase was pronounced in the Aldrich cellulose, whereas almost negligible in the case of cotton.
- 2) Further continuation of cellulose degradation at a slower rate.
- 3) A complete stopping of the degradation, resulting in incomplete cellulose degradation.

In the initial phase, the peeling reaction will be very dependent on the degree of polymerisation (DP) of the celluloses, whereas in the second phase, if chain scission is rate-limiting, then DP will not influence the degradation rate. In the three-phase model, the mid-scission degradation rate reduces to zero as the amount of accessible amorphous material decreases. In order to continue, the transformation of crystalline cellulose to amorphous cellulose would have to take place which would generate new end groups [Glaus 2004]. However, no experimental data exist to support this finding.

Furthermore, it was concluded that with respect to long-term predictions of cellulose degradation at room temperature, the kinetic parameters for alkaline hydrolysis as proposed in the work of [Pavasars 2003] (see above) are too large and that complete cellulose degradation at elevated temperatures occurs within time scales larger than hundreds of years [Glaus 2004]. Besides this, it was stated that the prediction of cellulose degradation proposed by the earlier publication of [Loon 1998] is probably also not on the safe side but that a complete transformation of cellulose to strong complexants within a few years under repository conditions may be also an over-conservative assumption [Glaus 2004].

In a further study by [Glaus 2008b], the results of the alkaline degradation studies at low and high temperature (25 ± 2 °C, 60 °C and 90 °C) have been extended to cover longer times (up to 12 years at room temperature; and up to 800 days for the experiments with elevated temperatures). Four different cellulose materials were contacted with $\text{Ca}(\text{OH})_2$ and artificial cement pore water in inert gas atmosphere under the exclusion of light and at pH 13.3. After certain reaction times, the samples were analysed on their ISA concentrations, pH and other parameters. The gathered data at room temperature however did not fit with the two-phase model proposed by [Loon 1998] (see above). Also, the data at room temperature did not demonstrate a stopping of cellulose degradation and the authors suggested that other undefined mechanisms ('decelerated peeling') by which crystalline or inaccessible reducing end groups of the polysaccharide chain become temporarily susceptible to alkaline attack maintain the cellulose degradation at these longer time frames (Figure 17). The experiments carried out at 90°C and 60°C showed similar results regarding the extent of cellulose degradation. However, it was found that a degradation model comprising the peeling-off reaction and mid-chain scission is not appropriate to describe the reaction course. No indication of the nature of the processes involved could be found by [Glaus 2008b]. Using the results gained from this long-term study it was found that the reaction rate constants proposed by [Pavasars 2003] are much too large. On the other hand, [Glaus 2008b] admitted that their previous work ([Loon 1998]) overestimated the cellulose stability since probably additional processes may take place which ultimately lead to degradation.

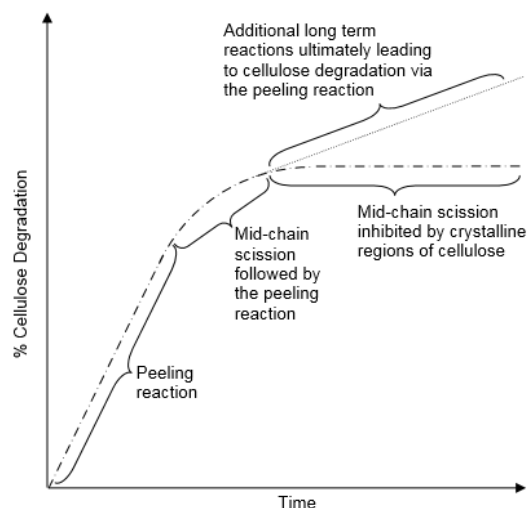


Figure 17: Scheme for potential cellulose degradation profile vs. time [Humphreys 2010]

Quantitative long-term calculations of the concentration of cellulose degradation products (i.e. ISA) in cement pore water can be undertaken by extrapolations from the laboratory scale experiments to geological time spans. However, the chemical processes involved are not sufficiently understood. Combined reactions as the peeling-off and mid-chain scission turned out to be sufficient to describe the chemical degradation of cellulose in a temperature range between room temperature and 200 °C for time scales of several hours. However, experiments carried out in [Glaus 2008b] showed that other reactions also play a role at extended time scales, whereas these reactions are not understood.

[Glaus 2008b] proposes that -in the view of the lack of a process-based understanding for the long-term degradation behaviour of cellulose- that the formation of α -ISA be scaled stoichiometrically to the amount of cellulose present in the wastes in a conservative performance assessment scenario.

5.3.1. Microbial degradation of cellulose

A microbe is understood as a living entity which contains all that it needs in order to perform a life cycle, including feeding, growth and reproduction, in one single cell. Microbes differ significantly in their size: bacteria diameters vary from about 200 nm to 1 mm or more (Pedersen 2000).

The initial conditions for microbial life in a cementitious repository are extreme and only very few if not any microbes are able to tolerate those conditions (high pH, very little water availability). All of the known micro-organisms need free liquid water and most of them depend on a moderate pH from 4 - 10. At reduced water activity, the activity of micro-organisms is impaired and the cells may die [Warthmann 2013]. Even further, water-consuming reactions such as the anaerobic steel corrosion will also keep the water availability on a very low level. The availability of nutrients is also limited in the cementitious environment. Therefore, it can be assumed that no extensive biocenosis will develop for very long time scales. Due to the heterogeneity of the wastes however small micro environments can develop in which good conditions for microbial activity may develop [Warthmann 2013].

According to [Askarieh 2000], micro-organisms cannot be excluded from a large engineering structure such as a nuclear waste repository. Various waste materials collected from diverse sources will carry microbial spores and vegetative cells, and the organic content of the waste provides a potential nutrient for cell growth [Askarieh 2000]. Further, also the groundwater may contain inorganic nutrients and also it may contain various sub-

classes of micro-organisms [Rosevear 1991]. However, how widespread microbial activity will become in the near-field and what the distribution of active microbial populations would be at any instant following repository closure remains uncertain [Askarieh 2000].

In LILW, cellulose is probably the most significant substrate for microbial growth. Cellulosic materials must however initially be broken down to more metabolisable sub-units in order for it to be available to microbes [Askarieh 2000]. This break-down process can occur either biologically or chemically. Under the expected high pH conditions (see section 4.1) the chemical process will dominate. Under neutral pH conditions, it is likely that micro-organisms mediate the cellulose degradation and this process will produce "glucose-type" monomers [Askarieh 2000].

During the post-closure period of a disposal site, anaerobic conditions are expected. Under such conditions, the microbial degradation of cellulose involves a wide variety of microbial groups which ultimately results in the generation of gases such as H₂, CO₂, CH₄ and H₂S and soluble organic compounds such as volatile fatty acids [Greenfield 1990, Askarieh 2000] (see Figure 18). Whether the micro-organisms will be able to survive and their activity in a repository depends on the prevailing chemical and physical conditions [Grant 1997, Grant 2001].

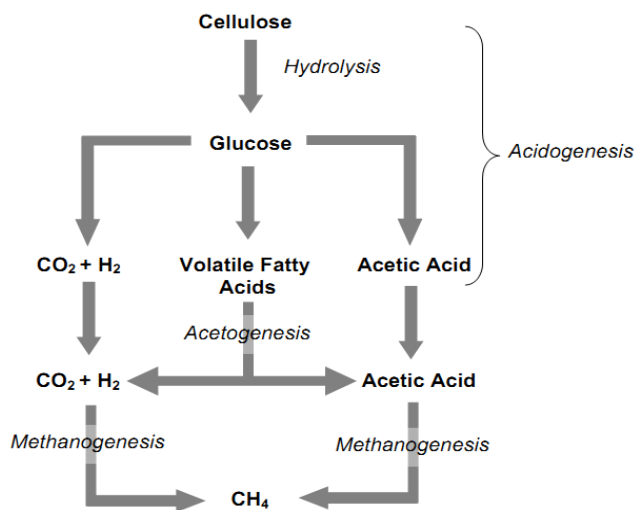


Figure 18: Microbial cellulose degradation under anaerobic conditions [Humphreys 2010]

Within the disposal concept of COVRA, there is a significant time period between waste generation, packaging and final disposal. During this period, the waste containers are placed in interim surface storage for several decades at COVRA followed by monitored retrievable storage which may last several hundred years prior to closure of a geological disposal facility (GDF). Initially, the microbial activity in the waste containers will be constrained by water activity since free water will be limited due to the cementation of the wastes. Note that water activity has a major impact on the microbiology since even the most specialized organisms will be inhibited once the water activity drops below 0.6 [Grant 1997, Brown 1976]. Consequently, it can be assumed that microbial cellulose degradation during storage at COVRA is likely to be limited providing the initial waste is dry and cemented. However, due to the heterogeneity of the cellulose-containing waste, it is not possible to determine niches within the waste where conditions may be favorable for microbial activity. Within these niches, if sufficient water and nutrients are present, microbial degradation of cellulose may proceed. Since some of the degradation products of anaerobic cellulose degradation are organic acids (see section 5.2.1), it cannot be excluded that microbial activity will also generate low pH niches within the waste [Chambers 2004].

The water activity will also continue to control the microbial cellulose degradation after backfilling and closure until the resaturation of the repository with groundwater takes place [Humphreys 2010]. The estimated times for resaturation can be estimated to be about five years (section 4.2). As stated in section 4.1, the equilibration with $\text{Ca}(\text{OH})_2$ is expected to maintain a pH above pH 12 for several thousand years until leaching allows evolved cement phases dominate the system and the pH falls continuously when the dissolution of CSH-phases generate a pH of 10.5 [Grant 1997, Grant 2007, Sonne 1997]. Anaerobic cellulose degrading bacteria able to live at high pH (alkaliphiles) of about 10 have already been described in the literature [Grant 1997, Grant 2007, Sonne 1997]. The bulk pH is however likely to be too high for extensive microbial cellulose degradation to occur for time frames of several thousands of years post closure. Thus, the cellulose degradation will possibly proceed during this period via chemical and radiolytical degradation [Humphreys 2010].

5.3.2. Radiolytic degradation of cellulose

In the planned nuclear waste repository, the waste will be exposed to a radiation field. This can also lead to cellulose degradation by radiolytic processes alone or in combination with chemical and microbial degradation processes. According to [Randall 2013], experimental studies of the combined impact of radiolytic and chemical cellulose degradation are rare.

Available experimental studies indicate that the irradiation of cellulose reduces the proportion of crystalline material [Arthur 1971] and thus increases the susceptibility of cellulose to subsequent alkaline degradation [Spevacek 1991]. One study confirmed this where the combined effects of an alkaline environment and radiation on the crystalline phase of paper tissues were examined [Baston 2002]. In those investigations, high levels of dissolved organic species and complexing agents were found but the nature of these products was not analysed. The experiments confirmed the expected synergy between the radiation and alkaline degradation, since the organic compounds generated by alkaline degradation only were very much lower (~ 10 ppm compared to 600 ppm when irradiated). It was found that at the dose of ~230 kGy about 10% of the cellulose was completely degraded. In the long term it is likely that a higher proportion of crystalline cellulose will be degraded since the accumulated doses will be higher. This will provide furthermore a continued source of sites for alkaline (chemical) degradation processes which would normally not take place due to stopping reactions.

Key difference between alpha and gamma radiation is their penetration power. Regarding gamma rays, the ionization, radical formation and the resulting degradation (i.e. chain-scission) will occur uniformly throughout the polymer. Regarding alpha-radiation, the degradation is expected to be heterogeneous, dependent on the radiation energy and likely to be limited to a surface layer of about 30 μm thickness [Humphreys 2010]. Besides alpha and gamma-radiation, also beta radiation will exist in the disposal environment. The effect of this radiation is expected to have an intermediate impact between that of alpha and gamma radiation.

The important issue regarding the cellulose degradation products is the production of insoluble organic liquid species on exposure to irradiation. However, studies regarding the degradation products are limited. The available information on the radiolysis of cellulose describe the generation of mainly water soluble degradation products [Humphreys 2010]. According to [Han1981], it has been observed that complete degradation and dissolution of cellulose happens at radiation doses of 500 kGy and above in aqueous environments for cellulose such as newspaper, cotton, sawdust and alpha-cellulose powder.

[Bludovsky 1984] examined the irradiation of cotton cellulose in oxygen-rich and inert environments and identified acetaldehyde, acetone, arabinose, deoxysaccharides,

formaldehyde, formic acid, glucuronic acids, glucose, malonaldehyde, oxalic acid and xylose as degradation products. The composition of the degradation products differed only little in oxygen-rich or inert environments, although the presence of oxygen increased the overall yield of the degradation products. Obviously the gaseous environment has little effect on the speciation of the degradation products of irradiated cellulose [Humphreys 2010].

5.3.3. Cellulose degradation kinetics: determining factors

Calcium concentration

The formation of sparingly soluble salts, e.g. with Ca^{2+} can limit the concentration of a ligand in cementitious pore waters. Thus, the formation of such salts will limit the effect of a ligand on radionuclide mobility. Regarding the safety of the nuclear waste repository, such an effect is desirable, especially for ligands with affinity towards tri- and tetravalent radionuclides such as isosaccharinic acid [Loon 1998].

Calcium present in the pore water of cementitious systems has the effect of catalyzing the benzylic acid rearrangements that lead to ISA and metasaccharinic acid (MSA) formation via the peeling and stopping reactions. The presence of Calcium enhances the rate of the stopping reaction to a greater extent than that of peeling and thus the overall effect of elevated Calcium concentrations is to reduce the degree of cellulose degradation. Another effect of the presence of Calcium is to enhance the formation of ISA relatively to the formation of smaller CDPs by fragmentation [Loon 1998].

According to [Small 2013], it is possible that under cementitious conditions ISA itself might control the Ca(II) and ISA concentrations, forming an upper limit on calcium concentrations through the solubility of calcium ISA salt. This might influence the rate of further ISA generation. According to [Hurdus 2000] the Ca salt of the α -ISA isomer has a solubility of $2.5\text{E-}2$ M [Hurdus 2000], which is similar to the Calcium concentration buffered by $\text{Ca}(\text{OH})_2$ at pH 12.5 [Small 2013]. According to [Small 2013], the β -ISA salt is even more soluble. If the Calcium concentration decreases from pH 12.5 to pH 11, then ISA concentrations $> 2.5\text{E-}2$ M would be required to maintain the Ca- α -ISA solubility product [Small 2013].

The Ca-Concentration in the early degradation stage of ordinary Portland cement is ~ 2 mM at pH 13.3. In the next stage of cement degradation, dissolution of $\text{Ca}(\text{OH})_2$ determines the pore water chemistry and the Ca-concentration is ~ 20 mM [Berner 1990]. By using the geochemical modelling tool PhreeqC, the maximum concentration of α -ISA in the cement pore water can be calculated using the solubility equilibrium for Ca(α -ISA):



and the complexation reaction:



Table 21 shows the maximum concentrations (solubilities) of α -ISA in equilibrium with Ca^{2+} for the two stages of cement degradation.

Table 21: predicted ISA concentrations at different pH values [Loon 1998]

pH	Ca [M]	Ionic strength [M]	[ISA] _{max} [M]
13.3	0.002	0.3	0.051
12.5	0.02	0.05	0.021

These calculations show that the solubility limit of Ca(α -ISA) leads to a relatively high concentration of α -ISA in cement pore water [Loon 1998]. According to [Loon 1998], the

solubility of Ca(α -ISA) is too high to limit the maximum concentration of α -ISA in cement pore waters where their effect on the sorption of radionuclides is negligible.

Temperature

[Haas 1967] was the first who investigated the effect of temperature on the alkaline degradation of cellulose and assessed reaction rate constants at different temperatures between 65 °C and 132 °C and a hydroxyl concentration of 1.25 M and cotton based cellulose. [Loon 1998] used the rate data to derive rate constants and activation parameters for 25°C. It was found that the activation parameter for the peeling reaction was greater than that for stopping reactions, indicating that the extent of cellulose degradation is smaller at lower temperatures than at higher temperatures.

5.4. Degradation processes of ISA

As was presented in the sections above, ISA is, concerning its eventually arising amounts and complexation properties, the main cellulose degradation product under alkaline conditions. Therefore, the stability of this ligand is discussed in the following sections.

5.4.1. Chemical Degradation

[Hurdus 2000] experimentally investigated the chemical degradation of cellulose in homogeneous alkaline solutions at room temperature and 80 °C over 10 and 12 months, respectively. Their results indicated a slight transformation of α -ISA under oxic conditions, whereas no transformation was detected under anoxic conditions. [Hurdus 2000] identified acetic, lactic and formic acids as ISA degradation products.

[Glaus 2008b] acquired similar results in their study which showed that ISA degradation only occurred in the presence of stoichiometric amounts of oxygen or a similar oxidant. Identified ISA degradation products were a mixture of lactic, formic and glycolic acids (which have less complexing strength as compared to α -ISA). [Glaus 2008b] concluded that the oxidative degradation of ISA could not be included as a significant process in reducing the concentrations of degradation products due to the limited period of oxidising conditions expected. This assumption is also true for the conditions expected in the near-field of the planned Dutch repository.

[Loon 1998] investigated the chemical stability of α -ISA under exclusion of oxygen in a homogeneous artificial cement pore water (pH 13.3, -25 °C, Na: 114 mM, K: 180 mM, Ca: 2.3 mM). No transformation of α -ISA could be detected. Figure 19 shows the results of the tests carried out by [Loon 1998]. The ISA concentrations were measured twice: immediately after sampling and after a certain time t after sampling. The time axis in Figure 19 shows the time difference between the first and the second measurement. The Y-axis represents the ratio of the first and the second measurement of the particular sample. In case both measurements have identical results, this ratio is one (represented by the solid line). As can be seen, the α -ISA concentration remains constant (within the measurement uncertainty), indicating that α -ISA (and probably also β -ISA) is stable under alkaline conditions of a cementitious repository and for the given time frame, i.e. three years.

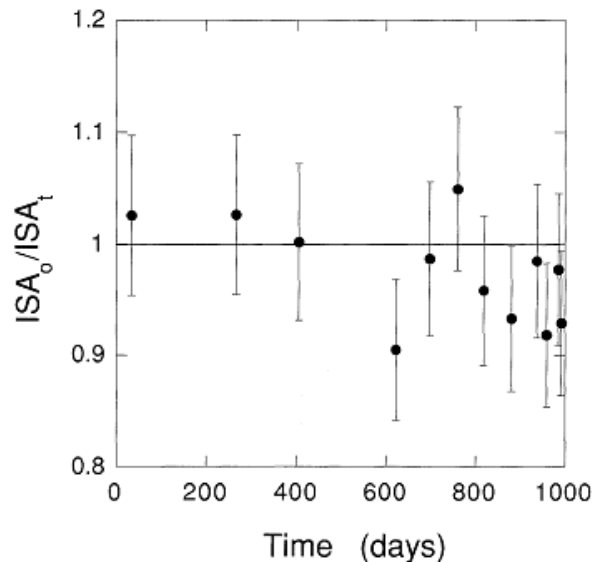


Figure 19: **Stability of α -ISA** at pH 13.3 as a function of time. Here, time represents the time difference between the first and the second measurement [Loon 1998]

It is not possible to demonstrate that α -ISA will be stable over repository time scales. However, such an assumption would be conservative in the sense of performance assessment, because the radionuclides complexed by α -ISA will be more mobile than in a situation in absence of α -ISA [Glaus 2008c].

5.4.2. Microbial degradation

As discussed above (section 5.2.1.1) the major cellulose degradation products are α - and β -ISA. Besides those compounds, a range of other organic acids are also generated under alkaline conditions (e.g. formic, lactic and acetic acids) [Knill 2003]. [Humphreys 2010] assumes that the microbial population will be initially mainly non-specialised and the ability to degrade ISA will be absent or very limited. The microbial communities may then develop the ability to degrade ISA provided that the conditions allow microbial activity.

In general, micro-organisms able to degrade both ISA-isomers under aerobic and denitrifying conditions (at pH 10.5) have been found in a range of environments [Grant 2002], e.g. from naturally occurring alkaline sites such as the Crater and Elmenteita Lakes in Kenya or Mono Lake in the USA [Grant 2002].

[Grant 2002] undertook studies on ISA degrading isolates and demonstrated ISA degradation between pH 7 and 11.5, with an optimum between pH 9 and 10. The ISA degrading isolates coupled the degradation of ISA to nitrate reduction with the concurrent oxidation of ISA to CO₂. However, the coupling of ISA oxidation to more reduced electron acceptors, such as sulphate and the degradation of ISA by methanogenic microbes has not been shown.

According to [Humphreys 2010], it is indicated that aerobic microbial populations in soil can adapt in a few decades to degrade ISA when it is the dominant carbon source. Micro-organisms isolated from such sites were shown to be able to degrade ISA in the absence of oxygen by using nitrate as a terminal electron acceptor (TEA) [Grant 2002]. This suggests that even when ISA degrading micro-organisms may not be active after repository closure, a mixed population could develop as ISA becomes the dominant carbon source within the system through the chemical degradation of cellulose [Humphreys 2010]. This hypothesis assumes that microbial ISA degradation under strongly reducing conditions may occur as was shown under aerobic and denitrifying conditions [Grant 2002, Strand 1984, Francis 2006]. Possibly, such microbes will grow preferentially in certain niches where the pH values are between 9 and 10, as reported by [Grant 2002].

The degradation of the mentioned cellulose degradation products under anaerobic conditions depends on methanogenic and acetogenic bacteria [Grant 2002, Pedersen 2000] (see Figure 18) or bacteria which couple the oxidation of the CDPs to the reduction of sulphate or ferric iron [Pedersen 2000]. However, under repository conditions, the degradation of these acidic, short chain organic molecules is probably inhibited by the high pH. Since the latter is expected to be > 12 for very long periods of time (see section 4.1), the removal of the CDPs will depend on the adaptation of the micro-organisms eventually present to the high pH environments. Also, their growth within biofilms or low pH niches within the waste may play a role.

[Bassil 2014] studied the microbial degradation of ISA under a number of biogeochemical conditions at high pH. In their study it was shown that bacteria are able to degrade ISA (as a sole carbon and energy source in minimal media) at high pH (~ pH 10) under a wide range of biogeochemical conditions, and that they can couple ISA metabolism to the bioreduction of a number of TEAs relevant to an evolving nuclear waste repository for LILW. It was found that the rates of ISA degradation, TEA reduction and the bacterial diversity of the cultures were proportional to the reduction potential of the TEA, in the order aerobic \approx nitrate > Fe(III), with no reduction detected at pH 10. [Bassil 2014] state that their results are consistent with the observation that a range of anaerobic processes can support ISA oxidation and that decreasing the reduction potential of the respiratory process redox couple results in progressively more streamlined microbial communities dominated by more specialist micro-organisms.

As discussed in section 4, the initial pH in the LILW section of the repository will be at ~13.5 due to the cementitious materials employed. The experiments of [Bassil 2014] were, however, conducted at pH 10. On the other hand, it can be expected that over prolonged timescales the starting hyperalkaline pH values will drop to pH ~ 10 [Berner 1992], the pH which supports the ISA degradation as shown in the study of [Bassil 2014]. [Bassil 2014] further argument, that at shorter time scales, when the pH is still very high inside the repository, there will be a pH gradient surrounding it that will result in regions of decreasing pH from hyperalkaline to ambient with increasing distance from the GDF. Any ISA generated within the LILW would migrate through the pH similar to that tested in the study of [Bassil 2014]. It cannot be excluded that the microbial metabolism of ISA will become more pronounced as the pH drops with time and distance from the repository and as the existent microbial communities adapt to the high pH conditions in and around the repository over long time-scales [Bassil 2014].

Furthermore, potential ISA degraders may also survive in the initial hyperalkaline pH as recalcitrant spores and then germinate when the conditions are more suitable for growth [Bassil 2014].

In general, ISA-metabolising bacteria have the potential to decrease the radionuclide mobility by degrading ISA-radionuclide complexes [Bassil 2014].

5.4.3. Radiolytic degradation

According to [Humphreys 2010], it is expected that the exposure of cellulose degradation products to ionizing radiation induces their decomposition by chain-scission to even lower molecular weight species and gas (decarboxylation). However, no data describing the degradation or degradation rates of CDPs during radiolysis could be found whether in the context of this study nor in the study of [Humphreys 2010]. According to [Humphreys 2010], it can be assumed that the factors that affect the radiolysis of the CDPs are likely to be the same as those affecting the original cellulose material. The influencing factors are radiation dose rate, the chemical nature of the CDP, the chemical environment and the irradiation temperature [Humphreys 2010]. Literature data concerning the chemical

stability of ISA indicate that this compound is stable in the absence of oxygen or other oxidising agents (see section 5.4.1). This suggests that potentially oxidising conditions generated by radiolysis could play a role in the degradation of ISA in the repository near-field.

5.5. Plastics

The word “plastic” is used as a general term for polymers such as polyethylene (PE), polypropylene (PP), polyamide (PA) and polyvinylchloride (PVC) [Warthmann 2013]. The plastic materials can be sub-divided into generic groups, each of which has a classification of materials, i.e. non-halogenated polymers and halogenated polymers. The exact composition of the particular plastic is often not specified [Warthmann 2013].

In the following sections, the properties and degradation processes and products of non-halogenated (section 5.5.2) and halogenated plastics (section 5.5.3) are discussed. In section 5.5.1 a knowledge basis regarding non-aqueous phase formation due to plastic degradation is given as this is necessary for the understanding of the subsequent sections.

5.5.1. Non-aqueous phase liquids

Non-aqueous phase liquids (NAPLs) are generally understood as oils and other organic materials that have limited miscibility with water and will thus form a separate phase if present in sufficient amounts [Dawson 2012].

NAPLs may be generated in the waste containers during storage or after disposal, mainly as breakdown products of the organic polymers in the waste [NDA 2012]. For example, a likely source of NAPLs in a repository could be the degradation products of PVC (and its additives) or PE which are present in the LILW [Dawson 2012].

Certain NAPLs are less dense than water (with a specific gravity $< 1 \text{ g/cm}^3$) and consequently tend to rise through aqueous systems; these NAPLs are known as light non-aqueous phase liquids (LNAPLs). Other NAPLs tend to sink in water and thus they are known as dense non-aqueous phase liquids (DNAPLs) [NDA 2012]. The potential effect of those liquids on radionuclide migration is one of the key uncertainties in the performance of a geological waste repository [Pöyry 2010].

LNAPLs may become mobile due to their buoyance if present in sufficient quantity and thus provide an additional pathway for the migration of eventually present radionuclides. Generally, LNAPLs are thought to be more likely than DNAPLs to have an effect on the post closure performance of a nuclear waste repository. The amount of uptake of radionuclides into the NAPL will depend on the relative stabilities of the relevant radionuclide species in the two liquid phases. Species which are ionic and polar will tend to favour the aqueous phase, uncharged less-polar species will however favour the NAPL. Neutral radionuclide-organic complexes containing significant hydrophobic groups are particularly likely to lead to uptake in the NAPL [NDA 2012]. The extent of radionuclide however also depends on the nature of the NAPL.

Another aspect of NAPLs is that they might affect the surface properties of solids (e.g. cement phases) with which they come into contact and thus have the potential to affect e.g. the sorption reduction of radionuclides onto cement phases in the near-field. Furthermore, small droplets of NAPLs may also contribute directly to radionuclide migration due to colloidal transport. Transport by this mechanism would be essentially the same as that considered for colloids in general [NDA 2012].

Another effect NAPLs may have is to provide a nutrition source for microbial communities and thus potentially enhance microbially induced corrosion or degradation. If, e.g., metal corrosion were enhanced in an anaerobic corrosion regime, this could lead to increase gas generation rates. However, NAPLs may also provide a protective film on metal surfaces, which limit gas production [NDA 2012].

5.5.2. Non-halogenated plastics

Non-halogenated plastics cover a large range of polymers with widely different properties. Polymers that may be found in the non-halogenated polymer waste are PE, polymethylmethacrylate (PMMA) and Vinylesterstyrene (VES) encapsulant. Furthermore, the presence of other polymers such as polypropylene (PP), polystyrene (PS), Nylon polyesters, epoxies, phenolics and other non-PMMA acrylics may be present in the waste. Many of the mentioned polymers are used in the medical, pharmaceutical or food packaging industries. PE is in its generic form probably the most common material in the non-halogenated polymer waste inventory. This material is often used to manufacture bottles, sheet, containers and film [Dawson 2012]. It is assumed that all non-halogenated waste is made up of PE and thus an amount of max. 10,500 t (see section 3.1.1) is present in LILW. In the framework of this report only PE (as a representative of non-halogenated plastics) is discussed.

PE is a linear polymer of ethylene, with the formula $(-CH_2CH_2-)_n$ [Vasile 2005]. It is semi-crystalline and consists of molecules closely packed in crystalline regions which are linked together by amorphous tie molecules. The ratio of amorphous to crystalline phase can vary significantly from about 50-90 % and is dependent on the degree of branching and the molecular weight [Dawson 2012].

PE grades are mainly classified according to their density. The following grades are distinguished [Vasile 2005]:

- High-density PE (HDPE)
- Medium-density PE (MDPE)
- Low-density PE (LDPE)
- Linear low-density PE (LLDPE)
- Ultra low-density PE (ULDPE)
- Very low-density PE (VLDPE)
- Low medium-density PE (LMDPE)

The grades are shown in Figure 20 and separated by their density and melt flow index.

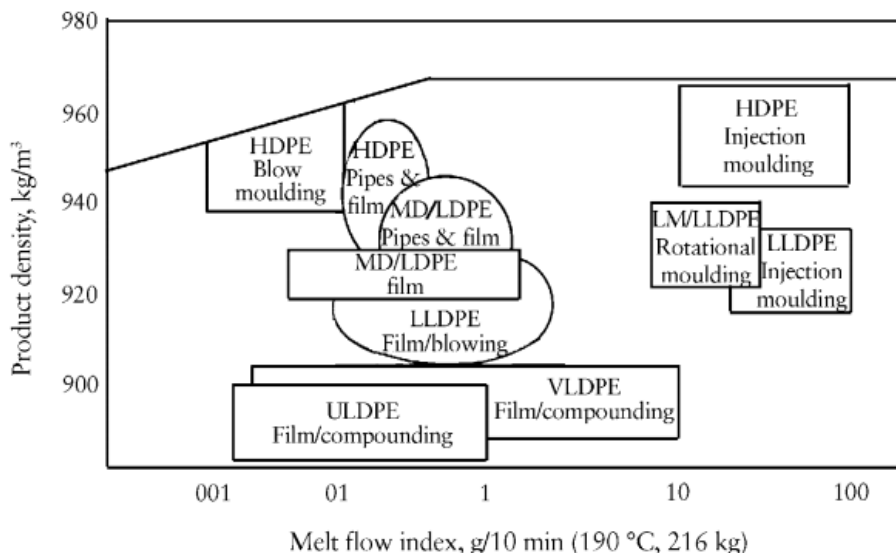


Figure 20: Classification of PE grades (Redrawn from Tecnon Orbichem. Copyright Tecnon Orbichem) [Vasile 2005]

Detailed information regarding the properties of the different PE grades can be found in [Vasile 2005].

[Dawson 2012] states that the polymers such as PE, PP and many of the fluoropolymers usually contain very few additives and that in most cases the additives are stabilisers present in amounts less than one percent. Hence the presence of additives eventually present in PE is neglected in the framework of this study (although it cannot be excluded that they influence the PE degradation behavior). For completeness, a brief overview of common additives in ultra-high molecular weight PE is shown in Table 22.

Table 22: Common additives of ultra high weight PE [Vasile 2005]

Property enhancement	Additive
Surface lubricity	Silicone oil, molybdenum disulfide, carbon black, graphite, polar waxes, vegetable oils, mineral oils
Abrasion resistance	Dicumyl peroxide
Surface hardness	Talc, hollow glass spheres, kaolin, short glass fibres, wood flour
UV resistance	Carbon black, hindered amine stabilisers
Electrical conductivity	Carbon black, graphite, carbon fibres

Generally, polymeric materials in the environment can undergo physical, chemical and biological degradation or a combination of all these due to the presence of moisture, air, temperature, light (photo-degradation, which is excluded under repository conditions), high energy radiation or micro-organisms (bacteria or fungi).

In the following sections, the chemical, radiolytic and microbial degradation processes of PE will be discussed.

5.5.2.1. Chemical degradation of polyethylene

The chemical structure of polymers controls their stability against chemical attack. Chemical degradation of polymers is initiated by a nucleophilic attack of OH⁻ ions on a carbon atom with a partial positive charge. Such carbon atoms are generally not present in addition polymers (i.e. PE and polystyrene, the basic material for ion exchange resins) but abundant in condensation polymers such as cellulose (see section 5.2). Thus, addition polymers are insensitive to OH⁻ and chemical (alkaline) degradation will be very limited and does not lead to the formation of organic ligands [van Loon 1995].

Generally, non-polar solvents (e.g. hydrocarbons and chlorinated solvents) are more easily absorbed by PE than polar solvents (e.g. soaps, alcohols). PE is extremely resistant to inorganic environments and is not affected by aqueous solutions of inorganic salts or mineral acids, even when concentrated. However, PE is altered by oxidising agents such as chlorosulfuric acid, pure fuming, nitric and sulfuric acids and halogens [Vasile 2005].

To summarize, PE has outstanding chemical resistance and it can be assumed that pure PE will not be prone to chemical degradation under the assumed repository conditions.

5.5.2.2. Radiolytic degradation of polyethylene

Irradiation of PE with lower doses (0-60 kGy) is used for, e.g., the improvement of the polymer properties (e.g. crosslinking of PE pipes, cables etc.). The exposure to a dose of about 25 kGy of radiation is a popular method of sterilising PE. At higher doses, in the presence of oxygen or at a long period of time, the degradation of PE takes place. Generally, radiochemical degradation occurs by three distinct and simultaneously competing processes: oxidative scission in amorphous phases, crosslinking and crystal destruction and/or chemocrystallisation. The latter produces an apparent increase of crystallinity and density due to the formation of polar groups which increase the intermolecular attraction forces resulting in high density [Landy 1988, Wright 1992]. Which of the mentioned processes dominates depends on the irradiation conditions.

Radiolytic processes generally may degrade plastics directly and may also contribute to their long-term biodegradability by altering their chemical and physical properties. The

likelihood of significant radiolytic effects on the degradation of plastics depends in general on the dose. Furthermore, the presence of oxygen in the repository before its closure and for a certain time period after closure may also affect radiolytic (and also microbial) processes [Cohen 2006].

[Chytiri 2006] analysed the generation of radiation degradation products from γ -irradiated LDPE via GC-MS. In their study, [Chytiri 2006] irradiated a polythene bag made of LDPE film with 30 kGy (average dose rate: 1,4 kGy/h). The irradiation was carried out in air at room temperature. Table 23 shows the major identified liquid species (C_5 and higher) with significant yields. The main degradation products were found to be hydrocarbons and alkenes. Further products are aldehydes, ketones, alcohols, carboxylic acids and esters. According to [Chytiri 2006], an unusual species is 3,3-dimethyl-butanamide, which is not expected from a PE based material and may be a lubricant degradation product [Dawson 2012]. The G-values (determined by [Dawson 2012]) in Table 23 give the number of products (here molecules) generated for every 100 eV of radiation energy absorbed.

Table 23: Degradation product G-values after irradiation of PE to 30 kGy [Chytiri 2006 and NDA 2012]

Degradation product	Yield at 30 kGy [mg/L]	Molecular weight	mM (in 100 mL)	G-value (molecules per 100 eV)
5-methyl-2-hexanone	7.8	114	0.007	1.5
2,4-dimethyl-2-pentanol	12	116	0.010	2.2
2,4,4-trimethyl-hexane	7.3	128	0.006	1.2
2-(1,1-dimethylethyl)-oxirane	8.6	72	0.012	2.6
2,2,4-trimethyl-3-pentanone	31.1	128	0.024	5.2
S,3,3-dimethyl-butanamide	35.3	115	0.031	6.5
S,1-octen-3-ol	11.8	128	0.009	2.0
2,2,4-trimethyl-3-pentanol	9.1	130	0.007	1.5
2,2,4-trimethyl-1-pentanol	5.9	130	0.005	1.0
2,4,4-trimethyl-1-pentanol	6.8	130	0.005	1.1
2,3,3-trimethyl-1-butene	30	98	0.031	6.7
2,6-dimethyl-undecane	8.1	184	0.004	0.9
2,2,4,4-tetramethyl-octane	6.2	170	0.004	0.8
2,2,4,6,6-pentamethyl-heptane	6.2	169	0.004	0.8
2,4-dimethyl-1-pentene	5.8	98	0.006	1.3
3,6-dimethyl-undecane	12.2	184	0.007	1.4

S= the sinister form of the polymer enantiomorph

Other work carried out by [Buchalla 2000] using GC-MS for the investigation of polymer degradation due to radiolysis has also shown that the radiolysis products of different PE materials irradiated to 25 kGy are similar to those shown in Table 23. A mixture of hydrocarbons, ketones, alcohols, aldehydes and carboxylic acids was found.

[Guest 1985] suggests that α - and γ -radiation generally produce qualitatively similar degradation effects in the polymers, whereas this is also supported by [Buchalla 2000].

Regarding the PE degradation during waste storage conditions it may be assumed that at low dose rates, with the probable availability of oxidising radicals, oxidative chain scission probably dominates and occurs predominantly in the amorphous phase of PE. Hence oxidised species are generated. Assuming that the polymers in the repository may be continuously irradiated to a dose of 10 MGy, the initially produced degradation products are likely to undergo radiolytic degradation or react with water radiolysis products [Dawson 2012].

[Dawson 2012] gives generic radiolysis reactions for the typical degradation products from PE:

- Ketones → radiolysis → Alcohols + gas [Riesz 1964]
- Alcohols → radiolysis → Aldehydes + gas [Pozzi 2005]
- Aldehydes → radiolysis → carboxylic acids + gas [Kovalenko 1994]
- Carboxylic acids → radiolysis → Alcohols, Aldehydes, Hydrocarbons + gas (decarboxylation [Wu 1975])

The generated degradation products will depend on the many different factors that control polymer radiolysis. The authors however infer that as polymer degradation products are generated under constant irradiation, they will also degrade to lower molecular weight species and gas. It is likely that during radiation exposures the concentrations of the individual degradation products reach a steady state determined by the balance between their rates of production and degradation [Dawson 2012].

Another aspect regarding the release of PE degradation products was described by [Buchalla 2000]: it was observed in sterilised polymers that the degradation products may be trapped within the polymer for extended periods of time unless using solvents or high temperatures. This is due to the complicated morphologies of the polymers. Once those degradation products are trapped, they can also degrade in-situ until they become small enough to become disentangled or the surrounding molecules have degraded [Dawson 2012].

No observation of liquid species has ever been made in irradiated polymers except for plasticised materials such as PVC and rubbers. [Dawson 2012] concludes from this, that in terms of the generation of NAPLs from PE it is likely that some potential NAPL products will be generated in the initial stages of waste storage. Their migration from the polymer is however likely to be restricted due to the PE morphology and the amounts are expected to be low. At high doses and extended periods of time, [Dawson 2012] suggests that the potential NAPL products will themselves degrade to water soluble species or gases if they are still present in the radiation field. It thus can be expected that the release of NAPLs from PE wastes is likely to be very low [Dawson 2012].

Only one study could be found which investigated the radiolytic degradation of PE under alkaline (aqueous) conditions. [Dawson 2013] carried out an experimental study investigating the radiolysis of LDPE. LDPE bottles (a material used as, e.g., storage bottles) were cut into pieces of sides ~ 10 mm. Samples of 20 g of the LDPE pieces were placed in separate glass vessels; six with demineralized water at pH 7 and six with saturated Ca(OH)_2 solution with an excess of solid Ca(OH)_2 to maintain a pH of 12.5. The two different pHs were used to assess potential differences in degradation rates brought about by synergy between chemical conditions and radiation [Dawson 2013]. Since the experiments with high pH are relevant, only the results of those experiments will be presented here.

Besides the 10 mm square LDPE pieces, also smaller pieces (~ 3mm) were cut from the bottles for gas analysis and high dose rate data. 12 samples of the smaller LDPE pieces were placed in separate glass ampoules to assess gas evolution. Two 20 g samples of the smaller LDPE pieces were placed in glass vessels containing demineralized water and two more 20 g samples placed in saturated Ca(OH)_2 solution in the same manner as described above for the larger pieces [Dawson 2013].

Note that the LDPE materials were commercial polymers which may contain a mixture of additives such as stabilisers, antioxidants and fillers, whereas their formulation was proprietary [Dawson 2013].

The vessels were either placed in a Co-60 irradiation facility and irradiated at the dose rates as shown in Table 24 or kept as unirradiated controls.

Table 24: Material samples and irradiation conditions [Dawson 2013]

Material	Conditions			
2 x 20 g LDPE in Ca(OH) ₂ solution in glass vessel (10 mm and 3 mm pieces)	High dose rate (4 kGy/h) to 10 MGy	Low dose rate (45 Gy/h) to 150 kGy	High dose rate (4 kGy/h) to 150 kGy	Unirradiated controls

Before and on completion of the irradiations, pH measurements were carried out on the aqueous solutions in each vessel [Dawson 2013].

An organic screening analysis of the aqueous solutions by GC-MS in which the LDPE samples were irradiated was carried out as a preliminary assessment of whether organics of C₅ or above had leached from the polymers as a result of exposure of radiation [Dawson 2013].

Table 25 shows the results of the recorded pH values and measured TOC of the experiments with alkaline pH. The pH of the Ca(OH)₂ solutions in which the LDPE samples were irradiated remained greater than 12. This is expected since Ca(OH)₂ buffers the pH at a value of ~12.5. The higher pH values measured ("final pH") can be explained by the uncertainty associated with these data [Dawson 2013].

Table 25: pH measurements for LDPE irradiated in aqueous solutions [Dawson 2013]

Aqueous solution	Dose rate [Gy/h]	Total dose [kGy]	Initial pH	Final pH	TOC (by UV) [mg/L]	TOC (by GC-MS) [mg/L]
Ca(OH) ₂ #1	0	0	12.99	12.99	10.6	7.5
Ca(OH) ₂ #2	0	0	12.94	12.99	10.1	8.9
Ca(OH) ₂ #1	~4,000	10,000	12.80	13.04	11.9	2.7
Ca(OH) ₂ #2	~4,000	10,000	12.81	13.03	7.7	4.0
Ca(OH) ₂ #1	~45	150	12.98	12.96	10.4	5.1
Ca(OH) ₂ #2	~45	150	12.97	12.99	9.8	4.9
Ca(OH) ₂ #1	~4,000	150	13.00	12.95	4.8	2.4
Ca(OH) ₂ #2	~4,000	150	13.00	12.95	4.9	0.7

According to [Dawson 2013], the TOC content of the solutions in which the LDPE samples were irradiated appeared to be largely unaffected by irradiation in either de-ionised water or Ca(OH)₂ solution. Under alkaline conditions (pH 12.5), the highest TOC value was found to be 11.9 mg/L by using a dose rate of ~4,000 Gy/h and a total dose of 10,000 kGy.

The GC-MS analyses carried out by [Dawson 2013] of the solutions in contact with LDPE and irradiated to 150 kGy at 4 kGy/h showed very low levels of organic compounds (Table 26).

Table 26: GC-MS analysis results of solutions irradiated to 150 kGy at 4 kGy/h [Dawson 2013]

Material	Sample	Organic compound detected	Concentration [µg/L]
LDPE	Ca(OH) ₂ #1	Benzenedicarboxylic acid	15
	Ca(OH) ₂ #2	Long chain alkanes	180

Besides the aspects discussed above, furthermore ion chromatography analyses were carried out by [Dawson 2013] to investigate the presence of low molecular weight organic anion species. The only anion which could be observed and quantified in Ca(OH)₂ solution and LDPE irradiated to 10⁶MGy was Oxalate (COO)₂²⁻ with a concentration of about ~0.2 mg/L.

[Dawson 2013] also analysed the light gas of irradiated LDPE in air. The results are shown in Table 27 and are given as ppm of the headspace volume in sealed headspace vials. Significantly more hydrogen and low molecular weight hydrocarbons were evolved at 10 MGy as compared to the data gained at 150 kGy.

Table 27: Gas analysis results for irradiated LDPE. Gas concentrations are in ppm [Dawson 2013]

Dose [kGy]	H ₂	CO ₂	CO	CH ₄	C ₂ H ₂	C ₂ H ₄	C ₂ H ₆	C ₃ H ₈	O ₂ %
10,000 at 4 kGy/h	604,386	329	62	2,932	< 1	< 1	4,036	420	0.6
150 at 4 kGy/h	52,138	525	846	251	< 1	< 1	922	111	< 0.1
150 at 45 Gy/h	15,354	1,638	668	164	< 1	< 1	367	43	< 0.1
Nil	18	401	5	3	< 1	< 1	< 1	< 1	2

[Dawson 2013] furthermore calculated G-values for the the irradiated LDPE under the different radiation conditions. G-values are understood as the number of molecules per 100 eV of radiation energy absorbed. The G-values for the hydrogen evolution (G_{H₂}) are given in Table 28.

Table 28: G_{H₂} values for irradiated LDPE [Dawson 2013]

Irradiation conditions	G _{H₂} molecules per 100 eV
Air, 10 MGy at 4 kGy/h	0.7
Air, 150 kGy at 4 kGy/h	4.0
Air, 150 kGy at 45 kGy/h	1.2

[Dawson 2013] furthermore investigated the volatile organic compounds (VOC) by mass spectral data, searched against an established compounds library and semi-quantified against the response of hexane from standards of known amounts of hexane in helium.

Table 29 shows the data of the irradiated LDPE ampoules. In the unirradiated control ampoules, no VOC were detected.

Table 29: Determined VOC concentrations for irradiated LDPE expressed in ppm/Mol hexane [Dawson 2013]

Compound	10 MGy air	150 kGy high dose rate air	150 kGy low dose rate air
Butane	185	358	66
2-Methylbutane	11	10	
Pentane	48	93	12
Acetone		3.2	1.2
2-Methylpentane	5.5		
Isopropyl alcohol		10	
2-Methyl-2-propanol		28	7.6
3-Methylpentane	5.5	71	8.5
Hexane	23	30	4.0
2-Butanol		2.7	
3,3-Dimethylpentane	2.0		
3-Methylhexane		8.5	10
5-Methyl-1-hexene	7.0		
3-Ethylpentane		3.4	6.5
Heptane	13	5.8	5.8
3,4-Dimethylhexane	16		
3-Methylheptane		11	0.9
2,4-Dimethylheptane		3.3	3.2
Octane	6.6	3.8	3.6
2,3-Dimethyloctane		2.1	3.6
3,3,4-Trimethylhexane	5.9		
3-Ethyl-2-methylheptane	2.6		
Nonane	2.2		

Blank cell: not detected

The VOC analyses showed that the degradation products from LDPE were mainly low molecular weight alkanes. The major gases detected in the VOC analyses of irradiated LDPE were found to be butane, pentane and 3-methyl pentane. Under standard temperature and pressure, butane is a gas. The other compounds appear as liquids at 20 °C, whereas many of them are volatile [Dawson 2013].

In order to estimate a limit for total organics generated from irradiated LDPE in Ca(OH)₂ solution, the highest determined TOC value was taken as 11,9 mg/L (as determined at a dose rate of ~ 4,000 Gy/h and a total dose of 10,000 kGy; see above). The sample was 20 g in weight and was irradiated in 100 cm³ of saturated Ca(OH)₂ solution. Thus, there were ~ 1.19 mg of organics arising from the 20 g sample. This equates to ~ 60 µg of all organics arising per gram of LDPE when irradiated to 10 MGy.

Regarding the highest total amount of organics in the gas phase arising from irradiated LDPE, the identified organic gases in the light gas analyses were CH₄, C₂H₆ and C₃H₈ at 2,932, 4,036 and 420 ppm (Table 27) [Dawson 2013]. According to [Dawson 2013], the volume of the headspace vial was ~22 cm³ which was assumed to have contained approximately 1 mM of gas. Thus, 2932 ppm of CH₄ converts to a mass of ~47 µg ($2,932 \times 10^{-6} \times 16 \times 10^{-3}$ g). The amounts of C₂H₆ and C₃H₈ can be estimated as ($4,036 \times 10^{-6} \times 30 \times 10^{-3}$) g or ~121 µg and ($420 \times 10^{-6} \times 44 \times 10^{-3}$) g or ~18 µg, respectively. Thus, a total organic gas content from the light gas analyses of ~186 µg is estimated which converts to ~248 µg of light organic gas per gram of LDPE (the light gas analyses were carried out on 0.75 g samples).

In the context of the VOC analysis of the LDPE irradiated to 10 MGy in air, a total of 333 ppm of VOC were detected (Table 26). [Dawson 2013] estimated the total mass of VOC by using a similar approach to that adopted for the light gas but the molecular weight of hexane has to be used. Thus, the total mass of VOC was estimated as ($333 \times 10^{-6} \times 86 \times 10^{-3}$) g to ~29 µg for a 0.75 g sample. Thus, ~39 µg of VOC per gram of LDPE is generated. The total amount of gases arising from the irradiation of LDPE to 10 MGy in air (light gas plus VOC) can therefore be estimated as 248 + 39 = ~ 287 µg/g of LDPE [Dawson 2013].

When comparing the amount of organics in solution determined by TOC for LDPE at a dose of 10 MGy with the amount of organics in air at the same dose, 60 µg/g in Ca(OH)₂ compared to 287 µg/g in air, the amounts differ by a factor of ~4,8. It might be expected that the amount of organics in solution are lower due to the potential volatilization and escape of gases when the LDPE is irradiated in solution which may not occur when the samples were irradiated in sealed ampoules [Dawson 2013].

In the framework of their study [Dawson 2013] also investigated the potential generation of NAPLs from the irradiation of LDPE. Organic molecules with 5-22 carbon atoms are often liquid and eventually have limited solubility in water. GC-MS is sensitive of compounds of C₅₋₆ and greater, so the organic screening data acquired by GC-MS analyses (Table 25) was used by [Dawson 2013] to estimate the potential NAPL generation. An upper bound estimate for NAPL generation from LDPE when irradiated in solution has thus been made from the highest estimate of TOC from the data given in Table 25. The highest value of TOC in Table 25 is 5,1 mg/L when the sample is irradiated to 150 kGy at ~45 Gy/h. Thus, 20 g of LDPE in 100 cm³ saturated Ca(OH)₂ solution generate a maximum of 510 µg (= ~26 µg/g or 26 g/t) which may form NAPLs.

The highest value of TOC in Table 25 is 8,9 mg/L when the sample is unirradiated. Thus, 20 g of LDPE in 100 cm³ generate a maximum of 890 µg (= 45 µg/g or 45 g/t) of high molecular weight organics which eventually form NAPL.

According to [Dawson 2013], an upper bound estimate of the amounts of $\sim C_5$ and higher molecular weight species from irradiated LDPE in the gas phase can be made by examining the VOC data in Table 29. The highest concentration of $\sim C_5$ and higher VOC was observed at ~ 242 ppm/Mol of hexane for the sample irradiated to 150 kGy at 4 kGy/h in air. Thus, approximately 242 ppm/M of hexane of VOC that may be NAPL were generated from this LDPE sample which correlate to ~ 21 μg of organics ($242 \times 10^{-6} \times 86 \times 10^{-3}$) g from 0.75 g of LDPE or ~ 28 $\mu\text{g/g}$ (= 28 g/t) of potential NAPL in the gas phase from irradiated LDPE. The upper bound estimates for potential NAPL production from LDPE is summarised in Table 30.

Table 30: Upper bound estimates for NAPL production from LDPE [Dawson 2013]

Environment	Upper bound estimate of NAPL in g/t of material
Aqueous solution (Ca(OH) ₂) irradiated	26
Aqueous solution (Ca(OH) ₂) unirradiated	45
Gas phase	28

When the estimates for irradiated conditions given in Table 30 are applied to the PE inventory (10,500 t), this means that 0,6 t of NAPL could be generated due to radiolysis. Thus, the amounts are so small that they are negligible when compared to the whole waste inventory.

5.5.2.3. Microbial degradation of polyethylene

Polyethylene seems to be one of the most inert polymers [Hadad 2005]. It is widely accepted that its resilience concerning biological degradation is due to its hydrophobicity (the surfaces have only CH₂ groups), water repellency, high molecular weight and lack of functional groups recognizable by microbial enzymic systems [Vasile 2005, Hadad 2005].

For example, it was found that after 10 years of incubation in soil, < 0.5 % carbon (as CO₂) by weight was evolved from an UV-irradiated polyethylene sheet [Albertsson 1990]. On the other hand, nonirradiated PE generated < 0.2 % CO₂ during the same time.

Thus, it can be assumed that pure PE (when no additives are present) will not be degraded microbially (in case microbes are active which can also considered to be very unlikely in high pH conditions (see also section 5.3.1)) when radiation is excluded.

Studies investigating biodegradation of PE under alkaline (repository) conditions expected in the LILW section do not exist. Regarding PE degradation under normal environmental conditions, the mechanisms of biodegradation involve the following steps [Arutchelvi 2008]:

1. Attachment of micro-organisms to the polymer surface
2. Growth of the micro-organism utilising the polymer as the carbon source
3. Primary degradation of the polymer
4. Ultimate degradation

When initial physical or chemical degradation takes place (e.g. photo- or thermo-oxidation (both will not occur in the repository) or radiolysis), hydrophilic groups on the polymer surface are inserted making it more hydrophilic and thus organisms may attach on the surface (otherwise step 1 is not possible) [Hakkarainen 2004, Arutchelvi 2008]. Microbes may then use the polymer as carbon source and start growing. In the primary step, the polymer main chain cleaves, leading to the formation of low molecular weight fragments. The generated lower molecular weight degradation products are further utilised by the microbes as carbon and energy sources. Furthermore, also small oligomers can also diffuse into the organism and get assimilated. The final degradation products would be CO₂, H₂O and biomass under aerobic conditions. Anaerobic micro-organisms are able to degrade

these polymers under anoxic conditions, where the final degradation products are CO₂, H₂O, CH₄ and biomass under methanogenic conditions or H₂S, CO₂ and H₂O under sulfidogenic conditions [Arutchelvi 2008].

To conclude, regarding the low probability of microbial activity in the cementitious repository and furthermore the lacking knowledge on microbial degradation of PE under alkaline conditions, it may be deemed appropriate to neglect microbial PE degradation under (alkaline) repository conditions.

5.5.3. Halogenated plastics

Halogenated plastics are understood as polymers whose structures contain fluorine, chlorine, and sometimes bromine and iodine. Halogenated plastics commonly available include PVC, polychlorotrifluoroethylene, polyvinylidene fluoride, polychlorotrifluoroethylene, ethylene-tetrafluoroethylene polymer and chlorinated polyethylene. Regarding PVC, its early discovery, cost effectiveness and the ability to vary its properties have made it the most commonly used halogenated plastic of all [Dawson 2012].

In the framework of this study, it is assumed that the halogenated plastics inventory consists solely of PVC. However, there is no information regarding the exact composition of the PVC, i.e. there is no data regarding the amounts of additives in the PVC materials. Thus, assumptions regarding the PVC composition have to be made.

Based on the information given in [Meeusen 2014] and [Verhoef 2016], halogenated plastics amount in LILW to 305 - 643 tonnes ($\pm 20\%$). Generally, PVC is distinguished into PVC-U (unplasticised PVC) and PVC-P (plasticized PVC) [Warthmann 2013]. It is assumed that 25% of the PVC materials contains 40% of plasticiser (similar assumptions were made in the framework of [Warthmann 2013] in the context of investigations for a LILW repository in Switzerland). Thus, according to the assumptions made, the total mass of plasticiser in the LILW inventory would amount to 31 - 64 t.

5.5.3.1. General information on PVC

Plastic materials are a part of everyday life around the world and they have a wide range of applications (e.g. in building and construction, films and sheet, flooring and cables, packaging, furniture, glove box posting bags or protective suits) [Smith 2013]. In terms of consumption, PVC is one of the important plastic materials used today due to its unmatched material properties in many applications [Lindström 2007].

Figure 21 shows the application areas of PVC.

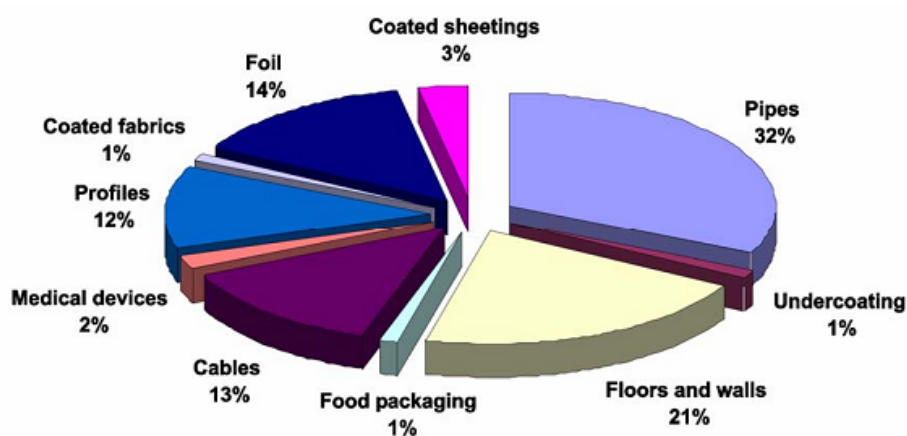


Figure 21: Applications of PVC [Lindström 2007]

PVC is made up of a polyhalogenated chains with a repeat unit $[\text{CH}_2\text{-CHCl}]_n$, which is similar to polyethylene but with a chlorine atom bonded to alternate carbon atoms in the particular chains (Figure 22) [Smith 2013]. This provides many points of dipolar interaction along its chain which give rise to strong interchain interactions and the consequent rigidity of the polymeric material [Vinhas 2003].



Figure 22: PVC chain structure [Vinhas 2003]

PVC has a mainly amorphous structure and is not flexible. By using additives, in particular plasticisers, the material can also be made flexible and its rigidity adjusted [Smith 2013]. Furthermore, certain material properties can be developed. Parameters considered when choosing a product formulation are, e.g. cost effectiveness, flexibility, chemical and fire resistance.

Depending on its application and required flexibility or hardness, plasticised PVC contains about 20 to 50 % plasticiser [Lindström 2007]. However, soft plastic bags used in the medical industry can have plasticiser contents as high as 70 % [Smith 2013]. Furthermore, varying amounts of fillers, impact modifiers, stabilisers, pigments and other additives may be added to the mixture. The additives in PVC however have large differences regarding their range, quantities and nature. Thus, it is very difficult to generalize the properties of PVC as different additives can impart different properties to the material [Smith 2013]. Note that PVC is by nature a flame-resistant material but, when organic plasticisers are used, the material is not self-extinguishing and flame retardants need to also be added [Lindström 2007].

Table 31 shows a list of commonly used generic compounding agents for PVC.

Table 31: Compounding agents found in PVC components [Humphreys 2010]

Additive Function	Range of % by volume in PVC	Generic additives used
Plasticisers	20 - 50	Esters (phthalates, adipates, azelates, phosphates), epoxies, trimellitates
Heat stabilisers	1 - 5	Lead compounds, cadmium compounds, organotins, barium/zinc compounds, calcium/zinc compounds
Fillers	10 - 20	Silicates, barium/calcium sulphate, calcium carbonate
Pigments	1 - 3	Metal oxides and silicates, organic dyes
Flame retardants	up to 5	Chlorinated or brominated organics, antimony oxide

Heat stabilisers suppress the thermal decomposition during manufacturing processes and protect the material from ultra-violet radiation [Howick 1995, Zahran 1986]. The type and amount of a particular stabiliser used in a PVC formulation can affect many of its properties, e.g. its physical properties, its chemical and radiation resistance, electrical, optical, rheological and toxicological properties and also its processability [Maura 2002]. As is shown in Table 31, stabilisers are added to PVC in small amounts (1-5 %).

Fillers can be added to PVC to enhance their mechanical properties and processability. Since they are normally much cheaper than the PVC resin, they are also used to reduce the amount of PVC and thus the manufacturing costs [Smith 2013]. Generally, there exist two types of fillers classed as organic and inorganic. Furthermore, both categories may be subdivided into fibrous (reinforcing) and non-fibrous compounds.

According to [Howick 1995, Zahran 1986], pigments and fire retardants are also added to PVC formulations depending on the component requirements.

5.5.3.2. Specific additives: Plasticisers

Due to their importance and comparatively high amount in the PVC formulations, the plasticisers and their properties will be discussed in this section in detail. The other additives presented in Table 31 are not discussed in the framework of this study.

Plasticisers are usually liquid and low molecular weight organic compounds which are incorporated into a material in order to increase its flexibility, workability and distensibility by breaking intermolecular forces within the material. Preferable properties of plasticisers are good miscibility, i.e. strong intermolecular forces between the plasticiser and the polymer resin, low volatility and diffusivity and low specific gravity [Lindström 2007]. Note that PVC polymers may even contain more than one type of plasticiser to achieve the desired functionality [Smith 2013].

Because a wide range of polymers with different structures exist, there is also a range of plasticisers for the different polymers and applications [Dawson 2012]. The dominant group of plasticisers used are phthalic acid esters of which bis(2-ethylhexyl)phthalate (DEHP) also known as dioctylphthalate (DOP), di-butylphthalate (DBP), butyl benzyl phthalate (BBP), di-isodecyl phthalate (DIDP) and di-isononyl phthalate (DINP) are most commonly used. According to [Smith 2013], DEHP, DINP and DIDP constitute well over 80 % of all PVC plasticiser applications. A detailed list of PVC additives is found in the Appendix 2.

Approximately 93 % of the plasticisers used in PVC are phthalates and ca. 95 % of all phthalate production is for use in PVC compounds [Mersiowsky 2001]. Figure 23 shows the chemical structure of the two most common phthalate esters DINP and DEHP.

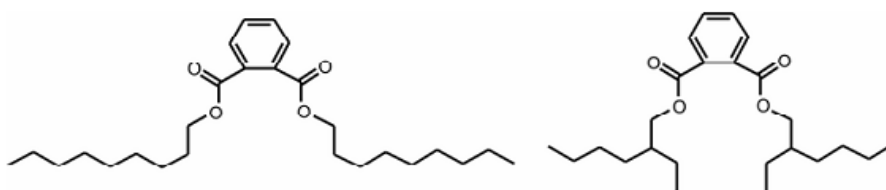


Figure 23: Chemical structure of two common phthalate esters; left: di-isononyl phthalate (DINP), right: (bis(2-ethyl hexyl) phthalate (DEHP) [Lindström 2007].

Table 32 shows a compilation of the existing wide range of plasticisers. All the mentioned plasticisers have very low water solubility and specific gravities less than 1 g/cm³. Thus, in their natural form, they are potentially buoyant non-aqueous phase liquids (NAPLs).

Table 32: Phthalate consumption in Europe [Harris 1997, Smith 2013, Ritchie 1972]

Phtalate	Specific gravity [g/cm ³]	Water solubility [% by weight]	European consumption [kt/a]
Bis(2-ethylhexyl)phthalate	0.9861*	Nil* (0.3 mg/l at 25 °C)	400 - 500
Di-isononyl phthalate	0.974	Nil	100 - 200
Di-isodecyl phthalate			100 - 200
Butyl benzyl phthalate			20 - 50
Di-butyl phtalate	1.071	0.1	20 - 40
Di-hexyl-phtalate	0.992	Nil	
Di-ethyl-hexyl-phtalate	0.985	0.01	
Di-capryl-phthalate	0.971	0.03	
Di-decyl-phtalate	0.964	0.01	
Di-octyl-phtalate	0.986	Nil	
Di butyl -adipate	0.961	Nil	
Di-ethyl-hexyl-adipate	9.926	0.01	
Di-butyl-sebacate	0.935	0.01	
Di-iso-octyl sebacate	0.935	Nil	
Di-2-ethyl-hexyl-sebacate	0.911	Nil	
Di-2-ethyl-hexyl-azelate	0.918	Nil	
Tri-butyl-phophate	0.978	0.6	
Tri-ethyl-hexyl-phophate	0.926	0.01	
Di-isobutyl phtalate			20 - 40
Di-tridecyl phthalate			3 - 10
Di-ethyl phthalate			10 - 20
Di-methyl phthalate			10 - 20

*: <http://scorecard.goodguide.com/chemical-profiles/html/dehp.html>

5.5.3.3. Specific additives: Stabilisers

Two different types of stabilisers are usually incorporated into the PVC structure. One stabiliser type reacts with and removes HCl whilst the other stabiliser type is usually a free radical scavenger [Smith 2013]. The following text gives a brief overview regarding stabilisers.

Heat stabilisers

The term heat stabiliser describes both types of stabiliser as HCl and free radical production occurs at elevated temperatures. Thermal degradation (i.e. dehydrochlorination) can occur in PVC during the processing and also at a very slow rate at room temperature. Heat stabilisers are used to minimise the chemical breakdown of the PVC by reacting with degradation products such as HCl. The main types of heat stabiliser are lead, cadmium, barium, calcium, zinc, organo-tin and epoxy compounds [Smith 2013].

Antioxidants

Peroxy radicals generated by the reaction of free radicals with oxygen may attack a polymer and break it down via chain scission. This mechanism can be inhibited by adding an antioxidant which will react with the peroxy radical species to form a less reactive product that cannot facilitate chain-scission. Besides phenolic antioxidants and those based on amides they are composed of e.g. sulphate or phosphate [Richie 1972].

Ultra-violet Absorbers

Ultra-violet light is able to break covalent bonds and thus cause degradation in various polymers including PVC. Additives which absorb UV and dissipate the heat may be added to the polymer to reduce these damaging effects. Common additives are, e.g., alkylated hydroxyphenylbenzotriazoles and 2- and 2,2'-hydroxybenzophenones and salicylates [Richie 1972].

Fillers

The addition of fillers to polymers has different aims: to improve their general properties or particular characteristics or to reduce the cost of the polymer compound. Generally, there are two types of fillers: organic and inorganic, whereas both categories can be further sub-divided into fibrous (reinforcing) and non-fibrous compounds. Organic (fibrous) fillers are, e.g. cotton and wood flour. Carbon Black and shell flour are, on the other hand, organic non-fibrous fillers. Furthermore, asbestos and glass fibre (fibrous) are commonly used inorganic fillers. Non-fibrous inorganic fillers are e.g., clay and calcium carbonate.

Lubricants

Lubricants are mixed to the PVC polymer to aid processing. Lubricating additives are classified as either internal (improving flow properties) or external (reducing melt viscosity). According to [Richie 1972], common lubricants in PVC are hydrocarbon, ester and amide waxes, fatty acids, fatty acid salts (calcium stearate), glycerol esters and paraffin oils.

5.5.3.4. Chemical Degradation of PVC

The dehydrochlorination of PVC in alkaline solution is used as a method for the disposal and recycling of PVC wastes [Blazevska-Gilev 2007]. Hence, several studies exist regarding the chemical (alkaline) attack on PVC at elevated temperatures. However, no studies could be found investigating the chemical degradation of (pure) PVC at room temperature. Selected studies undertaken on the PVC degradation under alkaline conditions (but temperatures far higher than room temperature) are presented here.

[Baston 2014] investigated the stability of a plasticised PVC material (Weston Vinyls PVC film, typically used as glove-box posting bag) by ageing it in different solutions, among them a $\text{Ca}(\text{OH})_2$ solution at 80 °C for 7, 30, 61, 90 or 120 days in air. This temperature was chosen to maximise the probability that significant ageing would occur in the PVC [Baston 2014]. In the framework of these measurements, the PVC weight, solution pH, TOC and GS-MS analyses were carried out.

Generally, when a generic plasticized PVC material is subjected to thermal ageing two processes take place simultaneously which will alter the physical properties of the material. Depending on the ageing temperature, one of these processes tends to dominate [NDA 2012]:

- The leaching of plasticiser which causes the PVC to become hard, rigid and brittle
- Thermal degradation: a complex and insufficiently understood process where the attack of the PVC polymer chains occurs leading to the release of HCl and unsaturation

According to [NDA 2012], thermal degradation usually dominates at temperatures above ~80 °C. At lower temperatures plasticiser leaching dominates, whereas the plasticiser diffusion is also dependent on the molecular structure of the PVC.

The study of [Baston 2014] showed that the PVC degraded quickly in the $\text{Ca}(\text{OH})_2$ solution, with differences in the appearance of both the PVC and the $\text{Ca}(\text{OH})_2$ solution observable after just seven days. [Baston 2014] suggested that the PVC underwent alkaline degradation in the $\text{Ca}(\text{OH})_2$ solution and released chloride. After 120 days of ageing, a weight loss of ~30 % was measured in the PVC. The TOC rose to 18 g/L after 120 days of ageing. GC-MS analyses detected phenol compounds in the solution with high phenol levels detected after 61 days of ageing. The levels reduced significantly at 120 days possibly due to hydrolysis of their primary decomposition products to secondary/tertiary species [Baston 2014].

It is expected that PVC releases HCl during its degradation (e.g. at high temperatures) [Baston 2014]. Hence, [Baston 2014] carried out additional analyses on the chloride concentrations in the solutions in which the PVC film was aged for 120 days. In the Ca(OH)₂ solution, a concentration of $2,6 \times 10^{-2}$ M was measured.

Table 33 shows the measured TOC data.

Table 33: Measured TOC in Ca(OH)₂ solutions for PVC aged at 80 °C [Baston 2014]

Experimental Code	Time (days)	TOC [mg/L]
pH 12/1	7	4,340
pH 12/2	7	4,580
pH 12/3	30	11,934
pH 12/4	30	12,574
pH 12/5	61	11,065
pH 12/6	61	11,295
pH 12/7	90	15,100
pH 12/8	90	15,600
pH 12/9	120	18,000
pH 12/10	120	16,700

The results of the (semi-quantitative) GC-MS analysis for the PVC film aged in the Ca(OH)₂ solution are shown in Table 34. Most abundant organic compounds were phenols. In the Ca(OH)₂ solutions, the concentrations were observed to be as high as 5,000 mg/L. [Baston 2014] suggest that in case of their study the source of the phenolic compounds was alkaline degradation of the PVC additives (mainly DEHP). It was not clarified why the degradation products were mainly phenols and the degradation path of DEHP did not follow the classical hydrolysis route into phthalate and aliphatic alcohol (see also section 5.5.4). It was speculated by [Baston 2014] that this occurs due to the influence of other (unknown) additives in the PVC film.

Table 34: Results of the GC-MS screening of the Ca(OH)₂ solution [Baston 2014]

Exp. code	Ageing period [d]	Organic compound	Concentration [mg/L]
PVC 12/1	7	2,3,6-trimethylphenol	980
PVC 12/2	7	2,4,6-trimethylphenol	890
		2,3,6-trimethylphenol	610
PVC pH 12/3	30	2,3,6-trimethylphenol	170
		4-isopropylphenol	160
		2,4-isopropylphenol	29
		Phthalic anhydride (phthalate anion)	28
		Benzoic acid	22
		3,4-dimethylphenol	22
		2,3,6-trimethylphenol	320
PVC pH 12/4	30	Phthalic anhydride (phthalate anion)	43
		2,4-diisopropylphenol	40
		Benzoic acid	29
		2,4,6-triisopropylphenol	26
PVC pH 12/5	61	2-isopropylphenol	5,000
		Phenol	4,000
PVC pH 12/6	61	Phenol	1,000
		3-isopropylphenol	1,000
		2,3-diisopropylphenol	200
PVC pH 12/9	120	4,4-methylenebisphenol (Bisphenol F)	2.6
		4,4-isopropylidenediphenol (Bisphenol A)	2.3
		4,4-ethylidenebisphenol (Bisphenol E)	2.1
		2,4-methylenebisphenol (2,4 Bisphenol F)	1.4
		4,4-dihydroxybenzophenone	1.0
PVC pH 12/10	120	2,6-di-tert-butyl-4-methylphenol	3.6
		4,4-methylenebisphenol (Bisphenol F)	2.8
		4,4-isopropylidenebisphenol (Bisphenol A)	2.5
		4,4-ethylidenebisphenol (Bisphenol E)	2.2
		Ethylmethoxyphenol	1.8
		2,4-methylenebisphenol (2,4 Bisphenol F)	1.3

In their ageing experiments, [Baston 2014] found also that a viscous, oily residue developed on the PVC after exposure to the Ca(OH)₂ solutions after 30 days ageing. [Baston 2014] investigated this solid residue. The results are shown in Table 35. According to [Baston 2014], the compounds detected by GC-MS seemed to be only a small fraction of the total solid mass. It was suggested that this may be due to the technique employed which was only able to identify those components that readily dissolved in the solvent used (dichloromethane). Thus, the nature of the residue remained uncertain because only a few percent could be dissolved in dichloromethane for GC-MS analysis. However, the soluble component of the residue contained phenol species similar to those found by the GC-MS analysis of the aqueous solutions. Despite the observation of the oily residue, no buoyant NAPL was observed at any time during the experiments.

Table 35: GC-MS analysis results of the solid residue [Baston 2014]

Compound	Concentration mg/kg of residue	% by mass
2-isopropylphenol	10,000	1.00
3-isopropylphenol	10,000	1.00
2,3-diisopropylphenol	4,000	0.40
Phenol	2,000	0.20
2,4,6-triisopropylphenol	500	0.05
Didecyl phthalate	200	0.02

The authors suggested that plasticiser migrated from the PVC, resulting in the high weight loss and underwent hydrolysis on contact with the Ca(OH)₂ solution.

To conclude, the experiments carried out by [Baston 2014] showed that the Weston Vinyls PVC film was unstable in alkaline solution at 80 °C and a wide range of organic degradation products is formed - both in solution and as a separate oily phase. Because the oily phase was solid, it was not considered to be a NAPL. Although the PVC appeared to release its phthalate additives when exposed to aqueous environments, the additives appeared to react so that no separate liquid phases are formed from the PVC film.

Generally, the release of HCl during the ageing of PVC is important because if HCl is allowed to remain in close proximity to the PVC, an unzipping reaction can catalyse and further degrade the polymer [Baston 2014]. When PVC ages in alkaline solution, HCl will however readily be neutralized and thus these conditions have a stabilising effect. However, experiments from [Baston 2014] showed that that PVC degrades even more readily at higher pH.

[Blazevska-Gilev 2007] reported that when (plasticised) PVC is exposed to high pH conditions, the dehydrochlorination and unsaturation occur within its structure. Although the end results of the alkaline and thermal degradation processes are similar (i.e. HCl release and unsaturation) the reactions mechanisms are difficult to compare due to a number of factors. One factor is the difficulty in comparing the size and chemical activity of the reactive hydroxyl anion in alkaline degradation to the mechanism of free radicals from a high molecular weight PVC chain subjected to high temperature thermal ageing.

According to [Baston 2014], their observation made during the ageing of the Weston Vinyls PVC are consistent with alkaline attack by the $\text{Ca}(\text{OH})_2$ solution rather than thermal ageing at 80 °C. Instead of suppressing the unzipping reaction in PVC by neutralizing HCl, the alkaline environment appeared to have attacked the PVC itself, as it was observed in the references [Yoshioka 1999, Blazevska-Gilev 2007].

To conclude, the data acquired by [Baston 2014] show that the Weston Vinyls PVC film is unstable in alkaline conditions at elevated temperatures and produces a wide range of organic degradation products in solution but also as a separate oily phase. The study of [Baston 2014] gives an initial insight into the chemical alkaline degradation of plasticised PVC at elevated temperatures but the transferability to conditions with lower temperatures remains uncertain.

Additional information regarding chemical degradation of PVC is also discussed in section 5.5.3.6 where, in the framework of PVC irradiation experiments in alkaline solution also unirradiated samples were investigated.

5.5.3.5. Microbial Degradation of PVC

In contrast to natural macromolecules which practically all can be degraded microbially, many synthetic polymers are durable for decades and cannot be biodegraded. The high molecular mass of synthetic polymers makes their incorporation into the cell impossible since an enzymatic cleavage of the polymers by exoenzymes is necessary. These enzymes must have access to the polymer binding which is often not possible due to the dense and crystalline form of the polymers [Munk 2008]. Since synthetic polymers are a development of the past decades, the evolution possibly has not yet developed enzymes which are able to cleave synthetic polymers such as PVC or polystyrene [Warthmann 2013].

There is no clear evidence in the literature regarding the microbial degradation of PVC. In landfills, as well as in the laboratory experiments simulating landfill conditions, the degradation of PVC was investigated. However, the degradation of the PVC could not be shown [Mersiowsky 2002a, Mersiowsky 2001, Mersiowsky 2002b].

To conclude, according to current literature, the PVC framework does not seem to be biodegradable, especially not under anoxic conditions and in absence of UV-radiation. The plasticisers (mostly phthalates) present in the PVC are on the other hand rather easy

biodegradable under anaerobic and aerobic conditions (see section 5.5.4.2) [Warthmann 2013].

5.5.3.6. Radiolytic degradation of PVC

A polymer with aromatic ring groups in its structure is usually more radiation stable than a polymer which has a purely aliphatic structure. The aromatic rings provide a protective effect by their ability to distribute the radiation energy across their de-localised bonding orbitals [Smith 2013]. [Szymanski 1979] has shown, for example, that the radiation stability of PVC compounds can be generally enhanced by the incorporation of phthalate plasticisers. However, as the plasticisers diffuse out of the PVC, the protective effect decreases which in turn results in more radiation damage and potentially faster diffusion rates of plasticiser out of the PVC. Thus, an accelerating sequence of processes that could lead to significant radiation damage in the PVC and the release of potentially significant amounts of plasticiser can take place. On the other hand, in a repository environment, the plasticisers themselves will be subject to radiolysis and possible degradation [Smith 2013] (see section 5.5.4).

When PVC is exposed to ionizing radiation, it may readily degrade to HCl and conjugated C=C double bonds (polyene structures) replacing the C-C single bonds on the polymer chains where HCl has been released (Figure 24).

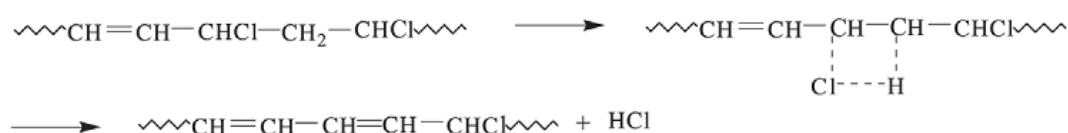


Figure 24: Generation of insaturations at PVC chain due to the „zipper“ effect (see text) [Vinhas 2003]

The result of the exposure to irradiation of PVC generally depends on competing reactions between cross-linking, chain-scission and recombination reactions. The balance of these reactions depends however on various factors such as the polymer structure, composition, radiation type, dose rate and environment (e.g. oxygen content). The range of commercial PVC formulations is very variable so that it is very difficult to predict the detailed results of the irradiation of a range of samples even under a fixed set of irradiation conditions [Smith 2013].

[Vinhas 2003] investigated the degradation of plasticized PVC films irradiated by gamma-radiation (and also irradiated an unplasticised PVC sample). In their study, four commercial PVC/plasticiser systems (DEHP: di(2-ethylhexyl)phthalate, DEBP (diisobutyl phthalate), TOTM (tris(2-ethylhexyltrimellitate) and viernol (a polymeric plasticiser)) were irradiated with different doses of gamma radiation (from a ⁶⁰Co source with a dose rate of about 6 kGy/h and doses of 10, 25 and 60 kGy). The samples were then analyzed by IR-spectroscopy and viscosimetry [Vinhas 2003]. The results of these investigations showed that the non-plasticised PVC as well as the plasticized systems PVC/DEHP, PVC/TOTM and PVC/viernol have suffered degradation due to chain-scission upon irradiation. The system PVC/DEHP suffered the highest degree of degradation [Vinhas 2003]. On the other hand, the system PVC/DIBP has not suffered scission of the polymer chains at any irradiation dosage. The viscosimetric molecular weight was related to the degradative process by the degradation index, DI, calculated by:

$$DI = \left[\frac{M_V}{M_{V_i}} - 1 \right]$$

where M_v and M_{v_i} are the viscosimetric molecular weight of the non-irradiated and irradiated samples, respectively [Vinhas 2003]. Figure 25 shows the results of the degradation index for the PVC and PVC/plasticiser systems as function of radiation doses.

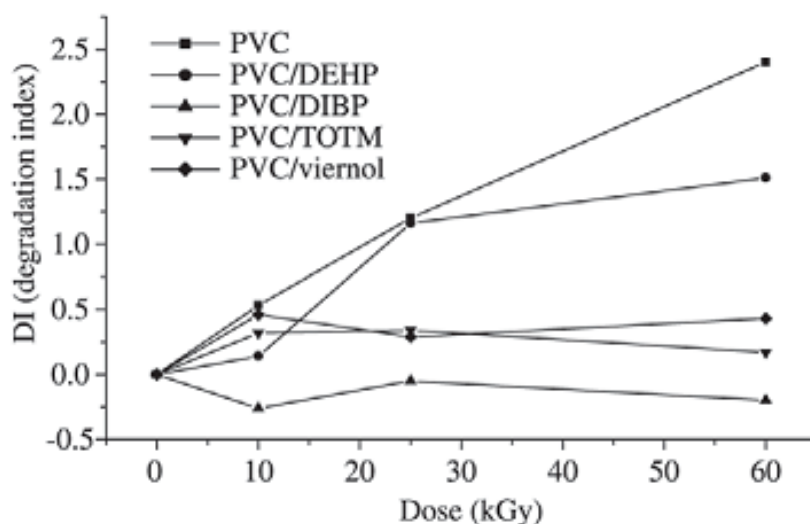


Figure 25: Degradation index of pure and plasticized PVC irradiated films vs. radiation dose [Vinhas 2003]

[Vinhas 2003] furthermore observed that PVC darkens and loses transparency due to irradiation whereas the darkening was proportional to the radiation dose. This observation is explained by the formation of double bonds along the chain in a process known as the zipper effect (Figure 24).

To summarise, results of the study of [Vinhas 2003] showed that plasticised PVC as well as non-plasticised PVC film degrade when exposed to γ -radiation. Chain-scission and double bond formation due to radiation were observed via infrared-spectroscopy. Among the irradiated plasticized PVC, the PVC/DEHP film has shown the highest degradation due to chain scission, especially when exposed to a dose of 25 kGy which is the sterilization dosage used for medical devices and packaging materials [Vinhas 2003].

[Reed 1993] carried out α -irradiation of a PVC material at about 120 kGy and has shown that various degradation products are formed but with the addition of chlorinated compounds. The ten major degradation products found via GC-MS analysis are shown in Table 36.

Table 36: GC-MS analysis results of the α -irradiation of PVC film at about 120 kGy [Reed 1993]

Degradation product	Amount detected ppmV
Acetone	14
Heptane	5.3
Butanal	2.4
3-heptane	1.9
3-methyl-heptane	1.7
Pentanal	1.4
3-chloromethyl-heptane	1.4
Benzene	1.1
1 chloro-2-butanol	1.1
Hexanal	1.1

Acetone was found to be the most abundant species, a low molecular weight soluble compound, possibly due in part to the degradation of intermediates.

[Dawson 2013b] carried out a study investigating the combined chemical and radiolytic degradation of plasticised PVC (which plasticiser was employed was unknown). Samples of PVC in the form of bag material were irradiated separately under the following conditions in room temperature:

- Deionized water at pH 7 to 10 MGy at 4 Gy/h
- Deionised water at pH 7 to 150 kGy at 42 Gy/h and at 4 kGy/h
- Ca(OH)₂ solution, at pH 12.4 to 10 MGy at 4 kGy/h
- Ca(OH)₂ solution, at pH 12.4 to 150 kGy at 42 Gy/h and at 4 kGy/h

Furthermore, unirradiated control samples were investigated.

Samples of each polymer were also irradiated at ambient temperature in sealed stainless steel vessels or glass ampoules under the following dry conditions for the analysis of evolved gases:

- Air to 10 MGy at 4 kGy/h
- Air to 150 kGy at 42 Gy/h and at 4 kGy/h
- Nitrogen to 10 MGy at 4 kGy/h
- Nitrogen to 150 kGy at 42 Gy/h and at 4 kGy/h

In all the experiments with the liquids, no non-aqueous phases could be detected [Dawson 2013b]. Due to the relevance of the high pH solutions and for space saving reasons, the results of only the experiments with alkaline solutions will be discussed in the following text. It was found that the pH of 12.4 was maintained in the Ca(OH)₂ solutions due to the presence of excess solid calcium hydroxide - which buffers released HCl in the alkaline solutions. Regarding the pH of the unirradiated PVC sample solutions, no significant change in pH was observed in any of the solutions. The results showed furthermore, that the total organic carbon content had increased in the solutions containing the irradiated PVC and the level of increase was dependent on the radiation environment.

The TOC content of the solutions containing the irradiated PVC increased on irradiation (see Table 37).

Table 37: TOC data for the solutions in which the PVC samples were irradiated [Dawson 2013b]

Dose rate [Gy/h]	Absorbed dose [kGy]	Solution	TOC [mg/L]
4,000	10,000	Saturated Ca(OH) ₂	66
4,000	150	Saturated Ca(OH) ₂	18
42	150	Saturated Ca(OH) ₂	38
0	0	Saturated Ca(OH) ₂	9

The semi-quantitative analyses by means of GC-MS of the dissolved species in the sample solutions showed a range of degradation products, including hydrocarbons, ketones, carboxylic acids, alcohols and aldehydes. Results of the analyses of the sample solutions are shown in Table 38. The data show that ketones and carboxylic acids, namely benzoic acid (C₇H₆O₂) at 200 µg/L were present when (plasticized) PVC is irradiated to 10 MGy in Ca(OH)₂ solution. An alcohol was furthermore detected (300 µg/L) and the amount of phthalic anhydride was (20 µg/L) [Dawson 2013b].

Table 38: GC-MS analysis results for PVC irradiated to 10 MGy in Ca(OH)₂ solution [Dawson 2013b]

PVC irradiated to 10 MGy in Ca(OH) ₂ solution	Species tentatively identified	Concentration [µg/L]	TOC [µg/L]
Sample 1	Isobenzofuranone	8	66,000
	Phthalic anhydride	20	
	Unknown	100	
	Propanol, (methoxy-methylethoxy)-	300	
	Benzoic Acid	200	
Sample 2	Propanol, (methoxy-methylethoxy)-	200	
	Benzoic Acid	100	

Table 39 shows the results of the GC-MS analyses for the PVC irradiated to 150 kGy in the Ca(OH)₂ solution at 42 Gy/h.

Table 39: GC-MS analysis results for PVC irradiated to 150 kGy in Ca(OH)₂ solution at 42 Gy/h [Dawson 2013b]

PVC irradiated to 150 kGy in Ca(OH) ₂ solution at 42 Gy/h	Species tentatively identified	Concentration [µg/L]	TOC [µg/L]
Sample 1	Octadecanoic acid, oxo methylester	3	38,000
	Phthalic anhydride	10	
	Phenol, bis dimethylethyl	50	
	Furancarboxaldehyde, hydroxymethyl	50	
	Nonane	100	
	Tetrachloroethylene	200	
Sample 2	Tetrachloroethylene	100	
	Unknown	40	
	Phenol, bis dimethylethyl	9	

In their study, [Dawson 2013b] also carried out light gas analyses of the headspace above dry irradiated PVC. It was found that these gases were dominated by hydrogen, methane, carbon monoxide and carbon dioxide. The results are summarised in Table 40. In the mentioned Table also G-values are given for the release of hydrogen (G_{H_2}) from the PVC material. According to [Daswon 2013b], the estimated G_{H_2} values are in reasonable agreement with values for plasticised PVC in the literature.

Table 40: Light gas analysis results in ppm of irradiated PVC in air and nitrogen [Daswon 2013b]

Light gas species	10 MGy N ₂	150 kGy 42 Gy/h N ₂	150 kGy 4 kGy/h N ₂	10 MGy Air	150 kGy 42 Gy/h Air	150 kGy 4 kGy/h Air
Methane CH ₄	20,000	380	655	18,000	480	240
Carbon Monoxide (CO)	18,000	2,300	1,790	11,000	390	1,680
Carbon Dioxide (CO ₂)	80,000	16,000	7,790	54,000	6,000	7,030
Ethane (C ₂ H ₆)	7,500	140	209	6,600	115	117
Ethene (C ₂ H ₄)	< 2	5	< 2	< 2	< 2	44
Ethyne (C ₂ H ₂)	< 2	< 2	< 2	< 2	< 2	115
Total C ₃	1,000	61	92	850	27	94
Hydrogen (H ₂)	270,000	1,200	11,600	260,000	4,400	1,300
GH ₂ molecules per 100 eV	0.12	0.03	0.33	0.11	0.13	0.04

Besides the light gas analysis, also the generated volatile organic compounds (VOC) generated during irradiation were analysed for the samples that had been irradiated to 10 MGy at 4 kGy/h and 150 kGy at 42 Gy/h. The results are shown in Table 41. Note that a range of unknown compounds were also detected by [Dawson 2013b] which are not shown in Table 41.

Table 41: Identified VOC in ng for irradiated PVC [Dawson 2013b]

Identified VOC	10 MGy N ₂	150 kGy 42 Gy/h N ₂	10 MGy Air	150 kGy 42 Gy/h Air
Dichloromethane	1,900	1,300	1,200	450
2-Butanone	38,00	660	3,600	3,200
Ethyl Acetate	610	< 15	510	< 15
1,1,1 Trichloroethylene	210	< 15	< 60	< 15
1-Butanol	< 80	330	< 60	< 15
Benzene	7600	580	6400	440
Toluene	84	17	65	17

Generally, more VOC were generated at the higher irradiation doses, whereas the identified VOC were aliphatic and aromatic hydrocarbons, chlorinated hydrocarbons, an ester, ketone and an alcohol. Since pure PVC contains chlorine, the observation of certain chlorinated species (e.g. dichloromethane) can be expected. The high benzene concentration might be due to the degradation of the plasticiser in the PVC material.

[Dawson 2013b] observed in their study that plasticiser appeared to be released from the PVC irradiated under dry conditions as could be seen by the waxy appearance these samples showed as compared to samples irradiated in contact with solution.

[Dawson 2013b] concluded from their study, that the detected amounts of species suggested that NAPL production seemed unlikely to occur as a result of radiolytic degradation of PVC in contact with aqueous solutions. NAPLs could not be directly observed in the aqueous phases. It was stated that the release of plasticiser may be a more significant route to NAPL formation from PVC. The observed plasticiser release from dry irradiated PVC together with the aqueous solution analyses suggested it is possible that

plasticiser or its degradation products may have diffused out of the polymer into the solution but then degraded under irradiation in the aqueous phase. Thus, plasticisers eventually diffuse from dry, irradiated PVC components during the primary stages of waste storage.

The potential for the production of NAPL may thus depend on a balance between the rate of diffusion out of the polymer and the rate of its radiolytic degradation. Degradation processes of plasticisers are discussed in section 5.5.4.

[Dawson 2013b] estimated the potential NAPL yields from their acquired GC-MS data. By banding all of the GC-MS data for the particular conditions and assuming that all identified organic compounds are potential NAPL (as a worst case), the particular concentrations were summed up and shown in Table 42.

Table 42: Estimates of potential NAPL generation from GC-MS screening data [Dawson 2013b]

Irradiation conditions	Total concentration of identified species by GC-MS [$\mu\text{g/L}$]	Estimates of potential NAPL yield in g/t of PVC
10 MGy at 4 kGy/h in Ca(OH)_2	628	~3
10 MGy at 4 kGy/h in Ca(OH)_2	300	~1.5
150 kGy at 42 Gy/h in Ca(OH)_2	149	~0.75
150 kGy at 42 Gy/h in Ca(OH)_2	413	~2

According to [Dawson 2013b], the potential NAPL yield for the investigated PVC material are surprisingly low since the PVC was expected to have 30 - 40 % by weight of plasticiser (and thus 300 - 400 kg of plasticiser per tonne of PVC material).

When the estimates for irradiated conditions given in Table 42 are applied to the PVC inventory (1,160 t), this means that max. 3,5 kg of NAPL could be generated due to radiolysis. Thus, the amounts are so small that they are negligible when compared to the whole waste inventory.

5.5.4. Degradation processes of PVC plasticisers

In this section, the stability of the most common PVC plasticisers under conditions relevant to the planned repository will be discussed. It can be considered possible that an aqueous alkaline environment will have a significant effect on the stability of PVC plasticisers and any subsequent migration [Smith 2013].

Plasticisers are usually employed for their ability to remain contained within a polymer during normal service. However, they can leach from the polymer as a result of elevated temperature, exposure to absorbent materials or due to degradation of the polymer itself. It is known that even at ambient temperatures, plasticisers can slowly leach from PVC [Baston 2014]. Due to their limited solubility in water, leached plasticisers could exist at some point as NAPL. Thus, it is important to understand the stability of those plasticisers in environments representative of the planned nuclear waste repository, e.g. under irradiation in contact with aqueous solutions at alkaline pH.

In the following sections, the chemical, microbial and radiolytic degradation of plasticisers commonly employed in PVC will be discussed. Note that the thermal stability of plasticisers (i.e. phthalates) has shown to be good at temperatures above <80 °C. So at the expected temperature in the LILW section (25 °C), the phthalates are expected to be thermally stable [NDA 2012].

Over time, the plasticisers may gas out of the PVC or be leached out and the PVC becomes brittle. It can be assumed, that the PVC wastes only have a lower proportion of plasticisers. In a Swiss study regarding chemical risk assessment it was found that plasticisers are in about 25 % of the products with about 40 % [Warthmann 2013].

5.5.4.1. Chemical and radiolytic degradation

There exist only very few data which describe the plasticiser behavior under combined chemical and radiolytic conditions (or only radiolytic degradation) expected in a geological waste repository. The additives are expected to be thermally stable under the expected temperatures (~ 25 °C) but under the aqueous alkaline conditions the esters are likely to undergo hydrolysis to the precursor alcohol and phthalate. Furthermore, the exposure to radiation of the plasticisers and their alkaline hydrolysis products may lead to further degradation [NDA 2012].

The three plasticisers most commonly used in PVC are DEHP, DINP, DIDP and they all have similar structures. The main difference between those compounds is the nature and the size of the aliphatic groups which are attached to the phenolic structure by the two ester linkages. Alkaline hydrolysis might be expected in each of the mentioned plasticisers and generate phthalate or (in a cementitious environment) calcium phthalate and an aliphatic alcohol. As an example for this process, Figure 26 shows the chemical structure of DEHP and its hydrolysis products in acidic and alkaline environments, respectively. The hydrolysis occurs at the two ester linkages [Smith 2013].

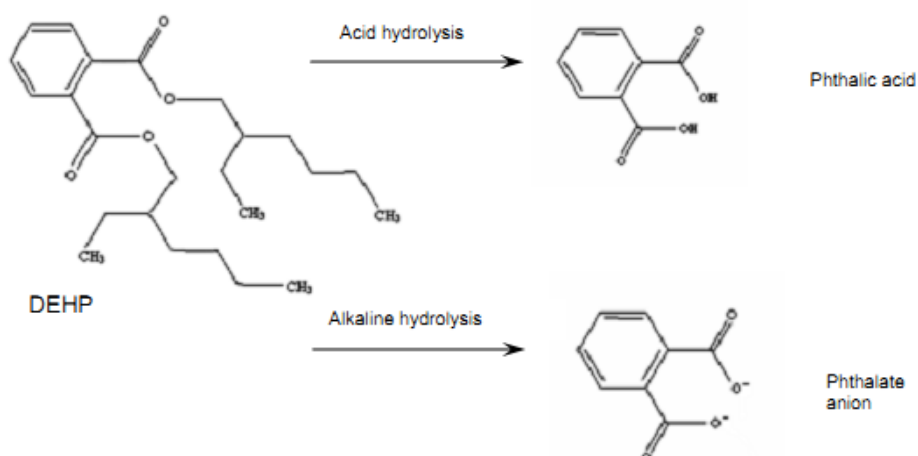


Figure 26: Potential phthalic degradation products due to hydrolysis of DEHP in acidic and alkaline environments, respectively [Smith 2013]

Note that the solubility of the aliphatic alcohol will depend on the number of carbon atoms in its structure, e.g. DEHP can undergo hydrolysis and generate, depending on the pH, phthalic acid or phthalate and ethylhexanol [Smith 2013]. Furthermore, the phthalic acid/phthalate is soluble whereas ethylhexanol has low water solubility and specific gravity and could therefore exist as a discrete, buoyant NAPL.

The recycling of (plasticised) PVC aims at generating low molecular weight products by chemical or thermal treatment. One established recycling process is the dehydrochlorination in alkaline media [Braun 2002]. Several studies regarding this method have shown that phthalate ester plasticisers such as DEHP and DOP degrade via alkaline hydrolysis in NaOH solution and generate iso-octyl alcohol or poly(vinyl alcohol) and phthalic acid [Shin 1999, Saravanane 2007].

[Baston 2014] carried out an investigation regarding the radiation stability of plasticisers in contact with aqueous solutions over a wide pH range. [Baston 2014] used (among others) aqueous solutions of Ca(OH)₂ (pH ~ 12.4) and approximately 20 g of DEHP was floated on the surface of the solutions. The process was repeated for DINP. The samples were then irradiated at a dose rate of ~ 4 kGy/h to a dose of ~10 MGy.

TOC measurements of the aqueous solutions in contact with DEHP and DINP, unirradiated controls and solutions irradiated to 10 MGy are shown in Table 43. As can be seen, the irradiation caused a significant increase of the dissolved organic carbon concentration.

Table 43: TOC for solution in contact with plasticisers: controls and at 10 MGy [Baston 2014]

Plasticiser	Aqueous solution	Unirradiated pH	pH in irradiated experiment	Unirradiated TOC [mg/L]	TOC in irradiated experiment [mg/L]
DEHP	Ca(OH) ₂ solution	12.6	11.7	30	1,430
DINP	Ca(OH) ₂ solution	12.6	11.2	45.7	664

Furthermore, unirradiated controls of both plasticisers were also aged for 120 days in contact with the Ca(OH)₂ solution. The GC-MS analysis results of the aqueous Ca(OH)₂ solutions in contact with unirradiated DEHP control are shown in Table 44. The experiments have shown that fewer species went into solution in the absence of radiation. The data in Table 44 show that the phthalate anion and Phtalanone were found in the Ca(OH)₂ control solution.

Table 44: GC-MS analysis data for unirradiated aqueous solution controls in contact with DEHP [Baston 2014]

Sample	Organic compound detected	Concentration [mg/L]
Ca(OH) ₂ solution in contact with DEHP unirradiated control	Phtalic anhydride (phtalate anion)	< 1
	Phtalanone	< 1
	DEHP	23

In the presence of gamma radiation, besides the hydrolysis products, many different organic compounds were detected in the DEHP and DINP materials themselves and also in the aqueous solutions. However, most of these compounds could not be identified [Baston 2014]. The analysis results of the Ca(OH)₂ solutions that were irradiated to ~10 MGy in contact with DEHP are shown in Table 45. Note, that in the latter experiments also 13 components were found which could not be identified (not shown in Table 45).

Table 45: GC-MS analysis data for aqueous Ca(OH)₂ solutions irradiated to 10 MGy in contact with DEHP [Baston 2014]

Sample	Organic compound detected	Concentration [mg/L]
Ca(OH) ₂ solution in contact with DEHP	Ethylhexanol	49
	Phtalic anhydride (phtalate anion)	3.0
	DEHP	990

Table 46 shows the result of the GC-MS analysis with unirradiated Ca(OH)₂ solution in contact with DINP.

Table 46: GC-MS analysis results for unirradiated aqueous solution controls in contact with DINP [Baston 2014]

Sample	Organic compound detected	Concentration [mg/L]
Ca(OH) ₂ solution in contact with DINP unirradiated control	Unknown	< 1
	Methyloctanol	< 1
	Phtalic anhydride (phtalate anion)	1,1
	Phtalanone	4,7
	Phtalate (DINP)	3,000

Table 47 shows the result of the GC-MS analysis with irradiated Ca(OH)₂ solution in contact with DINP.

Table 47: GC-MS analysis results for irradiated aqueous solution in contact with DINP [Baston 2014]

Sample	Organic compound detected	Concentration [mg/L]
Ca(OH) ₂ solution in contact with DINP irradiated to 10 MGy	Unknown	1.7
	Unknown	1.5
	Unknown	2.0
	Unknown	8.4
	Unknown	1.9
	Methyloctanol	4.9
	Phtalanone	1.0
	Phtalate (DIDP)	1,100

By evaluating the GC-MS analysis results, it was suggested by [Baston 2014], that the principal mode of degradation of phtalates in both the irradiated samples and unirradiated controls was hydrolysis. It was found that this process forms phtalic acid or phtalate and alcohol for both plasticisers. As with the experiments with DEHP, similar generic observations were made for the solutions which were in contact with DINP when aged. Many compounds were detected after irradiation compared with few in the controls [Baston 2014]. According to [Baston 2014], fewer compounds were detected in the solutions in contact with DINP as compared to those with DEHP.

One focus of the research of [Baston 2014] was to examine the stability of the two plasticisers and of other PVC leaching products. In this context [Baston 2014] carried out GC-MS analyses on the non-aqueous phase residues that remained in the vessels after irradiation and on the controls.

GC-MS analysis results for unirradiated DEHP control residues are shown in Table 48. Data for the irradiated residues are given in Table 49.

Table 48: GC-MS analysis data for unirradiated DEHP residues in contact with Ca(OH)₂ solution [Baston 2014]

Sample	Organic compound detected	Concentration [mg/L]
DEHP residue in contact with Ca(OH) ₂ solution control	Ethylhexanol	44
	5,6-dipropyldecane	6.4
	Unknown	12
	Phtalic anhydride (phtalate anion)	6.8
	Benzoic acid, 2-ethylhexyl ester	34
	Unknown	5.6
	Bis (2-ethylhexyl) maleate	30
	DEHP	6,700

Table 49: GC-MS analysis data of irradiated DEHP residues in contact with aqueous solutions [Baston 2014]

Sample	Organic compound detected	Concentration [mg/L]
DEHP residue in contact with Ca(OH) ₂ solution irradiated to 10 MGy	3-heptanol	1.1
	Heptanone	1.1
	Ethylhexanal	5.1
	Ethylhexanol	90
	Ethylhexanoic acid	8.6
	Unknown	3.1
	Phtalic anhydride (phtalate anion)	29
	Benzoic acid, 2-ethylhexyl ester	35
	Unknown	25
	unknown	15
	Methyl butyl phtalate	9.4
	DEHP	18,00

The GC-MS analysis results showed that the unirradiated DINP controls and the irradiated residues consisted of an array of different organic species [Baston 2014] (see Table 50 and

Table 51). According to [Baston 2014], phthalic anhydride was identified in each of the residue samples, both the unirradiated controls and the irradiated residues, which again was probably a result of hydrolysis.

Table 50: GC-MS analysis results for unirradiated DINP residues in contact with aqueous solutions [Baston 2014]

Sample	Organic compound detected	Concentration [mg/L]
DINP residue in contact with Ca(OH) ₂ solution control	Unknown	135
	Methyloctanol	95
	1-nonanol	35
	Phtalic anhydride (phtalate anion)	110
	unknown	29
	unknown	30
	unknown	31
	unknown	29
	unknown	32
	DINP	450,000

Table 51: GC-MS analysis results for irradiated DINP residues in contact with aqueous solutions [Baston 2014]

Sample	Organic compound detected	Concentration [mg/L]
DINP residue in contact with Ca(OH) ₂ solution irradiated to 10 MGy	Unknown	280
	Unknown	320
	Unknown	1,100
	Unknown	280
	Phtalic anhydride (phtalate anion)	420
	Unknown	70
	Unknown	90
	Unknown	86
	Unknown	100
	Unknown	60
	Unknown	50
	Unknown	50
	Unknown	40
	DINP	260,000

The experiments with DINP showed similar effects as those with DEHP where the irradiated residue consisted of an array of different organic species (degradation products). Phtalic anhydride was detected in each of the residue samples, both in unirradiated controls and the irradiated residues which was probably a result of hydrolysis [Baston 2014]. In both irradiation experiments the concentrations of phtalic anhydride were significantly higher than in the unirradiated controls [Baston 2014].

To conclude, the experiments regarding the radiation stability of DEHP and DINP in contact with Ca(OH)₂ produced high levels of TOC in the solutions in absence of gamma radiation. The measured TOC levels for the solution in contact with the phtalates and irradiated to 10 MGy were, however, significantly higher [Baston 2014].

The plasticisers DEHP and DINP showed signs of hydrolysis when aged in contact with the unirradiated aqueous solutions and the quantity of hydrolysis products increased significantly when exposed to 10 MGy of radiation. Both plasticisers generated phtalic anhydride and the appropriate alcohols as hydrolysis products. The findings suggested that although hydrolysis occurs in the phtalates in absence of radiation, the exposure to radiation appears to accelerate the hydrolysis reactions at the different solution pHs and a

wide range of organic degradation products are produced but remained unidentified [Baston 2014].

In the framework of their study, [Baston 2014] analysed the aqueous solutions irradiated in contact with the plasticisers DEHP and DINP by using ion chromatography. Considering the high TOC measured (see above), according to [Baston 2014] it was surprising to observe that the organic anion concentrations were low. Irradiation to 10 MGy seemed to have generated more acetate and formate/lactate ions in solution than the controls. It could not be found why the concentrations of organic anions are so low despite the high levels of TOC [Baston 2014]. Table 52 (DEHP) and Table 53 (DINP) shows the results of these investigations.

Table 52: Ion chromatography data in mg/L for organic anions in the solutions in contact with DEHP: unirradiated controls and at 10 MGy [Baston 2014]

Condition	Glycolate (OCH ₂ CH ₂ O ²⁻)	Acetate (CH ₃ COO ⁻)	Lactate (CH ₃ CH(OH)COO ⁻) or Formate HCOO ⁻	Propionate C ₂ H ₅ COO ⁻	Oxalate (COO) ₂ ²⁻
Ca(OH) ₂ solution, pH ~ 12.4 control	ND	X	X	ND	~ 1,4
Ca(OH) ₂ solution, pH ~ 12.4;10 MGy	~ 0.1	~ 1.4	~ 1.6	X	~ 2.7

X: the peak was present but could not be quantified. ND: peak was not observed.

Table 53: Ion chromatography data in mg/L for organic anions in the solutions in contact with DINP: controls and at 10 MGy [Baston 2015]

Condition	Glycolate (OCH ₂ CH ₂ O ²⁻)	Acetate (CH ₃ COO ⁻)	Lactate (CH ₃ CH(OH)COO ⁻) or Formate HCOO ⁻	Propionate C ₂ H ₅ COO ⁻	Oxalate (COO) ₂ ²⁻
Ca(OH) ₂ solution, pH~12.4 control	ND	X	X	ND	~ 1,5
Ca(OH) ₂ solution, pH~12.4;10 MGy	X	~ 0,5	~ 0,8	ND	~ 1,5

To conclude, a scoping study regarding the radiation stability of plasticisers in contact with Ca(OH)₂ solution was carried out by [Baston 2014]. The samples were aged under irradiation and in absence of irradiation, respectively. GC-MS analyses results suggested that the principal mode of degradation in the irradiated and unirradiated samples was hydrolysis, resulting in the formation of phtalic acid or phtalate and alcohol for both plasticisers. When gamma radiation is present, in addition to hydrolysis products many different organic compounds were detected (but many could not be identified) in the DEHP and DINP materials themselves and also in the aqueous solutions.

5.5.4.2. Microbial degradation

No specific studies regarding the microbial degradation of plasticisers/NAPLs under expected near-field conditions (high pH) exist. Most of the available literature on microbial degradation of PVC and its additives regard landfill conditions [Smith 2013]. Thus, the fate of plasticisers under landfill conditions is presented in this section to act as generic indicator (landfill conditions are not strictly comparable to a cementitious waste repository) of the effect on PVC and its additives.

The evolution of a landfill can be distinguished in four phases [Jonsson 2003]:

- 1) oxic phase with aerobic degradation
- 2) acidogenic conditions with acid fermentation
- 3) methanogenic phase, production of methane
- 4) diffusion of O₂ into the landfill, commencement of oxic degradation

Under these conditions, no PVC degradation was ever observed. However, the leaching of the plasticisers employed in the organic materials is considered to be of most concern. The degradation pathways of phthalic acid esters (present at intermediate pH levels) and their corresponding diesters have been studied under oxic and anoxic conditions. The primary degradation pathway is the hydrolysis of the phthalates to diesters, alcohols and monoester intermediates before finally forming phthalic acid. Monoesters occur under aerobic and anaerobic conditions since the mechanism is similar in both regimes.

The fate of the phthalic acid depends however on the environment. In aerobic conditions, phthalic acid is oxidised to 4,5- or 3,4-dihydroxyphthalate before being converted to key intermediates in common biochemical pathways. In anaerobic conditions, phthalic acid is decarboxylated to benzoate which then is reduced and the ring structure cleaved. Final products are H_2 , CO_2 and acetates [Mersiowsky 2001]. Typical plasticisers have thus been shown to be biodegradable by microbes present in landfills. High concentrations of phthalic acid were found in landfill leachates, indicating that the phthalic diesters and monoester intermediates are hydrolysed to phthalic acid but that conversion from phthalic acid to final degradation products (CH_4 and CO_2) by microbes occurs much less readily [Smith 2013]. It can be concluded that under landfill conditions, the micro flora should be capable of a complete biodegradation of phthalates into biogas dependent upon contact time and concentration [Smith 2013].

In the cementitious waste repository, highly alkaline conditions are expected and maintained for a long time. It cannot be excluded that areas evolve with lower pH where microbial activity (and thus phthalate degradation) may take place. However, there remains uncertainty whether this localisation of microbes will be the case over the long-term or whether the microbes will adapt to the conditions and become more widespread [Smith 2013]. Thus, the levels to which microbial degradation of plasticisers occur in a cementitious waste repository is also uncertain.

To summarise, the expected geochemical conditions in the planned repository will be hostile to phthalate plasticisers. In the moment they diffuse out of the polymer, they are in contact with high pH cementitious pore water and ionizing radiation, all of which are likely to promote the decomposition into calcium phthalate (which is not a NAPL) and alcohol, which however could be a NAPL. In the longer term, it cannot be excluded that microbes start to contribute to plasticiser degradation - if the latter are still present at that point in time. Thus, although there is a possibility that plasticisers may form NAPLs, the fate of the plasticisers themselves can be expected to be short lived. Note that the likely production of $C_8 - C_{10}$ alcohols from the most common plasticisers DEHP, DINP and DIDP will also be subject to the discussed degradation mechanisms and their fate will be probably determined by their radiation stability (as they are expected to be stable at alkaline pH). Radiolysis of these alcohols will eventually result in the generation of low molecular weight and gaseous species but their eventual fate is at this stage unknown [Smith 2013].

5.6. Rubbers

5.6.1. General information

Rubbers or elastomers are polymers with high molecular weights that usually have been crosslinked. Crosslinking is an irreversible process where the elastomers undergo a change in their chemical structure. Thus, the elastomer becomes less plastic and more resistant to swelling by organic liquids and their elastic properties are improved. By means of crosslinking, the molecules are tied together by permanent chemical bonds to give the material a three-dimensional network. Most common methods use sulfur as the crosslinking agent forming mainly polysulfide ($-C-S_x-C-$), disulfide ($-C-S-S-C-$) or monosulfide ($-C-S-C-$) crosslinks [Cohen 2006]. Elastomers have the property of long-range reversible extensibility

under relatively small applied stress. Rubbers can be natural or synthetic. Natural rubbers (or caoutchouc) refer to a coagulated or precipitated product obtained from latex of rubber plants (*Hevea brasiliensis*), which develops nonlinked but partially vulcanisable polymer chains with molecular masses of $\sim 10^6$ Da with elastic properties [Rose 2005]. Natural rubber is a polymer and consists of isoprene (C_5H_8) monomer units each containing one double bond in the cis configuration. Examples of synthetic rubbers are polyisoprene (Figure 27), styrene butadiene rubber and butyl rubber [Cohen 2006].

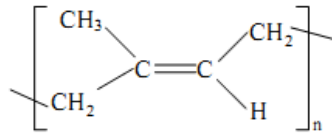


Figure 27: Structure of polyisoprene [Cohen 2006]

Further synthetic rubbers are Neoprene and Hypalon®. Neoprene is based on polychloroprene $[(C_4H_5Cl)_n]$ (Figure 28) and Hypalon® is a chlorosulfonated polyethylene rubber trademarked by Dupont [Cohen 2006]. Neoprene is used in the industry for more than 75 years. The structure of neoprene can be chemically modified (e.g. by adding additives or by copolymerisation with sulphur) to generate an elastomer with the required properties. Thus, neoprene can be obtained in a wide range of compositions according to their specific application [Dawson 2013c]. According to [Dawson 2013c], Hypalon® is available as a series of materials with various formulations to suit different applications. Its production by DuPont™ however ceased in 2010.

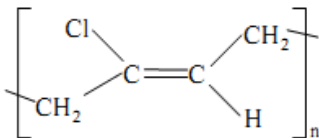


Figure 28: Structure of Neoprene (poly(2-chloro-trans-2-butene)) [Cohen 2006]

In general, elastomers have a large amount of unsaturation (C=C bonds) in their polymer backbone. Through crosslinking, the elastomer molecules are bound together by a few permanent chemical bonds which give the material a 3-dimensional network with a stable form improving the rubber properties. The most common method uses sulfur as the crosslinking agent. The crosslinks generated by this system are mainly polysulfide (-C-S_x-C-), disulfide (-C-S-S-C-) or monosulfide (-C-S-C-) which have different properties [Cohen 2006].

Rubber materials likely to be present in the LILW of the potential Dutch repository are Neoprene and Hypalon since they are used in the form of gaiters, gloves and seals. These materials are soft rubber formulations and therefore their plasticiser content will be high [Dawson 2012].

Further rubber materials, which also cannot be excluded to be present, are natural rubber, nitrile, silicone, ethylene-propylene rubbers, ethylene vinyl acetate and fluoroelastomers [Dawson 2012].

Rubbers generally differ widely regarding their formulations and their composition varies considerably from manufacturer to manufacturer. The typical rubber might contain a polymeric component of only about 50 % of the total composition [Dawson 2012]. Typical Neoprene and Hypalon® formulations are shown in Table 54. It can be seen that the main constituents of rubbers are the base polymer, fillers and plasticisers with further additives such as anti-oxidants, dispersants and vulcanizing agents [Dawson 2012]. According to [Dawson 2012], the principal organic materials that would be expected to contribute to NAPL formation are the base polymers and the plasticisers.

Table 54: Example Neoprene and Hypalon rubber formulations [NDA 2012]

Neoprene			Hypalon		
Ingredient Generic	Ingredient Specific	Parts per hundred parts of base polymer	Ingredient Generic	Ingredient Specific	Parts per hundred parts of base polymer
Base Polymer	Neoprene	100	Base Polymer	Hypalon	100
Filler/Stabiliser	Clay	35	Filler/stabiliser	MgO	10
Plasticiser	Typically phthalate esters	32	Plasticiser	Typically phthalate esters	30
Others (vulcanising agents, dispersants, antioxidants)		14	Others (vulcanising agents, dispersants, antioxidants)		13

It is assumed that only Neoprene will make up the rubber LILW inventory. According to [Dawson 2012], the plasticiser loading for this material is 0-50 parts per hundred of rubber component. The plasticiser content in a gaiter/glove formulation will be high and when assessed in terms of all the additives, a mean average plasticiser content of about 20 % by total weight can be assumed. Typical plasticisers employed are esters (phtalates, adipates, azelates, phosphates), epoxidised soya bean oil, aromatic petroleum oils and rapeseed oil. All those substances have very limited solubility, low density and are potential buoyant NAPL [Dawson 2012]. For this study, an upper-bound estimate of 20 % plasticisers is assumed as the bulk of the inventory will possibly be soft rubber. If it is assumed that 5 % of the LILW in the 200 L containers are rubbers, the total rubber mass is 1,285 t.

5.6.2. Chemical degradation

Studies researching the chemical degradation of rubbers under relevant alkaline (cementitious) conditions could not be found. However, an experimental study investigating the radiolytic degradation of neoprene under alkaline conditions investigated the degradation products of also unirradiated samples. The results of that study will be - for space-saving reasons - discussed in section 5.6.3.

5.6.3. Radiolytic degradation

The mechanism of rubber decomposition due to ionizing radiation strongly depends on whether oxygen is present [Cohen 2006]. According to [Cohen 2006], the radiation induced degradation of rubber is likely to proceed via different mechanisms during the initial aerobic phase and during the later anaerobic phase of the potential repository. Many of the past studies regarding radiation effects on different rubbers focused on the physical properties and not on the chemical changes [Cohen 2006]. As discussed by [Blow 1982], all vulcanized rubbers deteriorate under prolonged exposure to radiation, mostly by hardening. However, butyl rubber and polysulfide rubber soften, eventually resulting in a tarry residue. The rubbers most resistant to irradiation are natural, styrene butadiene and polyacrylate elastomers. The least resistant rubbers are known to be silicone-, fluorosilicone-, and fluorocarbon rubbers [Blow 1982].

Studies regarding radiolytic degradation of rubbers under cementitious conditions are very limited. The results of a selected relevant study are presented in the following text.

As discussed in section 5.7.3, [Dawson 2013c] carried out investigations regarding the NAPL production of ion exchangers under irradiation. In the context of this study, also the irradiation behavior of rubbers was investigated.

The irradiation effects in aqueous environments on neoprene samples were investigated under the following (amongst others) conditions in glass vessels under air [Dawson 2013c]:

- Ca(OH)_2 solution (+ solid Ca(OH)_2) at pH 12.4 to 10 MGy at 4 kGy/h
- Ca(OH)_2 solution (+ solid Ca(OH)_2) at pH 12.4 to 150 kGy at 49 Gy/h and 4 Gy/h

In order to analyse evolved gases, samples of each polymer were also irradiated separately in glass vessels under the following conditions [Dawson 2013c]:

- Air to 10 MGy at 4 kGy/h
- Air to 150 kGy at 49 Gy/h and 4kGy/h
- Nitrogen to 10 MGy at 4 kGy/h
- Nitrogen to 150 kGy at 49 Gy/h and 4 kGy/h

A flexible neoprene sheet (thickness 2 mm) was obtained from the company RS Components to be used for the experiments. The samples were cut from the sheet in squares weighing appr. 20 g and placed in separate, stoppered glass vessels with the Ca(OH)_2 solution [Dawson 2013c].

The values of the pH for the leachates from the irradiation of the neoprene samples are shown in Table 55. As neoprene is a polychloroprene, an increase in acidity due to HCl release might have been expected but was not observed by [Dawson 2013c]. Due to the solid Ca(OH)_2 present in the solutions, the pH remained about 12.4. TOC values ranged from 10 - 33 mg/L [Dawson 2013c]. Table 55 shows that increases in TOC were observed after irradiation.

Table 55: pH values of solutions with irradiated Neoprene samples [Dawson 2013c]

Polymer	Liquid	Dose rate [Gy/h]	Dose [kGy]	pH	TOC [mg/L]
Neoprene	Ca(OH)_2	4k	10,000	12.52	10
		49	150	12.60	20
		4k	150	12.50	33
		0	0	12.58	8.7
None	Ca(OH)_2	0	0	12.56	-

As for the experiments with the ion exchangers (see section 5.7), [Dawson 2013c] carried out organic screening tests by means of GC-MS in the context of the experiments described above. Aim was to establish whether organic degradation products of sufficient molecular weight could be NAPL. Table 56 shows the identified species from the irradiation of neoprene. According to [Dawson 2013c], some of the identified species are potential NAPL, for example n-methyl-aniline. The most abundant organic compound that was tentatively identified was n-methyl-aniline ($\text{C}_6\text{H}_5\text{NH}(\text{CH}_3)$). Besides the organic compounds identified from the irradiated neoprene, also organic species were identified from the unirradiated control in Ca(OH)_2 solution. In the unirradiated Ca(OH)_2 solution, tricosane ($\text{C}_{23}\text{H}_{48}$), hexadecane ($\text{C}_{16}\text{H}_{34}$) and tetramethyl hexadecane ($\text{C}_{20}\text{H}_{42}$) were the most abundant identified components. According to [Dawson 2013c], these compounds diffused out of the neoprene into the Ca(OH)_2 solution. Thus, these compounds can be expected to be present if only chemical degradation under alkaline conditions takes place. Exposed to gamma radiation, the mentioned compounds likely have undergone radiolysis to lower molecular weight species and were not detected in the later GC-MS analyses [Dawson 2013c].

Table 56: GC-MS analysis results for neoprene irradiated in solution with TOC data for comparison [Dawson 2013c]

Irradiation conditions	Tentative identification of Amberlite degradation products	Concentration [µg/l]	Detection level [µg/l]	TOC [µg/l]
150 kGy at 49 Gy/h in Ca(OH) ₂ , pH 12	Tetrachloroethylene	50	70	33,000
	N-methyl-aniline C ₆ H ₅ NH(CH ₃)	100		
	Nitro-benzene	30		
	Isothiocyanato-cyclohexane	30		
	Benzothiazole	70		
	Benzothiazolone	20		
	Mercaptobenzothiazole	20		
No irradiation, Ca(OH) ₂ , pH 12	N-methyl-aniline, C ₆ H ₅ NH(CH ₃)	100	60	8,700
	Nonadecane	40		
	Eicosane	40		
	Chloro-octadecane	20		
	Ditertbutyloxaspirodecadienedione	20		
	Heptadecane	30		
	Methanobenzocyclodecene	2		
	Tricosane (C ₂₃ H ₄₈)	200		
	N-methyl-chlorobenzenesulfonamide	50		
	Docosane	5		
	Heneicosane	30		
	Hexadecane (C ₁₆ H ₃₄)	400		
	Tetramethyl-hexadecane (C ₂₀ H ₄₂)	500		
	Dimethylpentyl-cyclohexane	20		
	Dimethylsilafuorene	60		
	Hydrazono-hydroxyimino-tetrahydrobenzofuroxane	70		

Regarding the visual appearance of the solutions after irradiation of neoprene, [Dawson 2013c] could not identify any visible signs of NAPL as bulk insoluble phase in the Ca(OH)₂ solutions. No changes were observed in the neoprene appearance after irradiation, although the flexibility decreased on irradiation in all environments but the flexibility decreased on irradiation.

As a first estimate for potential NAPL yields, in the analyses for the liquids in which the neoprene was irradiated, all of the GC-MS data for each condition were banded by [Dawson 2013c]. As a worst case, it was assumed that all organic compounds identified by GC-MS are potential NAPL and the concentrations of each of the identified compounds were summed at the particular conditions (Table 57). Since the original sample weights were 20 g and irradiated in 100 cm³ of solution, it can be estimated based on these data that the neoprene produced 35.5 µg of potential NAPL. Extrapolation to larger masses would equate to 1.8 g/t at 10 MGy. The estimates for the other conditions are given in Table 57. The generated amount of NAPLs due to degradation of rubber is -when the data in Table 57 is used- negligible.

Table 57: Sum of identified species in the particular experiments and estimated amounts of NAPL [Dawson 2013c]

Irradiation conditions	Total concentration of identified species [µg/L]	Estimates of potential NAPL [g/t]
10 MGy at 4 kGy/h, pH >12	355	~1.8
150 kGy at 49 Gy/h, pH >12	320	~1.6
No irradiation, pH>12	1,587	~7.9

As also for the ion exchangers (see section 5.7), [Dawson 2013c] report also evaluated the amount of gas evolved during irradiation of neoprene and investigated the effect of the irradiation atmosphere.

[Dawson 2013c] used irradiation to 10 MGy at 4 kGy/h and 150 kGy with doses rates of 49 Gy/h and 4 kGy/h. The gas analysis results are shown in Table 58. G-values (the number of gas molecules generated per 100 eV of radiation absorbed) are also given for CO₂ (GCO₂) [Dawson 2013c]. According to [Dawson 2013c], the light gas data for the neoprene samples irradiated in air and nitrogen suggest that there was no major difference between the gases evolved and the environment in which they were irradiated.

Table 58: Gas analysis data [ppm] after irradiation of neoprene in air and nitrogen [Dawson 2013c]

Light gas species	10 MGy, N ₂	150 kGy, 49 Gy/h, N ₂	150 kGy, 4 kGy/h, N ₂	10 MGy, Air	150 kGy, 49 Gy/h, Air	150 kGy, 4 kGy/h, Air
Methane (CH ₄)	37	< 2	7	45	< 2	15
Carbon Monoxide (CO)	26	24	42	29	48	350
Carbon Dioxide (CO ₂)	2,440	1,240	4,650	2,770	1,720	3,930
GCO ₂ (molecules per 100eV)	0.001	0.04	0.13	0.001	0.05	0.11
Ethane (C ₂ H ₆)	7	>2	2	3	2	< 2
Ethene (C ₂ H ₄)	< 2	< 2	2	< 2	< 2	< 2
Ethyne (C ₂ H ₂)	< 2	< 2	< 2	< 2	< 2	< 2
Total C ₃	< 2	< 2	< 2	3	2	< 2
Hydrogen (H ₂)	< 5	< 5	8	< 5	< 5	22

[Dawson 2013c] found that the irradiation environment experiments with irradiated neoprene showed no significant effect associated with the irradiation environment but the light gas analysis suggests that there may be a dose rate effect. In general, larger concentrations of organic species were observed in the solutions with samples irradiated to 150 kGy compared to those at 10 MGy. According to [Dawson 2013c], this is attributed to the continued radiolysis of polymer degradation products to lower molecular weight organic species which can eventually reduce to carbon dioxide and water.

5.6.4. Microbial degradation

Efforts to investigate the microbial degradation of natural rubber have been undertaken since the beginning of the 20th century [Rose 2005]. However, no literature data could be found regarding the investigation of microbial (natural or synthetic) rubber (i.e. neoprene) degradation under high pH conditions. The reason is probably due to the recent development and manufacture of synthetic rubbers and the very slow rate of degradation in natural environments [Shah 2013]. However, a brief overview regarding the current level of knowledge on biodegradation of synthetic rubbers will be given.

In general, studies of biodegradation of natural and synthetic rubber are made difficult due to several facts. The degradation of rubber is a slow process and the growth of bacteria using rubber as a sole carbon source is also slow. Additives eventually present in the polymers may also hinder or promote biodegradation. In general, incubation times

extending weeks or even months are needed to gain enough cell mass or rubber degradation products for further analysis [Rose 2005].

Biodegradation is generally influenced by different factors which include the polymer characteristics, organism type and nature of pretreatment. Polymer mobility, tacticity, crystallinity, molecular weight and the type of functional groups and substituents all influence its degradation [Shah 2013]. When O₂ is available (e.g. in the aerobic phase of the repository), aerobic microbes are responsible for the degradation and the degradation products will be CO₂, H₂O and microbial biomass. In anoxic conditions, anaerobic microbes will degrade polymers and the degradation products will CO₂, CH₄ and H₂O under methanogenic conditions or H₂S, CO₂ and H₂O under sulfidogenic conditions.

Rubber-degrading bacteria are divided into two groups characterized by their growth type and other characteristics. The first group are Actinomycetes forming clear zones on latex plates and metabolize polyisoprene by secretion of one or more enzymes. Most of the representatives of this group show relatively weak growth on natural or synthetic rubber. Members of the second group do not grow on latex plates and require direct contact with a polymer. However, members of this group grow relatively strong on polyisoprene. The microbes belong to the Corynebacterium-Nocardia-Mycobacterium group [Rose 2005]. The actual degradation mechanisms for both groups have not been completely identified but it has been found by analyses of natural and synthetic rubbers isolated from various bacterial cultures, that both natural and synthetic rubbers are degraded by all strains (e.g. Nocardia Psuedomonas citronellosis) by an oxidative cleavage of the double bond in the polymer backbone [Bode 2001, Enoki]. Most degradation products contain aldehyde and keto groups that result from endo-type cleavage of the rubber, in which the polymer chains are cleaved somewhere within the chain [Rose 2005].

Several studies were carried out with different strains of rubber-degrading bacteria (e.g. Streptomyces coelicolor, Thermomonospora curvata, Streptomyces sp. strain K30 and Gordonia polyisoprenivorans strain VH 2 [Rook 1955, Tsuchii 1985, Tsuchii 1990, Heisey 1995, Jendrossek 1997, Gallert 2000, Bode 2001, Rose 2005]. The majority of these bacteria is aerobic and thus will only be active for the brief period of time until oxygen is consumed in the repository following closure.

For example, Nocardia sp. strain 835A was one of the first strains which was investigated regarding its ability to degrade synthetic rubber. It was postulated that there was oxidative cleavage of poly(cis-1,4-isoprene) at the double-bond position. This resulted in weight losses of the rubber material used of 75 and 100 %.

[Kanwal 2009] found that Bacillus sp. S-10 are able to not only degrade natural but also synthetic rubber. Rubber tyre pieces were treated with Bacillus sp. S-10 in mineral salt medium with no additional carbon source for 28 days at different temperatures. Pits and erosion in the samples were found by means of microscopy and high amounts of CO₂ were detected.

5.7. Ion exchangers

5.7.1. General information

The LILW contains besides organic material such as e.g. cellulose and plastics also spent ion-exchange resins. Ion exchange resins serve the nuclear industry in e.g. nuclear fuel reprocessing, radioisotope separation, waste management and removal of radionuclides from reactor coolants. Although the resins are designed to perform under the harsh conditions found in the nuclear industry, those polymers undergo radiation-induced chemical decomposition [Baidak 2010].

In general, ion exchangers are distinguished between cation and anion exchangers and materials which are able to remove organic compounds from the aqueous phase. The

functional groups work as base or acid (e.g. SO_3 for cation exchange resins and $\text{N}(\text{CH}_3)_3$ for anion exchange resins [Neall 1994]). Regarding its surface properties, ion exchange resins are hydrophilic as compared to pure polystyrene [Warthmann 2013].

Figure 29 shows an example of the structure of ion exchange material.

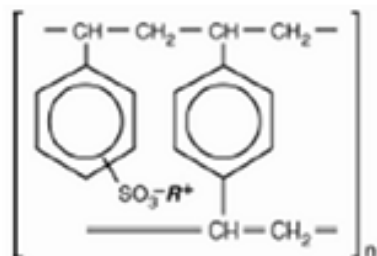


Figure 29: Chemical structure of ion exchange material based on polystyrene. The material is made of a polystyrene matrix with a functional group, here $\text{SO}_3\text{-R}^+$ ($\text{R} = \text{H}^+$ or Na^+) [Warthmann 2013]

According to [Verhoef 2016], details on the ion exchange resins in the LILW inventory are unknown and therefore [Verhoef 2016] presumes that the most common type of synthetic ion exchange resin used is polystyrene divinylbenzene in powdered form with diameters from 5-150 μm or in form of beads with diameters from 0.5 - 2 mm. Thus, in the following sections the degradation processes and products of only the mentioned type of exchange resin are discussed.

It can be assumed, that spent ion exchangers are loaded with anions, cations and eventually organic substances. Examples of spent powder ion exchange resin loadings can be found in [Verhoef 2016].

5.7.2. Chemical degradation of ion exchangers

As discussed already in section 5.5.2.1, the chemical attack of addition polymers is very limited and does not lead to the formation of organic ligands. Therefore, a purely chemical degradation of ion exchanges will not be discussed.

5.7.3. Radiolytic degradation of ion exchangers

Almost all organic substances are sensitive to irradiation. It is well known, however, that especially aromatic compounds show a large resistance to irradiation because such molecules are able to dissipate the absorbed energy without destroying the chemical bonds [Manion 1952, Burton 1954]. Strong acidic ion exchange resins can tolerate a radiation dose between 1 and 10 MGy. On the other hand, strong basic anion exchange resins have a slightly lower resistance against irradiation between 0.1 and 1 MGy absorbed dose [van Loon 1995]. The radiation effects on organic substances often require radiation sources with a high dose rate in order to carry out the experiments in a reasonable timescale. Often, the results of such experiments are extrapolated to conditions where the dose rate is significantly lower - a procedure which has often been criticised. According to [van Loon 1995] however, there exists some experimental evidence that the dose rate has no or at least little influence on the degradation processes and on the nature of the degradation products formed. Apparently, the total absorbed dose determines the amount of degradation products that will be formed. On the other hand, a minimum amount of energy is required to break bonds to initiate the degradation process.

The radiation damage induced in organic substances depends on their chemical composition and on environmental factors such as the presence of oxygen [van Loon 1995]. The chemical alterations organic substances undergo are the [van Loon 1995]:

- 1) formation of chemical bonds between different molecules

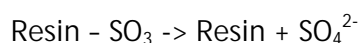
- 2) irreversible cleavage of bonds resulting in fragmentation
- 3) formation of unsaturated bonds
- 4) disappearance of unsaturated bonds.

Thus, irradiation of polymers may also have a significant effect on their physical properties [van Loon 1995]. Regarding the radiolytic degradation of polymers, process 2) is very important since it is generally observed that irradiation of polymers leads to the production of small radicals such as $\cdot\text{H}$, $\cdot\text{CH}_3$, $\cdot\text{CO}$, $\cdot\text{CO}_2$. The mentioned radicals may recombine with the polymer itself or with each other, the latter resulting in the formation of H_2 , CH_4 , C_2H_4 . Irradiation of polymers thus leads mainly to the formation of small gaseous products [van Loon 1995].

[van Loon 1995] investigated the effects of irradiation on polystyrene-based ion exchange resins under alkaline conditions. Irradiation experiments with two strong acidic cation exchange resins (Lewatite S-100 and Powdex PCH) both based on a styrene-divinylbenzene copolymer with SO_3^- groups attached to the benzene ring, were carried out. Initially, both resins were converted to the sodium form and after a set of procedures a final mixture of 100 g resin and 1000 cm^3 of 0.05 M NaOH (pH 12.7) was obtained and separated into 2 equal parts. One part was irradiated with a total absorbed dose of 1.7 MGy. The other part was not irradiated (and thus is actually a chemical degradation experiment). All solutions were analysed for pH, Na^+ , inorganic carbon (IC), DOC, SO_4^{2-} and oxalate.

In their study, [van Loon 1995] also investigated the interaction of the ion exchanger degradation products with metals. This required the development of a new technique since the ligands were present at low concentrations. In this context the ion exchange method was further developed for element quantification. This method employs trace metal concentrations to determine the stability constants of metal-ligand complexes by measuring the solid-liquid distribution coefficient of the metal in absence and presence of the ligand. In case of an unknown ligand at trace level concentrations, its concentration (and stability constant) can be determined by using the ion exchange method: a solution is titrated with a metal (i.e. Cu and Ni) in presence of the ion exchange resin. By monitoring the partition coefficients of the metals in presence and absence of the ligand as a function of the total concentration of the metal in solution, the end-point of the titration can be determined [Van Loon 1995]. By solving a number of equations and regarding the mass balance of metal and ligand in solution, the free metal concentration for a given total ligand and metal concentration can be calculated. Please refer to [Van Loon 1995] for further information regarding the theory of the ion exchange method.

Table 59 shows chemical compositions of the different solutions with and without irradiation. In absence of irradiation, no evidence for the formation of complexing ligands was found. This is explained by the high resistance of addition polymers towards alkaline solutions (see section 5.7.2). In the irradiated resin solution, the concentrations of Na^+ , SO_4^- , DOC, inorganic carbon and oxalate are significantly higher than in the non-irradiated waters [van Loon 1995]. According to [van Loon 1995], the SO_4^{2-} concentration in the solutions is caused by splitting off of the sulfonic acid groups, followed by oxidation of the SO_3 formed to SO_4^{2-} :



[van Loon 1995] could not explain the increase in oxalate concentration but assumed that it might have been formed by $\cdot\text{COO}^-$ radicals generated by the oxidative degradation of the resins because two such radicals can condense to form an oxalate molecule.

Table 59: Water compositions with irradiated and non-irradiated strong acidic cation exchange resins [van Loon 1995]

Name	Dose [Mgy]	pH	DOC [mM]	IC [mM]	SO ₄ ²⁻ [mM]	Ox [mM]	Na ⁺ [mM]
Lewatite S-100 (Cu-titration)							
LB1	1.7	11.80	2.8	9.3	24.8	0.23	71
LU1	0	12.74	1.0	0.8	0	0	48
Powdex PCH (Cu-titration)							
PB1	2.17	10.21	8.7	13.3	25.5	0.46	76
PU1	0	12.81	0.3	1.7	0	0	48
Lewatite S-100 (Ni-titration)							
LB2	1.7	11.73	2.9	9.8	21.6	0.31	70
LU2	0	12.75	1.3	1.5	0	0	48
Powdex PCH (Ni-titration)							
PB2	1.7	11.85	4.2	10.9	17.0	0.26	68
PU2	0	12.60	0.4	3.2	0	0	49

Ox = Oxalate, PB = Powdex, irradiated; PU = Powdex, non-irradiated, LB = Lewatite, irradiated, LU = Lewatite, non irradiated

According to [van Loon 1995], Oxalate contributes to only 10-15 % of the DOC for the Powdex resin and to 20-30 % in case of the Lewatite resin. The remainder could not be identified. It was furthermore concluded, that the rather low DOC/SO₄²⁻ ratio indicates that the radiolytic degradation of these resins is mainly the splitting off of the SO₃ groups and that the organic backbone of the resins seem hardly to be affected due to its aromatic character. [van Loon 1995] further observed that the generated CO₃²⁻ in solution was produced by the CO₂ generated from the organic matrix by irradiation. The formation of CO₃²⁻ and SO₄²⁻ is accompanied by H⁺ generation which leads to a pH decrease which also was observed in the irradiated solutions. The pH drop is caused mainly by the oxidation of SO₃ to SO₄²⁻ [van Loon 1995]. [Van Loon 1995] furthermore carried out complexation studies with Cu²⁺ and Ni²⁺ (for details please refer to the mentioned study) which showed the presence of two organic compounds: oxalate and a so-called unidentified ligand X. This ligand was characterized by its concentration (10⁻⁵ - 10⁻⁶ M) and a complexation constant for the NiX complex (log K_{NiX} ~ 7.0 at I =1 and 25 °C).

In their study, [Van Loon 1995] found by means of thermodynamic modelling that oxalate has a significant influence on Ni speciation at concentrations above 0.1 M in fresh cement pore water (pH > 12.5). However, according to [Van Loon 1995] such high oxalate concentrations will not be reached because the precipitation of calcium oxalate solids limits the oxalate concentration in solution. [Van Loon 1995] found that the maximum aqueous oxalate concentration is 10⁻⁴ M based on the solubility of Ca-oxalate (no Ni-oxalate complexes are formed at this low oxalate concentration). Thus, for oxalate no significant influence can be expected on the Ni speciation in cement pore waters. [Van Loon 1995] furthermore investigated the effect of the unidentified ligand X on Ni speciation. According to their modelling results, Ligand X is predicted to have a significant effect on Ni speciation in fresh cement pore water (pH > 12.5) only if the ligand concentration is higher than 10⁻³ M.

Regarding oxalate, no significant influence on the speciation of radionuclides is expected. The stronger complexing ligand X may exert some influence depending on its concentration and the values of other parameters. In the absence of irradiation, no evidence for the formation of complexing ligands was found [Van Loon 1995].

In their study, [van Loon 1995] also irradiated strong basic anion exchange resins (Powdex PAO and Lewatite M-500, both based on a styrene-divinylbenzene copolymer). In the framework of their experiments, the anion exchange resins were converted to the OH-form. Part of the solution was put into a container for irradiation in a ⁶⁰Co-cell. Volatile

degradation products could also be collected in the experimental setup employed. The temperature of the reaction mixture was kept at 25 °C and irradiated for about 10 days.

Table 60 shows the most important degradation products and measured concentrations arising during the radiolytic degradation of anion exchange resins compiled by [van Loon 1995]. According to [van Loon 1995], the most important radiolytic degradation products observed are amines such as ammonia, methylamine, dimethylamine and trimethylamine. These compounds do not form stable complexes with most metal cations and thus cannot influence their speciation under alkaline conditions [Van Loon 1995].

[van Loon 1995] furthermore found in complexation studies with Eu^{3+} , that the complexing capacity of the degradation products under near-field conditions was negligible but that the speciation of cations (Ag, Pd and to a smaller extent also Ni and Cu) can be influenced by the presence of amines. According to [van Loon 1995], the strongest amine-complexes are formed with Pd. In the absence of irradiation, also with the anion exchange resins no evidence for the formation of ligands was found.

[Van Loon 1995] investigated furthermore the irradiation of a mixed bed ion exchange resin (Amberlite MB1, composed of an Amberlite IR-120 cation exchange resin and an Amberlite IRA-420 anion exchange resin, ratio 1:1). The resin was equilibrated with 0.05 M NaOH and irradiated in a ^{60}Co -cell for 10 days. The solutions were analysed for pH, DOC, sodium, oxalate, sulphate and amines.

The results (i.e. water compositions) of the irradiation experiments carried out by [van Loon 1995] with the mixed bed resin (Amberlite MB1) are also shown in Table 60. As can be seen, only small amounts of sulphate (the main degradation product of cation exchange resins) and amines (the main degradation products of anion exchange resins) are present in the solution. According to [van Loon 1995], the carbon calculated from the amines present in the solution is only 3 % from the measured carbon. Furthermore, the sulphate is only a small fraction (0.1 %) of the total sulphur present in the solution. [van Loon 1995] concludes from these facts that other degradation products were formed during the irradiation of the mixed bed resin. Since the Na^+ and pH are increased in the irradiated solution, [van Loon 1995] concludes that surface $-\text{SO}_3$ and $-\text{N}(\text{CH}_3)_3$ groups have been split off from the polymer backbone. The authors assume that the low concentrations of sulphate and amines are due to recombination of the radicals produced from both types of resins, resulting in a kind of sulpho-amine product [van Loon 1995].

As Table 60 shows, the DOC content of the irradiated water is high compared to the non-irradiated waters.

Table 60: Water compositions with irradiated and non-irradiated anion (Powdex/Lewatite) and mixed bed (Amberlite) exchange resins [van Loon 1995]. Concentrations given in [mM]

Name	Dose [MGy]	pH	DOC	SO ₄ ²⁻	Ox*	Na ⁺	NH ₃	Methyl amine	Dimethyl amine	Trimethyl amine
Powdex PAO										
P-PAO-B	1.7	12.45	139	0.29	nd	48	21	5.6	11.1	11.4
P-PAO-U	0	12.7	3.2	0.12	nd	50	nd	n.d.	nd	nd
¹)P-H ₂ SO ₄		nm	64.0	nm	nm	nm	5.3	0.93	0.42	0.26
Lewatite M-500										
L-M500-B	1.7	12.66	268	0.08	nd	53	18	9.8	19.0	14.0
L-M500-U	0	12.67	0.78	0.08	nd	53	nd	nd	nd	nd
¹)L-H ₂ SO ₄		nm	58.8	nm	nm	nm	1.9	0.51	2.4	17.0
Amberlite MB1										
A-MB1-B	1.7	12.92	20.5	²)0.12	nd	89	1.1	0.23	0.13	0.04
A-MB1-U	0	12.66	0.26	nd	nd	49	0.2	nd	0.03	0.07
¹)A-H ₂ SO ₄		nm	7.4.	nm	nm	nm	6.3	0.30	0.62	3.53

*Ox: Oxalate

nd: not detectable; nm: not measured

P-PAO-B: Powdex, irradiated; P-PAO-U: Powdex, not irradiated; L-M500-B: Lewatite, irradiated; L-M500-U: Lewatite, not irradiated; A-MB1-B: Amberlite, irradiated; A-MB1-U: Amberlite, not irradiated

¹) H₂SO₄ phase used to collect the volatile degradation products (amines)

[Van Loon 1995] concluded from their study that the radiolytic and chemical (alkaline) degradation products of organic ion exchange resins in general will have no or only negligible influence on the radionuclide speciation in a cementitious near-field.

[Dawson 2013c] carried out an empirical investigation into the potential for the production of non-aqueous phase liquids (NAPL) from sulphonated styrene-divinylbenzene cation exchange resin (Amberlite IR-120, H⁺-form, spherical beads) (and also polychloroprene (neoprene)). The irradiation effects in aqueous environments on Amberlite cation exchange resin beads was investigated under the following conditions (excerpt) in glass vessels under air [Dawson 2013c]:

- Ca(OH)₂ solution (+ solid Ca(OH)₂) at pH 12.4 to 10 MGy at 4 kGy/h
- Ca(OH)₂ solution (+ solid Ca(OH)₂) at pH 12.4 to 150 kGy at 49 Gy/h and 4 Gy/h

In order to analyse evolved gases, samples of each polymer were also irradiated separately in glass vessels under the following conditions [Dawson 2013c]:

- Air to 10 MGy at 4 kGy/h
- Air to 150 kGy at 49 Gy/h and 4kGy/h
- Nitrogen to 10 MGy at 4 kGy/h
- Nitrogen to 150 kGy at 49 Gy/h and 4 kGy/h

According to [Dawson 2013c], no non-aqueous phases (NAPL) were visually observed in the liquids after irradiation. Furthermore, high levels of TOC were detected in the solutions in which the amberlite was irradiated but the compounds in the range C₅-C₂₂ could not be identified. [Dawson 2013c] suggested that if any C₅-C₂₂ compounds were formed, they could have experienced further radiolytic degradation to lower molecular weight species [Dawson 2013c].

Regarding the pH values recorded for the leachates, it was shown that the pH of saturated Ca(OH)₂ solutions remained at ~ 12.6 as expected due to the solid Ca(OH)₂ present. The values of the measured pH in solution in presence and absence of amberlite in Ca(OH)₂ solution are shown in Table 61. Furthermore, the results of the TOC measurements of the irradiation experiments with Amberlite IR-120 are shown. The TOC values range from 12 mg/L to 280 mg/L in Ca(OH)₂ solution. According to [Dawson 2013c], these data indicate that a significant amount of organic content is present in the solutions. Also, in

the unirradiated Amberlite sample solution, significant levels of organic species were found [Dawson 2013c].

Table 61: pH values of solutions with irradiated Amberlite samples [Dawson 2013c]

Polymer	Liquid	Dose rate [Gy/h]	Dose [kGy]	pH	TOC [mg/L]
Amberlite IR-120	Ca(OH) ₂	4k	10,000	12.58	12
		49	150	12.62	220
		4k	150	12.68	280
		0	0	12.61	164
None	Ca(OH) ₂	0	0	12.56	-

[Dawson 2013c] carried out also organic screening tests by means of GC-MS in the context of the experiments described above. Aim was to establish whether organic degradation products of sufficient molecular weight could be NAPL. Only for one Ca(OH)₂ solution (irradiated to 150 kGy at 49 Gy/h) individual organic species could be identified (see Table 62). The most abundant species identified was limonene. Another compound with a concentration as high as 900 µg/L was also detected but could not be identified. [Dawson 2013c] argues that if liquid organics of high carbon content were generated in any quantity from the irradiated Amberlite above their solubility limits, they would most likely be observed as a separate immiscible phase. However, no evidence of an immiscible liquid phase (NAPL) in any of the irradiated solutions could be found. On the other hand, [Dawson 2013c] also could not exclude that any immiscible phase that was generated may have been degraded down to lower molecular weight species due to radiolysis, especially at the high dose of 10 MGy.

Table 62: GC-MS analysis results for Amberlite IR-120 irradiation in solution with TOC data for comparison [Dawson 2013c]

Irradiation conditions	Tentative identification of Amberlite degradation products	Concentration [µg/L]	TOC [mg/L]
150 kGy at 49 Gy/h in Ca(OH) ₂ , pH 12	Tetrachloroethylene	80	280
	Dodecadienone, dimethyl	90	
	Ethane, tetrachloro	70	
	Limonene (C ₁₀ H ₁₆)	100	
	Hexadecane, methyl	50	
	unknown	10	
	unknown	900	
	unknown	70	
150 kGy at 4,000 Gy/h in Ca(OH) ₂ , pH 12	not measured	not measured	220
10 MGy at 4,000 kGy/h in Ca(OH) ₂ , pH 12	No unknowns detected above 70 %	Nil	12
No irradiation, Ca(OH) ₂ , pH 12	No unknowns detected above 70 %	nil	164

[Dawson 2013c] also evaluated the amount of gas evolved during irradiation of Amberlite and investigated the effect of the irradiation atmosphere (N₂ or air). [Dawson 2013c] used irradiation to 10 MGy at 4 kGy/h and 150 kGy with doses rates of 49 Gy/h and 4 kGy/h. The gas analysis results are shown in Table 63. G-values (the number of gas molecules generated per 100 eV of radiation absorbed) are also given for CO₂ (GCO₂) [Dawson 2013c]. [Dawson 2013c] concludes the following from the gas analyses:

- G_{CO₂} is of two orders of magnitude lower for Amberlite irradiated to 10 MGy compared to 150 kGy
- a higher amount of methane was produced at 150 kGy at 4 kGy/h compared to 49 Gy/h in both air and nitrogen and also, more methane was generated at 10 MGy in air compared to nitrogen
- significant amounts of H₂ could only be observed in the samples irradiated for the shortest time period (150 kGy at 4 kGy/h)

- significantly more H₂ was generated from Amberlite in air compared to nitrogen over the shorter time period.

Table 63: Gas analysis data [ppm] after irradiation of Amberlite in air and nitrogen [Dawson 2013c]

Light gas species	10 MGy, N ₂	150 kGy, 49 Gy/h, N ₂	150 kGy, 4 kGy/h, N ₂	10 Mgy, Air	150kGy, 49 Gy/h, Air	150 kGy, 4 kGy/h, Air
Methane (CH ₄)	< 2	< 2	15	71	8	39
Carbon Monoxide (CO)	26	123	78	257	45	78
Carbon Dioxide (CO ₂)	1,530	2,930	2,420	2,480	1,380	2,670
G _{CO₂} (molecules per 100 eV)	0.0003	0.04	0.03	0.0005	0.02	0.04
Ethane (C ₂ H ₆)	< 2	3	10	5	< 2	15
Ethene (C ₂ H ₄)	< 2	< 2	7	< 2	< 2	10
Ethyne (C ₂ H ₂)	< 2	< 2	2	< 2	< 2	3
Total C ₃	9	10	3	3	7	5
Hydrogen (H ₂)	< 5	< 5	55	< 5	< 5	580

As a first estimate for potential NAPL yields, in the analyses for the liquids in which the amberlite was irradiated, all of the GC-MS data were banded by [Dawson 2013c] (see also the corresponding irradiation experiments with neoprene in section 5.6.3).

For the experiment with 150 kGy at 49 Gy/h in Ca(OH), a potential NAPL yield was calculated as 6.9 g/t.

5.7.4. Microbial degradation of polystyrene

According to [Warthmann 2013] and own research, no literature regarding the microbial degradation of ion exchange material is available. As discussed in section 5.3.1, due to the extreme conditions in a cementitious repository, it is unlikely that an extensive biocenosis will develop.

In the context of their study, [Warthmann 2013] interviewed several experts on their opinion regarding the microbial degradation of ion exchange resins. Mr Schink stated in [Warthmann 2013] that polystyrene possesses a hydrophobic surface which delivers no point of attack for microbes and their enzymes (proteins with a specific structure). According to Mr. Schink, polystyrene can however be degraded microbially very slowly under aerobic conditions. Regarding the polystyrene degradation under anaerobic conditions, nothing is known according to Mr. Schink.

[Warthmann 2013] poses the question if it is possible that microbes in the distant future will be able to degrade polystyrene anaerobically after their mutation and gene transfer. According to the interviewed expert Mr. van der Meer, gene transfer and mutation of the microbes will take place but, however, it has to be doubted that the degradability of polystyrene (and also PVC) is increased in this way. According to Mr. van der Meer, firstly a microbial strain has to be developed through genetic alteration which is able to attack polystyrene (and PVC) in order to obtain enough carbon and/or energy to generate a new cell. Secondly, a mutant must have a selective advantage in degrading polystyrene (or PVC), otherwise it will not be able to extend its population. Since polystyrene (and PVC) is

insoluble in water, mutants eventually present will be in the difficult situation gaining sufficient carbon and energy, even if they would be able to degrade these substances [Warthmann 2013].

[Warthmann 2013] also interviewed Mr. Humphreys who stated that for the depolymerisation of polystyrene to the styrene monomer suitable enzymes are needed. To the knowledge of Mr. Humphreys, these enzymes do not exist and it cannot be predicted whether these enzymes will be developed within a few thousands of years due to selection pressure. The interviewee thinks it is more likely that depolymerisation is a radiolytic/chemical process which would then, after depolymerisation, allow microbial activity [Warthmann 2013].

According to [Warthmann 2013], the functional groups of ion exchangers (and plasticisers present in plastics) are relatively easy biologically degradable. The largest obstacle regarding the microbial degradation of synthetic polymers is the depolymerisation of polymers to utilizable monomers [Warthmann 2013].

5.8. Varnish

As stated in section 3.1.1, the 200 L waste drums are varnished with vinylcopolymer resin. However, the exact composition of the varnish is unknown.

Vinyl resins used in solvent-based coatings and adhesives are low-to medium molecular weight co- and tercopolymers of vinyl chloride, vinyl acetate or other monomers to improve solubility. Certain functional monomers contribute specific properties. For example, carboxylic acid-containing monomers provide adhesion, while hydroxyl-containing monomers contribute to reactivity, compatibility with other resins and polymers or adhesion to specific surfaces. These modified vinyl resins are used e.g. as solvent-soluble lacquers [Koleske 1995].

According to [Koleske 1995], the important characteristic features of vinyl resins are:

- 1) relatively high glass transition temperature
- 2) excellent resistance to water, alcohols, aliphatic hydrocarbons, dilute acids and alkali

In general, vinyl resin films can be degraded by the exposure to high temperatures or by long-term exposure to UV light. Therefore, vinyl resins may possess also certain pigments to help protect from attack by UV light. Furthermore, suitable heat stabilizers are employed that allow the processing of vinyl coatings at high temperature [Koleske 1995].

Another additive in vinyl resins may be plasticisers in order to improve their flexibility, formability and impact resistance of the coating. Monomeric as well as polymeric plasticisers may be used to plasticise a vinyl coating [Koleske 1995].

No information could be found in the literature regarding the degradation of the mentioned varnish under cementitious repository conditions. However, the effect of possible varnish degradation products on radionuclide migration has probably only little (if any) relevance: the maximum amount of paint per 200 L container is 720 g. Since 140,000 of those containers are intended for disposal, a maximum amount of paint of about 100 t can be expected [Meeusen 2014]. Based on the data given in [Verhoef 2016], an estimated maximum amount of organic waste contained in all the 200 L containers is 16,000 t. Thus, the amount of paint is < 1 % of the total organic material and can be considered negligible.

5.9. Cement admixtures

Commercial cement admixtures are generally mixtures of a number of different substances. The main components of the cement admixtures employed in the OPERA disposal concept

are given in the particular product safety data sheets (when available) but their exact composition is proprietary and remains unknown. Furthermore, other components may also be present which are not indicated in the product safety sheets. Thus, the compositions of the candidate products envisaged for use in the planned repository should be better known before use when more certainty regarding their behavior is needed [Hakanen 2006].

Cement is employed in the potential waste repository because of its ability to maintain a high pH for long time scales and retain radionuclides as low solubility hydroxides. Commercially available organic additives are used to improve the cement properties. However, the additives can leach from the solid phase over time and affect the radionuclide solubility. Currently, there is very little information in the literature regarding their leaching rates, the stability constants of the radionuclide complexes or their biodegradability.

Cement admixtures are generally used to improve the cement handling properties, e.g. to decrease the amount of water needed to produce adequate fluidity. The European standard EN 934-2 [CEN 2004] divides the cement admixtures into water reducers (or plasticisers) and superplasticisers (or high-range water reducers), depending on the degree of their effect [Bertolini 2004].

According to [Hayes 2012], there are five general classes of chemicals that are used as organic plasticisers and superplasticisers:

- 1) sulphonated melamine-formaldehyde (SMF) condensate salts;
- 2) sulphonated naphthalene-formaldehyde (SNF) condensate salts;
- 3) modified lignosulphonates;
- 4) vinyl co-polymers;
- 5) aliphatic polycarboxylate polyether graft co-polymers - new generation superplasticisers known as comb polymers.

Figure 30 shows building blocks of different types of plasticisers and superplasticisers.

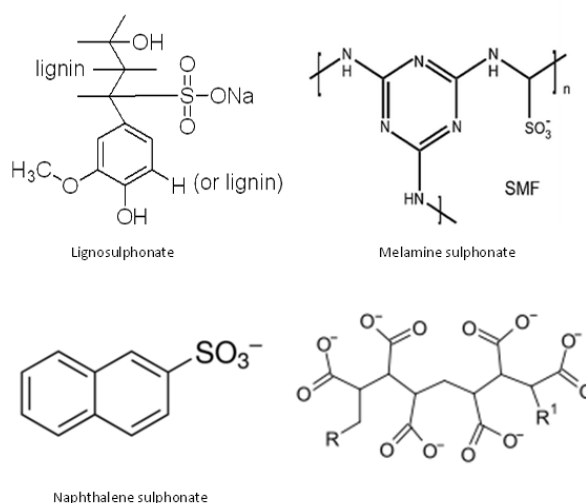


Figure 30: Schematic representation of building blocks of different types of plasticisers and superplasticisers.

The materials 1) - 4) act as surfactants and fluidity enhancement is achieved by electrostatic repulsion between cement particles thus preventing their agglomeration. Additionally, they also disperse particles via steric hindrance effects [Hayes 2012]. The admixtures are also often combinations of lignosulphonate to reduce water surface tension, and naphthalene to increase the negative surface charge on cement particles and melamine to generate a lubricating film on the particle surface [Hakanen 2006].

In general, organic superplasticisers are a special category of High Range Water Reducing (HRWR) admixtures and are designed to achieve the following functions in a cement formulation [Hayes 2012]:

- maintaining the fluidity while permitting large water reductions, or
- introduce extreme workability without increasing the water content, and/or
- lead to high early strength development.

Note that the water content determines the porosity of the concrete. Lower water contents leads to lower porosity but also to a decrease of the workability. By using superplasticisers, the production of concretes with low porosity, but still good workability has become feasible [Glaus 2004b].

The discrimination between plasticisers (water reducers) and superplasticisers is primarily based on their effect on the working properties of the resulting cementitious material. The discrimination is less distinct regarding their chemical structures and commercial products, e.g., lignosulfonates are sometimes termed as plasticisers but in other places also superplasticisers [Hayes 2012].

The polycarboxylate based superplasticisers are the only class of superplasticiser in general use. This product also increases grout fluidity by adsorption primarily on the aluminate cement hydration products, ettringite and to a lesser extent monosulfate, thereby imparting an overall negative surface charge on hydrating cement grains [Hayes 2012]. Thus, electrostatic repulsion again prevents particles from agglomerating. Furthermore, the polymeric structure of this superplasticiser contains polyethylene oxide graft side chains that stretch out and thus steric hindrance prevents particles from agglomerating [Glaus 2004b].

Table 64 shows the cement additives employed in the OPERA disposal concept in the different compartments.

Table 64: Information of cement additives used in the OPERA disposal concept [Verhoef 2014b, Verhoef 2016]

Compartment	Additive	Concentration	Comment
Gallery lining	Plasticiser: Woerment BV 514	1.33 [kg/m ³]	No information found
	Superplasticiser: Woerment FM 30	3.65 [kg/m ³]	Now named BASF MasterRheobuild 30; based on naphthalene sulphonate (SNF)
Backfill	Foaming agent TM 80/23, no plasticiser	1 [kg/m ³]	No detailed information found, supplier: Tillman Chemische Bouwstoffen B.V.
Containment LILW	Superplasticiser TM OFT II B84/39 CON 35 % (BT-SPL)	3-5 [kg/m ³]	Supplier: Tillman Chemische Bouwstoffen B.V., superplasticiser according to product information sheet, product description. Polymerised sulphonated naphthalene condensate combined with a lignine sulphonate ¹⁾ . Their widespread occurrence throughout the cement indicates that they are a substantial source of organic material.
Containment (TE)NORM	Same as LILW	3.3 [kg/m ³]	See LILW
Containment molybdenum waste per 1000 L waste container	Retarder CUGLA MMV con. 25% BT	1.6 kg in 180 L processes Mo waste	Not considered due to little amount
Reinforced 1,000 L concrete container	Glenium 51 35 %	2.95 [kg/m ³] for waste stream I; 1.7 [kg/m ³] for waste stream II.	Superplasticiser: Modified polycarboxylate ether
200 L container spent ion exchanger waste	Plasticiser: Sikament; Retarder: Sika retarder	Plasticiser: 3.6 kg for waste stream with beads, powder and sludge	Retarder not considered in this study

¹⁾ Personal message from Tillman Chemische Bouwstoffen B.V.

Thus, according to Table 64, (super)plasticisers of the following classes are present in the LILW sections and will be discussed in the following sections:

- superplasticisers based on naphthalene sulphonate (SNF)
- superplasticisers based on polymerised sulphonated naphthalene condensate combined with a lignine sulphonate
- modified polycarboxylate ether superplasticisers

5.9.1. Chemical degradation

Research regarding the chemical (alkaline) degradation of cement plasticisers/superplasticisers is very limited. For example, [Glaus 2004b] investigated a few selected concrete admixtures, i.e. sulfonated naphthalene-formaldehyde condensates, lignosulfonates and others on their sorption properties of Ni(II), Eu(III) and Th(IV) on cement. Degradation of additives was investigated rather marginally and mainly in an indirect fashion in the framework of their study. In the context of their experiments no

chemical degradation or transformation of the admixtures was detected (duration of experiments up to 14 months) and the authors regarded them as stable under cementitious conditions (~ pH 13.3) and 25 °C.

[Yilmaz 1993] investigated the degradation of sulfonated melamine formaldehyde condensates (SMF) and sulfonated naphthalene formaldehyde condensates (SNF). These superplasticisers (2 g) were treated in 1 M KOH (= pH 14) solutions for up to 20 days (under air-tight conditions). At pre-determined points in time, the solutions were sampled, filtered and neutralized. Afterwards, the concentrations of SMF and SNF were determined by UV spectroscopy. It was found that the concentrations of superplasticiser in the solutions decreased with time but the SMF and SNF behaved differently. The SMF concentration decreased over time and a white solid precipitate was observed. The analysis showed that more than 65 % of the original SMF had precipitated. SNF, however, showed a different behavior. A small decrease in concentration was observed after a day of the preparation and the SNF concentration did not change afterwards. No precipitation was observed in the SNF solutions. The investigations by UV spectroscopy showed only a reduction of 10 % of the initial SNF concentration.

According to the literature data found it can be concluded that SNF may be stable towards chemical degradation under alkaline conditions. However, since the exact compositions of the additives employed in the OPERA disposal concept and also those of the experimental investigations, there remains uncertainty and the transferability of the laboratory results onto realistic conditions may be questioned.

5.9.2. Microbial degradation

Literature regarding the research of microbial degradation of cement plasticisers/superplasticisers under cementitious conditions could not be found. For completeness, the results of a study investigating the degradation of a superplasticiser at neutral pH are presented. [Ruckstuhl 2002] carried out investigations regarding the biodegradation of sulfonated naphthalenes and their formaldehyde condensates (SNF). These technical mixtures consist of various mono- and disulfonated monomers and their condensed oligomers. Cause for the research of [Ruckstuhl 2002] was the discovery of SNF in groundwater samples 5 meters away from a construction site which employed the superplasticiser. Laboratory degradation experiments were conducted in which the pH (= 7) and sulphate/oxygen concentration were similar to the ones at the field sampling site. Generally, the degradation pathway of sulfonated naphthalenes was found to be desulfonation followed by a ring cleavage. According to [Ruckstuhl 2002], in their experiments (observation time: 195 d) it was found that the monosulfonated monomers were depleted more quickly than the disulfonated analogues (Naphthalene-1,5-disulfonate). Furthermore, it was found that disulfonated monomers and the oligomers are persistent in the environment. This information is, however, due to the different geochemical conditions, not transferable to a cementitious waste repository.

5.9.3. Radiolytic degradation

Literature studies regarding the radiolytic degradation of cement additives are sparse. The results of a selected study are presented in the following text.

[Chandler 2008] investigated the irradiation of grout and aqueous samples containing ADVA Cast 550 (a polycarboxylate ether superplasticiser). Two types of samples (cementitious and an aqueous) were irradiated at a Co-60 irradiation facility. The cementitious samples consisted of 3:1 pulverized fly ash (PFA) : ordinary Portland cement (OPC) grout containing 0.8 % (w/v) ADVA Cast 550 and 9:1 blast furnace slag : OPC containing 0.8 % (w/v) ADVA Cast 550.

The samples were placed in two positions in the irradiation chamber whereas the first was at the high dose rate position receiving a dose rate of 4 kGy/h to a total dose of 9 MGy. The second was subjected to a low dose rate of 1 kGy/h to a total dose of 2 MGy. After irradiation, the pore fluid from these samples was extracted by squeezing for analysis [Chandler 2008].

The aqueous samples were prepared in Ca(OH)₂ solution (pH~12.5), whereas one sample contained 1 % (w/v) ADVA Cast 550 and the second one contained 10 %. Three different dose rates were used to irradiate the samples:

- 4 kG/h to a total dose of 9 MGy
- 300 Gy/h to a total dose of 674 kGy
- 30 Gy/h to a total dose of 6.75 kGy

The samples were analysed then by GC-MS and ion chromatography (IC).

It was shown that irradiation decreases the TOC of the samples whereas the effect was greater at higher dose rates. The TOC measured from the pore squeeze solutions was observed to be dependent on the grout formulation: TOC measured from the BFS:OPC samples were higher than the PFA:OPC.

The organic screening by GC-MS indicated that for the ADVA Cast 550 samples (at low radiation doses), a broad range of degradation products was observed. The products were found to be degraded by chain scission (the molecule backbone is broken and lower molecular weight fragments are generated) since the products systematically decrease in molecular size. Regarding the pore squeeze samples, identified compounds were alcohols, ketones, carboxylic acid and hydrocarbons, whereas these species were different from those generated in the aqueous samples. By means of IC, low concentrations of organic ions in the 1 % aqueous solutions -consistent with the results of the TOC and GC-MS analysis- were identified. The sample containing 10 % ADVA Cast 550 showed a significant amount of organic anions, in particular acetate and lactates which was again consistent with the TOC and GC-MS analysis results. [Chandler 2008] concluded that there was no evidence for the formation or generation of undesirable complexing agents.

5.10. Metal corrosion processes and products

A variety of metals (i.e. carbon steel, zinc, aluminium) is assumed present in the LILW. Furthermore, steel is also used as reinforcement material of waste containers (see section 3.1). Corrosion processes and products of carbon steel are described in section 5.10.1, those of zinc in 5.10.2 and those of aluminium in 5.10.3.

5.10.1. Carbon Steel

The term carbon steel is used for alloys of iron and carbon with a C content of < 2 wt.% and typically containing Mn (< 1.65 wt.%), Si (< 0.6 wt.%) and Cu (< 0.6 wt.%) with minor amounts of other alloying elements (Cr, Ni, Mo, W, V, Zr). Low carbon and mild steels possess C contents of 0.05 - 0.15 wt.% and 0.16-0.29 wt.%, respectively. There exists a large number of individual designations for carbon and mild steels defined by various standards organisations. In this context, the general term carbon steel will be employed to refer to all low carbon and mild steels [King 2010].

In the LILW section of the planned Dutch repository, carbon steel is present in the form of waste containers, constituents of the waste and as reinforcement steel of the containers. (Carbon) steel corrosion processes are described in detail in [Kursten 2015] and thus will be presented only very briefly here.

According to [Kursten 2015], steel corrosion is an electrochemical process which involves two separate, but coupled chemical reactions proceeding simultaneously at two different sites on the steel surface and thus the transfer of electrons takes place.

The following, simultaneously occurring processes are required for the corrosion of steel in concrete to take place [Bertolini 2004]:

- a reduction reaction, consuming electrons,
- an oxidation reaction, liberating electrons,
- an electrical current flowing within the metal resulting from the electron flow from the oxidation reaction area to the reduction reaction areas,
- an electrical current flowing through the concrete pores due to the movement of charged ions.

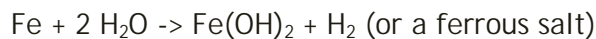
According to [Kursten 2015], the corrosion rate is determined by the slowest of the mentioned processes.

In the expected highly alkaline environment (pH > 12.5) and without the ingress of aggressive species, carbon steel is protected by a passive oxide film, which is believed to lead to very low uniform corrosion rates [Kursten 2015].

Air eventually present after waste emplacement (see section 4) will initially lead to aerobic corrosion of the carbon steel containers with the formation of ferric (III) corrosion products, according to the following reaction [Kursten 2015]:



Since any residual oxygen or oxidising radiolysis products will be consumed, the environment surrounding the particular LILW will become anoxic and the main corrosion reaction is described by the following reaction [Kursten 2015]:



When finally anoxic conditions prevail and depending on temperature and pH, the ferrous hydroxide (Fe(OH)_2) may not be the stable corrosion product and may be transformed into magnetite (Fe_3O_4), as described by the Schikorr reaction [Kursten 2015]:



Under the mentioned conditions, Fe(III) oxides that may have formed in the initial oxidising environment will react with Fe(II) and also lead to magnetite formation [Ishikawa 1998]. Thus it can be assumed that magnetite, which will be present in large quantities, will have a strong effect on the redox conditions. By means of galvanic coupling of magnetite and elemental Fe the redox potential close to the particular canister surfaces will be very low [King 2000]. Furthermore, with increasing distance from the particular steel surfaces, spalled-off magnetite [Johnson 2000] may also affect redox conditions [Wersin 2003].

It can be assumed that corrosion of the steel will occur throughout the lifetime of the repository producing iron hydroxide and oxide products, e.g. magnetite (Fe_3O_4) and hematite (Fe_2O_3). Such mineral phases have a significant sorption capacity for radionuclides due to their large surface areas and surface structures. At alkaline pH values, iron oxides are particularly effective sinks for actinides.

Carbon steel corrosion rates

Carbon steel corrodes both under aerobic and anaerobic conditions. Under aerobic conditions, the steel corrosion rate will be controlled by the rate of supply of O_2 to the

corroding surfaces. Under anaerobic conditions, the carbon steel corrosion rate will be controlled by the rate of film growth, whereas protective passive magnetite (Fe_3O_4) films form on the metal surface [King 2010].

Carbon steel present in cementitious backfill will become passive [Kursten 2008]. The duration of the passivity requires that the cementitious pore water pH remains above ~ pH 9-10, which can be expected for long time scales in the planned repository (see section 4.1). The passive film on carbon steel may be locally attacked (pitting, crevice corrosion) and eventually destroyed [Kursten 2008]. The localised attack can be initiated by reductive dissolution of Fe(III) corrosion products formed during the aerobic phase, non-uniform wetting of the surface as the repository saturates or the breakdown of a passive film. The mechanism of passive film breakdown is more likely in a cementitious system than, e.g., at lower pH-values, when a true passive film may be present or in the presence of high carbonate concentrations. Localised attack is most likely as the cementitious pore water pH decreases as a result of cement degradation processes (e.g. carbonation) and will be a function of time-dependent $\text{Cl}^- : \text{OH}^-$ ratio [King 2010].

[Kursten 2015] carried out a literature study to compile corrosion rates of carbon steel. The results of the corrosion rate data compilation will be shown here for the sake of completeness since selected data will be used for further considerations undertaken in the framework of this project. Figure 31 summarizes the corrosion rate data compiled by [Kursten 2015] for carbon steel in oxic and alkaline chloride-free solutions. According to [Kursten 2015], corrosion rates range from 0.1 to ~ 10 $\mu\text{m/a}$ and have been reported for temperatures up to 80 °C in alkaline environments.

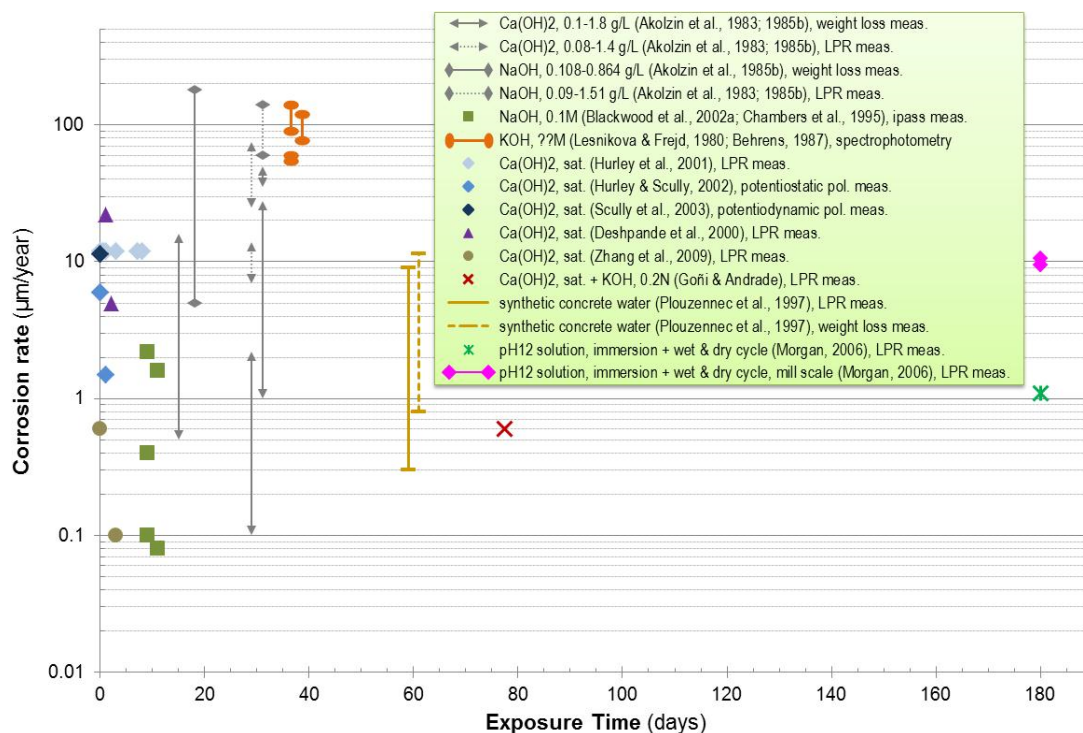


Figure 31: Compilation of uniform corrosion rates for carbon steel in oxic and alkaline chloride free solutions at pH 12 - 13.5 [Kursten 2015]

In their study, [Kursten 2015] also compiled the corrosion rate literature data for mild steel in anoxic and alkaline chloride-free solutions as shown in Figure 32.

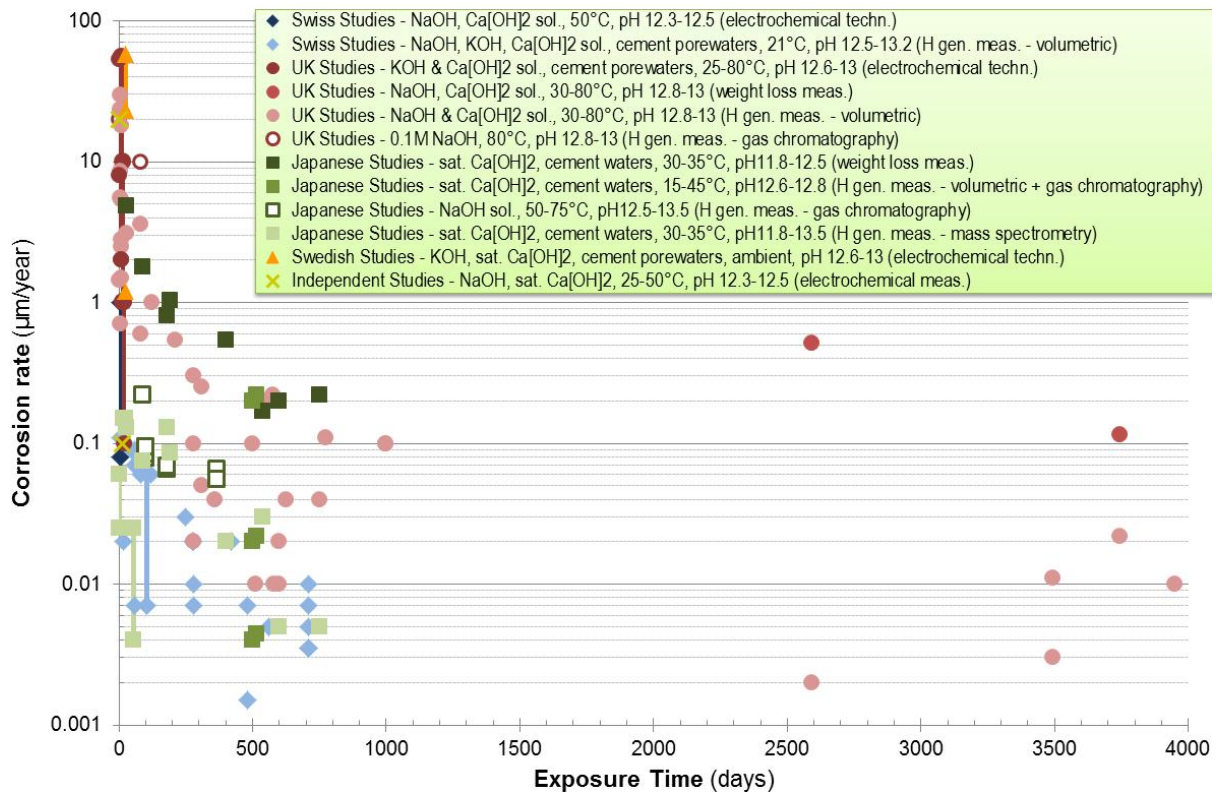


Figure 32: Compilation of uniform corrosion rates of carbon steel in anoxic and alkaline chloride-free solutions (pH 12 - 13.5) [Kursten 2015]

According to [Kursten 2015], the data in Figure 32 exhibits a decreasing tendency of the uniform corrosion rate with increasing time of exposure towards a constant and very low value.

Table 65 shows a compilation from [Kursten 2015] with corrosion rates generated from measurements of the rate of H₂ evolution. For more information, please refer to [Kursten 2015].

Table 65: Anaerobic corrosion rates of carbon steel in high pH solutions determined from long-term H₂-generation experiments [Kursten 2015]

Environment	pH	T [°C]	Test duration [days]	V _{CORR} [µm/year]	R&D programme
0.1 M NaOH	12.8	21	initial 60 120 280 710	0.09 - 0.11 0.07 0.06 0.02 0.005	Swiss Studies
KOH	12.8	21	60 280 710	0.09 0.01 0.0035	Swiss Studies
sat. Ca(OH) ₂	12.8	21	18 280 710	0.02 0.007 0.0035	Swiss Studies
0.1 M NaOH	12.8	30	initial 280 625 750 3949	1.5 - 3.11 0.1 0.04 0.04 0.01	UK Studies
0.1 M NaOH	12.8	50	initial 80 210 310 600 3492	5.5 - 8.6 0.6 0.54 0.005 0.02 - 0.01 0.011	UK Studies
0.1 M NaOH	12.8	80	initial 80 125 311 2591	18 - 29.6 3.6 1 0.25 0.002	UK Studies
sat. Ca(OH) ₂	12.8	50	initial 360 500 580 3494	5.1 - 5.4 0.84 0.1 0.01 0.003	UK Studies
sat. Ca(OH) ₂ + 0.1M NaOH	12.8	30	initial 280 510 1000 3743	0.7 - 1.43 0.3 0.2 0.1 0.022	UK Studies
sat. Ca(OH) ₂ + 0.1M NaOH	12.8	50	initial 510 773 1000	2.5 - 2.8 0.2 0.11 0.1	UK Studies
cement equilibrated water	11.8	30	30 90 400 600 750	0.13 0.075 0.02 0.005 0.005	Japanese Studies

[Kursten 2015] state that under the expected high pH conditions, the surface of carbon steel will be passivated and will remain so for at least the duration of the thermal phase.

This results in very low uniform corrosion rates and under normal evolution conditions carbon steel will only prone to uniform corrosion [Kursten 2015].

5.10.2. Zinc

As stated in section 3.1.1, the drum walls of the 200 L containers are galvanized with zinc with a thickness of 40 μm . Furthermore, it cannot be excluded that zinc may be also present in the waste. The zinc corrosion processes and products under alkaline conditions are discussed in this section.

[Macias 1983] investigated the corrosion kinetics of galvanized steel in $\text{Ca}(\text{OH})_2$ saturated solutions of pH 12 - 13.8 in presence of NaOH, KOH and SO_4^{2-} to simulate cementitious pore water. The corrosion rate of the galvanized steel was determined by its electrochemical polarisation resistance.

In their corrosion experiments, [Macias 1983] used galvanized steel of 6 mm in diameter and 8 cm length with a 60-80 μm zinc coating. These samples were placed in corrosion cells with different alkaline solutions and a constant temperature of 25 $^\circ\text{C}$ for an immersion period of 33 days. Table 66 and Table 67 show the composition and pH of the test solutions [Macias 1983].

Table 66: Compositions, pH and behaviour type of the solutions with $\text{Ca}(\text{OH})_2$, KOH and NaOH [Macias 1983]

Cell no	Added proportions			Determined proportions			
	Conc $\text{Ca}(\text{OH})_2$	KOH [M]	NaOH [M]	pH	KOH [M]	NaOH [M]	[g/L] Ca^{2+}
1	sat.	0.1		12.97			0.258
2	sat.	0.5		13.59			0.053
3	sat.	1.0		13.89	1.10		0.032
4	sat.	1.5		14.00	1.48		0.022
5	sat.	-	-	12.60			0.892
6	sat.	-	0.01	12.61			0.722
7	sat.	-	0.05	12.80			0.408
8	sat.	-	0.1	12.99			0.220
9	sat.	-	0.2	13.17		0.25	0.112
10	sat.	0.5	0.05	13.61			0.048
11	sat.	0.7	-	13.72			0.049
12	sat.	0.35	-	13.45			0.072
13	sat.	0.2	-	13.24			
14	sat.	0.6	0.1	13.69			0.038
15	sat.	-	0.5	13.50		0.5	0.050

Table 67: Composition, pH and behaviour type of the solutions with $\text{Ca}(\text{OH})_2$, CaSO_4 , Na_2SO_4 and K_2SO_4 [Macias 1983]

Cell no	Added proportions				Determined proportions				
	Conc $\text{Ca}(\text{OH})_2$	CaSO_4 [g/L]	K_2SO_4 [g/L]	Na_2SO_4 [g/L]	pH	Ca^{2+} [g/L]	K^+ [g/L]	Na^+ [g/L]	SO_4^{2-} [g/L]
16	saturated	5	-	-	12.43	1.132	-	-	0.94
17	saturated	-	-	5.22	12.70	0.856	-	1.75	2.56
18	saturated	-	6.41	-	12.77	0.784	3.13	-	2.48
19	saturated	5	-	5.22	12.71	0.858	-	1.84	2.41
20	saturated	5	6.41	-	12.77	0.872	2.37	-	2.51
21	saturated	5	6.41	5.22	12.72	0.480	2.84	1.62	5

The determined corrosion rates of galvanized steel determined after immersion of 33 days in the different solutions are shown in Figure 33. [Macias 1983] showed that the galvanized coating was shown to be a function of pH. A threshold value of 13.3 ± 0.1 divided two types of behaviour: at $\text{pH} < 13.3 \pm 0.1$ the medium was able to produce effective

passivation of the galvanised coating while at $\text{pH} > 13.3 \pm 0.1$ the galvanized coating was increasingly corroded until total dissolution had occurred.

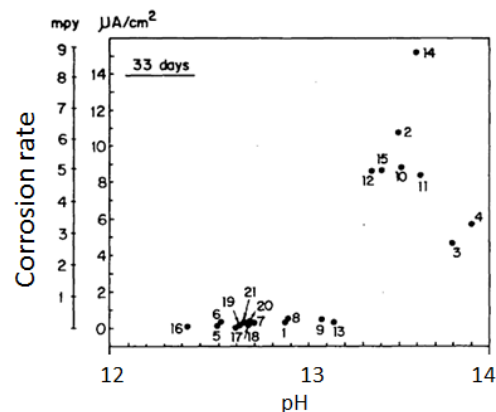


Figure 33: determined corrosion rates in mpy (milli-inch/year); 1 mpy = 25.4 $\mu\text{m/a}$ [Macias 1983]. Solutions 2, 10, 12 and 15 have pH values in the range of that expected in the initial phase of cement degradation ($\sim \text{pH} 13.5$) and lie in the area of no passivation

The passivating product was identified (by means of x-ray diffraction) as calcium hydroxyzincate ($\text{Ca}(\text{Zn}(\text{OH})_3)_2 \cdot \text{H}_2\text{O}$). Since the Ca^{2+} concentration of the solution decreases as the pH increases, Macias [1987] assume that for $\text{pH} > 13.3 \pm 0.1$ there is not enough Ca^{2+} present to form a compact, insulating layer of calcium hydroxyzincate, and consequently the dissolution of the galvanized coating, with formation of $\text{Zn}(\text{OH})_2$ and ZnO continues [Macias 1983]. According to Macias [1987], the controlling factors in the attainment of galvanized coating stability by the formation of a continuous and compact layer of $(\text{Ca}(\text{Zn}(\text{OH})_3)_2 \cdot \text{H}_2\text{O})$ were thought to be pH and Ca concentration.

To conclude, it can be assumed that the zinc coatings of the 200 L barrels will corrode rapidly since the pH values of the cementitious pore water will be initially about 13.5 [Seetharam 2015]. If a zinc corrosion rate of 5 mpy (= 127 $\mu\text{m/a}$, which is in the range of solutions 12, 15, 10 and 11, see Figure 33) is used, the coating will be destroyed in less than a year.

The zinc corrosion also generates hydrogen. Calculations regarding the generated gas amounts due to metal corrosion can be found in section 5.13.

5.10.3. Aluminium

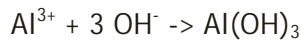
Aluminium is known as a reactive metal but it still is used for many practical applications because of the protective oxide and hydroxide films which develop on its surface. On the other hand, as oxides are amphoteric, aluminium is not resistant to corrosion in acidic and alkaline conditions due to the dissolution of the protective films [Hoch 2010].

According to [Fujisawa 1997], it is known that aluminium corrodes at a high rate under alkaline conditions but the corrosion rate can be reduced due to film formation when it is embedded in a cement structure.

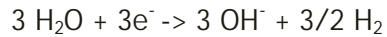
If aluminium is in contact with alkaline solutions such as cementitious pore water, the air formed oxide (amorphous Al_2O_3) is dissolved and corrosion follows [Hoch 2010]:



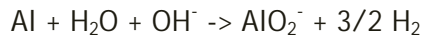
Under alkaline conditions, the aluminium ion reacts with hydroxide ions and aluminium hydroxide is generated [Hoch 2010]:



At high pH the cathodic reaction is the reduction of water [Hoch 2010]:



which gives the overall reaction [Hoch 2010]:



The overall behaviour of aluminium is shown in potential - pH diagrams (Pourbaix diagrams) for the aluminium-water system at 25 °C (Figure 34).

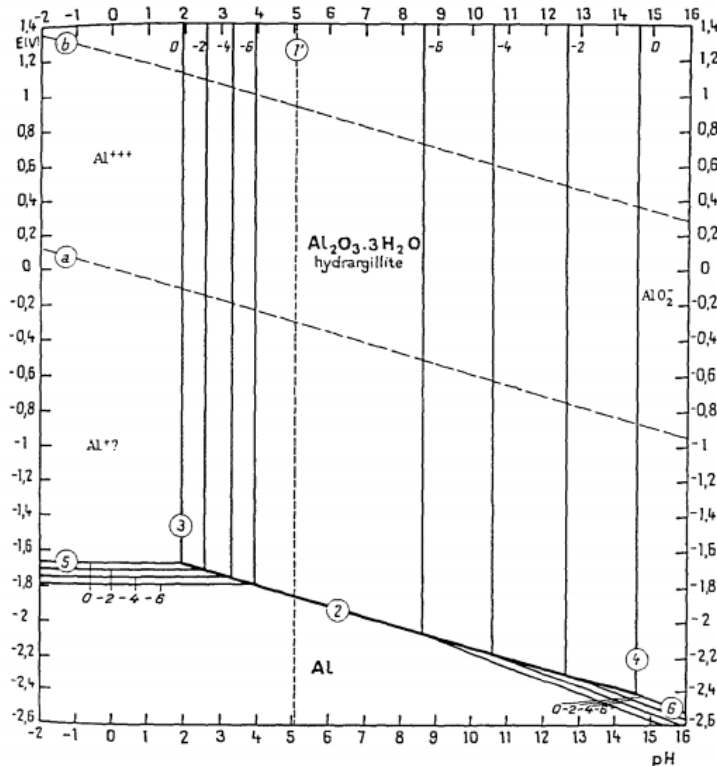


Figure 34: Pourbaix diagram for aluminium with regions of stability. At high pH values, AlO_2^- is the stable form of aluminium [Pourbaix 1974]

According to [Diomidis 2014], the corrosion rate of aluminium tends to increase at increased pH due to the increased solubility of its oxides and hydroxides. In the presence of $\text{Ca}(\text{OH})_2$ or cement, the corrosion rate of aluminium decreases with time due to the formation of calcium aluminates such as $\text{CaO} \cdot \text{Al}_2\text{O}_3 \cdot x \text{H}_2\text{O}$ and $\text{Al}_2\text{O}_3 \cdot 6 \text{CaO} \cdot 3 \text{SO}_3 \cdot 32 \text{H}_2\text{O}$ [Hoch 2010].

Literature data on aluminium corrosion under alkaline ($> \text{pH } 12.5$) and anoxic conditions are very limited. Only one study could be found. [Fujisawa 1997] carried out aluminium corrosion experiments with specimens of commercial pure aluminium and pulverized mortar. The mortar was prepared by mixing an ordinary Portland cement, water and sand at a ratio of 1:0.35:1. In these experiments, aluminium corroded in contact with the mortar equilibrated water and pulverized mortar at 15 °C, respectively. The corrosion rate was determined by the amount of H_2 generated.

In the initial period, aluminium corroded rapidly with a corrosion rate of 10 - 20 mm/a. However, the corrosion rate decreased with time, and after 1,000 hours the rate reached 1 - 10 $\mu\text{m}/\text{year}$ at pH 12.6. The authors observed on the surface of the aluminum specimens placed in the pulverized mortar films composed of the corrosion products which were

identified as $\text{Al}(\text{OH})_3$ (gibbsite) [Fujisawa 1997]. The reduction in the corrosion rate was attributed by [Fujisawa 1997] to the decomposition of gibbsite on the aluminum surface.

5.11. Behaviour of U_3O_8

As discussed in section 3.1.3, DU from the URENCO Uranium enrichment plant is stored in the form of Uranium oxide (U_3O_8) and will be, after its conditioning, re-packed in Konrad type II containers.

The release of Uranium from its cement matrix requires (after corrosion of the containers has taken place) different processes, e.g.

- the dissolution of U_3O_8 ,
- the desorption of sorbed Uranium from cement phases,
- leaching of Uranium from a solid phase without the macroscopic destruction of the latter ("leaching").

The basic requirement for the release of radionuclides to take place is the presence of water. The radionuclide release rate depends, among others, on the chemical composition of the pore water, the continuousness of the aqueous phase in the pore space and the water flow.

The Uranium mobility due to dissolution of U_3O_8 is mainly controlled by the solubility and the chemical properties of the particular solid phase.

U^{6+} can be bound in cementitious materials in the form of Ca-Uranates or Ca-Uranium-silicates, whereas the generation of the silicate phases requires a sufficiently high concentration of silicic acid [Atkins 1992, Moroni 1995, Serne 1996]. There have been several investigations to investigate the uptake mechanisms of U^{6+} with calcium silicate hydrates (CSH phases) - the main component of hardened cement past (HCP) [Gaona 2012]. In the framework of their geochemical modelling study, [Gaona 2012] compiled literature data regarding experiments (e.g. sorption isotherms, spectroscopic data) on U^{6+} interaction with CSH phases. The authors concluded from their literature review, that U^{6+} is neither adsorbed nor incorporated in the Ca-O octahedral layers of the CSH structure, but rather is located in the interlayer, similar to Ca^{2+} and other cations (Figure 35). The authors concluded that their observations indicated the U^{6+} uptake is driven by the formation of a solid solution [Gaona 2012].

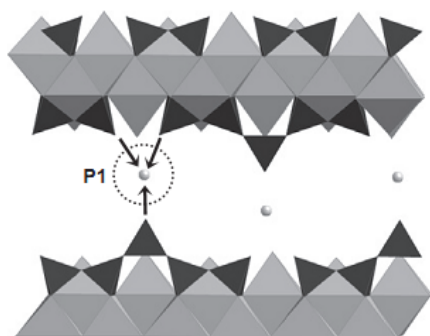


Figure 35: Site proposed for the incorporation of U^{6+} into the CSH-interlayer (P1) [Gaona 2012]

Besides the generation of the above mentioned compounds, also U^{4+} (in the form of $\text{U}(\text{OH})_4(\text{aq})$) as well as the anionic uranyl-complexes (e.g. $\text{UO}_2(\text{OH})_3^-$ or $\text{UO}_2(\text{OH})_4^{2-}$) may sorb onto the CSH gel [Heath 1996, Heath 2000b, Bond 2001, Fujita 2004]. Furthermore, uranium (especially in the form of UO_2^{2+}) may sorb onto Calcite or be incorporated into Calcite due to coprecipitation processes [Elzinga 2004, Reeder 2000, Reeder 2001, Kelly 2003].

According to the NAGRA/PSI Chemical Thermodynamic Database 01/01 [Hummel 2002] the dissolved Uranium concentration in cementitious pore waters and redox-potentials of ca. - 500 mV could be limited on a level of 10^{-9} M, whereas the only relevant dissolved specie is $U(OH)_4(aq)$. At higher redox potentials, U^{6+} species will dominate whereas no solubility limitation will exist using the U^{6+} solid phases Schoepit ($(UO_2)_8O_2(OH)_{12} \cdot H_2O$) and Rutherfordin (UO_2CO_3) as implemented in the thermodynamic database.

Based on experimental investigations regarding the Uranium solubility in cementitious systems [Moroni 1995, Serne 96, Tits 2001], [Berner 1999] recommended using $1E-8$ M as best estimate for dissolved Uranium in cementitious systems (and $5E-7$ M were recommended for an upper limit).

In general, Uranium can occur in the oxidation states +III, +IV, +V and +VI, whereas in natural systems only the oxidation states +IV and +VI are relevant (Figure 36).

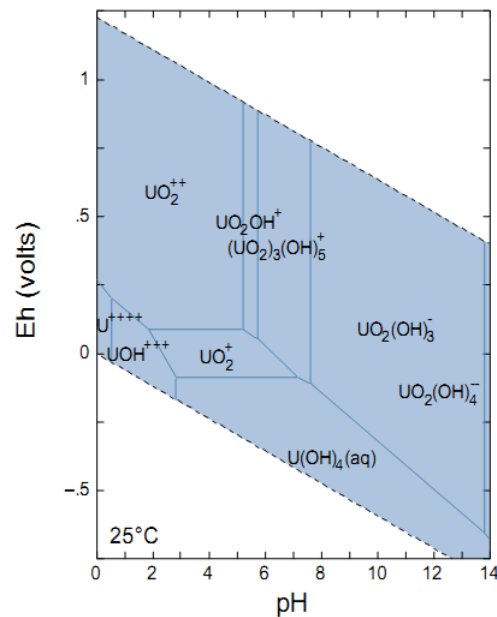


Figure 36: Stability fields of aquatic species in the system U-H₂O in dependence of the E_H-pH-conditions (a_U = 10^{-9}) [Deissmann 2005]

In cementitious systems, the hexavalent Uranium, occurring as the uranyl-ion (UO_2^{2+}), is relevant since in strongly alkaline conditions tetravalent uranium (occurring as $U(OH)_4(aq)$) only dominates at E_H-values of < -500 mV. U^{6+} forms a multitude of stable complexes with OH^- and CO_3^{2-} ions whereas under the relevant conditions of cementitious pore waters the hydroxospecies $UO_2(OH)_3^-$ and $UO_2(OH)_4^{2-}$ are dominant [Deissmann 2005]. The speciation of the dissolved Uranium species was undertaken with Geochemists Workbench 4.0 [Bethke 1996, Bethke 2002] by [Deissmann 2005]. Thermodynamic data was mainly taken from the NAGRA/PSI -Chemical Thermodynamic Data Base 01/01 [Hummel 2002]. The approximation of the activity coefficients was undertaken by employing the Davies-equation, since the ionic strength in cementitious pore water is normally below 0.5 M [Deissmann 2005]. Figure 37 shows the calculated U^{6+} speciation as function of pH and $[CO_3^{2-}]$.

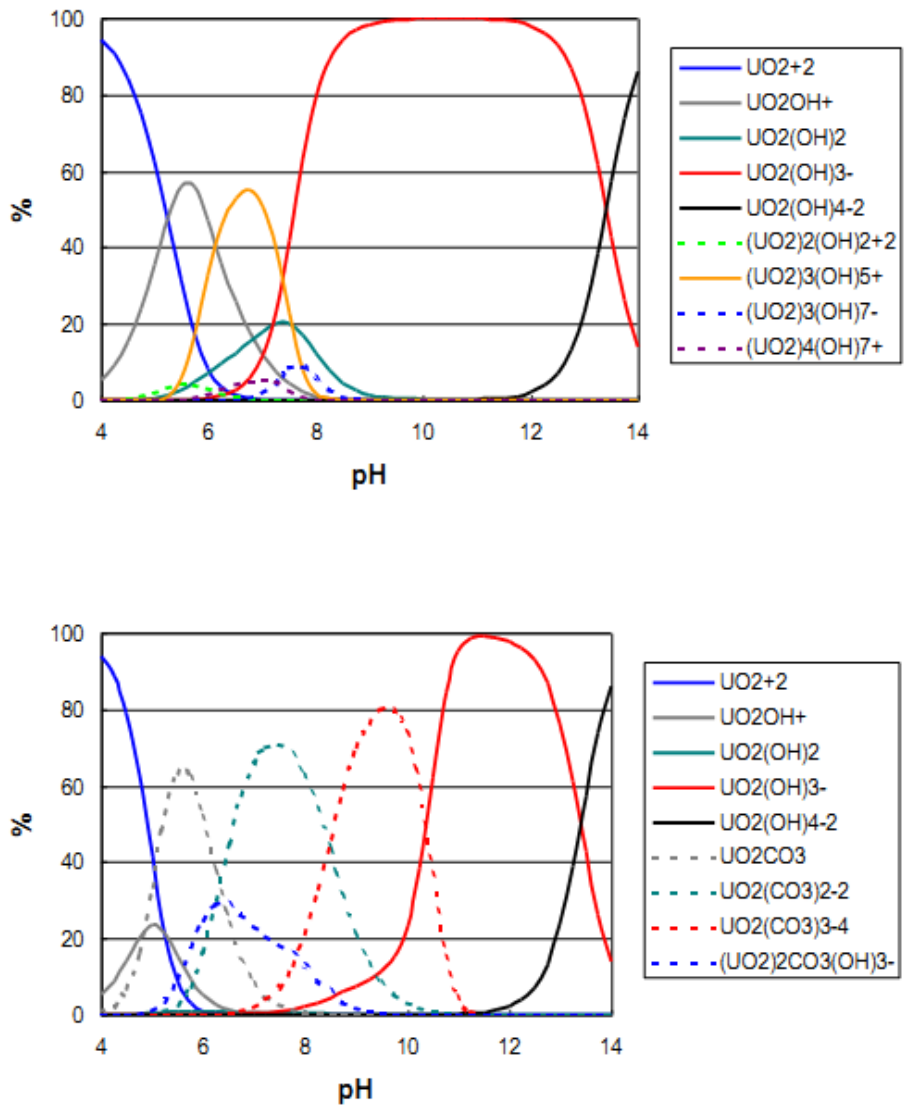


Figure 37: Fractions of different dissolved U⁶⁺ species of total dissolved U-concentration as a function of pH (above: $\Sigma\text{CO}_3 = 0$; below: $\Sigma\text{CO}_3 = 1 \text{ mM}$) [Deissmann 2005]

5.12. Degradation of processed liquid molybdenum waste

The properties of the processed molybdenum wastes are shown in section 3.1.2.1. As discussed in that section, (closed) 200 L drums are placed in 1,000 L containers and mortar is poured into the containers. The liquid waste streams are fixed within the cementitious matrix. It can be expected that the waste in the 200 L drums will come into contact with water in several 1,000 years. After the 200 L drums come in contact with water, they also will start to corrode. When the wastes are finally in contact with water, leaching of the radionuclides takes place and the diffusion gradient between the chemical elements present in the waste and the pore water will lead to the diffusion of the radionuclides into the near-field.

¹³⁷Cs has a half-life of about 30.08 a [Magill 2012]. About 95 % decays by beta emission to a metastable nuclear isomer of barium: ^{137m}Ba. The remainder directly populates the ground state of ¹³⁷Ba, which is stable. ^{137m}Ba has a half-life of about 153 seconds and is responsible for all of the emissions of gamma rays in samples of ¹³⁷Cs. One gram of ¹³⁷Cs has an activity of 3.215 terabecquerel (TBq).

Due to its short half-life, ^{137}Cs will be mostly decayed to Ba-137 at the point of time when the waste can be expected to be in contact with water.

Ru^{106} has a half-life of 1.02 a and thus will also be decayed when the waste is in contact with water. Ru^{106} decays via ^{106}Rh ($t_{1/2} = 29.8$ s) to stable ^{106}Pd .

Regarding the retarder employed in the cement (CUGLA MMV con. 25% BT) only limited information was available. According to its product specification sheet, the effective component is gluconate. Since the amount of retarder per 1,000 L waste container is however very small (0.5 % for waste streams I and II) its degradation processes and products are negligible and not investigated. More information regarding cement admixtures is given in section 5.9.

Regarding the fission products in the waste streams, it can be assumed that they diffuse into the pore water. For performance assessment considerations, an instantaneous release of the radionuclides contained should be taken into account whereas the solubility limits of the particular elements must be considered (see section 6).

5.13. Gas generation

5.13.1. Gas generation processes

In the planned nuclear waste repository significant quantities of gas may be generated as a result of various processes, e.g. anaerobic corrosion of metals, radiolysis of water or polymers, radioactive decay or eventually microbial degradation of organic substances. The most important gases generated are hydrogen, methane and carbon dioxide.

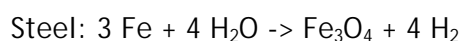
The following metals are considered as corrodible and their generated gas amounts are calculated: iron (including carbon steel and various stainless steels), aluminium and zinc. The molar quantities of hydrogen etc. are estimated.

Two broad categories of organic wastes can be defined: easily degradable organics such as cellulose and organic materials such as plastics that may be resistant to complete degradation.

5.13.1.1. Gas generation due to metal corrosion

H_2 is generated by anaerobic corrosion of metals. Microbial degradation of organics under anaerobic conditions and $\text{pH} > 12$ is up not proven and thus neglected in the framework of this study. It can be assumed, that some moisture, due to pore water in the cementitious materials, will be present at the time of repository closure, permitting the immediate initiation of corrosion of at least some of steel waste containers. Aerobic corrosion, with no gas generation, eventually occurs for a short time is also neglected due to its minor significance [Johnson 2002].

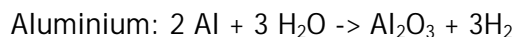
The H_2 gas volumes are calculated from the stoichiometry of the particular corrosion reactions and the molar mass of the corresponding metals. The stoichiometry factor of the corrosion reaction depends on the reaction product. For the calculations the most stable corrosion product under the given chemical conditions in the repository is assumed to be the final reaction product. The following corrosion reactions of are used for the calculations of the potential gas amounts which may be generated:



The resulting stoichiometry factor is 4/3, which means that 1.33 M of hydrogen per M of corroded iron are formed.



The resulting stoichiometry factor is 1, which means that 1 M of hydrogen per M of corroded zinc is formed.



The resulting stoichiometry factor is 3/2, meaning that 1,5 M of hydrogen per M of corroded aluminium is formed. Table 68 summarizes the data for the calculations of gas amounts. The estimated gas volumes relate to an ideal gas under standard conditions (T = 273,15 K, 101325 Pa).

Table 68: Data for calculation gas amount

Metals	Molecular mass [kg/moles]	Stoichiometry [M H ₂ /M metal]	m ³ Gas / kg metal
Carbon steel (Fe)	0.05585	1.33	0.534
Aluminium	0.02698	1.5	1.246
Zinc	0.06538	1	0.343

Estimations regarding the generated gas amounts are based on the waste inventory (given for the year 2130) for LILW and (TE)NORM as published in [Meeusen 2014] and shown in Table 69.

Table 69: Estimated waste matrix composition in the OPERA disposal facility in the year 2130 [Meeusen 2014]

Material	LILW		(TE)NORM		Total	
	min [kg]	max [kg]	min [kg]	max [kg]	min [kg]	max [kg]
concrete	4.20E+07	5.94E+07	0	0	4.20E+07	5.94E+07
cement	1.20E+07	2.40E+07	4.70E+07	4.70E+07	3.60E+07	7.10E+07
plasticiser	7.55E+05	1.17E+06	6.58E+05	6.58E+05	1.41E+06	1.83E+06
steel	8.77E+06	1.90E+07	3.00E+06	5.00E+06	1.17E+07	2.40E+07
stainless steel	0	0	0	0	0	0
U ₃ O ₈	0	0	8.62E+07	9.23E+07	8.62E+07	9.23E+07
Net LILW	1.24E+07	2.62E+07	0	0	1.24E+07	2.62E+07
Zinc	2.24E+05	9.57E+05	0	0	2.24E+05	9.57E+05
Paint	1.57E+04	1.03E+05	0	0	1.57E+04	1.03E+05
Aluminium	0	0	0	0	0	0

Table 70 shows the calculated gas amounts for steel and zinc corrosion of the container materials.

Table 70: Calculated total gas amounts for steel and zinc corrosion (waste excluded)

Material	LILW		(TE)NORM		Total	
	min [m ³]	max [m ³]	min [m ³]	max [m ³]	min [m ³]	max [m ³]
Steel	4.68E+06	1.01E+07	1.60E+06	2.67E+06	6.28E+06	1.28E+07
Zinc	7.68E+04	3.28E+05			7.68E+04	3.28E+05

Table 71 shows the calculated gas amounts of steel and zinc corrosion.

Table 71: Calculated total gas amounts for steel and zinc corrosion expressed in Moles

Material	LILW		(TE)NORM		Total	
	min [M]	max [M]	min [M]	max [M]	min [M]	max [M]
Steel	~2E+08	~4.5E+08	~7E+07	~1.2E+8		
Zinc	~3.4E+06	~1.4E+07			~3.4E+06	~1.4E+07

As shown in Table 6, the total net waste in the 200 L containers was estimated to range between 1.22E+07 kg and 2.57E+07 kg. The data given in Table 7 is used to estimate the total gas amounts due to steel and aluminium corrosion. Both metals were estimated to amount to 30 % ± 20 % in the waste. Table 72 shows the estimated gas amounts due to corrosion of metals in the waste.

Table 72: Estimated minimum and maximum generated gas amounts due to degradation of steel and aluminium present in the waste

Material	Minimum amount in waste [kg]	Maximum amount in waste [kg]	Minimum gas amounts [m ³]	Maximum [m ³]
Steel	9.15E+05	4.57E+06	4.88E+05	2.44E+06
Aluminium	3.05E+05	1.52E+06	3.80E+05	1.89E+06
Total	1.22E+06	6.09E+06	8.68E+05	4.33E+06

Using the data in Table 72, the potential gas amounts are calculated and given in Moles in Table 73.

Table 73: Calculated gas amounts in Moles

Material	Minimum amount in waste [M]	Maximum amount in waste [M]	Minimum gas amounts [M]	Maximum [M]
Steel	1.6E+07	8.1E+07	2.1E+07	1.08E+08
Aluminium	1.1E+07	5.6E+07	1.65E+07	8.4E+07
Total	2.7E+07	1.37E+08	3.75 E+07	1.92E+08

5.13.1.2. Gas generation due to microbial activity

It can be assumed that microbial activity is not significant at pH values > 12 as it is assumed to prevail in the planned repository. However, for completeness, assuming that microbes would be active and degrade organic matter (i.e. polyethylene and cellulose) the generated gas amounts (under anaerobic conditions) are also estimated.

Degradation of polyethylene (described by the monomer C₂H₄; 28 g/mol) can take place due to the following processes:

Denitrification:

Reaction	Mol Gas/Mol C ₂ H ₄	m ³ Gas/kg Material
C ₂ H ₄ + 2,4 NO ₃ ⁻ + 2,4 H ⁺ <-> 2 CO ₂ + 1,2 N ₂ + 3,2 H ₂ O	3.2	2.562

Sulfate reduction :

Reaction	Mol Gas/Mol C ₂ H ₄	m ³ Gas/kg Material
C ₂ H ₄ + 1,5 SO ₄ ²⁻ + 3H ⁺ <-> 2 CO ₂ + 1,5 H ₂ S + 2H ₂ O	3.5	2.802

Fermentation:

Reaction	Mol Gas/Mol C ₂ H ₄	m ³ Gas / kg Material
$C_2H_4 + 8/3 SO_4^{2-} \leftrightarrow 4/3 CO_2 + 10/3 H_2S + 2/3 CH_4$	5.33	4.267

The fermentation reaction can be considered conservative due to the highest gas generation amounts.

The data given in Table 6 and Table 7 is used to estimate the mass of PE in the LILW. Since the total net waste in the 200 L containers was estimated to range between 1.22E+07 kg and 2.57E+07 kg, the non-halogenated plastics (assumed to consist solely of PE) mass can be estimated to range from 5.49E+05 kg (= 1.9E+07 M) to 1.04E+7kg (= 3.71E+08 M). Using the fermentation reaction, gas amounts due to microbial PE degradation would amount to 2.34E+06 m³ (=1.01E+08 M) - 4.56E+07 m³ (= 1.97E+09 M).

Degradation of cellulose (described by the monomer C₆H₁₂O₆ but using the molar mass of cellulose, 162 g/mol) can occur due to the following processes [Poppei 2002]:

Denitrification:

Reaction	Mol Gas/Mol C ₂ H ₄	m ³ Gas/kg Material
$C_6H_{12}O_6 + 4,8 NO_3^- + 4,8 H^+ \leftrightarrow 6 CO_2 + 2,4 N_2 + 8,4 H_2O$	8.4	1.162

Sulfate reduction:

Reaction	Mol Gas/Mol C ₂ H ₄	m ³ Gas/kg Material
$C_6H_{12}O_6 + 3 SO_4^{2-} + 6 H^+ \leftrightarrow 6 CO_2 + 3 H_2S + 6 H_2O$	9	1.245

Fermentation:

Reaction	Mol Gas/Mol C ₂ H ₄	m ³ Gas/kg Material
$C_6H_{12}O_6 + 2 H_2O \leftrightarrow 4 CO_2 + 4H_2 + 2 CH_4$	10	1.384

The data given in Table 6 and Table 7 is used to estimate the mass of Cellulose in the LILW. Since the total net waste in the 200 L containers was estimated to range between 1.22E+07 kg and 2.57E+07 kg, the Cellulose mass can be estimated to range from 1.83E+06 kg to 1.41E+07 kg. Using the fermentation reaction, gas amounts due to microbial PE degradation would amount to 2.53E+06 m³ (= 1.1E+08 M) - 1.95E+07 m³ (8.7E+08 M).

5.13.1.1. Volatile radioisotopes

Of the radionuclides present in the LILW (see section 3.2), ¹⁴C, ¹²⁹I, ³H and Rn need to be considered as having potential for formation of volatile forms. The release of ³H is not significant because of the short half-life of 12.3 years [Johnson 2004]. ¹⁴C that might be released from LILW (e.g. from ion exchangers) may occur in a volatile organic form such as CH₄ or in inorganic (carbonate) form in the aqueous phase and thus may produce carbonate phases. In the latter case, no transport in the gas phase is expected [Johnson 2004]. According to [Johnson 2004] ¹²⁹I is released to solution as iodide which is non-volatile. It appears unlikely that a volatile compound (e.g. CH₃I or I₂) is generated because these compounds are reactive or hydrolyse readily to reform iodide. ²²²Rn will be generated from decay of the Ra inventory in the repository. However, due to its short half-life of 3.82 days, most of the Rn would normally decay close to its source. If however, a bulk gas flow to the surface is established, eventually a carrier medium is thus provided capable of transporting significant fractions of Rn to the surface before it decays [Rodwell 1999].

5.13.1.1. Radiolysis of water

Radiolysis is understood as the decomposition of chemical compounds by radiation. It is distinguished between internal and external radiolysis. The former means processes taking place in the waste and its package. External radiolysis regards the backfill material and possibly the host rock. All kinds of radiation (α , β , γ , n) may contribute to gas generation inside the waste packages. The decomposition of water (H_2O) results under idealized conditions in the formation of hydrogen and oxygen gas. Normally oxygen reacts immediately with its environments since it is generated in atomic form. Thus, gas generation by radiolysis of water is commonly characterised by the amount of hydrogen produced per unit mass of substrate and applied radiation dose. The G-value describes this linear relationship [Rodwell 1999]:

$$B = G \cdot D$$

where

B: generated gas volume

D: radiation dose

G is specific for the gas generated and the irradiated material. It was defined historically as the number of molecules of gas produced per 100 eV of absorbed radiation energy [Rodwell 1999].

[Bouniol 2008] reviewed the basic mechanisms controlling the radiolysis in cementitious matrices in the context of gamma radiation at 25 °C with a pore solution representative of Portland cement paste. Regarding the gamma radiation of water, after 10^{-7} to 10^{-6} seconds of irradiation, the water decomposition leads to the formation of 8 primary species (H_2 , H_2O_2 , OH^\cdot , H_3O^+ , e^- , H^\cdot , OH^\cdot , HO_2^\cdot). Due to the variability of the alkali contents in industrial cements, there is no standard value of the primary yields for cement matrices. Thus, the G_{H_2} value can vary from 0.0435 to 0.384 between pH 12.45 and 14). After the primary step, generated species can react with the solvent (H_2O) and its main solute (OH^-) or between themselves. About 60 reactions are known (please refer to [Bouniol 2008] for details). The decomposition of alkaline water without any other solute leads to the secondary production of molecules and radicals, either already known as primary products or new products (O_2 , O_3 , etc.).

In the presence of $Ca(OH)_2$, H_2O_2 and its derived species can react to the metastable calcium peroxide octahydrate ($CaO_2 \cdot 8 H_2O$) when the solubility product ($2.51E-11$) is reached [Bouniol 2008].

6. Radionuclide Source-Terms and Migration in the Near-Field

6.1. Source terms

In order to define a model representation of the repository for safety assessment the 'source term' is necessary [Verhoef 2011]. In the following sections, the source terms for the waste matrix and radionuclide release are defined for the different fractions of LILW.

6.1.1. Compacted waste

The details of the compacted waste are discussed in section 3.1.1. The top of the 200 L drums containing the compressed waste are not covered with steel (as the rest of the particular drums). Thus, as soon as those containers come into contact with (cementitious pore) water, diffusion processes according to the prevailing concentration gradients will take place. As noted in section 3.1.1, the radionuclides present in the compacted waste can be expected to be present on the particular surfaces of the wastes (e.g. tissues). Thus, it

is proposed for performance assessment that as soon as the waste comes into contact with water, an instantaneous release of the radionuclides will take place.

Regarding degradation rates of organic material, most research was carried out on cellulose degradation (see section 5.3). However, up to date there still exist large uncertainties and the chemical degradation kinetics of cellulose are not sufficiently understood. For initial assessments, the rate equations given in section 5.3 may be used.

Regarding the other organic materials present in the compacted waste, no studies concerning the degradation kinetics under alkaline conditions exist. The plastic materials (PE, PVS, PC, i.e. addition polymers) however can be assumed to be relatively inert under cementitious near-field conditions.

6.1.2. Processed liquid molybdenum waste

The characteristics of the processed molybdenum waste are described in section 3.1.2.1. As soon as the 200 L containers (placed in the 1,000 L containers) are corroded, migration of the pore water into the waste and diffusion of the radionuclides from the waste into the pore water (due to a concentration gradient) will take place. Taking a wall thickness of 1 mm and a corrosion rate of 0.2 $\mu\text{m/a}$ (anoxic conditions) as given in Table 74, the container would be corroded in ~ 5000 a. The concentrations of the particular elements in the cementitious pore water will be controlled by their solubility.

6.1.3. Processed liquid waste with ion exchangers

The characteristics of the processed liquid waste with ion exchangers are described in section 3.1.2. In the first step, cementitious pore water will migrate through the 1000 L containers and reach the 200 L drum. After its corrosion (similar values as given in section 6.1.2 can be assumed), the cementitious waste matrix will come into contact with cementitious pore water and thus the radionuclides may be released. Since the ion exchanger materials are not in equilibrium with the cementitious alkaline conditions, a fast radionuclide release can be assumed.

6.1.4. (TE)NORM: depleted Uranium

As presented in section 3.1.3, DU is stored in KONRAD type II containers when placed in the repository. These containers are made of low carbon steel with at least 3 mm thickness.

[Kursten 2015] compiled low carbon steel corrosion rate data in alkaline media under anoxic and oxic conditions (see also section 5.10.1.).

[Kursten 2015] reviewed their compiled corrosion rate data and divided them into two ranges: a source (SR) and an expert range (ER). The SR and ER of corrosion rates for carbon steel in high alkaline environments (pH ~ 13.6) and without the ingress of aggressive species (e.g. chloride) are shown in Table 74. Source range is the range of values outside of which the value of the corrosion rate is very unlikely to lie, considering current knowledge. The expert range is understood as the range of values within which experts expect the value of the corrosion rates to lie. It is meant to be a more realistic corrosion rate range than the source range and is thus expected to be more narrow [Kursten 2015].

Table 74: Uniform corrosion rate of carbon steel in high alkaline environments (pH ~ 13.6) and without the ingress of aggressive species [Kursten 2015]

Condition	SR [$\mu\text{m/a}$]	ER
Oxic, alkaline media	0.005 - 2.2	0.005 - 2.2
Anoxic, alkaline media	0.0015 - 2.4	0.0015 - 0.2

By using corrosion rates as compiled by [Kursten 2015] (Table 74) the time of failure of the containers can be estimated as shown in Table 75.

Table 75: Calculated times of failure of the KONRAD II container using the data given in Table 74

Condition	Time of failure [a] using SR values	Time of failure [a] using ER values
Oxic, alkaline media	600,000 - 1,370	600,000 - 1,370
Anoxic, alkaline media	2 Ma - 1,250	2 Ma - 15,000

According to [Kursten 2015], 1 D thermo hydraulic analysis of the resaturation time of the concrete materials showed that the concrete will resaturate almost completely (95-98 %) after already one to five years. Assuming an oxic phase of 5 years and the maximum given corrosion rate of 2.2 $\mu\text{m/a}$, the canister is only corroded about 11 μm . In the following anoxic phase, the maximal expert value of 0.2 $\mu\text{m/a}$ is taken for the estimation when the KONRAD container is fully corroded. Considering the 11 μm steel already corroded in the oxic phase, another 15.000 years have to pass to corrode the steel completely (assuming uniform corrosion).

[Kursten 2015] also investigated the effect of chloride on the carbon steel corrosion rate. According to [Kursten 2015], lots of data are available on the effect of chloride on the aerobic corrosion rate of carbon steel. However, the authors found it very difficult to assign an absolute value to the effect of chloride concentration.

Regarding the anaerobic corrosion rate in presence of chloride, it was affected that the anaerobic long-term corrosion rate was not affected by the addition of chlorides up to 20,000 mg/L. For more information on this topic it is referred to [Kursten 2015].

When the container is corroded, the conditioned waste will come into contact with water. The uranium concentration in the pore water is controlled by the uranium solubility (see section 6.2.1 for radionuclide solubility data) whereas the migration of cementitious pore water into the cement matrix and the desorption and diffusion of uranium out of the conditioned waste matrix takes place.

6.2. Radionuclide migration in the near-field

Generally, the radionuclide concentrations in the repository near-field can be expected to be the highest because they will not increase along the migration path ways to the far-field and will only decrease due to retardation processes, e.g. due to sorption of radionuclides onto engineering or natural barriers in the repository.

Due to the complex nature of the radionuclide behavior, it is not possible to accurately determine the maximum radionuclide concentrations in the repository. The element concentrations in the pore water are determined by many processes such as the degradation rate of the waste and containers, dissolution and precipitation of secondary solids and their sorption onto repository materials. A possibility to determine the maximum concentrations of radionuclides in a geological repository would be to calculate the solubility of radionuclides by using chemical thermodynamic data [Wanner 2007]. According to [Wang 2013], it is justified within the radioactive waste community that solubility determined by equilibrium calculation represents the maximum released radionuclide concentration. Therefore, relevant radionuclide solubility data was compiled in the framework of this study and is presented in the following sections.

6.2.1. Solubility of radionuclides in a cementitious near-field

The leaching behavior and mobility of radionuclides in cementitious materials depends mainly on the chemical behavior of the particular nuclide and the chemical, physical and mineralogical properties of the material. In general, many nuclides may exist parallel in different binding forms. How the radionuclides are bound in the cementitious matrix is dependent on the particular radionuclides and their specific chemical behavior under alkaline conditions. An essential binding mechanism is the sorption/incorporation on and in

cement phases, whereas the calcium silicate hydrates have a high specific binding capacity for radionuclides. Furthermore, many nuclides can also be sorbed/incorporated on Calcite which is generated due to the carbonatisation of concrete. Radionuclides can sorb onto Fe-hydroxides (formed due to the degradation of steel) or eventually may also precipitate in alkaline cement pore waters also as discrete phases or exist as oxide particles (e.g. UO_2 or PuO_2) [Deissmann 2005].

[Wang 2013] determined the solubility values of 21 radionuclides in a foreseen engineered barrier system for the disposal of Belgian high-level waste in Boom Clay under the present day conditions. The solubility values were calculated by means of equilibrium calculations or taken from literature for conditions relevant for a cement pore water characterised by a high pH value. Equilibrium calculation assumes that the element solubility is reached when the solubility limiting solid phase of the particular element is in equilibrium with the pore water. According to [Wang 2013], most of the considered radionuclide solubilities are determined only by pH.

[Wang 2013] modelled in the first step the interaction of cement with Boom Clay porewater. The Boom Clay water was a 15 mM $NaHCO_3$ solution with minor concentrations of other species and a pH of 8.5. To calculate the evolution of the cement porewater, an initial amount of about 100 g cement was put in equilibrium with Boom Clay water of increasing amounts. In the result it was found that the porewater had an initial pH of ~ 13.5. Portlandite dissolved at $pH < 12.5$ and the CSH phases were depleting at $pH \sim 10.5$.

Thus, [Wang 2013] used for their further radionuclide solubility calculations 3 states of cement degradation (based on the change of pH and the cement phases stability). At 25 °C the following cement degradation stages were used:

Stage 1: $pH \sim 12.5 - 13.5$ (NaOH and KOH porewater)

Stage 2: $pH \sim 12.5$, controlled by the solubility of $Ca(OH)_2$

Stage 3: $pH 10.5 - 12.5$, pH is buffered by CSH-phases

The porewater compositions of the particular stages (used in the equilibrium calculations) are shown in Table 76. The redox potential was found to be very uncertain and no exact value was given by the authors.

Table 76: Simulated porewater compositions at 25 °C [Wang 2013]

Element [mM]	Stage 1	Stage 2	Stage 3
Ca	0.7-15.4	15.4	15.4-1.4
Na	141-15	15	15
K	370-0.2	0.2	0.2
Al	0.08-0.008	0.008	0.008 - 0.5
Si	0.1-0.002	0.002	0.002 - 5
Mg	$1E-7 - 1E-6$	$1E-6$	$1E-6 - 1E-4$
*Fe	$1E-4 - 1E-5$	$1E-5$	$1E^{-5} - 0.5$
C (TIC)	$0.4 - 7 \times 1E-3$	$7E-3$	$7E^{-3} - 0.02$
SO_4^{2-}	8 - 0.04	0.04	0.04 - 5.7
pH	13.5 - 12.5	12.5	12.5 - 10.5

*under oxidising conditions, Fe is in equilibrium with dissolved oxygen from air

For the calculation of the solubility values the thermodynamic database Thermochemie v7b was used. The equilibrium modeling was carried out by setting cement phases in equilibrium with Boom Clay pore water and the resulting pore water composition was calculated for different cement degradation stages as a function of time. The initial cement phases were Portlandite, afwillite or CSH, ettringite, hydrogarnet, iron oxide and

calcite. For more details regarding the equilibrium calculations it is referred to [Wang 2013]. Table 77 shows the determined solubilities found by [Wang 2013].

Table 77: Solubility values [M/kg water] of selected elements in cementitious pore water in the absence of ligands [Wang 2013]

Element	Stage	Upper bound	90 % confidence limit for upper bound	Lower bound	95 % confidence limit for lower bound
Ag	1	6E-5		VL	
	2	6E-6		VL	
	3	6E-6		VL	
Am	1	3E-9	3E-10 - 3E-8	3E-9	3E-10 - 3E-8
	2	3E-9	3E-10 - 3E-8	3E-9	3E-10 - 3E-8
	3	3E-9	3E-10 - 3E-8	3E-9	3E-10 - 3E-8
Be	1	1E-4		< 1E-4	
	2	< 1E-4		< 1E-4	
	3	< 1E-4		< 1E-4	
C	1	3E-4		8E-6	
	2	8E-6		8E-6	
	3	1E-5		8E-6	
Ca	1	1.5E-2		7E-4	
	2	1.5E-2		1.5E-2	
	3	1.5E-2			
Cl	1 - 3	not limited		not limited	
Cm	1	3E-9	3E-10 - 3E-8	3E-9	3E-10 - 3E-8
	2	3E-9	3E-10 - 3E-8	3E-9	3E-10 - 3E-8
	3	3E-9	3E-10 - 3E-8	3E-9	3E-10 - 3E-8
Cs	1 - 3	not limited		not limited	
I	1 - 3	not limited		not limited	
Mo	1	9E-4		5E-6	
	2	5E-6		5E-6	
	3	4E-5		5E-6	
Nb	1	1.1E-5	2E-6 - 2E-5	7E-9	4E-9 - 8E-9
	2	7E-9	4E-9 - 8E-9	7E-9	4E10-9 - 8E-9
	3	8E-7	1.8E-7 - 4.2E-7	7E-9	4E-9 - 8E-9
Ni	1	2.9E-7	2.4E-7 - 3.4E-7	2.9E-7	2.4E-7 - 3.4E-7
	2	2.9E-7	2.4E-7 - 3.4E-7	2.9E-7	2.4E10-7 - 3.4E-7
	3	2.9E-7	2.4E-7 - 3.4E-7	2.9E-7	2.4E-7 - 3.4E-7
Np (IV)	1	1E-8		1E-9	
	2	1E-8		1E-9	
	3	1E-8		1E-9	
Pa	1 - 3	1E-8		1E-8	
Pb	1	not limited		not limited	
	2	not limited		5E-2	
	3	not limited		1E-4	
Pd	1	1E-4		1E-5	
	2	1E-5		1E-5	
	3	1E-5		4E-6	
Pu (IV)	1 - 3	1E-8		1E-11	
Ra	1	1E-6		7E-9	
	2	1E-6		1E-6	
	3	1E-6		1E-8	
Se	1	not limited		5E-4	
	2	not limited		2E-5	
	3	not limited		1E-11	

Table 77 (continued): Solubility values [M/kg water] of selected elements in cementitious pore water in the absence of ligands [Wang 2013]

Element	Stage	Upper bound	90 % confidence limit for upper bound	Lower bound	95 % confidence limit for lower bound
Sn	1	2E-6		1E-8	
	2	1E-8		1E-8	
	3	1E-7		1E-8	
Sr	1	2.5E-3		1E-4	
	2	2.5E-3		2.5E-3	
	3	2.5E-3		3.4E-4	
Tc	1	not limited		1E-6 (Tc (IV))	
	2	not limited		1E-7 (Tc (IV))	
	3	not limited		not limited	
Th (IV)	1 - 3	1E-8	1E-9 - 1E-7	1E-8	1E-9 to 1E-7
U (VI)	1	3E-6			
	2	2E-6	1E-6 - 6E-6	2E-6	1E-6 - 6E-6
	3	3E-5		2E-6	1E-6 - 6E-6

[Berner 2003] carried out solubility calculations in cementitious pore water using the Nagra/PSI Chemical Thermodynamic Data Base (TDB) various elements (Table 78). The heading "Calculated" lists maximum concentrations based on data fully documented in the TDB. The results under the heading "Recommended" include data from other sources.

Table 78: Results of solubility calculations carried out by [Berner 2003]. Conditions: pH 12.55, E_H -230 mB, 25 °C

Element	CALCULATED			RECOMMENDED		
	Lower limit	Maximum solubility	Upper limit	Lower limit	Maximum solubility	Upper limit
Cm	-	-	-	3E-10	2E-9	1E-8
Am	3E-10	2E-9	1E-8	-	-	-
Pu	1E-11	4E-11	2E-10	-	-	-
Np	3E-9	5E-9	1E-8	-	-	-
U	-	not limited	-	-	1E-8	5E-7
Pa	-	-	-	-	~1E-8	-
Th	8E-10	3E-9	1E-8	-	-	-
Ra	-	1E-5	-	1E-6	-	2E-2

Table 78 (continued): Results of solubility calculations carried out by [Berner 2003]. Conditions: pH 12.55, E_H -230 mB, 25 °C

Element	CALCULATED			RECOMMENDED		
	Lower limit	Maximum solubility	Upper limit	Lower limit	Maximum solubility	Upper limit
Cs	-	not limited	-	-	-	-
I	-	not limited	-	-	-	-
Tc	-	not limited	-	-	-	-
Nb	-	not limited	-	-	-	-
Se	-	not limited (-0.1)	-	7E-6	1E-5	2E-5
Cl	-	not limited	-	-	-	-
C _{inorg}	-	-	-	-	9.7E-6	2E-4
Ac	-	-	-	4E-9	2E-6	2E-5
Sn	1E-8	1E-7	2E-7	-	-	-
Pd	-	insignificantly low	-	8E-8	8E-7	8E-6
Zr	-	6E-6	-	6E-7	-	6E-5
Sr	-	3E-3	-	1E-3	-	6E-3
Ni	1E-8	3E-7	8E-6	-	-	-
Po	-	-	-	-	-	-
Pb	-	-	-	-	3E-3	2E-2
Hf	-	-	-	6E-7	6E-6	6E-5
Ho	-	-	-	4E-9	2E-6	2E-5
Eu	-	2E-6	2E-5	4E-9	-	-
Pm	-	-	-	4E-9	2E-6	2E-5

Table 78 (continued): Results of solubility calculations carried out by [Berner 2003]. Conditions: pH 12.55, E_H -230 mB, 25 °C

Element	CALCULATED			RECOMMENDED		
	Lower limit	Maximum solubility	Upper limit	Lower limit	Maximum solubility	Upper limit
Sb	-	not limited	-	-	-	-
Cd	-	-	-	-	4E-6	3E-5
Ag	-	-	-	-	insignificant -ly low	3E-6
Ru	-	-	-	-	-	high
Mo	-	-	-	-	3E-5	2E-3
Co	-	-	-	-	7E-7	8E-6
Fe	-	-	-	-	1E-7	1E-6
Ca	-	2E-2	-	1.8E-2	-	2.2E-2
Be	-	-	-	-	-	high

6.2.2. Effects of (organic) LILW degradation products on radionuclide solubility

Data regarding the effects of ligands on radionuclide solubility have been found for isosaccharinic acid and certain cement additives. The findings are summarised in the following text.

Isosaccharinic acid (ISA)

The effect of cellulose degradation products (CDPs) such as ISA on the behavior of radionuclides, e.g. through increase of their solubility (= maximum amount of a species), has been recognised since the early 1980s [Heath 2005]. A number of experimental and modelling studies were carried out to understand and quantify the impact of CDPs. Results of selected studies on effects of CDPs on radionuclide solubility are presented in this section.

Previous studies (see also section 5.2.1.1) showed that ISA is the most abundant CDP with complexation potential; however, it was also shown that numerous other short chain organic acids are also generated during degradation. ISA, however, has received the most attention in the literature but in general it is necessary to understand the behaviour of the other CDPs generated and their influence on radionuclide transport in order to predict their impact on the long-term performance of the repository.

[Berner 2014] carried out solubility calculations with the GEMS/PSI software [Kulik 2013] using the PSI/Nagra Chemical Thermodynamic Data Base 12/07 [Thoenen 2012a, Thoenen 2012b]. Solubility limits for the safety relevant elements Be, C, Cl, K, Ca, Co, Ni, Se, Sr, Zr, Nb, Mo, Tc, Pd, Ag, Sn, I, Cs, Sm, Eu, Ho, Pb, Po, Ra, Ac, Th, Pa, U, Np, Pu, Am and Cm in the pore water of a concrete system characterised by portlandite ($\text{Ca}(\text{OH})_2$) saturation (pH 12.5) and by the absence of (Na,K)OH solutes were evaluated according to the principles of equilibrium thermodynamics [Berner 2014]. Furthermore, the impact of a maximum concentration of ISA present in the cementitious system on the solubility of the mentioned elements was investigated and solubility enhancement factors (SEF) were derived [Berner 2014].

The modelled impact of ISA on the radionuclide solubilities is summarized in Table 79 (SEF were derived by dividing the solubility in the presence of ISA^- by the solubility in the absence of ISA^-). For the solubility calculations, [Berner 2014] used an ISA concentration of $5\text{E-}3$ M/kg H_2O which is near the maximum concentration of $2\text{E-}2$ M/kg H_2O . The maximum concentration was assumed to be defined by the solubility of solid $\text{Ca}(\text{ISA})_2$.

Table 79: Influence of $5\text{E-}3$ [M/kg H_2O] of ISA^- on the solubility of selected elements [Berner 2014]

Element	Solubility w/o ISA^- [M/kg H_2O]	Solubility in the presence of $5\text{E-}3$ [M/kg H_2O] of ISA^- [M/kg H_2O]	SEF	Dominant complexes in solution Comments
Ca	$1.8\text{E-}2$	$2\text{E-}2$	1.1	Ca^{2+} ; Ca-ISA complexes only
Ni	$3\text{E-}6$	$3.5\text{E-}6$	1.2	$\text{Ni}(\text{OH})_3^-$; $\text{Ni}_2(\text{ISA})(\text{OH})_4^-$ only 6 %
Zr	$4.5\text{E-}9$	$4.9\text{E-}7$	109	$\text{Zr}(\text{OH})_4\text{ISA}^-$ exclusively based on analogy with Eu
Sm	$4.6\text{E-}7$	$2.9\text{E-}4$	630*	$\text{Sm}(\text{OH})_3\text{ISA}^-$ exclusively based on analogy with Eu
Eu	$1.9\text{E-}6$	$5\text{E-}4$	263	$\text{Eu}(\text{OH})_3\text{ISA}^-$
Ho	$1.9\text{E-}7$	$1.2\text{E-}4$	632*	$\text{Ho}(\text{OH})_3\text{ISA}^-$ exclusively based on analogy with Eu
Po	$6.4\text{E-}8$	$4.7\text{E-}5$	731	$(\text{Po}(\text{OH})_4)\text{ISA}^-$ exclusively based on analogy with Th
Ac	$1.9\text{E-}6$	$5\text{E-}4$	263	$\text{Ac}(\text{OH})_3\text{ISA}^-$ exclusively based on analogy with Eu.
Th	$1.3\text{E-}9$	$9.5\text{E-}7$	731	$\text{Th}(\text{OH})_4\text{ISA}^-$; $\text{ThCa}(\text{OH})_4(\text{ISA})_2(\text{aq})$
Pa	$1.8\text{E-}6$	$2.3\text{E-}6$	1.3	No thermodynamic data; analogy with Eu, Th, U, Np.
U	$7\text{E-}7$	$8.4\text{E-}7$	1.2	$\text{UO}_2(\text{OH})_4^{2-}$; $\text{U}(\text{OH})_4\text{ISA}^-$ only 10 %; ratio U(IV)/U(VI) increases from 0.004 to 0.11
Np	$1\text{E-}9$	$3.5\text{E-}9$	3.5	$\text{Np}(\text{OH})_4\text{ISA}^-$ and $\text{Np}(\text{OH})_4(\text{ISA})_2^{2-}$ (72 %)
Pu	$2.3\text{E-}12$	$8.1\text{E-}12$	3.5	No thermodynamic data; analogy (enhancement factor) with Np assumed
Am	$5.4\text{E-}10$	$8.9\text{E-}8$	165	$\text{Am}(\text{OH})_3\text{ISA}^-$
Cm	$1.1\text{E-}9$	$1.8\text{E-}7$	165	No thermodynamic data; analogy with Am assumed

* the difference in impact factors between Eu, Sm and Ho has its origin in differing formation constants for the $\text{Ln}(\text{OH})_4^-$ complexes.

The results of the study of [Berner 2014] have shown that the presence of ISA may be critical for the tri-valent elements Eu (Sm, Ho, Ac), Am and Cm, and for Th (Po, Zr). Obviously, the impact on Ca, Ni, Pa, U, Np and Pu is less significant. However, [Berner

2014] states that further work on evaluating complex formation constants with ISA is necessary. The author concludes that since a rather high ISA concentration was selected for the calculations, a potential impact of degrading organic materials on the solubility of safety relevant elements is not significant or at most restricted to tri-valent elements.

[Randall 2013] carried out cellulose degradation experiments to investigate the influence of cellulose degradation products on Th and Eu solubility. In the first step, cellulose degradation products were generated at temperatures 25 °C, 50 °C and 80 °C in saturated Ca(OH)₂ solution with a pH of ~12.4. Three types of material were investigated: paper, wood and cotton wool. All experiments were carried out in anaerobic and aerobic conditions. Experiment duration was 1 or 12 months. In the second step, the degradation products were identified in the samples for 1 and 12 months. The results from the analysis of the 1 month old leachates showed that the most significant degradation products were ISA, X-ISA, lactic acid, glycolic acid, 2-hydroxybutyric acid and formic acid. Thus, for the solubility studies, lactate, 2-hydroxybutyrate, glycolate, acetate, ISA and X-ISA were chosen.

The measured thorium solubility in saturated Ca(OH)₂ solution (in absence of organic compounds) at pH 12 as determined by [Randall 2013] is shown in Table 80.

Table 80: Experimentally determined thorium solubility in absence of organic compounds [Randall 2013]

Target pH	Replicate	pH after 28 days	Average pH	Th [M]	Th error, [M]	Average [Th], M	Average [Th] error, M
12	1	12.24	12.20	1.78E-7	2.16E-9	7.19E-8	2.05E-9
	2	12.19		2.02E-8	4.31E-10		
	3	12.16		1.8E-8	3.58E-9		
12	1	12.20	12.19	6.63E-8	8.62E-10	2.28E-7	2.01E-9
	2	12.19		1.51E-7	8.62E-10		
	3	12.19		4.66E-7	4.31E-9		

[Randall 2013] made a comparison of the Thorium solubilities determined in the framework of their study with selected experimental results from the open literature (Figure 38). As can be seen, their determined solubilities are higher than many experimental determinations.

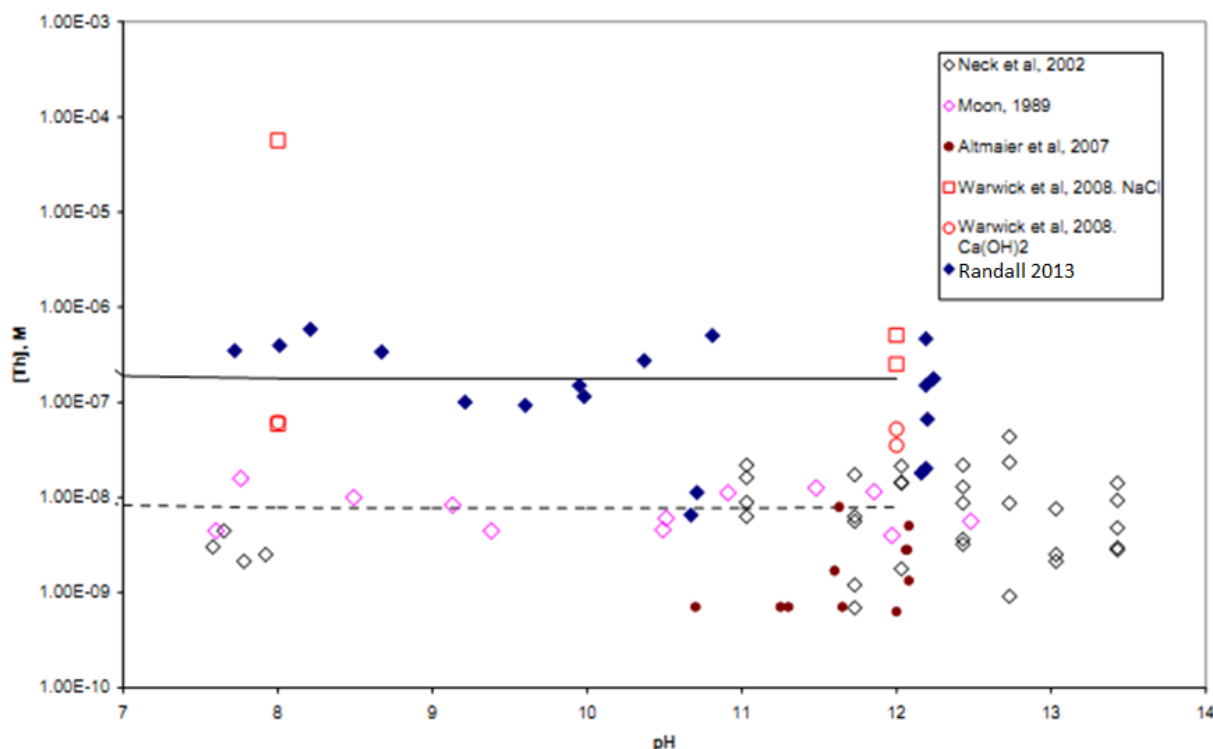


Figure 38: Comparison of thorium solubility in absence of organic compounds determined by [Randall 2013] with other work [Randall 2013]

[Randall 2013] investigated in the framework of their study furthermore the thorium solubility in the presence of different cellulose degradation products. The results, shown in Table 81, present the measured thorium solubility in the presence of lactic acid, acetic acid, hydroxybutyric acid and glycolic acid (all at initial concentrations of 1E-3 M).

Table 81: Experimental results for thorium solubility in the presence of different organic acids [Randall 2013]

Test product	pH	Final pH	Average pH	Th [M]	Th Error [M]	Average Th [M]	Average Th error, [M]
Lactic acid [1E-3 M]	12	12.15	12.15	2.41E-7	4.74E-9	6.93E-5	5.65E-7
		12.17		7.07E-7	9.05E-9		
		12.13		2.07E-4	1.68E-6		
Glycolic acid [1E-3 M]	12	12.09	12.19	5.78E-7	2.37E-9	3.63E-7	3.09E-9
		12.22		1.13E-7	1.29E-9		
		12.26		3.97E-7	5.6E-9		
Acetic Acid [1E-3 M]	12	12.20	12.21	1.54E-7	2.37E-9	2.57E-6	1.86E-8
		12.23		5.3E-6	4.31E-8		
		12.20		2.25E-6	1.03E-8		
2-hydroxybutyric acid [1E-3 M]	12	11.90	11.9	4.48E-8	4.31E-10	1.69E-7	0
		11.93		2.65E-7	5.17E-9		
		11.92		1.97E-7	2.16E-9		

[Randall 2013] concluded that the presence of lactic acid at pH 12.2 at an initial concentration of 10^{-3} M had no impact on thorium solubility. Furthermore, it was found that glycolic acid also has no effect regarding a solubility increase at pH 12.2. Concerning acetic acid, [Randall 2013] found that this compound increases thorium solubility by an order of magnitude at pH 12.5. Obviously, hydroxybutyric acid also has no impact on thorium solubility [Randall 2013].

In the framework of their research, [Randall 2013] investigated also the solubility of thorium in the presence of ISA and X-ISA. Table 82 and Table 83 show the experimental

results of the thorium solubility in the presence of ISA or X-ISA at concentrations ranging from 10^{-4} M to 10^{-2} M at pH ~ 12.

Table 82: Experimental results regarding the thorium solubility in the presence of ISA [Randall 2013]

Test Product	Target pH	Final pH	Average final pH	Th [M]	Th Error [M]	Average Th [M]	Average Th Error, [M]
ISA [$1\text{E-}2$ M]	12	11.98	11.99	$1.29\text{E-}4$	$1.25\text{E-}6$	$1.2\text{E-}4$	$6.32\text{E-}7$
		12.03		$1.13\text{E-}4$	$1.29\text{E-}7$		
		11.96		$1.17\text{E-}4$	$5.17\text{E-}7$		
ISA [$5\text{E-}3$ M]	12	12.19	12.21	$1.18\text{E-}5$	$4.31\text{E-}8$	$1.19\text{E-}5$	$1.01\text{E-}7$
		12.36		$1.19\text{E-}5$	$1.72\text{E-}7$		
		12.08		$1.21\text{E-}5$	$8.62\text{E-}8$		
ISA [$1\text{E-}3$ M]	12	11.98	11.95	$3.84\text{E-}7$	$5.17\text{E-}9$	$2.78\text{E-}7$	$2.59\text{E-}9$
		11.84		$1.08\text{E-}7$	$8.62\text{E-}10$		
		12.03		$3.4\text{E-}7$	$1.72\text{E-}9$		
ISA [$1\text{E-}4$ M]	12	12.10	12.10	$1.5\text{E-}7$	$2.59\text{E-}9$	$6.49\text{E-}7$	$8.48\text{E-}9$
		12.10		$1.33\text{E-}6$	$2.24\text{E-}8$		
		12.09		$4.7\text{E-}7$	$4.31\text{E-}10$		

Table 83: Experimental results regarding the thorium solubility in the presence of X-ISA [Randall 2013]

Test Product	Target pH	Final pH	Average final pH	Th, [M]	Th Error [M]	Average Th [M]	Average Th Error [M]
X-ISA [$1\text{E-}2$ M]	12	11.10	11.18	$2.56\text{E-}5$	$4.31\text{E-}8$	$9.65\text{E-}5$	$4.31\text{E-}7$
		11.22		$2.42\text{E-}4$	$1.08\text{E-}6$		
		11.23		$2.16\text{E-}5$	$1.72\text{E-}7$		
X-ISA [$5\text{E-}3$ M]	12	12.20	12.20	$6.90\text{E-}5$	$8.19\text{E-}7$	$7.04\text{E-}5$	$6.9\text{E-}7$
		12.21		$7.33\text{E-}5$	$8.62\text{E-}7$		
		12.20		$6.9\text{E-}5$	$3.88\text{E-}7$		
X-ISA [$1\text{E-}3$ M]	12	12.44	12.43	$1.54\text{E-}6$	$2.46\text{E-}8$	$2.88\text{E-}6$	$1.6\text{E-}6$
		12.43		$4.96\text{E-}4$	$4.74\text{E-}6$		
		12.43		$4.22\text{E-}6$	$3.36\text{E-}8$		
X-ISA [$1\text{E-}4$ M]	12	12.21	12.31	$3.11\text{E-}7$	$3.02\text{E-}9$	$5.09\text{E-}7$	$8.76\text{E-}9$
		12.35		$3.06\text{E-}7$	$2.59\text{E-}9$		
		12.37		$9.09\text{E-}7$	$2.07\text{E-}8$		

Figure 39 summarises the results of the experiments described above (Table 82 and Table 83) and shows the solubility of thorium at pH 12 in presence of ISA/X-ISA at concentrations between 10^{-4} M and 10^{-2} M. As can be seen, the concentration of thorium increases as the concentration of both organic compounds increase. Regarding ISA, the solubility of thorium is not significantly influenced at ISA concentrations $< 10^{-3}$ M. A similar trend is observed with X-ISA although thorium solubility appears to be more enhanced at concentrations of 10^{-3} M and 10^{-5} M X-ISA than in the case for ISA [Randall 2013].

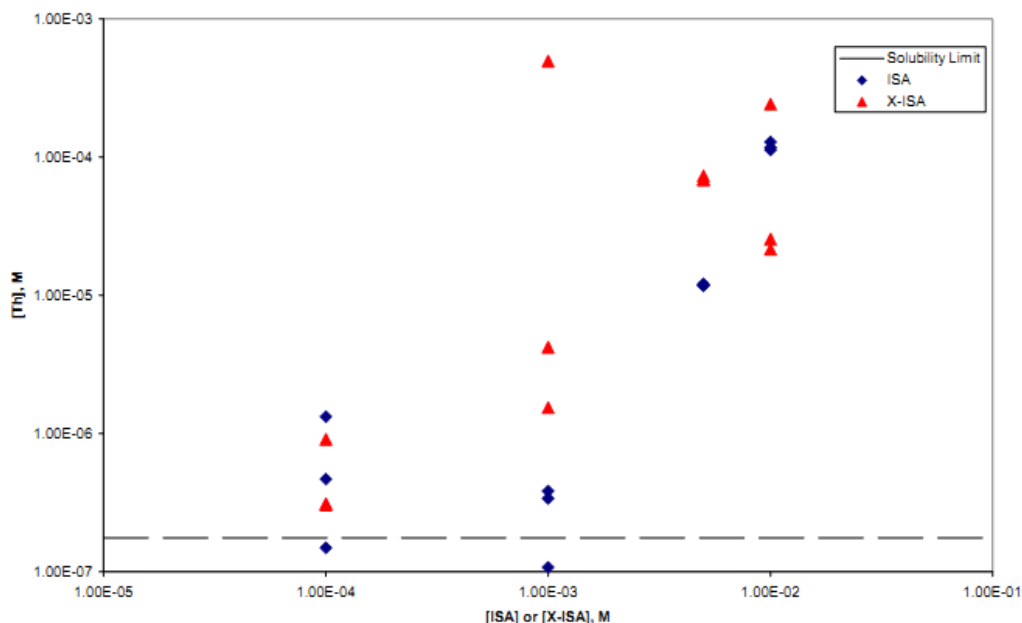


Figure 39: Thorium solubility in presence of varying concentrations of ISA and X-ISA at pH-12. The dashed line represents the thorium solubility limit in absence of organic compounds [Randall 2013]

[Randall 2013] carried out similar solubility experiments with europium in presence and absence of the same organic compounds as mentioned above. Table 84 shows the measured values of the europium solubility at pH ~ 12 in absence of organic compounds.

Table 84: Experimental results for europium solubility in the absence of organic compounds [Randall 2013]

Target pH	Final pH	Average pH	Eu [M]	Eu Error, [M]	Average Eu [M]	Average Eu error, [M]
12	12.14	12.14	2.91E-5	1.29E-7	1.07E-5	4.97E-8
	12.00		1.26E-6	4.74E-9		
	12.28		1.63E-6	1.51E-8		

[Randall 2013] investigated also the Europium solubility in the presence of lactic acid, acetic acid, hydroxybutyric acid and glycolic acid, all at initial concentrations of 10^{-3} M as a function of pH. The results of these investigations are shown in Table 85.

Table 85: Experimental results for Europium solubility in the presence of organic compounds [Randall 2013]

Test Product	Target pH	Final pH	Average final pH	Eu [M]	Eu Error [M]	Average [Eu], M	Average [Eu] error, M
Lactic acid [1E-3 M]	12	12	12	3.83E-4	3.09E-6	1.38E-4	1.15E-6
		12		1.35E-6	1.58E-7		
		12		2.84E-5	1.97E-7		
Glycolic acid [1E-3 M]	12	NS	12	NS	NS	2.19E-6	3.36E-8
		12		2.85E-6	4.54E-8		
		12		1.53E-6	2.17E-8		
Acetic acid [1E-3 M]	12	11.9	11.87	6.84E-4	2.5E-6	2.39E-4	8.9E-7
		11.5		6.58E-7	5.26E-9		
		12.2		3.32E-5	1.64E-7		
2-hydroxybutyric acid [1E-3 M]	12	11.7	11.7	9.34E-8	6.58E-10	3.74E-7	3.51E-9
		11.7		1.26E-7	1.32E-9		
		11.7		9.03E-7	8.55E-9		

NS: no sample (sample was lost during filtering)

As can be seen in Table 85, a solubility increase can be observed at pH 12 for both lactic and acetic acid.

As with thorium, [Randall 2013] carried out experiments to determine the impact of ISA and X-ISA on europium solubility over a range of concentrations. Table 86 shows the solubility of europium in the presence of ISA, Table 87 shows the data in the presence of X-ISA. An increase in solubility is also clear at an ISA concentration of 10^{-2} M. According to [Randall 2013], the apparent increase in solubility at ISA concentrations of 10^{-4} M is due to the large variation in the data. The experiments with X-ISA also show a solubility increase of europium with increasing X-ISA concentrations.

Table 86: Experimentally determined europium solubilities in the presence of ISA [Randall 2013]

Test product	Target pH	Final pH	Average final pH	Eu [M]	Eu Error [M]	Average Eu [M]	Average Eu Error [M]
ISA [1E-2 M]	12	12	11.99	2.38E-4	3.88E-7	8.75E-4	1.38E-5
		12		2.33E-3	4.05E-5		
		11.97		5.67E-5	4.31E-7		
ISA [5E-3 M]	12	12.17	12.17	4.05E-6	2.63E-8	3.18E-6	2.5E-8
		12.17		1.45E-6	5.6E-9		
		12.16		4.04E-6	4.31E-8		
ISA [1E-3 M]	12	11.75	11.75	1.92E-7	8.62E-10	8.93E-7	1.72E-9
		11.72		2.1E-7	1.29E-9		
		11.79		2.28E-6	3.02E-9		
ISA [1E-4 M]	12	11.9	12.09	1.05E-6	1.42E-8	5E-4	2.4E-6
		11.9		1.42E-3	6.9E-6		
		12.48		7.76E-5	3.02E-7		

Table 87: Experimentally determined europium solubilities in the presence of X-ISA [Randall 2013]

Test product	Target pH	Final pH	Average final pH	Eu [M]	Eu Error [M]	Average Eu [M]	Average Eu Error, [M]
X-ISA [1E-2 M]	12	11.93	11.92	7.11E-5	3.88E-7	2.73E-5	1.39E-7
		11.93		5.18E-6	1.94E-8		
		11.91		5.64E-6	9.48E-9		
X-ISA [5E-3 M]	12	11.66	11.85	4.91E-6	3.49E-8	9.83E-6	5.47E-8
		11.99		2.13E-5	8.62E-8		
		11.89		3.27E-5	4.31E-8		
X-ISA [1E-3 M]	12	12.15	12.15	5.89E-8	8.62E-10	2.43E-6	1.9E-8
		12.15		1.23E-6	3.32E-8		
		12.15		5.99E-6	2.28E-8		
X-ISA [1E-4 M]	12	12.20	12.2	7.76E-7	6.47E-9	7.32E-7	5.17E-9
		12.20		8.55E-7	5.17E-9		
		12.21		5.63E-7	3.88E-9		

[Randall 2013] concluded that the solubility of Eu and Th is predominantly controlled by the concentration of ISA. It would be a reasonable assumption that the effect of cellulose degradation on the radionuclide behavior can be represented by assuming that ISA is the dominant complexing species in a cellulose degradation leachate. Other components of such a leachate obviously either do not complex with these radionuclides or are not present at high enough concentrations, which appears to be the case for X-ISA. According to [Randall 2013] it is unlikely that any other unknown degradation product contributes to the increase in solubility of Eu or Th.

Sorption of CDPs onto repository components such as cement may also have a significant impact on the CDP migration and their ability to increase the radionuclide solubility and migration [Heath 2005, Evans 2004]. Obviously, the sorption behavior of ISA is determined

by the calcium-silicate-hydrate hydrate and calcium-aluminium-silicate hydrate phases present [Loon 1998]. Experiments carried out on ISA sorption indicated K_d values for ISA begin to fall as the initial ISA concentration increases beyond values of 0.01 mol/dm^3 .

[Loon 1998] carried out batch sorption experiments with α - and β -ISA and cement (hardened cement paste CPA 55 HTS cement, Lafarge, France) to determine sorption isotherms for ISA at 25°C . For the experiments artificial cement pore water with a pH of 13.3 was used. The found ISA adsorption data is shown in Figure 40. According to [Loon 1998], the sorption of ISA on cement is a fast process, almost reaching equilibrium after one day. The best fit to the experimental data was found by using a Langmuir adsorption isotherm. The total sorption capacity of the cement for ISA was found to be $\sim 0.3 \text{ M/kg}$.

[Loon 1998] carried out similar experiments with β -ISA and found a similar behavior with respect to the sorption on cement. This was deemed as expected since both molecules have a similar structure. The same sorption parameters as for α -ISA can be taken for β -ISA [Loon 1998].

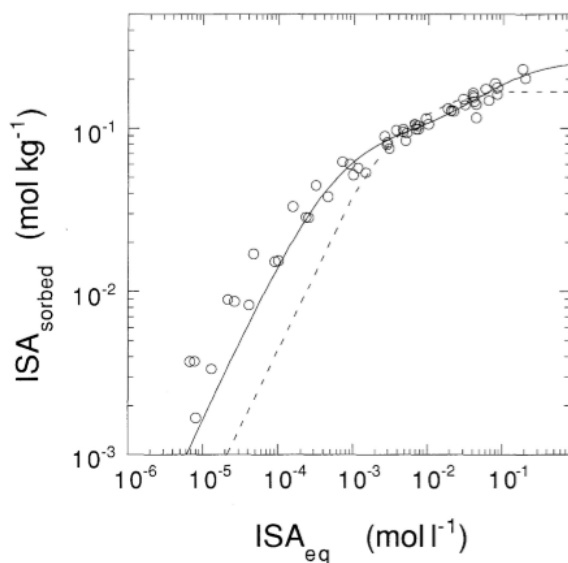


Figure 40: **Sorption isotherm of α -ISA on Portland cement at pH 13.3.** The symbols are experimental data for equilibrium times between 1 and 10 days. The dashed line shows the best fit by a Langmuir isotherm with one adsorption site; the solid line represents the best fit using a two site model with Langmuir adsorption behavior [Loon 1998]

To conclude, the sorption behavior of ISA on cement is important because sorption drastically reduces the ISA concentration in the cementitious pore water and consequently the adverse effect of ISA on radionuclide sorption. The underlying sorption mechanisms are however, still unknown, since ISA adsorption on cement is not consistent with electrostatic concepts. Specific interaction is deemed to be the most likely sorption mechanism [Loon 1998].

Cement additives (superplasticisers)

Cement additives (and their degradation products) are potential complexants which may increase the solubility and mobility of radionuclides. Some studies have reported on the effects of superplasticiser on metal solubilities. The results of selected studies are briefly summarised in the following.

Regarding the solubility data given in this section it is important to notice that the data is not determined with exactly the plasticisers/superplasticisers proposed in the framework of the OPERA disposal concept. Furthermore, also the cementitious porewater composition will not be identical to that used in the experiments for radionuclide solubility

determination. However, the master variable „pH“ is in the same range as to be expected in the planned Dutch repository and the plasticisers used in the experiments are in the compound groups as those used in the OPERA disposal concept.

[Greenfield 1998] investigated the effects of two Japanese cement additives (a naphtalene sulphonic acid condensation (HS-100) and a superplasticiser, i.e. a polycarboxylic acid polymer (HS-700)) on the solubility of Tc(IV), U(IV), Pu(IV) and Am(III) in a cement equilibrated water (pH 12 - 12.4). In the experiments with HS-100 an additive:water ratio of 30 g:1 kg and 0.3 g:1 kg. The experiments with HS-700 were carried out with an additive:water ratio of 50 g:1 kg and 0.5 g:1kg, respectively. All of the metals showed a significant solubility enhancement in the presence of the additives, whereas the highest solubility increase was observed in the presence of Am(III). The results and the solubility enhancement factors (SEF) are shown in Table 88 (with HS-100) and Table 89 (with HS-700). The SEF is calculated by dividing the solubility in presence of superplasticiser through the solubility in absence of additives. [Greenfield 1998] conclude from their experiments, that it is not possible to predict radionuclide solubilities in typical porewaters from concretes containing these additives because the additives present in the mix water may be sorbed onto the cement phases as the cement cures and not released into solution completely. It was stated that it is likely that the additives undergo reaction thus reducing the soluble ligand concentration. The enhancements observed in the diluted solution of the two cement additives are seen as eventually more realistic of those in concrete porewater.

Table 88: Solubility determinations with HS-100 by [Greenfield 1998] including SEF

Element	Solubility in cement equilibrated water	Solubility in the presence of HS-100 [M] with additive:water ratio	SEF
Technetium (IV)	7E-9 M	5E-6 (30g:1kg)	714
		2E-8 (0.3 g:1kg)	2,9
Uranium (IV)	2E-7 M	5E-5 (30 g:1kg)	250
		5E-6 (0.3g:1 kg)	25
Americium (III)	5E-11 M	5E-6 (30 g:1kg)	100,000
		3E-7 (0.3 g:1kg)	6,000
Plutonium (IV)	2E-10 M	4E-6 (30 g:1kg)	20,000
		4E-9 (0.3 g:1kg)	20

Table 89: Solubility determinations with HS-700 by [Greenfield 1998] including SEF

Element	Solubility in cement equilibrated water	Solubility in the presence of HS-700 [M] with additive:water ratio	SEF
Technetium (IV)	7E-9 M	9E-8 M (50 g:1 kg)	12,9
		3E-8 M (0.5 g:1kg)	4,3
Uranium (IV)	2E-7 M	7E-5 M (50g:1kg)	350
		4E-6 M (0.5 g:1kg)	20
Americium (III)	5E-11 M	8E-6 M (50 g:1 kg)	160,000
		1E-8 M (0.5 g:1kg)	200
Plutonium (IV)	2E-10 M	6E-6 M (50 g:1 kg)	30,000
		2E-8 (0.5 g:1 kg)	100

[Boult 1998] investigated the effect of Sikament N (based on sulphonated naphtalene formaldehyde) on the plutonium solubility in cement equilibrated water. Sikament N was present with 0.5 % and 1 % (w/v), whereas the baseline solubility of Pu in cement equilibrated water is 1E-10 M/L at pH 12. [Boult 1998] found in their study that in addition of 0.5 % and 1 % Sikament N, the average plutonium solubility increases to 2E-6 M and 5E-6 M, respectively. Thus, in presence of Sikament N a significant increase of Pu in cement equilibrated water is observed.

Sikament 10

[McCrohon 1997] investigated the effect of Sikament 10 (a formaldehyde free, low alkali and water soluble vinyl co-polymer) on the solubility of Pu in cement equilibrated water (~pH 12.5). The plutonium solubility was investigated in the presence of 0.5 % and 1 % (w/v) Sikament 10. After adding 0.5 % Sikament 10, the average Pu solubility was $5E-5$ M. With a concentration of 1 % Sikament 10, the average Pu solubility was $9E-5$ M. The baseline solubility of Pu in cement equilibrated water in absence of Sikament 10 at pH 12 was $1E-10$ M. Thus, an increase in the solubility of Pu(IV) over several orders of magnitude takes place in the presence of Sikament 10.

[Young 2012] investigated the effect of a commercial polycarboxylated poly ether comb type superplasticiser (ADVA Cast 551 which has a similar structure as the above mentioned HS-700) on the behaviour of U(VI), Th(IV), Eu(III) and Ni(II) in blended cements. Besides blast furnace slag (BFS) also pulverised ash (PFA) blends with ordinary portland cement (OPC) were investigated. The solubility experiments were carried out in a range of high pH aqueous solutions representative of cement pore waters. The results showed that the superplasticisers increase the solubility of all the mentioned metals but that the extent of the solubility increase depends on the metal investigated and the nature of the high pH solution. According to [Young 2012], U(VI) and Eu(III) display a solubility enhancement over several orders of magnitude while Ni(II) and Th(IV) solubility is enhanced to a lesser extent. A summary of the results including experimental data is given in Table 90.

Table 90: Experimental solubility data with SEF values with 1 % ADVA Cast 551 [Young 2012]

Aqueous solution	pH	Solubility in absence of ADVA Cast 551 [M]				SEF			
		U(VI)	Th(IV)*	Eu(III)	Ni(II)	U (VI)	Th (IV)	Eu(III)	Ni(II)
95 % saturated Ca(OH) ₂	12.5 ± 0.5	1E-7 ± 5E-9	1E-9	5E-7 ± 2E-8	8E-6 ± 4E-6	3,152	3	936	6
0.1 M NaOH	12.5 ± 0.5	3E-5 ± 2E-5	1E-9	1E-6 ± 5E-8	5E-6 ± 1E-6	24	3	531	2
BFS:OPC equilibrated water	12.5 ± 0.5	2E-6 ± 3E-7	1E-9	1E-6 ± 5E-8	5E-6 ± 2E-6	125	4	338	30
PFA:OPC equilibrated water	12.5 ± 0.5	1E-5 ± 1E-5	1E-9	3E-6 ± 2E-7	2E-6 ± 1E-7	45	4	160	2
PFA equilibrated water (pH adjusted)	12.5 ± 0.5	2E-6 ± 3E-7	1E-9	1E-6 ± 2E-7	7E-6 ± 2E-6	214	5	343	11
BFS equilibrated Water	12.5 ± 0.5	1E-5 ± 1E-5	1E-9	1E-6 ± 1E-7	4E-6 ± 3E-6	17	5	340	68
OPC equilibrated water	12.5 ± 0.5	2E-6 ± 3E-6	1E-9	1E-6 ± 2E-7	1E-5 ± 9E-6	186	6	42	7

*Th(IV) values were taken from experimental work reported [Wierczinski 1998], [Neck 2003], [Altmaier 2008]

[Young 2012] repeated the solubility experiments on U(VI), Th(IV), Eu(III) and Ni(II) to investigate the effect of irradiated superplasticiser ADVA Cast 551. The superplasticiser was irradiated to a dose of 65 kGy (dose rate 3.23 Gy/min) and solutions of irradiated ADVA Cast 551 were prepared at a variety of concentrations and cement equilibrated

solutions. As with the experiments with unirradiated plasticiser, the results show that the presence of irradiated superplasticiser increases the solubility of all metals (Table 91).

Table 91: Experimental solubility in presence of irradiated ADVA Cast 551 data with SEF values with 1 % [Young 2012]

Aqueous solution	pH	Solubility in absence of irradiated ADVA Cast 551 [M]				SEF in presence of 1% irradiated ADVA Cast 551			
		U(VI)	Th(IV)*	Eu(III)	Ni(II)	U (VI)	Th (IV)	Eu(III)	Ni(II)
95 % saturated Ca(OH) ₂	12.5 ± 0.5	7E-8 ± 1E-08	1E-9	4E-8 ± 1E-8	9E-8 ± 4E-9	70,561	5,953	7,883	262
0.1 M NaOH	12.5 ± 0.5	7E-6 ± 6E-7	1E-9	1E-7 ± 1E-8	2E-8 ± 1E-8	419	3,884	199	23,041
BFS:OPC equilibrated water	12.5 ± 0.5	2E-7 ± 6E-8	1E-9	9E-8 ± 3E-8	4E-8 ± 5E-9	46,114	3,946	5,577	2,060
PFA:OPC equilibrated water	12.5 ± 0.5	4E-8 ± 7E-9	1E-9	2E-7 ± 1E-8	5E-8 ± 5E-9	94,447	4,583	1,840	10,368
BFS equilibrated Water	12.5 ± 0.5	2E-6 ± 3E-8	1E-9	1E-7 ± 2E-8	3E-8 ± 2E-8	1,631	3,755	4,466	18,381
PFA equilibrated water (pH adjusted)	12.5 ± 0.5	3E-6 ± 4E-7	1E-9	2E-7 ± 6E-8	8E-8 ± 1E-7	203	3,215	2,675	4,584
OPC equilibrated water	12.5 ± 0.5	7E-7 ± 7E-8	1E-9	2E-7 ± 2E-8	1E-7 ± 1E-7	1,935	4,650	1,705	910

*Th(IV) values were taken from experimental work reported in [Wierczinski 1998], [Neck 2003], [Altmaier 2008]

[Young 2012] concludes that in comparison to HS-100 and HS-700, and using the example of U(VI), ADVA Cast 551 has a significantly higher solubilising effect than either of the two polymers. However, since ADVA Cast 551 and HS-700 are both polycarboxylate superplasticisers, which suggests that they are based on a similar structure, the exact nature of the interactions with aqueous species is different.

[Clacher 2011] investigated the effect of varying superplasticiser (ADVA Cast 551) concentrations (0.01 %, 0.1, 0.3 %, 1%) on the solubility of Pu(IV) and U(VI) in a near-saturated calcium hydroxide solution. Furthermore, the role of colloidal size material was investigated by measuring the solubilities in equilibration solutions after filtration through both 0.45 µm and 30,000 Dalton nominal molecular weight cut off (NMWCO) filters. Besides this, the effect of irradiated ADVA cast 551 solution on the solubility of Pu(IV) and U(VI) at pH ~12 was investigated.

It was shown that U(VI) solubility in saturated Ca(OH)₂ solution (pH ~12.5) was significantly increased by the presence of ADVA Cast 551 at 1 % in both the 0,45 µm and 30,000 NMWCO filtered solutions. A colloidal fraction was found to be present that passes through a 0,45 µm filter unit but is removed by 30,000 NMWCO filtration. The lowest concentration of ADVA Cast 551 employed was 0.01 %; here only negligible enhancement regarding the U (VI) solubility was observed in calcium hydroxide solution. The irradiated ADVA Cast 551 at 1% concentration lead to U(VI) solubility of up to two orders of magnitude lower than for the non-irradiated solution. The results are summarized in Table 92.

Table 92: Effects of ADVA Cast 551 on U(VI) solubility in saturated Ca(OH)₂ solution [Clacher 2011]

ADVA Cast 551 Concentration	Filtration	Mean U concentration [M]
0.01 %	0.45 µm	2.6 ± 4.9E-6
	30,000 NMWCO	1.1 ± 0.3E-7
0.1 %	0.45 µm	8.5 ± 4.8E-5
	30,000 NMWCO	8.1 ± 5.6E-6
0.3 %	0.45 µm	2.9 ± 0.4E-4
	30,000 NMWCO	6.8 ± 20E-5
1.0 %	0.45 µm	6.2 ± 0.9E-4
	30,000 NMWCO	2.2 ± 4.4E-4
0.1 % Irradiated	0.45 µm	8.8 ± 5.5E-8
	30,000 NMWCO	1.1 ± 0.8E-7
1.0 % Irradiated	0.45 µm	5.3 ± 10E-6
	30,000 NMWCO	5.0 ± 16E-6

The solubility of Pu (IV) in saturated Ca(OH)₂ solution was significantly increased in the presence of ADVA Cast 551 at 1 % concentration from the baseline 1.2E-10 M in both the 0.45 µm and the 30,000 NMWCO filtered solutions. Furthermore, it was found that gamma irradiation to 1 MGy decreased the TOC content of the 1 % ADVA Cast 551 solutions from 1600 ppm to 1000 ppm. In the 0.1 % ADVA Cast 551 solutions, the TOC was reduced from 190 ppm to 6 ppm [Clacher 2011]. The results are shown in Table 93.

Table 93: Effects of ADVA Cast 551 on Pu(IV) solubility in saturated Ca(OH)₂ [Clacher 2011]

ADVA Cast 551 Concentration	Filtration	Mean Pu concentration [M]
0.01 %	0.45 µm	2.1 ± 0.4E-7
	30,000 NMWCO	1.2 ± 0.4E-7
0.1 %	0.45 µm	2.1 ± 0.2E-7
	30,000 NMWCO	5.8 ± 2.3E-8
0.3 %	0.45 µm	2.3 ± 0.2E-7
	30,000 NMWCO	1.5 ± 0.3E-7
1.0 %	0.45 µm	2.4 ± 0.1E-7
	30,000 NMWCO	2.1 ± 0.5E-7
0.1 % Irradiated	0.45 µm	5.5 ± 8.1E-8
	30,000 NMWCO	3.8 ± 5E-9
1.0 % Irradiated	0.45 µm	3.4 ± 0.6E-7
	30,000 NMWCO	2.3 ± 0.3E-8

The irradiated ADVA Cast 551 at 1 % concentration leads to a Pu solubility a magnitude lower than that obtained for unirradiated ADVA Cast 551. The gamma irradiation reduced the solubility enhancement because the irradiation decreases the complexing ability of an ADVA Cast 551 solution compared to unirradiated superplasticiser [Clacher 2011].

[Clacher 2011] notes that the concentrations of ADVA Cast 551 used in their study are of the order of the concentration of the addition rate (0,3 - 0,8 w/v) of superplasticiser to cement mixture. They state, that even at a concentration of 0.01 %, ADVA Cast 551 causes a large increase in solubility.

To conclude, several studies have shown an increase of radionuclide solubility in presence of cement admixtures. This is due to the strong complexation of the radionuclides with the plasticisers. However, experiments with plasticiser/superplasticiser in free solution (as described above) are not realistic since those additives are part of the cementitious materials and it is expected that a significant fraction of the additives are bound in the cement matrix and will not be readily released into solution. Thus, the use of solubility data for fresh (super)plasticiser solutions eventually overestimates the potential impact of additives on the radionuclide solubility [Clacher 2013]. Thus, whilst „free solution“ solubility experiments can be used as a simple screening test, the assessment of the performance of additives should include experiments with realistic concentrations.

Further research with realistic (super)plasticiser concentrations and geochemical conditions are needed.

Some studies have shown that leaching (even under aggressive leaching conditions) of several superplasticisers, including polycarboxylated ether copolymer, from concrete is minimal [Dransfield 2005]. According to [Hayes 2012], an understanding of the nature and stability of the complexes formed and reversibility of superplasticiser sorption behaviour is required to predict the fate of radionuclides within the repository. Furthermore, the release rate of pore water from the cementitious materials and concentration of superplasticisers and associated degradation products are not known and hence their effects on post closure performance in terms of solubility and sorption of radionuclides is at present difficult to quantify.

The interaction of organic ligands with elements can be described by complexation constants. A compilation of the latter can be found in the Appendix 3.

7. Conclusions

In this study, the LILW degradation processes and products and their behavior in the repository near-field were investigated and discussed on the basis of the defined environmental conditions in the OPERA disposal facility. The particular wastes present in the LILW inventory (i.e. cellulose, plastics, rubbers, metals, depleted uranium) were investigated with respect to their chemical, microbial and radiolytic degradation.

Furthermore, potential amounts of gas generated by metal corrosion or cellulose degradation were estimated.

Thermodynamic data (complexation constants) and radionuclide solubilities in presence and absence of selected ligands are also provided in this report.

Finally, radionuclide source-terms suggested to be used in PA and the radionuclide migration behaviour in the repository near-field are also addressed.

The following text summarises the main findings of this study and the knowledge gaps found.

Source-terms

- For performance assessment, an instantaneous release of radionuclides from the compacted waste can be assumed. Regarding the processed liquid molybdenum waste, the waste with ion exchangers and DU, an instantaneous release of the radionuclides can be assumed after corrosion of the particular containers. The concentrations of the particular elements in the cementitious pore water will be controlled by their solubility.
- Element concentrations in the pore water are determined by many processes. Using the solubilities determined by thermodynamic equilibrium calculations would represent the maximum released radionuclide concentration. Solubilities may be enhanced by certain organic ligands. Section 6.2.2 presents the according data. Furthermore, complexation constants of different relevant organic ligands with metals are given in Appendix 3.
- Cellulose degradation kinetics are comparatively well known but still there are large bandwidths regarding the degradation rates. Regarding the other organic materials, no studies regarding their degradation kinetics under alkaline conditions exist.

Table 94 briefly summarises potential implications of LILW degradation processes on post closure safety functions.

Table 94: Potential implications of LILW degradation processes on post closure safety functions

Post closure safety functions in system containment phase	Contributing components	Implication of processes
C: Engineered containment	Supercontainer	not applicable for LILW
R: delay and attenuation of releases R1: Limitation of contaminant release from waste forms	Waste forms	<p><u>Degradation of organics and formation of complexing ligands:</u> facilitated contaminant release from cemented waste forms due to reduced sorption and enhanced solubility of some radionuclides;</p> <p><u>Carbonation:</u> Carbonation decreases the concrete porosity (which is positive) but lowers the pH. At a pH of about 9, the passive films on the steel surfaces are no longer stable and corrosion is enhanced;</p> <p><u>NAPLs:</u> NAPL coating on cement surfaces may affect the cement sorption properties;</p> <p>NAPLs may coat a waste form, limiting the quantity of radionuclides leached into the porewater;</p> <p>Radionuclides may partition into NAPL in a wasteform;</p> <p>If NAPLs were to be released as colloidal dispersions, any associated radionuclides could migrate by the groundwater pathway;</p> <p><u>Gas generation:</u> potential crack formation due to gas pressure</p>
R2: Limitation of water flow through the system	Boom Clay, EBS (backfill, plugs, seals)	<u>Gas generation:</u> potentially reduced water flow due to partly unsaturated conditions and gas overpressure; potential crack formation due to gas pressure
R3: retardation and spreading of contaminants	Boom Clay, EBS (backfill)	<p><u>Degradation of organics and formation of complexing ligands:</u> increase in mobility due to reduced sorption and enhanced solubility of some radionuclides;</p> <p><u>Carbonation:</u> Carbonation decreases the concrete porosity (which is positive) but lowers the pH to about 9 which may increase the solubility of some radionuclides;</p> <p><u>NAPL coating on surfaces of the backfill could affect its sorption properties and wettability;</u></p> <p>NAPLs may pool in the crown space above the backfill;</p> <p>Radionuclides may partition into NAPL in backfill or in the crown-space;</p> <p><u>Gas generation:</u> facilitated transport of volatile radionuclides</p>
I: Isolation	Boom Clay, geological coverage	geological stability not impaired by LILW degradation processes

In the framework of this study it was found that there exist various knowledge gaps. Major knowledge gaps, together with proposed research are listed here.

Cellulose degradation and isosaccharinic acid

- ∅ The cellulose chemical and radiolytic degradation pathways are well known. However, microbial activity at pH > 11 under cementitious conditions is unlikely and cellulose degradation at this high pH and anaerobic conditions is not proven. How widespread microbial activity will become in the near-field and what the distribution of active microbial populations would be at any instant following repository closure remains uncertain.
- ∅ Only few studies investigating the combined impact of radiolytic and chemical cellulose degradation and the generated degradation products are available. Studies investigating these aspects should vary parameters (anaerobic/aerobic, pH, temperature, cement composition, dose rate, type of irradiation etc.) and quantify the degradation products.
- ∅ Regarding the cellulose alkaline degradation kinetics, conflicting views exist concerning how much time is needed for cellulose to be degraded under repository conditions. Significant uncertainties exist regarding the degradation rates. Further investigations are necessary to completely understand the chemical processes involved, especially investigating longer time scales.
- ∅ It was found that ISA is chemically stable at pH 13.3 for a time scale of 1,000 days. However, it cannot be shown that this compound will be stable (under otherwise the same conditions) for repository time scales.
- ∅ There is no evidence that microbial ISA degradation occurs under alkaline anaerobic conditions at pH > 12. However, the presence of niches with lower pH cannot be ruled out. Here, a microbial degradation of ISA could take place (i.e. at pH 10 as was shown by [Bassil 2014]).
- ∅ Currently no experimental data concerning radiolytic impacts on cellulose degradation products and rates could be found. It is however likely, that the factors that affect the radiolysis of the CDPs are the same as those affecting the original cellulose material (e.g. dose rate).
- ∅ Impact of radiolysis on near-field complexant concentrations is lacking.
- ∅ The extent to which the behaviour of radionuclides in CDP leachates can be represented simply by assuming ISA is the dominant species present is unclear.

Non-halogenated plastics (polyethylene)

- ∅ The exact formulation of the material to be disposed (e.g. type of PE, amount of plasticisers, stabilisers etc.) is unknown. Thus the exact prediction of the degradation products that will arise is not possible.
- ∅ Only one study was found which investigated the radiolytic degradation of PE under alkaline conditions (pH 12.5). Further studies are necessary to consolidate the knowledge of radiolytic PE degradation under cementitious conditions, e.g. with different relevant types of PE. When possible, the exact formulation of the material investigated should be known. Degradation products and degradation rates need to be quantified.

- ∅ It is likely that PE will not be degraded microbially under repository conditions- however, it is not sure if that is still the case if microbes adapt to the conditions in the long-term. Furthermore, studies are lacking which investigate microbial degradation of possible PE radiolytic/chemical degradation products
- ∅ Radiolytic degradation of PE under repository (alkaline) conditions is not sufficiently understood
- ∅ Adaptability of microbes concerning plastics degradation is unknown. It is not known for certain if microbial degradation of PVC/PS will (ever) take place under repository conditions.

Halogenated plastics (PVC)

- ∅ The exact formulation of the material to be disposed (e.g. amount of PVC, plasticisers, stabilisers etc.) is unknown.
- ∅ The studies found investigating chemical (plasticised) PVC degradation were carried out at elevated temperatures.
- ∅ Only one study was found which investigated the combined chemical and radiolytic degradation of (plasticised) PVC. Studies investigating the combined degradation under a variety of conditions (e.g. pH values even higher than 12.5, i.e. pH 13.4) and PVC/additive combinations are needed. Degradation products should be identified and quantified.
- ∅ The (plasticised) PVC ageing experiments of [Baston 2014] found that a viscous, oily residue was developed on the PVC which could not be exactly identified.
- ∅ No PVC degradation rates under cementitious repository conditions could be found in the literature
- ∅ It is not known for certain if microbial degradation of PVC will (ever) take place under repository conditions. The adaptability of microbes concerning plastics degradation is unknown.
- ∅ PVC degradation rates under alkaline (cementitious) repository conditions were not found
- ∅ Some radiolytic and chemical degradation products of selected PVC plasticisers have been identified. However, it was found that several degradation products may be generated which have yet to be identified. Furthermore, from the wide range of plasticisers the degradation processes and products only few have been investigated until now.
- ∅ No specific studies regarding the microbial degradation of plasticisers or non-aqueous phase liquids under the expected near-field conditions exist.

Rubbers

- ∅ The exact amount and formulation of the material to be disposed (e.g. amount and identity of additives) is unknown
- ∅ Studies are lacking which investigate the neoprene degradation under (cementitious) repository conditions
- ∅ One study was found which investigated the combined radiolytic and alkaline degradation of neoprene. More studies under a variety of conditions and material compositions are necessary to acquire a solid knowledge base
- ∅ No research could be found which focused on the investigation of microbial neoprene degradation under high pH conditions
- ∅ No data concerning neoprene degradation rates could be found

Ion exchangers

- ∅ The exact amount and composition of the ion exchangers to be disposed (e.g. amount and identity of additives) is unknown
- ∅ One study was found which investigated the effects on irradiation of polystyrene-divinylbenzene cation exchangers under alkaline conditions. In this study, a large part of the degradation products however could not be identified. Another study also investigated the irradiation of a styrene-divinylbenzene cation exchange resin and found several unidentified degradation products
- ∅ It is not known for certain if microbial degradation of polystyrene will (ever) take place under repository conditions
- ∅ Degradation rates of ion exchangers under relevant repository conditions were not investigated up to date

Cement additives

- ∅ The exact formulation of the particular additives are proprietary and thus unknown
- ∅ Research concerning the chemical (alkaline) degradation of cement plasticisers/superplasticisers is very limited
- ∅ According to the literature data, it can be concluded that sulfonated naphthalene formaldehyde condensates are stable under alkaline conditions. However, since the exact compositions of the additives used in the cements employed in the OPERA disposal concept are not known, the transferability of laboratory results is questionable. Further experiments to identify and quantify degradation products under relevant conditions with the particular additives are necessary

- ∅ Literature research focusing on the microbial degradation of cement additives under alkaline conditions could not be found. Since the microbial activity at pH > 12 seems to be unlikely, the aspect of microbial degradation of additives may be neglected
- ∅ It was shown that the combined radiolytic and alkaline degradation of a selected additive (ADVA Cast 550) generates certain degradation products with lower molecular weights. Since the exact formulation of this additive and also of those employed in the OPERA disposal concept are not known, the transferability of such results has to be questioned

Microbial life in cement a cementitious repository

In the planned cementitious repository, the pH will be very alkaline (~12.5) for very long time scales and the availability of water will be very little. Most known micro-organisms depend on the availability of water and moderate pH (4-10). Thus, probably no significant biocenosis will be developed over long periods of time.

Furthermore, water-depleting reactions such as anaerobic steel corrosion will take place which will maintain the low water availability for long periods of time. Eventually, also a limit of nutrient availability will also hinder the development of microbes. However, due to the heterogeneity of the waste and conditioning procedures, small-scaled niches may be present in which relatively good conditions are present for microbial activity. A slow spread of microbes from these niches is conceivable.

It cannot be excluded that in the course of time (100,000 a) mutation of microbes will take place which allows for new degradation mechanisms/enzymes for e.g., PS and PVC. According to Mr. Schink, interviewed in [Warthmann 2013], such mutations may be possible. According to Mr. Jan Roelof van der Meer, also interviewed in [Warthmann 2013], genetic transfer and mutations in the microbial communities are very probable. However, it can be doubted, that the degradability of PVC and PS will be increased, since new bacterial strains must be able to metabolically attack PVC/PS to yield sufficient carbon and/or energy to generate a new cell. Furthermore, a mutant must find a selective advantage in the degradation of PVC/PS, otherwise it will not increase its population. In conclusion, the microbial degradation of PS and PVC under anaerobic, alkaline conditions with limited water availability can be considered as very unlikely [Warthmann 2013].

Non-aqueous phase liquids

The experimental programmes carried out to date have undertaken investigations with different organic polymers in both deionised water and Ca(OH)₂ solutions (pH ~12.4) in air (aerobic) and nitrogen (anaerobic) atmospheres. Some studies used irradiation of differing dose rates and lengths of time to simulate the effects of the gamma radiation field that eventually will be present in the repository. These empirical studies have shown that the NAPL yields from the radiolytic degradation of the respective polymer backbone chains are unlikely to be significant. However, obtaining a better mechanistic understanding of the polymer degradation and fate of any released products (i.e. NAPLs are generated but may be destroyed by radiolysis) would aid extrapolation of the empirical observations -as discussed in this report- to the timescales considered in performance assessments.

The eventual fate of polymer additives when released under the chemical and radiolytic conditions present is not well understood. Furthermore, it can be considered to be important to understand the timescales over which NAPLs are generated and whether this is compatible with the timescales over which radionuclides might be available [NDA 2012].

8. References

[Albertsson 1990] Albertsson AC, Karlsson S, The influence of biotic and abiotic environments on the degradation of polyethylene, *Progress in Polymer Science* 15 (1990) 177-192. Cited in [Hadad 2005].

[Alen 1985] Alen R, Lahtela M, Niemela, K, Sjoström E, Formation of Hydroxy Carboxylic-Acids from Softwood Polysaccharides During Alkaline Pulping, *Holzforschung* 39 (4) (1985) 235-238. Cited in [Humphreys 2010].

[Altmaier 2008] Altmaier M, Neck V, Fanghänel T, Solubility of Zr(IV), Th(IV) and Pu(IV) Hydrated Oxides in CaCl₂ Solutions and the Formation of Ternary Ca-M(IV)-OH-Complexes, *Radiochimica Acta* 96 (2008) 541-550. Cited in [Young 2012].

[Andra 2015] <https://www.thermochimie-tdb.com/>, 02.02.2016.

[Arthur 1971] Arthur JC, Reactions Induced by High Energy Radiation, in *Cellulose and Cellulose Derivatives*, Edited by Bikales NM, Segal L (1971). Cited in [Randall 2013]

[Arutchelvi 2008] Arutchelvi J, Sudhakar M, Arkatkar A, Doble M, Bhaduri S, Uppara PV, Biodegradation of polyethylene and polypropylene, *Indian Journal of Biotechnology* 7 (2008) 9-22.

[Askarieh 2000] Askarieh MM, Chambers AV, Daniel FBD, FitzGerald PL, Holtom GJ, Pilkington NJ, Rees, JH, The chemical and microbial degradation of cellulose in the near field of a repository for radioactive wastes, *Waste Management* 20 (2000) 93-106.

[Astbury 1944] Astbury WJ, Davies MM, Structure of Cellulose, *Nature* 154 (1944) 84.

[Atkins 1992] Aktins M, Glasser F, Application of Portland cement-based materials to radioactive waste immobilization, *Waste Management* 12 (1992) 105-131. Cited in [Deissmann 2005].

[Baidak 2010] Baidak A, LaVerne JA, Radiation-induced decomposition of anion exchange resins, *Journal of Nuclear Materials* 407 (2010) 211-219.

[Barlaz 1997] Barlaz MA, Microbial Studies of Landfills and Anaerobic Refuse Decomposition, in *Manual of Microbiology*, Edited by Hurst CH, Knudsen GR, McInerney MJ, Stetzenbach LD, Walter MW, American Society for Microbiology (1997) 541-557. Cited in [Humphreys 2010].

[Bassil 2014] Bassil NM, Bryan N, Lloyd JR, Microbial degradation of isosaccharinic acid at high pH, *The International Society for Microbial Ecology Journal* (2014) 1-11.

[Baston 2002] Baston GMN, Brownsword M, Cowper MM, Manning MC, Pilkington NJ, Williams SJ, The Influence of Gamma Irradiation on the Alkaline Degradation of Cellulose and the Effects on Plutonium Solubility, AEA Technology Report AEAT/ERRA-0346 (2002). Cited in [Humphreys 2010].

[Baston 2014] Baston, G., Dawson, J., NAPL Generation from PVC and the Fate of Plasticiser Additives when Aged in Aqueous Solutions, AMEC, AMEC/PPE/002834/003, Didcot, UK 2014.

[Berner 1990] Berner U, A Thermodynamic Description of the Evolution of Pore Water Chemistry and Uranium Speciation during the Degradation of Cement. *PSI Bericht* 62, Paul

Scherrer Institute, Villingen, Switzerland. Also published as Nagra Technical Report NTB 90-12 (1990).

[Berner 1992] Berner UR, Evolution of pore water chemistry during degradation of cement in a radioactive waste repository environment, *Waste Management* 12 (1992) 201-219.

[Berner 1999] Concentration Limits in the Cement Based Swiss Repository for Long-lived Intermediate-level Radioactive Wastes (LMA). PSI Bericht 99-10, Paul Scherrer Institute, Villingen, Switzerland.

[Berner 2003] Berner U, Radionuclide Concentration Limits in the Cementitious Near-Field of an ILW Repository, Nagra Technical Report 02-22 (2003) Paul Scherrer Institut Villingen PSI, Switzerland.

[Berner 2014] Berner U, Solubility of Radionuclides in a Concrete Environment for Provisional Safety Analyses for SGT-E2, Nagra Technical Report 14-07 (2014) 1-81

[Bertolini 2004] Bertolini L, Elsener B, Pedferri P, Redaelli E, Polder R, Corrosion of Steel in Concrete, Wiley VCH (2013) 1-414.

[Bethke 1996] Bethke CM, Geochemical reaction modeling, Oxford University Press (1996) 1-397. Cited in [Deissmann 2005].

[Bethke 2002] Bethke CM, The Geochemist's Workbench, release 4.0. A user's guide to Rxn, Act2, Tact, React and Gtplot. University of Illinois (2002) 1-224. Cited in [Deissmann 2005].

[Blazevska-Gilev 2007] Blazevska-Gilev J, Spaseska D, Chemical Recycling of Poly(Vinyl Chloride): Alkaline Dechlorination in Organic Solvents and Plasticizer Leaching in Caustic Solution, *Journal of the University of Chemical Technology and Metallurgy* 41 (1) (2007) 29-34.

[Blow 1982] Blow CM, Hepburn C, *Rubber Technology and Manufacture*, 2nd edition, published for the Plastics and Rubber Institute by Butterworth Scientific. Cited in [Cohen 2006]

[Bludovsky 1984] Bludovsky R, Prochazka M, Kopoldova J, The Influence of Oxygen on the Radiolytical Products of Cellulose, *Journal of Radioanalytical and Nuclear Chemistry* 87 (1984) 69-79. Cited in [Randall 2013].

[Bode 2001] Bode HB, Kerkhoff K, Jendrossek D, Bacterial degradation of natural and synthetic rubber, *Biomacromolecules* 2 (2001) 2295-303. Cited in [Rose 2005]

[Bond 2001] Bond KA; Linklater CM, Tweed CJ, Interpretation and modelling of radioelement sorption data obtained under alkaline conditions, UK Nirex Report AEAT/R/ENV/0214 (2001). Cited in [Deissmann 2005]

[Boult 1998] Boult K, McCrohon R, Williams SJ, Further Experiments on the Effects of Sikament 10 and Sikament N on Plutonium Solubility: A report produced for UK NIREX Ltd. (1998). Cited in [Young 2012].

[Bouniol 2008] Bouniol P, Bjergbakke E, A comprehensive model to describe radiolytic processes in cement medium, *Journal of Nuclear Materials* 372 (2008) 1-15.

[Braun 2002] Braun D, Recycling of PVC, *Progress in Polymer Science* 27 (2002) 2171-2195.

- [Brown 1976] Brown AD, Microbial Water Stress, *Bacteriological Review* 40 (4) (1976) 803-846. Cited in [Humphreys 2010].
- [Buchalla 2000] Buchalla R, Radiolysis Products in Gamma-Irradiated Plastics by Thermal Desorption-Gas Chromatography-Mass Spectrometry, PhD Thesis at the Technische Universität Berlin (2000) 1-216.
- [Burton 1954] Burton M, Patrick WN, Radiation Chemistry of Mixtures: Cyclohexane and Benzene-d₆, *Journal of Physical Chemistry* 58 (1954) 421-423.
- [CEN 2004] EN 934-2. Admixtures for Concrete, Mortar and Grout - Part 2: Concrete Admixtures - Definitions, Requirements, Conformity, Marking and Labelling, European Committee for Standardization. Cited in [Bertolini 2004].
- [Chambers 2004] Chambers AV, Holtom GJ, Hunter FMI, Ilett DJ, Tearle WM, Williams SJ, pH Evolution in Super Compacted Waste, Serco Assurance Report SERCO/ERRA-0444 (2004).
- [Chandler 2008] Chandler K, Constable M, Dawson J, Morgan S, Gamma Irradiation Testing of Grout and Aqueous Samples Containing ADVA Cast 550: A report produced for Magnox Electric Ltd. (North) (2008) (14-1007-08N). Cited in [Young 2012].
- [Clacher 2011] Clacher AP, Cowper MM, Effect of ADVA Cast 551 on the Solubility of Plutonium (IV) and Uranium (VI), SERVO/TAS/003145/001 Issue 02 (2011) 1-57.
- [Clacher 2013] Clacher A, Baston G, Glasser F, Jauffret G, Swanton S, Effects of ADVA Cast 551 Superplasticiser on Radionuclide Solubility, AMEC/006180/003 Issue 01 (2013) 1-104.
- [Cohen 2006] Preliminary Review of the Degradation of Cellulosic, Plastic, and Rubber Materials in the Waste Isolation Pilot Plant, and Possible Effects on Magnesium Oxide Safety Factor Calculations, Work Assignment No. 2-09 (2006) 1-55.
- [Dawson 2012] Dawson J, Magalhaes S, The Potential for Non-aqueous Phase Liquid Production in Irradiated Polymers, Serco Technical Consulting Services, SA/ENV/0997, Oxford (2012) 1-48.
- [Dawson 2013] Dawson J, NAPL Generation from the Radiolysis of Polyethylene and Chlorosulphonated Polyethylene Elastomer (Hypalon®), AMEC, AMEC/PPE/2834/002, Didcot, UK 2013.
- [Dawson 2013b] Dawson J, The potential for non-aqueous phase liquid production from irradiated PVC and Vinylesterstyrene (VES), AMEC, AMEC/PPE-1008/001 Issue 02, Didcot, UK (2013) 1-41.
- [Dawson 2013c] Dawson J, The potential for non-aqueous phase liquid production from irradiated neoprene and ion-exchange resin, AMEC, AMEC/PPE-000283 Issue 01, Oxford UK 2013.
- [Deissmann 2005] Deissmann G, Hoppe G, Schartmann F, Thierfeldt S, Wörlen S, Bath A, Jeffries S, Verbundprojekt Kontaminierter Beton: Betonfreigabe - Betonrezyklierung, Schlussbericht zum Fördervorhaben BMBF 02S 7900 (2005) 1-284.
- [Diomidis 2014] Diomidis N, Scientific basis for the production of gas due to corrosion in a deep geological repository, NAGRA Arbeitsbericht NAB 14-21 (2014) 1-74.

[Dransfield 2005] Dransfield JM, Leaching of organic admixtures from concrete, <http://www.efca.info/downloads/aes%209%20leaching%20of%20admixture.pdf>, (2005) 1-5.

[Elzinga 2004] Elzinga EJ, Tait CD, Reeder RJ, Rector KD, Donohoe RJ, Morris DE, Spectroscopic investigation of U(VI) sorption at the calcite-water interface, *Geochimica et Cosmochimica Acta* 68 (2004) 2437-2448. Cited in [Deissmann 2005]

[Enoki 2003] Enoki M, Doi Y, Iwata T, Oxidative degradation of cis- and trans-1,4-polyisoprenes and vulcanized natural rubber with enzyme-mediator systems. *Biomacromolecules* 4 (2003) 314-320. Cited in [Rose 2005].

[Evans 2004] Evans NDM, Heath TG, The Development of a Strategy for the Investigation of Detriments to Radionuclide Sorption in the Geosphere, Serco Assurance Report SA/ENV-0611 (2004). Cited in [Humphreys 2010].

[Francis 2006] Francis AJ, Dodge CJ, Microbial Transformations of TRU and Mixed Wastes: Actinide Speciation and Waste Volume Reduction, Brookhaven National Laboratories Report BNL-7300-2006 (2006). Cited in [Humphreys 2010].

[Fujisawa 1997] Fujisawa R, Cho T, Sugahara K, Takizawa Y, Horikawa Y, Shiomi T, Hironaga M, The corrosion behaviour of iron and aluminium under waste disposal conditions, *Materials Research Society Symposium Proceedings Volume 465* (1997) 675-682.

[Fujita 2004] Fujita T, Tits J, Harfouche M, Sugiyama D, Tsukamoto M, Wieland E, U(VI) uptake by co-precipitation and adsorption processes in cementitious systems. *Geochimica et Cosmochimica Acta* 68 (Suppl. 1) A112 (2004). Cited in [Deissmann 2005]

[Gallert 2000] Gallert C, Degradation of latex and of natural rubber by *Streptomyces* strain La7, *Systematic and Applied Microbiology* 23 (2000) 433-441. Cited in [Cohen 2006].

[Gaona 2012] Gaona X, Kulik DA, Macé N, Wieland E, Aqueous-solid solution thermodynamic model of U(VI) uptake in C-S-H phases, *Applied Geochemistry* 27 (2012) 81-95.

[Glaus 1999] Glaus MA, van Loon LR, Achatz S, Choruda A, Fischer K, Degradation of cellulosic materials under the alkaline conditions of a cementitious repository for low and intermediate level radioactive waste, Part I: Identification of degradation products, *Analytica Chimica Acta* 398 (1999) 111-122.

[Glaus 2004] Glaus MA, Van Loon LR, Cellulose Degradation at Alkaline Conditions: Long-Term Experiments at Elevated Temperatures, Nagra Technical Report 03-08 (2004) 1-70.

[Glaus 2004b] Glaus MA, van Loon LR, A Generic Procedure for the Assessment of the Effect of Concrete Admixtures on the Retention Behaviour of Cement for Radionuclides: Concept and Case Studies, Nagra Technical Report 03-09 (2004) 1-129.

[Glaus 2008] Glaus MA, Van Loon LR, Degradation of Cellulose under Alkaline Conditions: New Insights from a 12 Years Degradation Study, *Environmental Science and Technology* 42 (2008) 2906-2911 .

[Glaus 2008b] Glaus MA, Van Loon LR, Schwyn B, Vines S, Williams SJ, Larsson P, Puigdomenech I, Long-Term Predictions of the Concentration of α -isosccharinic Acid in Cement Pore Water, *Materials Research Society Proceedings Volume 1107* (2008).

[Glaus 2008c] Glaus MA, van Loon LR, Chemical reactivity of α -isocaccharinic acid in heterogeneous alkaline systems, Nagra Technical Report 08-10 (2008) 1-85.

[Grant 1997] Grant WD, Holtom GJ, Rosevear A, Widdowson D, A Review of Environmental Microbiology Relevant to the Disposal of Radioactive Waste in a Deep Underground Repository, Nirex Report NSS/R329 (1997). Cited in [Humphreys 2010].

[Grant 2002] Grant WD, Holtom GJ, O'Kelly N, Malpass J, Rosevear A, Watkiss P, Widdowson D, Microbial Degradation of Cellulose-Derived Complexants Under Repository Conditions, AEA Technology Report AEATERRA-0301 (2002). Cited in [Humphreys 2010].

[Grant 2007] Grant WD, Alkaline Environments and Biodiversity, in Extremophiles (Life Under Extreme Environmental Conditions), Edited by Encyclopedia of Life Support Systems (EOLSS), Unesco (2007). Cited in [Humphreys 2010].

[Grant 2001] Grant W, Greedy R, Holtom GJ, O'Kelly N, Rosevear, Widdowson D, The Survival of Micro-organisms in a Deep Cementitious Repository Under Alkaline, High Temperature Conditions, AEA Technology Report AEAT/R/ENV/0227 (2001). Cited in [Humphreys 2010].

[Grassie 1985] Grassie N, Scott G, Polymer Degradation and Stabilisation, Cambridge University Press (1985). Cited in [Smith 2013].

[Greenfield 1994] Greenfield BF, Hurdus MH, Pilkington NJ, Spindler MW, Williams SJ, The degradation of cellulose in the near field of a radioactive waste repository. In Barkatt A, Konynenburgh RA (Eds.), Scientific basis for nuclear waste management XVII (Vol 333), Materials Research Society Symposium Series (1994) 705-710.

[Greenfield 1998] Greenfield BF, Ilett DJ, Oto M, McCrohon R, Heath TG, Tweed CJ, Williams SJ, Yui M, The Effect of Cement Additives on Radionuclide Solubilities, Radiochimica Acta 82 (1998) 27-32.

[Greenfield 1990] Greenfield BF, Rosevear A, Williams SJ, Review of the Microbiological Chemical and Radiolytic Degradation of Organic Material Likely to be Present in Intermediate Level and Low Level Radioactive Waste, UK DoE Report DoE/HMIP/RR/91/002 (1990). Cited in [Humphreys 2010].

[Grant 2007] Grant WD, Alkaline Environments and Biodiversity, in Extremophiles (Life Under Extreme Environmental Conditions), Edited by Encyclopedia of Life Support Systems (EOLSS), Unesco (2007). Cited in [Humphreys 2010].

[Guest 1985] Guest MJ, Survey of Chemical Degradation Processes in Combustible PCM Wastes Immobilized in Concrete and Disposed of in Geological Repositories, AERE-G3671 (1985). Cited in [Dawson 2012].

[Haas 1967] Haas DW, Hrutfiord BF, Sarkanen KV, Kinetic Study on the Alkaline Degradation of Cotton Hydrocellulose, Journal of Applied Polymer Science 11 (1967) 587-600.

[Hadad 2005] Hadad D, Geresh S, Sivan A, Biodegradation of polyethylene by the thermophilic bacterium *Brevibacillus Borstelensis*, Journal of Applied Microbiology 98 (2005) 1093-1100.

[Hakanen 2006] Hakanen M, Ervanne H, The Influence of Organic Cement Additives on Radionuclide Mobility, Posiva Working Report 2006-06 (2006) 1-42.

[Hakkarainen 2004] Hakkarainen M, Albertsson A, Environmental Degradation of Polyethylene, *Advances in Polymer Science* 169 (2004), 177-199.

[Han 1981] Han YW, Timpa J, Ciegler A, Courtney J, Curry WF, Lambremont EN, γ -Ray-induced Degradation of Lignocellulosic Materials, *Biotechnology and Bioengineering* 23 (11) (1981) 2525-2535. Cited in [Dawson 2012]

[Harris 1997] Harris CA, Henttu P, Parker MG, Sumpter JP, The estrogenic activity of phthalate esters in vitro, *Environmental Health Perspectives* 105 (8) (1997). Cited in European Commission DGXI.E.3, *The Behaviour of Landfill, Final Report 2000*, ARGUS in association with University Rostock.

[Hart 2014] Hart, J, Determination of the Inventory, Part A: Radionuclides, OPERA-PU-NRG1112A (2014) 1-59.

[Hayes 2012] Hayes M, Angus M, Garland R, Current status paper on the potential use of Superplasticisers in a Geological Disposal Facility, *NNL (12) 11905 Issue 4* (2012) 1-54.

[Heath 1996] Heath TG, Illet DJ, Tweed CJ, Thermodynamic modelling of the sorption of radioelements on cementitious materials. *Material Resources Society Symposium Proceedings* 412 (1996) 443-4449. Cited in [Deissmann 2005]

[Heath 2000] Heath TG, Illet DJ, Pilkington NJ, Tweed CJ, Wiggin RM, Williams SJ, Predicting the Effect of Radioelement Solubility of Complexants Present in Waste or Derived from the Degradation of Non-Cellulosic Polymers, *AEA Technology Report, AEAT/ENV/0230 Issue 1* (2000). Cited in [Smith 2013].

[Heath 2000b] Heath TG, Illet DJ, Tweed CJ, Development of a near-field sorption model for a cementitious repository, *UK Nirex report AEAT/R/ENV/0029* (2000). Cited in [Deissmann 2005]

[Heath 2005] Heath TG, Williams SJ, Effects of Organic Complexants and their Treatment in Performance Assessments, *Serco Assurance Report SA/ENV-0726* (2005). Cited in [Humphreys 2010].

[Heisey 1995] Heisey RM, Papadato S, Isolation of microorganisms able to metabolize purified natural rubber, *Applied and Environmental Microbiology* 61 (1995) 3092-3097. Cited in [Cohen 2006].

[Hoch 2010] Hoch AR, Smart NR, Wilson JD, Reddy B, A Survey of Reactive Metal Corrosion Data for Use in the SMOGG Gas Generation Model, *SA/ENV-0895 Issue 2* (2010), 1-147.

[Howick 1995] Howick C, Plasticisers for Poly(Vinyl Chloride), *Progress in Rubber and Plastics Technology* 11(4) (1995) 239-260. Cited in [Smith 2013].

[Hummel 2002] Hummel W, Berner U, Curti E, Pearson FJ, Thoenen T, *NAGRA/PSI Chemical Thermodynamic Database 01/01*. Universal Publishers/uPublish.com, Parkland, Florida, USA (2002) 1-565. Cited in [Deissmann 2005].

[Hummel 2005] Hummel W, Anderegg G, Rao L, Puigdomènech I, Tochiyama O, *Chemical Thermodynamics of Compounds and Complexes of U, Np, Pu, Am, Tc, Se, Ni and Zr with Selected Organic Ligands*, Elsevier B.V. Amsterdam, The Netherlands (2005) 1-1081.

[Humphreys 2010] Humphreys PN, Laws A, Dawson J, A Review of Cellulose Degradation and the Fate of Degradation Products under Repository Conditions, SercoTAS/002274/001 Issue 2 (2010) 1-55.

[Hurdus 2000] Hurdus MH, Pilkington NJ, The solubility and sorption of 2-C-(hydroxymethyl)-3-deoxy-D-pentonic acid in the presence of Nirex Reference Vault Backfill and its degradation under alkaline conditions. AEA Technology Report AEAT/ERRA-0153. Cited in [Humphreys 2010].

[Ishikawa 1998] Ishikawa T, Kondo Y, Yasukawa A, Kandon K, Formation of Magnetite in the presence of ferric oxides, Corrosion Science 40 (1998) 1239-1251. Cited in [Wersin 2003].

[Jendrossek 1997] Jendrossek D, Tomasi G, Kroppenstedt RM, Bacterial degradation of natural rubber: a privilege of actinomycetes? FEMS Microbiology Letters 150 (1997) 179-188. Cited in [Cohen 2006].

[Jobe 1997] Jobe DL, Lemire RJ, Taylor P, Iron oxide redox chemistry and nuclear fuel disposal, AECL-11667, COG-96-487-1, AECL, Canada. Cited in [Wersin 2003].

[Johansson 1978] Johansson MH, Samuelson O, End-wise degradation of hydro-cellulose in bicarbonate solution, Journal of Applied Polymer Science (1978) 22-617. Cited in [Askarieh 2000].

[Johnson 2000] Johnson LH, Smith PA, The interaction of radiolysis products and canister corrosion products and the implications for radionuclide transport in the near field of a repository for spent fuel, Nagra Technical Report NTB 00-04 (2000). Cited in [Wersin 2003].

[Johnson 2002] Johnson L, Schneider J, Zuidema P, Gribi P, Mayer G, Smith P, Project Opalinus Clay Safety Report, Demonstration of disposal feasibility for spent fuel, vitrified high-level waste and long-lived intermediate-level waste (Entsorgungsnachweis), Nagra Technical Report 02-05 (2002) 1-360.

[Johnson 2004] Johnson L, Marschall P, Zuidema P, Gribi P, Effects of Post-disposal Gas Generation in a Repository for Spent Fuel, High-level Waste and Long-lived Intermediate Level waste Sited in Opalinus Clay, Nagra Technical Report 04-06 (2004) 1-151.

[Jonsson 2003] Jonsson S, Ejlertsson J, Svensson BH, Behaviour of Mono- and Diesters of O-phthalic Acid in Leachates Released During Digestion of Municipal Solid Waste Under Landfill Conditions, Advances in Environmental Research 7(2) (2003) 429-440. Cited in [Smith 2013]

[Kanwal 2009] Biodegradation of Rubber Tyres by Bacillus sp-10. Dissertation. Quaid-i-Azam University, Islamabad, Pakistan. Cited in [Shah 2013].

[Kelly 2003] Kelly SD, Newville MG, Cheng L, Kemner M, Sutton SR, Fenter P, Sturchio NC; Spötl C, Uranyl incorporation in natural calcite, Environmental Science and Technology 37 (2003) 1284-1287. Cited in [Deissmann 2005]

[Kienzler, 2013] Kienzler B, Altmaier M, Bube C, Metz V, Radionuclide source term for irradiated fuel from prototype, research and education reactors, for waste forms with negligible heat generation and for uranium tails, KIT Scientific reports 7635 (2013) 1-66.

[King 2000] King F, Stroes-Gascoyne S, An assessment of the long-term corrosion behavior of C-stell and the impact on the redox conditions inside a nuclear fuel waste disposal

container, Ontario Power Generation Report No 06819-REP-01200-10028-R00. Cited in [Wersin 2003].

[King 2010] King F, Watson S, Review of the Corrosion Performance of Selected Metals as Canister Materials for UK Spent Fuel and/or HLW, QRS-1394J-1, Version 2.1. (2010).

[Klemm 1998] Klemm D, Philipp B, Heinze T, Heinze U, Wagenknecht W, Degradation of cellulose, *Comprehensive cellulose chemistry* (Vol. 1). Fundamentals and analytical methods. Weinheim: Wiley (1998) 83-129. Cited in [Knill 2003].

[Knill 2003] Knill CJ, Kennedy JF, Degradation of cellulose under alkaline conditions, *Carbohydrate Polymers* 51 (2003) 281-300.

[Koleske 1995] Koleske JV (Editor), *Paint and Coating Testing Manual*, 14th Edition of the Gardner-Sward Handbook, ASTM Manual Series: MNL 17 (1995).

[Kovalenko 1994] Kovalenko NI, Glushonok GK, Ablameiko SV, Radiation Chemical Transformations of Glycol Aldehyde in Aqueous Solutions, *High Energy Chemistry* 28 (6) (1994). Cited in [Dawson 2012].

[Krupa 1998] Krupa KM, Serne RJ, Effects on Radionuclide Concentrations by Cement/Ground-Water Interactions in Support of Performance Assessment of Low-Level Radioactive Waste Facilities, Pacific Northwest National Laboratory (1998) 1-142.

[Kulik 2013] Kulik Da, Wagner T, Wagner T, Dmytrieva SV, Kosakowski G, Hingerl FF, Chudnenko KV, Berner U, GEM-Selektor geochemical modeling package: revised algorithm and GEMS3K numerical kernel for coupled simulation codes. *Computational Geosciences* 17 (2013) 1-24. Cited in [Berner 2014].

[Kursten 2008] Kursten B, Druyts F, Methodology to make a robust estimation of the carbon steel overpack lifetime with respect to the Belgian Supercontainer design. *Journal of Nuclear Materials* 379 (2008) 91-96.

[Kursten 2015] Kursten B, Druyts F, Assessment of the uniform corrosion behavior of carbon steel radioactive waste packages with respect to the disposal concept in the geological Durch Boom Clay formation, OPERA-PU-SCK 513 (2015) 1-107.

[Landy 1988] Landy MM, Walker PS, *Clinical Orthopaedics* 3 (1988) 1-73. Cited in [Vasile 2005].

[Lindström 2007] Lindström A, *Environmentally Friendly Plasticisers for PVC - Improved Material Properties and Long-Term Performance through Plasticizer Design*, PhD Thesis (2007) 1-74.

[Loon 1998] Van Loon LR, Glaus MA, Experimental and Theoretical Studies on Alkaline Degradation of Cellulose and its Impact on the Sorption of Radionuclides, Nagra Technical Report 97-04 (1998) 1-55.

[Machell 1957] Machell G, Richards GN, The alkaline degradation of polysaccharides, part II. The alkali-stable residue from the action of sodium hydroxide on cellulose, *Journal of the Chemical Society* (1975) 4500. Cited in [Askarieh 2000].

- [Macias 1983] Macias A, Andrade C, Corrosion Rate of Galvanized Steel Immersed in Saturated Solutions of Ca(OH)₂ in the pH Range 12 - 13.8, *British Corrosion Journal* 18, 2 (1983) 1-6
- [Macias 1987] Macias A, Andrade C, Corrosion of Galvanized Steel reinforcements in alkaline solutions, Part 1: Electrochemical results, *British Corrosion Journal* 22, 2 (1987) 1-6.
- [Magill 2012] Magill J, Pfenning G, Dreher R, Soti Z, *Karlsruher Nuklidkarte* (2012).
- [Manion 1952] Manion JP, Burton M, Radiolysis of Hydrocarbon Mixtures, *Journal of Physical Chemistry* 56 (1952) 560-569. Cited in [van Loon 1995].
- [Maura 2002] Maura G, Rinaldi G, Stabilizing Action of Polymeric Plasticisers in PVC, *Macromolecular Symposia* 176 (2002) 39-48. Cited in [Smith 2013].
- [McCrohon 1997] McCrohon R, Williams SJ, Effect of Sikament 10 superplasticiser on radionuclide solubility: A report produced for UK Nirex Ltd. Cited in [Young 2012].
- [Meeusen 2014] Meeusen JCL, Rosca-Bocancea E, Determination of the Inventory Part B: Matrix composition, OPERA-PU-NRG1112B (2014) 1-22.
- [Meeusen 2014b] Meeusen JCL, Rosca-Bocancea E, Reference list of waste-inventory-Part B: matrix composition (spread sheet) OPERA-IR-NRG1111B (2014).
- [Mersiowsky 2001] Mersiowsky I, Weller M, Ejlertsson J, Fate of Plasticised PVC Products under Landfill Conditions: a Laboratory-Scale Landfill Simulation Reactor Study, *Water Research* 35(13) (2001) 3063-3070. Cited in [Smith 2013].
- [Mersiowsky 2002a] Mersiowsky I, Fate of PVC polymer, plasticizers, and stabilizers in landfilled waste, *Journal of Vinyl & Additive Technology* 8 (2002) 36-44. Cited in [Warthmann 2013].
- [Mersiowsky 2002b] Mersiowsky N, Long-term fate of PVC products and their additives in landfills, *Progress in Polymer Science* 27 (2002) 2227-2277. Cited in [Warthmann 2013].
- [Moroni 1995] Moroni LP, Glasser FP, Reactions between cement components and U(VI) oxide, *Waste Management* 15 (1995) 243-254. Cited in [Deissmann 2005]
- [Munk 2008] Munk K (Ed.), *Taschenlehrbuch Biologie: Mikrobiologie* (2008) 507-508. Cited in [Warthmann 2013].
- [NDA 2012] Geological Disposal Summary of NAPL Studies March 2010, NDA Technical Note no. 17779488 (2012) 1-38.
- [Neall 1994] Neall F, Modelling of the Near-Field Chemistry of the SMA Repository at the Wellenberg Site: Application of the Extended Cement Degradation Model, *Nagra Technical Report* 94-03 (1994) 1-45.
- [Neck 2003] Neck V, Altmaier M, Muller R, Bauer A, Fanghänel T, Kim J, Solubility of Crystalline Thorium Dioxide, *Radiochimica Acta* 91 (5) (2003) 253-262. Cited in [Young 2012].

[Nevell 1985] Nevell TP, Degradation of cellulose by acids, alkalis and mechanical means. In: Nevell TP, Zeronian SH, editors. Cellulose chemistry and its applications (1985) 223-242. Cited in [Askarieh 2000].

[Pavasars 1999] Pavasars I, Characterisation of organic substances in waste materials under alkaline conditions. PhD Thesis, Linköping University, Sweden (1999).

[Pavasars 2003] Pavasars I, Hagberg J, Borén H, Allard B, Alkaline Degradation of Cellulose: Mechanisms and Kinetics, Journal of Polymers and the Environment 11 (2) (2003) 39-47.

[Pedersen 2000] Pedersen K, Microbial processes in radioactive waste disposal, SKB Technical Report TR-00-04 (2000) 1-98.

[Poppei 2002] Poppei J, Suter D, Niemeyer M, Wilhelm S, Modellierung der Gasentwicklung im Endlager für radioaktive Abfälle Morsleben, P151, Colenco Bericht 4651/76 (2002) 1-52.

[Pourbaix 1974] Pourbaix M, Atlas of Electrochemical Equilibria in Aqueous Solutions, N.A.C.E./Cebelcor, Houston, 1974. Cited in [Hoch 2010].

[Pöyry 2010] Pöyry, Nuclear Decommissioning Authority: Development of the Derived Inventory for ILW & LLW based on the 2007 UK Radioactive Waste Inventory, 390685/12 (2010), Cited in [Dawson 2012].

[Pozzi 2005] Pozzi OR, Zalutsky MR, Radiopharmaceutical Chemistry of Targeted Radiotherapeutics, Part 2: radiolytic Effects of ^{211}At α -particles Influence N-Succinimidyl 3- ^{211}At -Astatobenzoate Synthesis, Journal of Nuclear Medicine 46 (8) (2005) 1393-1400. Cited in [Dawson 2012].

[Randall 2013] Randall M, Rigby B, Thompson O, Trivedi D, Assessment of the effects of cellulose degradation products on the behavior of europium and thorium, NNL (12) 12239 Part A Issue 4 (2013) 1-178.

[Randall 2013b] Randall M, Rigby B, Thompson O, Trivedi D, Assessment of the effects of cellulose degradation products on the behavior of europium and thorium, NNL (12) 12239 Part B Issue 4 (2013) 1-95.

[Reed 1993] Reed DT, Molecke MA, Generation of Volatile Organic Compounds by Alpha Particle Degradation of WIPP Plastic and Rubber Material, Argonne National Laboratory, ANLI/CMT/CP-79852 (1993). Cited in [Dawson 2012].

[Reeder 2000] Reeder RJ, Nugent M, Lamble GM, Tait CD, Morris DE, Uranyl incorporation into calcite and aragonite: XAFS and luminescence studies, Environmental Science and Technology 34 (2000) 638-644. Cited in [Deissmann 2005]

[Reeder 2001] Reeder RJ, Nugent M, Tait CD, Morris DE, Heald SE, Beck KM, Hess WP, Lanzirrotti A, Coprecipitation of U(VI) with Calcite: XAFS, micro-XAS and luminescence characterization, Geochimica et Cosmochimica Acta 65 (2001) 3491-3503. Cited in [Deissmann 2005]

[Riesz 1964] Riesz P, The Radiolysis of Acetone in Aqueous Solutions, Radiation Research Supplement 4 (1964) 152-157. Cited in [Dawson 2012].

[Ritchie 1972] Ritchie PD, Plasticisers, Stabilisers and Fillers, The Plastics Institute, Iliffe Books LTd (1972). Cited in [Smith 2013]

[Rodwell 1999] Rodwell WR, Harris AW, Horseman ST, Lalieux P, Müller W, Ortiz Amaya L, Pruess K, Gas Migration and Two-Phase Flow through Engineered and Geological Barriers for a Deep Repository for Radioactive Waste, A Joint EC/NEA Status Report, EUR 19122 EN (1999) 1- 429.

[Rook 1955] Rook JJ, Microbial deterioration of vulcanized rubber, Journal of Applied Microbiology 3 (1955) 302-309. Cited in [Cohen 2006].

[Rose 2005] Rose K, Steinbüchel A, Biodegradation of Natural Rubber and Related Compounds: Recent Insights into a Hardly Understood Catabolic Capability of Microorganisms, Applied and Environmental Microbiology (2005) 2803-2812.

[Rosevear 1991] Rosevear A, A review of national reseach programmes on the microbiology of radioactive waste disposal, Nirex report NSS/R263 (1991). Cited in [Askarieh 2000].

[Ruckstuhl 2002] Ruckstuhl S, Suter MJF, Kohler HPE, Giger W, Leaching and Primary Biodegradation of Sulfonated Naphtalenes and Their Formaldehyde Condensates from Concrete Superplasticizers in Groundwater Affected by Tunnel Construction, Environmental Science & Technology 36 (2002) 3284-3289.

[Saravanane 2007] Saravanane R, Sudalai S, Muthukumaran T, Dechlorination Treatment and Thermal Effect on Degradation of Municipal Waste Plastics Contaminated with Saline Leachate in a Waste Dumping Site, Proc. Int. Conf. on Sustainable Solid Waste Management (2007) 293-307.

[Seetharam 2015] Seetharam S, Jacques D, Potential Degradation Processes of the Cementitious EBS Components, their Potential Implications on Safety Functions and Conceptual Models for Quantitative Assessment, OPERA-PU-SCK514 (2015).

[Serne 1996] Serne RJ, Rai D, Martin PF, Felmy AR, Rao L, Ueta S, Leachability of ND, U, Th and Sr from cements in a CO₂ free atmosphere. Material Resources Society Symposium Proceedings 412 (1996) 459-467. Cited in [Deissmann 2005]

[Shah 2013] Shah AA, Hasan F, Shah Z, Kanwal N, Zeb S, Biodegradation of natural and synthetic rubbers: A review, International Biodeterioration & Biodegradation 83 (2013) 145-157.

[Shaw 2013] Shaw PB, Studies of the Alkaline Degradation of Cellulose and the Isolation of Isosaccharinic Acids. Doctoral Thesis, University of Huddersfield (2013) 1-246.

[Shin 1999] Shin SM, Yoshioka T, Okuwaki A, Fundamental Behaviour of PVC Materials Degradation in Aqueous Solutions at Elevated Temperature, Proc Int Symp Feedstock recycle Plast 1 (1999) 87-90.

[Small 2013] Small J, Abrahamsen L, Warwick P, Review of the formation and degradation of isosaccharinic acid under LLWR Vault wasteform conditions, NNL (12) 12150 Issue 2 (2013) 1-45.

[Smith 2013] Smith V, Magalhaes S, Schneider S, The Role of PVC Additives in the Potential Formation of NAPLs, AMEC, AMEC/PPE/2834/001, Didcot, UK (2013) 1-41.

[Sonne 1997] Sonne-Hansen J, Kiaer J, Ahring B, Anaerobic Microbiology of an Alkaline Icelandic Hot Spring, FEMS Microbiology Ecology 23 (1) (1997) 31-38. Cited in [Humphreys 2010].

[Spevacek 1991] Spevacek J, Kafka D, High Resolution Solid State ¹³C Nuclear Magnetic Resonance Study of the Gamma-radiation Effect on Cellulose and Wood Structure, *Macromolecular Chemistry and Physics* 12 (1991) 359-365. Cited in [Humphreys 2010].

[Strand 1984] Strand SE, Dykes J, Chaing V, Aerobic Microbial Degradation of Glucoisosaccharinic Acid, *Applied and Environmental Microbiology* 47 (2) (1984) 268-271. Cited in [Humphreys 2010].

[Szymanski 1979] Szymanski W, Smietanska G, Synergistic effect in Gamma-irradiated Poly(vinyl chloride) Hard Foils Stabilised by Plasticizer-Stabilizer Systems, *Journal of Applied Polymer Science* 23 (1979) 791-795.

[Thoenen 2012a] Thoenen T, The PSI/Nagra Thermodynamic Data Base 12/07: Compilation of updated and new data with respect to the Nagra/PSI Chemical thermodynamic database 01/01. PSI Technical Report TM-44-12-06. Paul Scherrer Institute, Villingen PSI, Switzerland. Cited in [Berner 2014].

[Thoenen 2012b] Thermodynamic Data for Elements not considered in the PSI/Nagra Chemical Thermodynamic Data Base 12/07. PSI Internal Report AN-44-12-11. Paul Scherrer Institute, Villingen PSI, Switzerland. Cited in [Berner 2014].

[Tits 2001] Tits J, Wieland E, Radionuclide uptake by calcium silicate hydrates (CSH phases), PSI Internal report AN-44.01.10 (2001). Cited in [Deissmann 2005]

[Tsuchii 1985] Tsuchii A, Suzuki T, Takeda K, Microbial degradation of natural rubber vulcanizates, *Applied and Environmental Microbiology* 50 (1985) 965-970. Cited in [Cohen 2006].

[Tsuchii 1990] Tsuchii A, Takeda K, Rubber-degrading enzyme from a bacterial culture, *Applied and Environmental Microbiology* 56 (1990) 269-274. Cited in [Cohen 2006].

[van Loon 1995] van Loon LR, Hummel W, The Radiolytic and Chemical Degradation of Organic Ion Exchange Resins under Alkaline Conditions: Effect on Radionuclide Speciation, Nagra Technical Report 95-08 (1995) 1-112.

[van Loon 1999] van Loon LR, Glaus MA, Laube A, Stallone S, Degradation of cellulosic materials under the alkaline conditions of a cementitious repository for low- and intermediate-level radioactive waste. II. Degradation kinetics. *Journal of Environmental Polymer Degradation* 7 (1999) 41-51.

[Vasile 2005] Vasile C, Pascu M, Practical Guide to Polyethylene, Rapra Technology Limited (2005) 1-189.

[Verhoef 2011] Verhoef E, Schröder T, Research Plan, OPERA-PG-COV004 (2011) 1-24.

[Verhoef 2014] Verhoef EV, Neeft EAC, Grupa JB, Poley AD, Outline of a Disposal Concept in Clay, OPERA-PG-COV008 (2014) 1-18.

[Verhoef 2014b] Verhoef EV, de Bruin AMG, Wiegiers RB, Neeft EAC, Deissmann G, Cementitious materials in OPERA disposal concept in Boom Clay (2014) 1-17.

[Verhoef 2016] Verhoef EV, Neeft EAC, Deissmann G, Filby A, Wiegiers RB, Kers DA, Waste Families in OPERA, OPERA-PG-COV023 (2016) 1-39.

[Vinhas 2003] Vinhas, GM, Souto-Maior RM, Lapa CM, de Almeida YMB, Degradation Studies on Plasticized PVC Films Submitted to Gamma Radiation, *Materials Research* Vol. 6, No. 4 (2003) 497-500.

[Wanner 2007] Wanner H, Solubility data in radioactive waste disposal, *Pure and Applied Chemistry* 79 (2007) 875-882. Cited in [Wang 2013].

[Warthmann 2013] Warthmann R, Mosberger L, Baier U, Langzeit-Degradation von organischen Polymeren unter SMA-Tiefenlagerbedingungen, *Nagra Technischer Bericht* 13-04 (2013) 1-81.

[Wang 2013] Wang L, Solubility of radionuclides in Supercontainer concrete, *SCK CEN External Report* 239 (2013) 1-43.

[Wersin 2003] Wersin P, Johnson LH, Schwyn B, Berner U, Curti E, Redox Conditions in the Near Field of a Repository for SF/HLW and ILW in Opalinus Clay, *Nagra Technical Report* 02-13 (2003) 1-38.

[Westerscheldetunnel 2014] A representative composition of the prefabricated concrete sediments used for the Westerscheldetunnel has been provided by e-Mail on 19 March 2014. Cited in [Verhoef 2014b].

[Wieland 2001] Wieland E, Experimental studies on the inventory of cement-derived colloids in the pore water of a cementitious backfill material, *Nagra Technical Report* 01-02 (2001) 1-104.

[Wieland 2002] Wieland E, Van Loon LR, Cementitious Near-Field Sorption Data Base for Performance Assessment of an ILW Repository in Opalinus Clay, *Nagra Technical Report* 02-20 (2002) 1-87.

[Wierczinski 1998] Wierczinski B, Helfer S, Ochs M, Skarnemark G, Solubility Measurements and Sorption Studies of Thorium in Cement Pore Water, *Journal of Alloys and Compounds* 271 (1998) 272-276. Cited in [Young 2012].

[Wright 1992] Wright TM, Rimnac CM, Stulberg SD, Minz L, Tsao AK, Klein RW McCrae C, *Clinical Orthopaedics and Related Research* 276 (1992) 126.

[Wu 1975] Wu GS, Howton DR, γ -Radiolysis of Stearic Acid: Studies of Nongaseous Products, *Radiation Research* 61 (1975) 374-392. Cited in [Dawson 2012].

[Yilmaz 1993] Yilmaz VT, Odabasoglu M, Icbudak H, Ölmez H, The Degradation of Cement Superplasticisers in High Alkaline Solution, *Cement and Concrete Research* 23 (1993) 152-156.

[Young 2012] Young AJ, The Stability of Cement Superplasticiser and its Effect on Radionuclide Behaviour, *Doctoral Thesis, Loughborough University, UK* (2012) 1-301.

[Yoshioka 1999] Yoshioka T, Feedstock Recycling of PVC and PET by Wet-processes. *International Symposium on Feedstock Recycling of Plastics, Volume 1* (1999). Cited in [Baston 2014].

[Zahran 1986] Zahran AH, Ezz Eldin FM, Radiation Effects on Poly(vinyl Chloride) 2, Effect of Plasticisers on the Behaviour of pVC, *International Journal of Radiation Physics and Chemistry* 27(3) (1986) 175-183. Cited in [Smith 2013].

Appendix 1: Exemplary cement pore water compositions

Table A-1: Predicted composition of cementitious pore water in the early and later stage of cement degradation for different input groundwaters [Wieland 2002]. Repository in Opalinus Clay host rock.

Component	Early porewater [mM/L]	Later stage [mM/L]
Na	101	169
K	303	5.7
Ca	0.84	20.1
Mg	$< 10^{-4}$	10^{-4}
Al	0.01	0.005
CO ₃	0.20	0.01
SO ₄	0.75	0.10
Cl	-	160
F	0.76	0.10
H ₂ SiO ₄	0.05	0.016
pH	13.44	12.55

Table A-2: Simulated pore water compositions of near-field concrete for a repository in Boom Clay [Wang 2006]

Time scale [a]	Unsaturated t= 0	Saturated t = 5~10	Young concrete water t = 1000 ~ 10000	Evolved concrete water t > 80,000	CSH water
Ca	0.7	0.7	0.7	15.3	0.8/1.3*
Na	141	141	141	15.1	15.1
K	367	367	367	0.2	0.2
Al	0.06	0.06	0.06	0.005	9.4/2.9*
Si*	0.05/0.3	0.05/0.3	0.05/0.3	6e-3/3E-3	0.8/6.3
Mg	$\sim 10^{-7}$	$\sim 10^{-7}$	$\sim 10^{-7}$	4E-6	10^{-6}
Fe	10^{-5}	10^{-5}	10^{-5}	1E-6	10^{-7}
C (TIC)	0.3	0.3	0.3	8E-3	0.02
SO ₄ ²⁻	2	2	2	7E-3	0.05
S ₂ O ₃ ²⁻	-	-/1.9 [#]	1.9~6.4	-	-
HS-/S ₂ -	-	-/0.15 [#]	0.15~0.5	-	-
Cl-	-	0.2/3.6 [#]	0.2~12	0.2	0.2
pH	$\sim 12^s$	12^s	13.5	12.5	~ 12
Eh, mV	100~200	100~200	~ 800	~ 800	~ 800

Appendix 2: Additives in polymers

Table A-3: Examples for commercial polymers with typical plasticiser loading [Ritchie 1972]

Polymer Type	Plasticiser loading (parts per hundred of polymer)	Generic plasticiser type
Polyvinyl chloride	30-150	Esters, oils
Polyvinyl acetate	10-30	Esters
Polyvinyl alcohol	10-30	Water, glycol
Cellulose acetate	10-50	Esters
Cellulose nitrate	10-50	Esters
Ethyl cellulose	10-100	Esters, oils
Polyamides	0-20	Sulphonamides
Polymethylmethacrylate	0-20	Esters
Polyisoprene	0-50	Oils
Styrene-butadiene rubber	0-50	Oils
Polybutadiene	0-50	Oils
Butyl rubber	0-50	Oils
Ethylene propylene rubber	0-150	Oils
Polychloropene	0-50	Esters, oils
Nitrile rubber	0-100	Esters, oils
Chlorosulphonated polyethylene	0-50	Esters, oils
Polysulphides	0-30	Esters
Epoxies	0-50	Polyamides, polysulphides, esters
Melanime-formaldehyde	0-10	Sulphonamides
Phenol-formaldehyde	0-10	Esters

Table A-4: List of common PVC additives [Smith 2013]

Compound
Plasticisers
Di-butyl phthalate (DBP)
Tri-tolyl phosphate
Di-allyl phthalate
Tri-phenyl phosphate
Octyl-diphenyl phosphate
1,1-Dimethylethylphenyldiphenylphosphate
Di-ethylhexyl phtalate (DEHP or DOP)
Di-isodecyl phthalate (DIDP)
Epoxy resin (Shell EC57)
Di-n-octyl phthalate (BBP)
Di-isodecyl phthalate
Tribasic sulphate lead phosphite
Di-isononyl adipate (DINA)
Di-2-ethylhexyladipate (DEHA)
Trimethylol propane
Di-isoctyl adipate (DIOA)
Di-methyl phthalate (DMP)
Di-ethyl phthalate (DEP)
Di-isodenonyl phthalate (DINP)
Di-n-propyl phthalate (DPrP)
Di-n-pentyl phthalate (DPeP)
Di-n-hexyl phthalate (DHexP)
Di-cyclohexyl phtalate (DCHP)
Di-isoctyl Phtalate (DIOP)
Di-isononyl-cyclohexane-1,2-dicarboxylate (DINCH)
Stabilisers
Lead stearate/phtalate
Barium cadmium complex
Tinuvin P (2-/2H-benzotriazol-2-yl)-p-cresol
Irganox 1076 (octadecyl-3-(3'5'-di-tert-butyl-4'-hydroxy-phenyl)-propionate
Irgastab PVC 11 (2,4-dimethyl-6-(1-methyl-pentadecyl)phenol
Lead sulphate
Calcium/Zinc soaps
Butyltin
Epoxidised soya bean oil (ESBO)
Epoxidised sunflower oil (ESO)
Lead
Methyltin
Butyltin
Octyltin
Organotin stabiliser (dibultyn bis-(2-ethylhexylthioglycollate)
Tribasic lead sulphate
Antimony trioxide
Aluminium silicate
Bis-phenol A
Calcium stearate
Fillers
Kaolin
Calcium carbonate
Lead stearate
Antioxidants
Bisphenol
Curing Agents
Tetraethylene pentamine

Appendix 3: Complexation constants

The effect of organic LILW degradation products on radionuclide concentration and speciation can be calculated by using thermodynamic data from selected databases. Important ligands generated due to LILW degradation which have an influence on radionuclide solubility are regarded and their complexation constants (a measure for the affinity of the binding of ligands with radionuclides) and solubilities are presented in Table A-5. Data are given for the following ligands: isosaccharinic acid (Isa), gluconate (Glu), acetate, adipate, phthalate and oxalate as far as available.

Isosaccharinic acid is a major cellulose degradation product (see section 5.2.1.1). According to the [Andra 2015], simple polycarboxylic acids (such as gluconate) have been used as a surrogate of the polycarboxylate additives. This compound may represent the upper limit effect that a carboxylic ether superplasticiser could have on radionuclide mobilization. Adipates, acetate and oxalate are typical degradation products of organic polymers (e.g. ion exchangers, PE, plasticisers).

Table A-5: Complexation constants for organic ligands with metals (T = 25 °C)

Reaction	Log K	Source
Isosaccharinic acid (ISA)		
$\text{Am}^{3+} + \text{HIsa}^- + 3 \text{H}_2\text{O} \rightarrow \text{Am}(\text{OH})_3(\text{HIsa})^- + 3 \text{H}^+$	-21.5	Andra Thermochimie DB*
$\text{Ca}^{2+} + \text{Isa}^- \rightarrow \text{Ca}(\text{Isa})^+$	1.7 ± 0.3	[Hummel 2005]
$\text{Ca}^{2+} + \text{HIsa}^- \rightarrow \text{Ca}(\text{Isa}_{\text{H}})(\text{aq}) + \text{H}^+$	-10.4 ± 0.5	[Hummel 2005]
$\text{Ca}^{2+} + 2 \text{Isa}^- \rightarrow \text{Ca}(\text{Isa})_2(\text{cr})$	6.4 ± 0.2	[Hummel 2005]
$\text{Ca}^{2+} + \text{Th}^{4+} + \text{HIsa}^- + 4 \text{H}_2\text{O} \rightarrow \text{CaTh}(\text{OH})_4(\text{Isa}) + 4 \text{H}^+$	-9.0	Andra Thermochimie DB
$\text{HIsa}^- + \text{Eu}^{3+} + 3 \text{H}_2\text{O} \rightarrow \text{Eu}(\text{OH})_3(\text{HIsa})^- + 3 \text{H}^+$	-20.9	Andra Thermochimie DB
$\text{H}^+ + \text{HIsa}^- \rightarrow \text{H}_2\text{Isa}$	4.0	Andra Thermochimie DB
$\text{Ni}^{2+} + \text{HIsa}^- \rightarrow \text{Ni}(\text{HIsa})^+$	2.8	Andra Thermochimie DB
$\text{Ni}^{2+} + \text{HIsa}^- + 3 \text{H}_2\text{O} \rightarrow \text{Ni}(\text{OH})_3(\text{HIsa})^{2-} + 3 \text{H}^+$	-26.5	Andra Thermochimie DB
$\text{Np}^{4+} + \text{HIsa}^- + 3 \text{H}_2\text{O} \rightarrow \text{Np}(\text{OH})_3(\text{HIsa}) + 3 \text{H}^+$	3.27	Andra Thermochimie DB
$\text{Np}^{4+} + 2 \text{HIsa}^- + 3 \text{H}_2\text{O} \rightarrow \text{Np}(\text{OH})_3(\text{HIsa})^{2-} + 3 \text{H}^+$	5.38	Andra Thermochimie DB
$\text{Np}^{4+} + \text{HIsa}^- + 4 \text{H}_2\text{O} \rightarrow \text{Np}(\text{OH})_4(\text{HIsa})^- + 4 \text{H}^+$	-4.06	Andra Thermochimie DB
$\text{Np}^{4+} + 2 \text{HIsa}^- + 4 \text{H}_2\text{O} \rightarrow \text{Np}(\text{OH})_4(\text{HIsa})_2^{2-} + 4 \text{H}^+$	-2.2	Andra Thermochimie DB
$\text{Pu}^{4+} + \text{HIsa}^- + 3 \text{H}_2\text{O} \rightarrow \text{Pu}(\text{OH})_3(\text{HIsa}) + 3 \text{H}^+$	4.75	Andra Thermochimie DB
$\text{Pu}^{4+} + 2 \text{HIsa}^- + 3 \text{H}_2\text{O} \rightarrow \text{Pu}(\text{OH})_3(\text{HIsa})_2^- + 3 \text{H}^+$	6.86	Andra Thermochimie DB
$\text{Pu}^{4+} + \text{HIsa}^- + 4 \text{H}_2\text{O} \rightarrow \text{Pu}(\text{OH})_4(\text{HIsa})^- + 4 \text{H}^+$	-3.6	Andra Thermochimie DB
$\text{Pu}^{4+} + 2 \text{HIsa}^- + 4 \text{H}_2\text{O} \rightarrow \text{Pu}(\text{OH})_4(\text{HIsa})_2^{2-} + 4 \text{H}^+$	0.7	Andra Thermochimie DB
$\text{Th}^{4+} + \text{HIsa}^- + 3 \text{H}_2\text{O} \rightarrow \text{Th}(\text{OH})_3(\text{HIsa}) + 3 \text{H}^+$	-5.65	Andra Thermochimie DB
$\text{Th}^{4+} + 2 \text{HIsa}^- + 3 \text{H}_2\text{O} \rightarrow \text{Th}(\text{OH})_3(\text{HIsa})_2^- + 3 \text{H}^+$	-4.9	Andra Thermochimie DB
$\text{Th}^{4+} + \text{HIsa}^- + 4 \text{H}_2\text{O} \rightarrow \text{Th}(\text{OH})_4(\text{HIsa})^- + 4 \text{H}^+$	-13.2	Andra Thermochimie DB
$\text{Th}^{4+} + 2 \text{HIsa}^- + 4 \text{H}_2\text{O} \rightarrow \text{Th}(\text{OH})_4(\text{HIsa})_2^{2-} + 4 \text{H}^+$	-10.4	Andra Thermochimie DB
$\text{U}^{4+} + \text{HIsa}^- + 3 \text{H}_2\text{O} \rightarrow \text{U}(\text{OH})_3(\text{HIsa}) + 3 \text{H}^+$	0.29	Andra Thermochimie DB
$\text{U}^{4+} + 2 \text{HIsa}^- + 3 \text{H}_2\text{O} \rightarrow \text{U}(\text{OH})_3(\text{HIsa})_2^- + 3 \text{H}^+$	2.4	Andra Thermochimie DB
$\text{U}^{4+} + \text{HIsa}^- + 4 \text{H}_2\text{O} \rightarrow \text{U}(\text{OH})_4(\text{HIsa})^- + 4 \text{H}^+$	-6.7	Andra Thermochimie DB
$\text{U}^{4+} + 2 \text{HIsa}^- + 4 \text{H}_2\text{O} \rightarrow \text{U}(\text{OH})_4(\text{HIsa})_2^{2-} + 4 \text{H}^+$	-5.1	Andra Thermochimie DB
$\text{UO}_2^{2+} + \text{HIsa}^- \rightarrow \text{UO}_2(\text{HIsa})^+$	3.7	Andra Thermochimie DB
$\text{UO}_2^{2+} + 2 \text{HIsa}^- \rightarrow \text{UO}_2(\text{HIsa})_2$	6.6	Andra Thermochimie DB
$\text{UO}_2^{2+} + 3 \text{HIsa}^- \rightarrow \text{UO}_2(\text{HIsa})_3^-$	8.5	Andra Thermochimie DB
$\text{UO}_2^{2+} + \text{HIsa}^- + 4 \text{H}_2\text{O} \rightarrow \text{UO}_2(\text{OH})_4(\text{HIsa})^{3-} + 4 \text{H}^+$	-28.1	Andra Thermochimie DB
Gluconate (Glu)		
$\text{Am}^{3+} + \text{HGlu}^- + 3 \text{H}_2\text{O} \rightarrow \text{Am}(\text{OH})_3(\text{HGlu})^- + 3 \text{H}^+$	-19.7	Andra Thermochimie DB
$\text{Ca}^{2+} + \text{HGlu}^- \rightarrow \text{Ca}(\text{HGlu})^+$	1.73	Andra Thermochimie DB
$\text{Ca}^{2+} + \text{HGlu}^- + \text{H}_2\text{O} \rightarrow \text{Ca}(\text{OH})(\text{HGlu}) + \text{H}^+$	-10.4	Andra Thermochimie DB
$\text{Ca}^{2+} + \text{Th}^{4+} + \text{HGlu}^- + 4 \text{H}_2\text{O} \rightarrow \text{CaTh}(\text{OH})_4(\text{Glu}) + 4 \text{H}^+$	-9.0	Andra Thermochimie DB
$\text{Np}^{4+} + \text{HGlu}^- + 3 \text{H}_2\text{O} \rightarrow \text{Np}(\text{OH})_3(\text{HGlu}) + 3 \text{H}^+$	3.27	Andra Thermochimie DB

Reaction	Log K	Source
$\text{Np}^{4+} + \text{HGlu}^- + 4 \text{H}_2\text{O} \rightarrow \text{Np}(\text{OH})_4(\text{HGlu})^- + 4 \text{H}^+$	-3.7	Andra Thermochimie DB
$\text{Pu}^{4+} + \text{HGlu}^- + 3 \text{H}_2\text{O} \rightarrow \text{Pu}(\text{OH})_3(\text{HGlu}) + 3 \text{H}^+$	4.75	Andra Thermochimie DB
$\text{Pu}^{4+} + \text{HGlu}^- + 4 \text{H}_2\text{O} \rightarrow \text{Pu}(\text{OH})_4(\text{HGlu})^- + 4 \text{H}^+$	-2.7	Andra Thermochimie DB
$\text{Th}^{4+} + \text{HGlu}^- + 3 \text{H}_2\text{O} \rightarrow \text{Th}(\text{OH})_3(\text{HGlu}) + 3 \text{H}^+$	-6.7	Andra Thermochimie DB
$\text{Th}^{4+} + \text{HGlu}^- + 4 \text{H}_2\text{O} \rightarrow \text{Th}(\text{OH})_4(\text{HGlu})^- + 4 \text{H}^+$	-11.8	Andra Thermochimie DB
$\text{Th}^{4+} + 2 \text{HGlu}^- + 4 \text{H}_2\text{O} \rightarrow \text{Th}(\text{OH})_4(\text{HGlu})_2^{2-} + 4 \text{H}^+$	-9.9	Andra Thermochimie DB
$\text{U}^{4+} + \text{HGlu}^- + 3 \text{H}_2\text{O} \rightarrow \text{U}(\text{OH})_3(\text{HGlu}) + 3 \text{H}^+$	0.29	Andra Thermochimie DB
$\text{U}^{4+} + \text{HGlu}^- + 4 \text{H}_2\text{O} \rightarrow \text{U}(\text{OH})_4(\text{HGlu})^- + 4 \text{H}^+$	-5.94	Andra Thermochimie DB
$\text{H}^+ + \text{HGlu}^- \rightarrow \text{H}_2\text{Glu}$	3.9	Andra Thermochimie DB
Acetate		
$\text{Am}^{3+} + \text{Acetate}^- \rightarrow \text{Am}(\text{Acetate})^{2+}$	2.94	Andra Thermochimie DB
$\text{Am}^{3+} + 2 \text{Acetate}^- \rightarrow \text{Am}(\text{Acetate})_2^+$	5.07	Andra Thermochimie DB
$\text{Am}^{3+} + 3 \text{Acetate}^- \rightarrow \text{Am}(\text{Acetate})_3$	6.54	Andra Thermochimie DB
$\text{Ca}^{2+} + \text{Acetate}^- \rightarrow \text{Ca}(\text{Acetate})^+$	1.12	Andra Thermochimie DB
$\text{Cm}^{3+} + \text{Acetate}^- \rightarrow \text{Cm}(\text{Acetate})^{2+}$	3.01	Andra Thermochimie DB
$\text{Cm}^{3+} + 2 \text{Acetate}^- \rightarrow \text{Cm}(\text{Acetate})_2^+$	4.96	Andra Thermochimie DB
$\text{Cm}^{3+} + 3 \text{Acetate}^- \rightarrow \text{Cm}(\text{Acetate})_3$	6.3	Andra Thermochimie DB
$\text{Eu}^{3+} + \text{Acetate}^- \rightarrow \text{Eu}(\text{Acetate})^{2+}$	2.9	Andra Thermochimie DB
$\text{Eu}^{3+} + 2 \text{Acetate}^- \rightarrow \text{Eu}(\text{Acetate})_2^+$	4.8	Andra Thermochimie DB
$\text{Eu}^{3+} + 3 \text{Acetate}^- \rightarrow \text{Eu}(\text{Acetate})_3$	5.6	Andra Thermochimie DB
$\text{H}^+ + \text{Acetate}^- \rightarrow \text{HAcetate}$	4.76	Andra Thermochimie DB
$\text{Ni}^{2+} + \text{Acetate}^- \rightarrow \text{Ni}(\text{Acetate})^+$	1.34	Andra Thermochimie DB
$\text{Np}^{4+} + \text{Acetate}^- \rightarrow \text{Np}(\text{Acetate})^{3+}$	5.83	Andra Thermochimie DB
$\text{Np}^{4+} + 2 \text{Acetate}^- \rightarrow \text{Np}(\text{Acetate})_2^{2+}$	10.0	Andra Thermochimie DB
$\text{NpO}_2^+ + \text{Acetate}^- \rightarrow \text{NpO}_2(\text{Acetate})$	1.32	Andra Thermochimie DB
$\text{NpO}_2^+ + 2 \text{Acetate}^- \rightarrow \text{NpO}_2(\text{Acetate})_2^-$	3.42	Andra Thermochimie DB
$\text{NpO}_2^+ + 3 \text{Acetate}^- \rightarrow \text{NpO}_2(\text{Acetate})_3^{2-}$	3.57	Andra Thermochimie DB
$\text{Pu}^{3+} + \text{Acetate}^- \rightarrow \text{Pu}(\text{Acetate})^{2+}$	2.85	Andra Thermochimie DB
$\text{Pu}^{4+} + \text{Acetate}^- \rightarrow \text{Pu}(\text{Acetate})^{3+}$	5.93	Andra Thermochimie DB
$\text{Pu}^{3+} + 2 \text{Acetate}^- \rightarrow \text{Pu}(\text{Acetate})_2^+$	5.06	Andra Thermochimie DB
$\text{Pu}^{4+} + 2 \text{Acetate}^- \rightarrow \text{Pu}(\text{Acetate})_2^{2+}$	10.09	Andra Thermochimie DB
$\text{Pu}^{3+} + 3 \text{Acetate}^- \rightarrow \text{Pu}(\text{Acetate})_3$	6.57	Andra Thermochimie DB
$\text{PuO}_2^{2+} + \text{Acetate}^- \rightarrow \text{PuO}_2(\text{Acetate})^+$	2.87	Andra Thermochimie DB
$\text{PuO}_2^{2+} + 2 \text{Acetate}^- \rightarrow \text{PuO}_2(\text{Acetate})_2$	4.77	Andra Thermochimie DB
$\text{PuO}_2^{2+} + 3 \text{Acetate}^- \rightarrow \text{PuO}_2(\text{Acetate})_3^-$	6.19	Andra Thermochimie DB
$\text{TcO}(\text{OH})_2 + \text{H}^+ + \text{Acetate}^- \rightarrow \text{TcO}(\text{OH})(\text{Acetate}) + \text{H}_2\text{O}$	5.55	Andra Thermochimie DB
$\text{Th}^{4+} + \text{Acetate}^- \rightarrow \text{Th}(\text{Acetate})^{3+}$	5.24	Andra Thermochimie DB
$\text{Th}^{4+} + 2 \text{Acetate}^- \rightarrow \text{Th}(\text{Acetate})_2^{2+}$	9.44	Andra Thermochimie DB
$\text{Th}^{4+} + 3 \text{Acetate}^- \rightarrow \text{Th}(\text{Acetate})_3^+$	12.56	Andra Thermochimie DB
$\text{Th}^{4+} + 4 \text{Acetate}^- \rightarrow \text{Th}(\text{Acetate})_4$	14.38	Andra Thermochimie DB
$\text{Th}^{4+} + 5 \text{Acetate}^- \rightarrow \text{Th}(\text{Acetate})_5^-$	15.37	Andra Thermochimie DB
$\text{U}^{4+} + \text{Acetate}^- \rightarrow \text{U}(\text{Acetate})^{3+}$	5.64	Andra Thermochimie DB
$\text{U}^{4+} + 2 \text{Acetate}^- \rightarrow \text{U}(\text{Acetate})_2^{2+}$	9.81	Andra Thermochimie DB
$\text{UO}_2^{2+} + \text{Acetate}^- \rightarrow \text{UO}_2(\text{Acetate})^+$	3.02	Andra Thermochimie DB
$\text{UO}_2^{2+} + 2 \text{Acetate}^- \rightarrow \text{UO}_2(\text{Acetate})_2$	5.2	Andra Thermochimie DB
$\text{UO}_2^{2+} + 3 \text{Acetate}^- \rightarrow \text{UO}_2(\text{Acetate})_3^-$	7.03	Andra Thermochimie DB
Adipates (Adipate)		
$\text{Ca}^{2+} + \text{Adipate}^{2-} \rightarrow \text{Ca}(\text{Adipate})(\text{s})$	3.3	Andra Thermochimie DB
$\text{H}^+ + \text{Adipate}^{2-} \rightarrow \text{H}(\text{Adipate})^-$	5.45	Andra Thermochimie DB
$2 \text{H}^+ + \text{Adipate}^{2-} \rightarrow \text{H}_2(\text{Adipate})$	9.89	Andra Thermochimie DB
Phthalate (Phthalat)		
$\text{Am}^{3+} + \text{Phthalat}^{2-} \rightarrow \text{Am}(\text{Phthalat})^+$	4.93	Andra Thermochimie DB
$\text{Ca}^{2+} + \text{H}^+ + \text{Phthalat}^{2-} \rightarrow \text{Ca}(\text{HPhthalat})^+$	6.42	Andra Thermochimie DB
$\text{Ca}^{2+} + \text{Phthalat}^{2-} \rightarrow \text{Ca}(\text{Phthalat})$	2.49	Andra Thermochimie DB
$\text{Cm}^{3+} + \text{Phthalat}^{2-} \rightarrow \text{Cm}(\text{Phthalat})^+$	4.93	Andra Thermochimie DB
$\text{Eu}^{3+} + \text{Phthalat}^{2-} \rightarrow \text{Eu}(\text{Phthalat})^+$	4.96	Andra Thermochimie DB

Reaction	Log K	Source
$\text{Eu}^{3+} + 2 \text{Phthalat}^{2-} \rightarrow \text{Eu}(\text{Phthalat})_2^-$	7.34	Andra Thermochimie DB
$2 \text{H}^+ + \text{Phthalat}^{2-} \rightarrow \text{H}_2\text{Phthalat}$	8.32	Andra Thermochimie DB
$\text{H}^+ + \text{Phthalat}^{2-} \rightarrow \text{HPhthalat}^-$	5.34	Andra Thermochimie DB
$\text{Ni}^{2+} + \text{Phthalat}^{2-} \rightarrow \text{Ni}(\text{Phthalat})$	3.0	Andra Thermochimie DB
$\text{PuO}_2^{2+} + \text{Phthalat}^{2-} \rightarrow \text{PuO}_2(\text{Phthalat})$	5.76	Andra Thermochimie DB
$\text{UO}_2^{2+} + \text{Phthalat}^{2-} \rightarrow \text{UO}_2(\text{Phthalat})$	5.56	Andra Thermochimie DB
Oxalate (Ox)		
$\text{Am}^{3+} + \text{Ox}^{2-} \rightarrow \text{Am}(\text{Ox})^+$	6.51 ± 0.15	[Hummel 2005]
$\text{Am}^{3+} + 2 \text{Ox}^{2-} \rightarrow \text{Am}(\text{Ox})_2^-$	10.71 ± 0.2	[Hummel 2005]
$\text{Am}^{3+} + 3 \text{Ox}^{2-} \rightarrow \text{Am}(\text{Ox})_3^{3-}$	13.0 ± 1.0	[Hummel 2005]
$\text{Ca}^{2+} + \text{Ox}^{2-} \rightarrow \text{Ca}(\text{Ox})(\text{aq})$	3.19 ± 0.06	[Hummel 2005]
$\text{Ca}^{2+} + \text{H}_2\text{O} + \text{Ox}^{2-} \rightarrow \text{Ca}(\text{Ox}) \cdot \text{H}_2\text{O} (\text{cr})$	8.73 ± 0.06	[Hummel 2005]
$\text{Ca}^{2+} + 2 \text{H}_2\text{O} + \text{Ox}^{2-} \rightarrow \text{Ca}(\text{Ox}) \cdot 2 \text{H}_2\text{O} (\text{cr})$	8.3 ± 0.06	[Hummel 2005]
$\text{Ca}^{2+} + 3 \text{H}_2\text{O} + \text{Ox}^{2-} \rightarrow \text{Ca}(\text{Ox}) \cdot 3 \text{H}_2\text{O} (\text{cr})$	8.19 ± 0.04	[Hummel 2005]
$\text{Ca}(\text{ox})(\text{aq}) + \text{Ox}^{2-} \rightarrow \text{Ca}(\text{Ox})_2^{2-}$	0.83 ± 0.19	[Hummel 2005]
$\text{Ox}^{2-} + \text{Cm}^{3+} \rightarrow \text{Cm}(\text{Ox})^+$	6.48	Andra Thermochimie DB
$2 \text{Ox}^{2-} + \text{Cm}^{3+} \rightarrow \text{Cm}(\text{Ox})_2^-$	10.4	Andra Thermochimie DB
$3 \text{Ox}^{2-} + \text{Cm}^{3+} \rightarrow \text{Cm}(\text{Ox})_3^{3-}$	12.84	Andra Thermochimie DB
$\text{Eu}^{3+} + \text{Ox}^{2-} \rightarrow \text{Eu}(\text{Ox})^+$	6.55	Andra Thermochimie DB
$\text{Eu}^{3+} + 2 \text{Ox}^{2-} \rightarrow \text{Eu}(\text{Ox})_2^-$	10.93	Andra Thermochimie DB
$\text{Eu}^{3+} + 3 \text{Ox}^{2-} \rightarrow \text{Eu}(\text{Ox})_3^{3-}$	12.48	Andra Thermochimie DB
$\text{Fe}^{3+} + \text{H}^+ + \text{Ox}^{2-} \rightarrow \text{Fe}(\text{HOx})^{2+}$	9.3	Andra Thermochimie DB
$\text{Fe}^{2+} + \text{Ox}^{2-} \rightarrow \text{Fe}(\text{Ox})$	4.1	Andra Thermochimie DB
$\text{Fe}^{3+} + \text{Ox}^{2-} \rightarrow \text{Fe}(\text{Ox})^+$	9.53	Andra Thermochimie DB
$\text{Fe}^{3+} + 2 \text{Ox}^{2-} \rightarrow \text{Fe}(\text{Ox})_2^-$	15.75	Andra Thermochimie DB
$\text{Fe}^{2+} + 2 \text{Ox}^{2-} \rightarrow \text{Fe}(\text{Ox})_2^{2-}$	6.2	Andra Thermochimie DB
$\text{Fe}^{3+} + 3 \text{Ox}^{2-} \rightarrow \text{Fe}(\text{Ox})_3^{3-}$	20.2	Andra Thermochimie DB
$\text{Fe}^{2+} + 3 \text{Ox}^{2-} \rightarrow \text{Fe}(\text{Ox})_3^{4-}$	5.22	Andra Thermochimie DB
$\text{H}^+ + \text{Ox}^{2-} \rightarrow \text{H}(\text{Ox})^-$	4.25 ± 0.01	[Hummel 2005]
$\text{H}^+ + \text{Hox}^- \rightarrow \text{H}_2\text{ox}(\text{aq})$	1.4 ± 0.03	[Hummel 2005]
$3 \text{H}^+ + \text{Nb}(\text{OH})_6^- + \text{Ox}^{2-} \rightarrow \text{NbO}_2(\text{HOx}) + 4 \text{H}_2\text{O}$	13.7	Andra Thermochimie DB
$4 \text{H}^+ + \text{Nb}(\text{OH})_6^- + 2 \text{Ox}^{2-} \rightarrow \text{NbO}_2(\text{HOx})_2^- + 4 \text{H}_2\text{O}$	20.96	Andra Thermochimie DB
$2 \text{H}^+ + \text{Nb}(\text{OH})_6^- + \text{Ox}^{2-} \rightarrow \text{NbO}_2(\text{Ox})^- + 4 \text{H}_2\text{O}$	10.94	Andra Thermochimie DB
$\text{Ni}^{2+} + \text{Ox}^{2-} \rightarrow \text{Ni}(\text{Ox})(\text{aq})$	5.19 ± 0.04	[Hummel 2005]
$\text{Ni}^{2+} + 2 \text{Ox}^{2-} \rightarrow \text{Ni}(\text{Ox})_2^{2-}$	7.64 ± 0.07	[Hummel 2005]
$\text{Np}^{4+} + \text{Ox}^{2-} \rightarrow \text{Np}(\text{Ox})^{2+}$	11.16	Andra Thermochimie DB
$\text{Np}^{4+} + 2 \text{Ox}^{2-} \rightarrow \text{Np}(\text{Ox})_2$	19.94	Andra Thermochimie DB
$\text{Np}^{4+} + 3 \text{Ox}^{2-} \rightarrow \text{Np}(\text{Ox})_3^{2-}$	25.19	Andra Thermochimie DB
$\text{NpO}_2^+ + \text{Ox}^{2-} \rightarrow \text{NpO}_2(\text{Ox})^-$	3.9 ± 0.1	[Hummel 2005]
$\text{NpO}_2^+ + 2 \text{Ox}^{2-} \rightarrow \text{NpO}_2(\text{Ox})_2^{3-}$	5.8 ± 0.2	[Hummel 2005]
$\text{UO}_2^{2+} + \text{ox}^{2-} \rightarrow \text{UO}_2\text{ox}$	7.130 ± 0.16	[Hummel 2005]
$\text{UO}_2^{2+} + 2 \text{ox}^{2-} \rightarrow \text{UO}_2(\text{ox})_2^{2-}$	11.65 ± 0.15	[Hummel 2005]
$\text{UO}_2^{2+} + 3 \text{ox}^{2-} \rightarrow \text{UO}_2(\text{ox})_3^{4-}$	13.8 ± 1.5	[Hummel 2005]
$\text{UO}_2\text{ox}(\text{aq}) + 3 \text{H}_2\text{O} \rightarrow \text{UO}_2\text{ox} \cdot 3\text{H}_2\text{O} (\text{cr})$	1.8 ± 0.27	[Hummel 2005]
$\text{Mg}^{2+} + \text{ox}^{2-} \rightarrow \text{Mg}(\text{ox})(\text{aq})$	3.56 ± 0.04	[Hummel 2005]
$\text{Mg}^{2+} + 2 \text{ox}^{2-} \rightarrow \text{Mg}(\text{ox})_2^{2-}$	5.17 ± 0.08	[Hummel 2005]

*SIT V9 Database of PhreeqC, which used the Andra Thermochimie database from 21.1.2014. See also <https://www.thermochimie-tdb.com/>.

Appendix 4: Radionuclide Inventory

Table A-6: Activity per 200 L drum processed molybdenum waste (200 L drums contained in 1,000 L concrete containers), 130 years after collecting the waste [Verhoef 2016]

Radionuclide	Molybdenum waste stream I		Molybdenum waste stream II	
	Activity [Bq]	comments value	Activity [Bq]	comments value
Ac-226				
Ac-227				
Ag-108 m				
Am-241	1.24E+05	fraction uranium collection filters	8.59E+05	fraction uranium collection filters
Am-242m				
Am-243	3.17E+05	fraction uranium collection filters	2.20E+06	fraction uranium collection filters
Ba-133				
Be-10				
Bi-207				
Bi-214				
C-14				
Ca-41				
Cd-113 m				
Cf-249				
Cf-251				
Cf-252				
Cl-36				
Cm-241				
Cm-243	1.84E+05	fraction uranium collection filters	1.28E+06	fraction uranium collection filters
Cm-244	2.82E+05	fraction uranium collection filters	1.96E+06	fraction uranium collection filters
Cm-245	2.14E+03	fraction uranium collection filters	1.49E+04	fraction uranium collection filters
Cm-246	2.69E+02	fraction uranium collection filters	1.87E+03	fraction uranium collection filters
Cm-247	3.82E-01	fraction uranium collection filters	2.65E+00	fraction uranium collection filters
Cm-248	2.36E+00	fraction uranium collection filters	1.64E+01	fraction uranium collection filters
Co-60				
Cs-135	1.16E+07	Cs-137 (upon collection), 6.62%		
Cs-137	3.62E+10	upon collection max A2		
Eu-152	1.27E+01	fraction uranium collection filters	8.79E+01	fraction uranium collection filters
Eu-152 m				
H-3				
Ho-166m				
I-129	1.53E+05	Cs-137 (upon collection), 0.706%		
K-40				
Kr-81				
Kr-85				
Mo-93				
Mo-99				
Nb-93 m				
Nb-94		not calculated		not calculated
Ni-59				
Ni-63			1.06E+03	fraction uranium collection filters
Np-237	2.13E+03	fraction uranium collection filters	1.48E+04	fraction uranium collection filters
Pa-231	8.04E+00	fraction uranium collection filters	5.58E+01	fraction uranium collection filters
Pa-233				
Pa-234				

Table A-6 (continued)

Pb-202				
Pb-210				
Pb-214				
Pd-107	4.51E+03	fraction uranium collection filters	3.13E+04	fraction uranium collection filters
Pm-145			4.63E-02	fraction uranium collection filters
Po-209				
Pu-238	3.53E+04	fraction uranium collection filters	2.45E+05	fraction uranium collection filters
Pu-239	3.01E+06	fraction uranium collection filters	2.09E+07	fraction uranium collection filters
Pu-240	1.62E+05	fraction uranium collection filters	1.13E+06	fraction uranium collection filters
Pu-241	7.11E+03	fraction uranium collection filters	4.94E+04	fraction uranium collection filters
Pu-242	1.49E+00	fraction uranium collection filters	1.04E+01	fraction uranium collection filters
Pu-244				
Ra-226				
Re-186m				
Sb-125				
Se-79	5.20E+05	Cs-137 (upon collection), 0.0487%	4.69E+04	fraction uranium collection filters
Si-32				
Sm-146				
Sm-151	1.09E+08	fraction uranium collection filters	7.55E+08	fraction uranium collection filters
Sn-121m				
Sn-126	1.05E+06	Cs-137 (upon collection), 0.0594	3.05E+05	fraction uranium collection filters
Sr-90	3.07E+10	Cs-137 (upon delivery), 5.73%	4.30E+09	fraction uranium collection filters
Tc-99		filtered		
Tc-99 m				
Th-229				
Th-230				
Th-231				
Th-234				
Ti-44				
U-232				
U-233	2.71E+00	fraction uranium collection filters	1.88E+01	fraction uranium collection filters
U-234	1.40E+03	fraction uranium collection filters	9.70E+03	fraction uranium collection filters
U-235	1.84E+05	fraction uranium collection filters	1.28E+06	fraction uranium collection filters
U-236	6.67E+04	fraction uranium collection filters	4.63E+05	fraction uranium collection filters
U-238	3.84E+03	fraction uranium collection filters	2.67E+04	fraction uranium collection filters
U-239				
Zr-93	2.83E+05	fraction uranium collection filters	1.97E+06	fraction uranium collection filters

Table A-7: Activity per waste container for (processed) DU, spent ion exchanger and compacted waste 130 years after collecting the waste [Verhoef 2016]

Radionuclide	Depleted uranium	Spent ion exchanger		Compacted 90 litre drums with waste	
	Activity [Bq]	Activity [Bq]	comments value	Activity [Bq]	comments / source value
Ac-226					
Ac-227				1.31E+02	[COVRA,2012]
Ag-108 m		3.26E+08	[IAEA,2002]	1.50E+03	[COVRA,2012]
Am-241				1.50E+08	[COVRA,2012]
Am-242m					
Am-243				3.65E+02	[COVRA,2012]
Ba-133				1.82E+01	[COVRA,2012]
Be-10		8.00E+04	[IAEA,2002]	1.79E+04	[COVRA,2012]
Bi-207				3.41E+02	[COVRA,2012]
Bi-214					
C-14		7.09E+09	[IAEA,2002]	1.98E+07	[COVRA,2012]
Ca-41		2.00E+06	[IAEA,2002]		not reported
Cd-113 m					reported activity upon collection after 30 years < 1 MBq
Cf-249				1.32E+02	[COVRA,2012]
Cf-251					
Cf-252					
Cl-36		4.00E+06	[IAEA,2002]	4.53E+04	[COVRA,2012]
Cm-241					not reported
Cm-243					not reported
Cm-244				1.41E+04	[COVRA,2012]
Cm-245					not reported
Cm-246					not reported
Cm-247					not reported
Cm-248				1.83E+00	not reported, deduced from Cf-252
Co-60		1.51E+04	A2 value upon collection		
Cs-135		3.00E+06	[IAEA,2002]		not reported
Cs-137		3.00E+10	A2 value upon collection	9.16E+08	[COVRA,2012]
Eu-152				2.48E+02	[COVRA,2012]
Eu-152 m					
H-3		2.04E+04	from conditioning and waste characteristics	1.08E+07	[COVRA,2012]
Ho-166m					not reported
I-129		6.00E+05	[IAEA,2002]	2.22E+03	[COVRA,2012]
K-40				4.22E+04	[COVRA,2012]
Kr-81				2.84E+01	[COVRA,2012]
Kr-85				1.36E+04	[COVRA,2012]
Mo-93		3.91E+05	[IAEA,2002]		reported activity upon collection after 30 years < 1 MBq
Mo-99					
Nb-93 m				1.06E-01	[COVRA,2012]
Nb-94		4.78E+07	[IAEA,2002]	1.53E+03	[COVRA,2012]
Ni-59		4.39E+08	[IAEA,2002]	1.18E+04	[COVRA,2012]
Ni-63		2.27E+11	[IAEA,2002]	3.70E+08	[COVRA,2012]
Np-237				2.84E+02	[COVRA,2012]
Pa-231				3.97E+02	[COVRA,2012]
Pa-233					
Pa-234					
Pb-202					reported activity upon collection after 30

Table A-7 (continued)

Pb-210				7.71E+03	years < 1 MBq [COVRA,2012]
Pb-214					
Pd-107		6.00E+04	[IAEA,2002]		not reported
Pm-145					not reported
Po-209					reported activity upon collection after 30 years < 1 MBq
Pu-238				6.91E+07	[COVRA,2012]
Pu-239				1.26E+07	[COVRA,2012]
Pu-240				8.06E+05	[COVRA,2012]
Pu-241				3.68E+03	[COVRA,2012]
Pu-242				1.99E+06	[COVRA,2012]
Pu-244					reported activity upon collection after 30 years < 1 MBq
Ra-226				6.69E+06	[COVRA,2012]
Re-186m				2.37E+04	[COVRA,2012]
Sb-125					
Se-79		2.40E+06	[IAEA,2002]		not reported
Si-32					reported activity upon collection after 30 years < 1 MBq
Sm-146					reported activity upon collection after 30 years < 1 MBq
Sm-151				1.65E+04	[COVRA,2012]
Sn-121m		1.98E+06	[IAEA,2002]	5.30E+02	[COVRA,2012]
Sn-126		5.40E+06	[IAEA,2002]		not reported
Sr-90		6.11E+07	[IAEA,2002]	1.94E+07	[COVRA,2012]
Tc-99		6.00E+06	[IAEA,2002]	8.88E+05	[COVRA,2012]
Tc-99 m					
Th-229				2.25E+02	[COVRA,2012]
Th-230				2.84E+01	[COVRA,2012]
Th-231					
Th-234					
Ti-44					reported activity upon collection after 30 years < 1 MBq
U-232	4.68E+08			1.69E+02	[COVRA,2012]
U-233	0.00E+00			2.04E+03	[COVRA,2012]
U-234	1.73E+11			5.15E+05	[COVRA,2012]
U-235	3.46E+09			1.35E+06	[COVRA,2012]
U-236	4.10E+10			8.52E+01	[COVRA,2012]
U-238	1.50E+11			3.83E+07	[COVRA,2012]
U-239					reported activity upon collection after 30 years < 1 MBq
Zr-93		2.00E+05	[IAEA,2002]		not reported

OPERA

Meer informatie:

Postadres
Postbus 202
4380 AE Vlissingen

T 0113-616 666
F 0113-616 650
E info@covra.nl

www.covra.nl

